ESHID-602341

Los Alamos
NATIONAL LABORATORY
EST. 1943

Associate Directorate for Environmental Management
P.O. Box 1663, MS M992
Los Alamos, New Mexico 87545
(505) 606-2337

Environmental Management
1900 Diamond Drive, MS M984
Los Alamos, New Mexico 87544
(505) 665-5658/FAX (505) 606-2132

Date: APR 27 2017
Refer To: ADEM-17-0084
LAUR: 17-23076
Locates Action No.: n/a

John Kieling, Bureau Chief
Hazardous Waste Bureau
New Mexico Environment Department
2905 Rodeo Park Drive East, Building 1
Santa Fe, NM 87505-6303

Subject: 2016 Sandia Wetland Performance Report

Dear Mr. Kieling:

Enclosed please find two hard copies with electronic files of the 2016 Sandia Wetland Performance Report. Los Alamos National Laboratory (the Laboratory) has prepared this report in response to requirements set forth in the document Work Plan and Final Design for Stabilization of the Sandia Canyon Wetland. The requirement to design a Sandia wetland monitoring program was previously set forth in the New Mexico Environment Department's (NMED's) Approval with Modification, Interim Measures Work Plan for Stabilization of the Sandia Canyon Wetland, in response to the Laboratory's Interim Measures Work Plan for Stabilization of the Sandia Canyon Wetland. The report was modified to consider comments from NMED in its Approval with Modifications [for the] 2015 Sandia Wetland Performance Report, dated November 18, 2016, and during a pre-report submittal meeting on January 30, 2017. The document also satisfies Appendix B, Milestones and Targets, Milestone 9, of the 2016 Compliance Order on Consent.

An update on the status of Los Alamos County's construction activities related to the Segmental Retaining Wall Landfill Cap/Scar Repair Project will be provided in the 2017 Sandia Wetland Performance Report. This project has recently started the construction phase of the control that will prevent debris from the County landfill from washing into the Sandia Canyon grade-control structure.

If you have questions, please contact Steve Veenis at (505) 667-0013 (veenis@lanl.gov) or Ramoncita Massey at (505) 665-7771 (ramoncita.massey@em.doe.gov).

Sincerely,

Bruce Robinson, Program Director
Environmental Remediation Program
Los Alamos National Laboratory

Sincerely,

David S. Rhodes, Director
Office of Quality and Regulatory Compliance
Los Alamos Environmental Management
Field Office

BR/DR/SV:sm

Enclosures: Two hard copies with electronic files – 2016 Sandia Wetland Performance Report (EP2017-0038)

Cy: (w/enc.)
Ramoncita Massey, DOE-EM-LA
Steve Veenis, ADEM ER Program
Tadz Kostrubala, ADEM ER Program

Cy: (w/electronic enc.)
Laurie King, EPA Region 6, Dallas, TX
Raymond Martinez, San Ildefonso Pueblo
Dino Chavarria, Santa Clara Pueblo
Steve Yanicak, NMED-DOE-OB, MS M894
Amanda White, ADEM ER Program
emla.docs@em.doe.gov
Dea Musa (w/ MS Word files on CD)
Public Reading Room (EPRR)
ADESH Records
PRS Database

Cy: (w/o enc./date-stamped letter emailed)
lasomailbox@nnsa.doe.gov
Peter Maggiore, DOE-NA-LA
Kimberly Davis Lebak, DOE-NA-LA
David Rhodes, DOE-EM-LA
Bruce Robinson, ADEM ER Program
Randy Erickson, ADEM
Jocelyn Buckley, ADESH-EPC-CP
Mike Saladen, ADESH-EPC-CP
John Bretzke, ADESH-EPC-DO
Michael Brandt, ADESH
William Mairson, PADOPS
Craig Leasure, PADOPS
Records

LA-UR-17-23076
April 2017
EP2017-0038

2016 Sandia Wetland Performance Report

Prepared by the Associate Directorate for Environmental Management

Los Alamos National Laboratory, operated by Los Alamos National Security, LLC, for the U.S. Department of Energy (DOE) under Contract No. DE-AC52-06NA253 and under DOE Office of Environmental Management Contract No. DE-EM0003528, has prepared this document pursuant to the Compliance Order on Consent, signed March 1, 2005. The Compliance Order on Consent contains requirements for the investigation and cleanup, including corrective action, of contamination at Los Alamos National Laboratory.

EP2017-0038

2016 Sandia Wetland Performance Report

April 2017

Responsible project manager:

Printed Name	Signature	Title	Organization	Date
Steve Veenis	Steve Veenis	Project Manager	Environmental Remediation Program	4.18.17

Responsible LANS representative:

Printed Name	Signature	Title	Organization	Date
Randall Erickson		Associate Director	Associate Directorate for Environmental Management	4/18/17

Responsible DOE EM-LA representative:

Printed Name	Signature	Title	Organization	Date
David S. Rhodes		Office Director	Quality and Regulatory Compliance	4-27-2017

EXECUTIVE SUMMARY

The 2016 Sandia wetland performance report is the third annual performance report following the 2012 to 2014 baseline that assessed the overall condition of the wetland at the head of Sandia Canyon in the context of the wetland's ability to prevent or minimize migration of contaminants of concern (i.e., chromium, polychlorinated biphenyls [PCBs] and polycyclic aromatic hydrocarbons) detected in wetland sediments as a result of historical releases at Los Alamos National Laboratory (LANL or the Laboratory). The geochemistry and physical stability of wetland sediments and the extent of wetland vegetation are the indicators of wetland conditions. The condition of the wetland is assessed to evaluate the effectiveness of the grade-control structure (GCS) completed in 2013 at the terminus of the wetland and to monitor changes to the Laboratory's operational practices that have affected outfall volumes discharging to the wetland. This report presents the results of monitoring conducted for surface water, alluvial groundwater, vegetation, and geomorphology between January and December 2016. The data are assessed relative to baseline conditions presented in the "Sandia Wetland Performance Report, Baseline Conditions 2012–2014" and the data presented in the "Sandia Performance Report, Performance Period April 2014–December 2014" and "2015 Sandia Wetland Performance Report" to identify any physical and geochemical changes that occurred during the 2016 monitoring period. Monitoring data include water levels and water chemistry from 12 former piezometers and 12 newly installed alluvial wells that monitor the alluvial groundwater in the wetland; surface water and storm water data from 2 gaging stations located upstream of the wetland and 1 gaging station located downstream; vegetation monitoring; and geomorphic change detection data from ground survey points, field observations, and digital elevation models derived from aerial light detection and ranging (LiDAR) surveys.

The monitoring conducted during the performance period indicates the Sandia wetland remains stable following the installation of the GCS, even with generally lower, but variable, effluent volumes entering the wetland. The GCS continues to be effective in arresting headcutting at the terminus of the wetland. Groundwater within the shallow alluvium remains in a reducing condition, and no obvious detrimental temporal trends in chemistry have been observed. Water levels in the wetland remained similar to those noted in the last 3 yr, with a temporary drop in the easternmost transect during the summer of 2016. This decrease was similar to that noted in the summer of 2014 and 2015. The decrease in water level was possibly a result of enhanced evapotranspiration associated with meteorological conditions and robust growth of additional wetland vegetation planted as part of the GCS restoration effort. Despite the observed decrease, water levels remained sufficiently high to sustain obligate wetland vegetation, and analytical results indicate alluvial groundwater remained in strongly reducing conditions in the eastern portion of the wetland immediately upgradient of the GCS. Even the upper portion of reach S-2 (the second reach down from the headwaters of Sandia Canyon and the reach that encompasses the Sandia wetland), which had previously seen a significant drop in the water table when the outfall was moved from a location that directly discharged into the wetland to an outfall (001) located upstream, retains reducing conditions at depth within alluvial groundwater. Storm water data indicate the GCS has had a positive effect in reducing contaminant mobility, and this trend continued through 2016. Suspended sediment, PCBs, and chromium concentrations have decreased significantly compared with pre- and post-GCS data immediately downgradient of the wetland at gage E123, presumably from eliminating headcutting at the terminus of the wetland and from trapping efficiency because of the dense vegetation within the wetland.

Geomorphic change detection studies indicate the wetland is stable, with a greater likelihood that the wetland experienced overall aggradation when comparing post-2015 monsoon to post-2016 monsoon season topographic data. A small amount of erosion was detected within the side channel located on the south side of reach S-2 and has remobilized previously deposited sediment, advancing the fan eastward

along the edge of the wetland boundary. Overall, the thalweg was stable between 2015 and 2016. The thalweg nick point observed in 2015 has not eroded upstream. Likewise, the plunge pool at the head of the reach has remained stable. The installation of the straw bales upstream of the run-on cells by the former Los Alamos County landfill has stabilized the previous sediment inputs from the landfill. The side channel entering the wetland from the south continues to deposit a small amount of sandy gravel into the wetland but did not result in the loss of cattail vegetation in 2016.

Vegetation perimeter mapping and vegetation photograph comparison suggest that the wetland is stable and expanding. Between 2015 and 2016, wetland vegetation perimeter surveys indicate the area with obligate wetland plants expanded by approximately 21%. Most of the expansion is occurring along the northern bank of the Northern Willow Zone with the growth of willows away from the primary channel and at the head of the wetland and with an expansion of cattails and mixed cattail/willows along the channel.

Alluvial chemistry is stable and continues to indicate strong reducing conditions. Speciated arsenic and iron data collected from piezometers and alluvial wells installed in Sandia Canyon continue to confirm the reducing conditions of the wetland. Ongoing sampling of hexavalent chromium indicate it is at or below detection limit within the wetland.

Surface water and alluvial water analytical data collected in 2016 were compared with New Mexico water-quality criteria and groundwater standards, respectively. Exceedances of water-quality criteria are presented in this report and are determined to be associated with historical Laboratory releases, with developed areas in the upper watershed, and with the natural reducing conditions of the wetland within the alluvial system.

Overall, 2016 monitoring indicates the wetland is physically more stable and discharging lower concentrations of contaminants of concern in storm water relative to baseline conditions. Alluvial data collected in 2016 continue to demonstrate the reducing conditions of the wetland sediment.

CONTENTS

Figures

Tables

Appendixes

1.0 INTRODUCTION

In response to liquid effluent released by the Los Alamos National Laboratory (LANL or the Laboratory), the Sandia wetland, located at the head of Sandia Canyon, has expanded from a relatively small footprint in the early 1950s to its current size, encompassing a wetland species vegetated area of 16,333 m^2, as of 2016 (note that this does not constitute a formal wetland delineation). Throughout the course of Laboratory operations, the wetland has been supported by continued effluent releases to the canyon. Contamination is present in wetland sediments because of historical releases from Laboratory operations (LANL 2009, 107453).

The Laboratory has prepared this "2016 Sandia Wetland Performance Report" in response to requirements set forth in the "Work Plan and Final Design for Stabilization of the Sandia Canyon Wetland" (LANL 2011, 207053). In that plan, the Laboratory proposed reporting of Sandia wetland monitoring data to the New Mexico Environment Department (NMED) by April 30 of each year. The requirement for designing a Sandia wetland monitoring program was previously set forth in NMED's "Approval with Modification, Interim Measures Work Plan for Stabilization of the Sandia Canyon Wetland" (NMED 2011, 203806) in response to the Laboratory's "Interim Measures Work Plan for Stabilization of the Sandia Canyon Wetland" (LANL 2011, 203454). The monitoring plan was provided in the work plan (LANL 2011, 207053) and is summarized in section 1.5 of this report. The monitoring plan is designed to identify physical or chemical changes in the Sandia wetland related to (1) the installation of a grade-control structure (GCS) at the terminus of the wetland (LANL 2013, 251743) and (2) changes in outfall chemistry and discharge volumes related to the Sanitary Effluent Reclamation Facility (SERF) expansion (DOE 2010, 206433).

This report assesses the overall condition and stability of the wetland in the context of the GCS at the terminus of the wetland, and changes to the volume and chemistry of effluent released into Sandia Canyon resulting from changes in the Laboratory's water-management practices associated with SERF and National Pollutant Discharge Elimination System (NPDES) Outfall 001 (Figure 1.0-1). The results of monitoring conducted in 2016 for surface water, alluvial groundwater, vegetation, and geomorphology are presented herein. Data are assessed relative to baseline conditions presented in the "Sandia Wetland Performance Report, Baseline Conditions 2012–2014" (LANL 2014, 257590) and relative to data presented in the "Sandia Performance Report, Performance Period April 2014–December 2014" (LANL 2015, 600399) and the "2015 Sandia Wetland Performance Report" (LANL 2015, 600399) to identify any physical and geochemical changes during the monitoring period. Monitoring data include the following:

- Water levels and water chemistry from 12 former piezometers and 12 newly installed alluvial wells that monitor the alluvial groundwater in the wetland
- Surface water and storm water data from 2 gaging stations located upstream of the wetland and 1 gaging station located downstream
- Vegetation monitoring
- Geomorphic change detection data from ground survey points, field observations, and digital elevation models (DEM) derived from aerial light detection and ranging (LiDAR) surveys

Hexavalent chromium [Cr(VI)] was historically released into liquid effluent from the Technical Area 03 (TA-03) power plant at the head of Sandia Canyon from 1956 to 1972. Some of the Cr(VI) made its way to the regional aquifer beneath Sandia and Mortandad Canyons, and Cr(VI) concentrations in the regional aquifer presently exceed NMED groundwater standards and U.S. Environmental Protection Agency (EPA) maximum contaminant levels (MCLs). Historical releases of polychlorinated biphenyls (PCBs) from

a former transformer storage area and polycyclic aromatic hydrocarbons (PAHs) from an asphalt batch plant also discharged to the wetland, which still contains an inventory of these contaminants. Sandia Canyon wetland performance monitoring is related to the overall chromium remediation project because a large portion of the original chromium inventory and other contaminants (i.e., PCBs and PAHs, discussed in section 1.1 below) are currently sequestered in the wetland sediment. The results of characterization work conducted to date in Sandia Canyon are described in the "Investigation Report for Sandia Canyon" (hereafter, the Phase I IR) (LANL 2009, 107453) and in the "Phase II Investigation Report for Sandia Canyon" (hereafter, the Phase II IR) (LANL 2012, 228624).

New Mexico Water Quality Control Commission (NMWQCC) groundwater standards, EPA MCLs, NMED screening levels for tap water, and EPA regional screening levels for tap water that are used to establish a set of screening values for evaluating monitoring data. Base-flow and storm water analytical results were screened against the appropriate surface water–quality standards in 20.6.4 New Mexico Administrative Code.

Information on radioactive materials and radionuclides, including the results of sampling and analysis of radioactive constituents, is voluntarily provided to NMED in accordance with U.S. Department of Energy policy.

1.1 Project Goals

The overall objective of this project is to monitor the physical and chemical stability of the Sandia wetland in the context of its inventory of contaminants of concern. Monitoring was initiated to evaluate the influence of the GCS (which was installed to reduce erosion at the terminus of the wetland) and anticipated decreases in discharge volume associated with the expansion of SERF on the discharge of contaminants.

Geochemical reducing conditions within the Sandia wetland converted some of the Cr(VI) released from 1956 to 1972 to stable, relatively insoluble trivalent chromium [Cr(III)]. A significant inventory of chromium as Cr(III), possibly around 15,000 kg, remains in wetland sediment (LANL 2009, 107453). Studies presented in the Phase I IR have shown the trivalent form of chromium is unlikely to oxidize and convert to mobile hexavalent chromium whether sequestered in the saturated reducing conditions of the wetland alluvium or exposed to oxygen upon dewatering of wetland sediments (LANL 2009, 107453). Maintaining the saturated reducing condition, however, is a prudent measure to ensure stability of the chromium inventory as trivalent chromium within the wetland sediment and alluvial waters.

The wetland also contains an inventory of PCBs and PAHs from historical Laboratory releases that have adsorbed to sediment within the wetland. This inventory will remain in place as long as the sediment remains physically stable. Abundant vegetation stabilizes sediments through root binding and also enhances deposition of suspended solids from storm water. PCBs in wetland sediment are primarily attributed to releases of PCBs from a transformer storage area, Solid Waste Management Unit 03-056(c). The PCB inventory in the wetland sediments is estimated to be 5.5 kg, 3.3 kg, 31.1 kg, and 24.4 kg for Aroclor-1242, Aroclor-1248, Aroclor-1254, and Aroclor-1260, respectively (LANL 2009, 107453). Four PAHs (benzo[a]anthracene, benzo[a]pyrene, benzo[b]fluoranthene, and indeno[1,2,3-cd]pyrene) were identified in the Phase I IR as being the most important for evaluating human health risk. PAHs are primarily attributed to releases from a former asphalt batch plant located upgradient of the wetland. The highest concentrations of benzo[a]anthracene and benzo[a]pyrene in sediment were found in investigation reaches S-1N and S-1S above the wetland (Figure 1.0-1). Much smaller concentrations, typically less than 1 mg/kg, have been measured in reach S-2, which includes the Sandia wetland (Figure 1.0-1).

The monitoring presented in this report is intended, in part, to assess the stabilizing impacts of the GCS on the eastern terminus of the wetland. Before the GCS was constructed, the terminus of the wetland had an active headcut (up to 3 m high). Installation of the GCS at the former active headcut has arrested it, thereby stabilizing the grade (Figure 1.0-1). Stabilization of vegetation, hydrology, and geochemistry at the easternmost end of the wetland indicates the efficacy of the GCS, backing up groundwater because of its impervious subgrade face (section 1.3) (LANL 2015, 600399) and stabilizing the grade at the terminus of the wetland. Maintenance of physical and chemical stability will, in turn, help prevent potential physical mobilization of adsorbed contaminants associated with sediment and chemical mobilization of precipitated or reduced contaminants under changing geochemical conditions in groundwater (LANL 2011, 203454; LANL 2011, 207053).

The Sandia wetland has experienced generally decreased liquid outfall effluent volumes (both daily and annually) from NPDES-permitted Outfalls 001 and 03A027 as part of the SERF expansion project. As part of the SERF expansion, a portion of the effluent previously released to Sandia Canyon is now being rerouted to cooling towers at various facilities, including the Strategic Computing Complex (SCC). Though effluent releases to Sandia Canyon may be reduced further, discharge will be maintained at a level that is believed to be sufficient to maintain the ecologic, hydrologic, and geochemical functioning of the wetland. If future changes to effluent volume or chemistry are shown to adversely impact the wetland, adaptive management will be used to ensure wetland stability (e.g., engineered controls to manage sediment and water distribution to increase the area of wetland saturation).

More detailed background on the SERF-related outfall chemistry and discharge volume changes is provided in section 1.4. The monitoring plan and associated rationale designed to identify physical and chemical changes in the wetland are presented in section 1.5. A conceptual model for wetland performance is presented in section 1.6. Monitoring performed during the 2016 performance period is discussed in section 2. Detailed monitoring results are presented in Appendix D. Section 3 summarizes monitoring results in the context of wetland performance metrics and suggests proposed changes to the monitoring plan.

1.2 Timeline

A graphical timeline showing changes related to outfall discharge and chemistry, the construction of the GCS, the addition of piezometer and alluvial well monitoring locations, and associated sampling events is shown in Figure 1.2-1.

1.3 Design and Function of the GCS

The location of the GCS is shown in Figure 1.0-1. The overall objectives of the GCS were to arrest the headcut in the lower portion of the wetland and to maintain favorable hydrologic and geochemical conditions to minimize contaminant migration (LANL 2011, 203454, Figure 2.4-2). The GCS was designed to meet the following objectives:

- Minimize erosion during large flow events
- Provide an even grade to allow wetland expansion and further stabilization
- Be sufficiently impervious to prevent the draining of alluvial soils and promote a high water table
- Facilitate nonchannelized flow
- Support wetland function under potentially reduced effluent conditions

The GCS transitions the grade approximately 11 vertical feet from the elevation of the wetland just upgradient of the former headcut location to the natural stream bed just upstream of gage E123. To maintain grade and to reduce the overall fill and size of a single structure, a set of three steel-sheet-pile walls was installed with decreasing elevation drops. Downstream of the third sheet-pile wall, a cascade pool was constructed of boulders and cobbles to transition to the final grade. The transition from the wetland above the GCS to the stream channel below is gradual, smooth, and stepped to prevent erosive flows that could scour and destabilize the stream reach below the structure (LANL 2013, 251743). The design of the GCS should allow for a reduction of outfall effluent discharge into the wetland without compromising the physical and geochemical function of the wetland, particularly of the eastern terminus where the GCS controls wetland water levels. The area behind the GCS was backfilled and wetland vegetation was planted to allow expansion of the wetland area. These measures physically stabilize the wetland by reducing sediment and associated contaminant transport into the lower sections of the canyon and should also maintain reducing conditions within the sediment near the terminus of the wetland, thus contributing to the goal of reducing potential contaminant transport (LANL 2013, 251743). A set of as-built diagrams for the GCS is presented in Appendix C of the completion report for the construction of the GCS (LANL 2013, 251743).

1.4 Sandia Canyon Outfalls and SERF

Outfalls have released liquid effluent to Sandia Canyon since the development of TA-03 in the early 1950s. Currently, three NPDES-permitted outfalls release to upper Sandia Canyon upstream of the wetland: Outfalls 001, 03A027, and 03A199 (EPA 2007, 099009) (Figure 1.0-1). Effluent releases at these outfall discharge points are monitored in compliance with the Laboratory's industrial NPDES permit (Permit No. NM0028355, EPA 2014, 600257). Operational changes that impact these outfalls have occurred since mid-2012. Figure 1.4-1 shows daily, monthly, and yearly average effluent volumes from 2006 to 2016 for Outfall 001, which releases the greatest volume of effluent to Sandia Canyon. Figure 1.4-1 also shows daily releases from August 2007 to January 2010 and from November 2012 to December 2016 for the two smaller outfalls, Outfalls 03A027 and 03A199. (The record for these two outfalls is incomplete.) The 2015 Sandia wetland performance report discusses liquid effluent releases to Sandia Canyon from 2006, when the Laboratory's chromium investigation began, to 2015. Late 2015 and 2016 releases and operations are discussed below:

September 18, 2015, to March 7, 2016: Operational changes at the SERF plant resulted in an increase discharge at Outfalls 001 and 03A027 in late 2015 and early 2016, as illustrated in Figures 1.4-1 and 1.4-2. During this time, incoming flows from the Sanitary Waste Water System (SWWS) plant increased, resulting in a corresponding increase in discharge at Outfall 001. In addition, the SERF plant discharged more effluent to Outfall 001 and sent less SERF-blended water for reuse in the SCC cooling towers. This combination of increases resulted in an additional 95,000 gallons per day (gpd) (58%) of effluent at Outfall 001 compared with the same period from September 2014 to March 2015. Makeup water for the SCC cooling towers was largely potable water (70%) rather than SERF-blended makeup water during this period (Figure 1.4-2). As a result, effluent volumes have increased by approximately 11,500 gpd at Outfall 03A027 because fewer cycles could be run using the silica-rich potable water. These changes represented a significant increase in the water input to the wetland but did not negatively affect wetland stability. Changes in water chemistry entering the wetland are discussed in Appendix D. The SERF product water has continued to be blended at a 4:1 ratio with SWWS effluent. However, a second blending point available near Outfall 001 was employed during this time period to mix SERF product water with SWWS effluent water; the blending of SERF to SWWS water (from the reuse and fire protection tank) at that point is not maintained at a constant ratio and likely has a higher ratio of SWWS water than usual when more water comes in from the SWWS plant.

March 8, 2016, to December 31, 2016: The operational changes at the SERF plant described above were temporary, and a return to reuse of SERF-blended water in the SCC cooling towers occurred on March 8, 2016. During this period, more than 99% of the water used by the SCC cooling towers was SERF-blended water. As a result, discharges at Outfall 001 decreased to an average of 152,000 gpd. One other operational change is also noted. Since September 9, 2016, discharges from the SCC cooling towers have been directed to Outfall 001 through the wet well (Figure 1.4-3) rather than to Outfall 03A027. Since then, the SCC blowdown effluent volumes are accounted for in the Outfall 001 discharge volumes and releases to Outfall 03A027 have been zero. This change is illustrated in Figure 1.4-1, which shows discharges at Outfall 03A027 dropping to zero, and in Figure 1.4-2, which shows the "combined Outfalls 001 and 03A027" data (turquoise line) converging with the Outfall 001 data (dashed light-green line). This change in discharge location and in accounting for the SCC cooling tower blowdown volume is expected to be permanent; Outfall 03A027 will be used only during maintenance or in the event of an emergency.

Future: Future plans allow for the SERF to run at full capacity so Laboratory computing facilities have access to larger amounts of SERF-blended water for cooling. This change would result in a further decrease in discharge to Outfall 001 and therefore less surface water entering the wetland. The variability in effluent volumes and water chemistry that may be released to the wetland will depend on return flow from facilities to outfalls that release to the wetland.

1.5 Monitoring Planned during the 2016 Performance Period

The original monitoring plan for the Sandia wetland is described in section 6.0 of the "Work Plan and Final Design for Stabilization of the Sandia Canyon Wetland" (LANL 2011, 207053). Proposed revisions to the monitoring plan were presented in the "Sandia Wetland Performance Report, Baseline Conditions 2012-2014" (LANL 2014, 257590); in the "Sandia Wetland Performance Report, Performance Period April 2014–December 2014" (LANL 2015, 600399); and in the "2015 Sandia Wetland Performance Report" (LANL 2016, 601432).

The initial work plan (LANL 2011, 207053) called for a multiphased approach to monitoring to evaluate hydrologic and geochemical changes associated with the GCS and/or with the SERF expansion and subsequent effluent reduction:

- Evaluate changes in hydrology and key geochemical indicators to monitor the health of the wetland at 12 alluvial sampling locations
- Evaluate transport of metals and organic chemicals through the wetland by monitoring surface-water base flows and storm flows at 3 gaging stations
- Monitor vegetation every 2 yr via photographic surveys
- Conduct periodic geomorphic surveys to evaluate erosion and aggradation of sediments within the wetland.

Monitoring of alluvial chemistry until February 2016 had been accomplished through a series of 13 drive-point 1-in.–inside diameter wells (henceforth denoted as "piezometers" because of their small well-casing diameter and method of installation) arranged in 4 transects in the wetland that were scheduled to be sampled quarterly. In the pilot sampling method comparison performed in 2015 and discussed in Appendix E of the "2015 Sandia Wetland Performance Report" (LANL 2016, 601432), alluvial wells were deemed the best method to obtain ample amounts of water and provide representative samples and field parameters. By October 2016, all the piezometers (prefix: SCPZ) were removed and replaced with 12 alluvial wells (prefix: SWA), placed in undisturbed locations adjacent to the piezometers with

approximately the same screening depth (Table 1.5-1). These alluvial wells are constructed of a 2-in.–inside diameter polyvinyl chloride casing (PVC) and a 2-in. slotted PVC casing to act as a screen surrounded by a filter pack consisting of 1/20 silica sand (Figure 1.5-1). As the piezometers were gradually replaced with alluvial wells in 2016, water from the piezometers was sampled until the alluvial wells were installed. Only water from the alluvial wells will be sampled in the coming years. The alluvial well name will be used to refer to the approximate location shared by the former piezometers and the current alluvial wells (the piezometers and wells are cross-walked in Table 1.5-2) through the rest of this report.

The alluvial well (piezometer) transects are as follows.

- Alluvial wells SWA-1-1 (SCPZ-1), SWA-1-2 (SCPZ-2/SWA-1), and SWA-1-3 (SCPZ-3) are located on a sand-and-gravel terrace near the active channel (c1 geomorphic unit) towards the western end of the wetland, which has experienced channel incision and dewatering relative to historical conditions. These alluvial systems are located on the c3 geomorphic unit (Figure D-4.0-1 and Appendix D for maps and definitions of geomorphic surfaces from the "2015 Sandia Wetland Performance Report" [LANL 2016, 601432]), away from the active channel and associated inset terrace (c2a geomorphic unit), which are locations of recent cattail expansion. Well SWA-1-1 is screened towards the base of alluvial fill, while the tops of the screens in wells SWA-1-2 and SWA-1-3 are approximately 6 ft and 3 ft below ground surface (bgs), respectively (Table 1.5-1).
- Wells SWA-2-4 (SCPZ-4), SWA-2-5 (SCPZ-5), and SWA-2-6 (SCPZ-6/SWA-2) form a transect in the widest portion of the wetland. The tops of the well screens are 2–3 ft bgs because the wetland water level is at or very near the ground surface at this transect. It is at these shallowest depths that changes in water level and sediment oxidation state are expected to manifest as a result of reduced effluent discharge. Similarly, the lateral margins of the wetland may dewater before the longitudinal axis of the wetland as a result of reduced effluent volumes. This effect could be most pronounced where the wetland is widest and water flux is most spread out. It is also at such locations that preferential flow paths within the alluvium may form.
- Wells SWA-3-7 (SPCZ-7), SWA-3-8 (SCPZ-8/SWA-3), and SWA-3-9 (SCPZ-9) are located in a narrow part of the wetland closer to its distal (eastern) end. This transect includes two shallow wells, SWA-3-7 and SWA-3-9, with the tops of the screens at 0.6 and 2.2 ft bgs, respectively, and the SWA-3-8 well with the top of the screen at 4.8 ft bgs (Table 1.5-1). The wetland water level is at or just below the ground surface at this transect. These alluvial locations provide indications of changes near the surface of the wetland and at depth in a narrow portion of the wetland where preferential flow paths are less likely to develop.
- The final transect of wells SWA-4-10 (SCPZ-10), SWA-4-11 (SCPZ-11B), and SWA-4-12 (SCPZ-12/SWA-4) have responded most to the rewatering that has occurred at the eastern terminus of the wetland because of the effect of the GCS. The wetland water level is at or near the surface at this transect. Water was routed around this area during the period of construction of the GCS.

The 2016 sampling and analysis plan for the piezometers and alluvial wells is provided in Table 1.5-3. Most of the analyses were designed as indicators of redox changes associated with potential dewatering of the wetland. Alluvial locations were also instrumented with sondes for continuous monitoring of water levels, specific conductance, and temperature.

Samples from base flow were collected quarterly with the alluvial wells. The same analytical suite, with the addition of unfiltered metals, PCB congeners, PAHs, and suspended sediment concentration (SSC), was monitored in base flow at surface water gaging stations E121, E122, and E123 (Figure 1.0-1).

Storm water flow rates into and out of the wetland are measured at gaging stations E121, E122, and E123, during sample-triggering storm events. Analyses of storm water samples collected in 2016 were planned as presented in Table 1.5-4. Analytical results with data plots are discussed in Appendix D and analytical data is available on CD (Appendix F).

Since 2015, two methods of topographic survey were employed: aerial LiDAR and ground-based global positioning system (GPS) surveying. Details of the monitoring scheme and results are presented in Appendix B.

The Laboratory resurveyed the vegetation perimeter of the Sandia wetland and photographed established locations to define the extent of obligate wetland species that depend upon saturated wetland conditions as well as to ascertain trending of vegetation conditions from 2015 to 2016. Details of the monitoring scheme and the results from this vegetation monitoring are presented in Appendix C. This monitoring effort replaces and supersedes that originally proposed in the “Work Plan and Final Design for Stabilization of the Sandia Canyon Wetland” (LANL 2011, 207053).

The GCS is inspected twice a year and following rain events with discharges greater than 50 cubic feet per second (cfs) (LANL 2014, 600083). If erosion or any indications of instability are observed, appropriate actions will be taken to ensure continued stability and functionality of the GCS. Inspections also assess sediment inputs from the former Los Alamos County landfill such as those that occurred during the September 2013 flooding (LANL 2014, 600083). Inspection results for 2016 are provided in Appendix E.

1.6 Conceptual Model for Assessing Wetland Performance

1.6.1 Hydrologic Status

The Sandia wetland is an effluent-supported cattail wetland. Surface water is generally present in a discrete channel (though in some areas surface water spreads from bank to bank) and passes through the wetland with a short residence time relative to alluvial water (LANL 2009, 107453; LANL 2014, 257590). Wetland sediments are underlain by Bandelier Tuff upon which alluvial groundwater is perched. A water-balance analysis conducted in 2007 and 2008 showed little surface water loss (approximately 2% of both effluent and runoff) occurs through the wetland (LANL 2009, 107453). A direct-current (DC) electrical-resistivity–based geophysical survey found that large continuous areas of the wetland are underlain by highly resistive welded tuffs (Qbt 2 of the Tshirege Member of the Bandelier Tuff) that represent a significant barrier to the infiltration of alluvial water into the subsurface (LANL 2012, 228624). In several areas, the survey also identified subvertical conductive zones that penetrate the upper bedrock units and, in some cases, appear to correlate with mapped fault and/or fracture zones. These conductive zones may represent present-day or historical infiltration pathways. However, the DC resistivity data do not differentiate between conductive zones that contain higher water content (possibly representing active infiltration) and wetted clay-rich fracture fill that may hinder infiltration.

Installation of the GCS has led to cessation of headcutting at the terminus of the wetland and has created an impermeable barrier to subsurface flow such that alluvial water must resurface before exiting the wetland. Given the impermeable nature of this barrier and the largely impermeable tuff underlying the wetland, to the first order the system can conceptually be thought of as a bathtub that effectively holds water with excess water spilling over the GCS at the wetland terminus. Annual evaluation of base-flow

rates confirms this “bathtub” assumption as rates entering and exiting the wetland are similar, although this assumption breaks down during storm events because of additional flow from subtributaries such as from the former Los Alamos County landfill (Figure 1.0-1). However, as long as water inputs from the outfalls exceed wetland evapotranspiration, even significantly reduced outfall discharge may sustain water levels and sufficient saturation within wetland sediments. Extreme decreases in effluent input volumes into the wetland, however, could potentially result in wetland dewatering. The wetland sediment is typically saturated at the eastern end of the wetland; these conditions extend westward, but near-surface sediment is unsaturated at the margins and at the western end of the wetland. The west end of the wetland previously supported a large cattail expanse; however, the area was largely dewatered more than a decade ago when the outfall that discharged directly into the wetland was relocated upstream to the current location of Outfall 001 and the associated channel was incised. Channel meandering and sediment redistribution are resulting in the reestablishment and expansion of cattails in this area (LANL 2016, 601432). Recent decreases in effluent volume to the wetland have not resulted in a lowering of the water table (dewatering) or decreased wetland vegetation cover (LANL 2016, 601432). The wetland vegetation community is important in mitigating storm water–related mobilization of contaminants through root binding and physical trapping of suspended sediments.

1.6.2 Contamination in Wetland Sediment

Detailed sediment mapping was performed during the Phase I IR (LANL 2009, 107453). Canyon reach S-2, which contains the Sandia wetland, contains high concentrations and proportions of the originally released contaminant inventory because of its proximity to contaminant sources, the large volume of sediment deposited during the period of active contaminant releases, the presence of high concentrations of organic matter in the wetland, and the presence of large amounts of silt and clay (Figure 1.0-1). Contaminants commonly adsorb to, or are precipitated in association with, sediment particles or organic matter.

Chromium is the major inorganic contaminant of concern in the wetland that could be affected by both redox changes in the wetland and physical destabilization. Sections 1.0 and 1.1 present the background of chromium contamination in wetland sediments. Arsenic may also be released from wetland sediments upon dewatering (LANL 2009, 107453). Two organic contaminants of concern, PCBs and PAHs, are primarily subject to physical transport in floods because of low solubility and a strong affinity for organic material and sediment particles. Important source areas for these contaminants are the former outfall for the power plant cooling towers in upper Sandia Canyon (chromium), a former transformer storage area along the south fork of Sandia Canyon (PCBs), and the former asphalt batch along the north fork of Sandia Canyon (PAHs) (LANL 2009, 107453).

1.6.3 Cr(III) Stability in the Sandia Wetland

The inventory of chromium contamination within the Sandia Wetland exists primarily in the form of Cr(III) because of reducing conditions. Alluvial saturation, along with significant amounts of solid organic matter (SOM) produced from wetland vegetation, results in reducing alluvial aquifer conditions as indicated by detectable concentrations of ammonia and sulfide, high dissolved iron and manganese concentrations, and low nitrate and sulfate in alluvial water (LANL 2014, 257590; LANL 2015, 600399; LANL 2016, 601432). Theoretically, oxidation by manganese oxides under aqueous conditions is the primary mechanism responsible for oxidation of Cr(III) to Cr(VI) (Rai et al. 1989, 249300). Complete oxidation of Cr(III) to Cr(VI) is likely to occur if the molar concentrations of Mn(IV) exceed those of Fe(II), Cr(III), and organic carbon. This situation, however, is unlikely within the active Sandia wetland because concentrations of total iron, consisting mainly of Fe(II), and SOM are present at much higher weight-percent concentrations than Mn(IV), which is usually present in the parts per million range (discussed in more detail in Appendix J of the Phase I IR [LANL 2009, 107453]). In addition, drying and leaching

experiments conducted on Sandia wetland sediments to quantify the potential release of Cr(VI) during drying of the wetland material showed that Cr(III) appears to remain stable, suggesting insufficient Mn(IV) is produced to oxidize appreciable amounts of Cr(III) to Cr(VI) (LANL 2009, 107453). Total "dissolved" chromium in leachates was primarily in the form of Cr(III), indicating most chromium measured in a filtered wetland performance monitoring sample occurs as colloids. This explanation is supported by analyses of Cr(VI), which is generally below the method detection limit (LANL 2016, 601432).

1.6.4 Current State of the Sandia Wetland

Data from geochemical studies presented in the Phase I IR (LANL 2009, 107453) and previous performance reports (LANL 2015, 600399; LANL 2016, 601432) indicate chromium in wetland sediments is predominantly geochemically stable as Cr(III) and is not likely to become a future source of chromium contamination in groundwater, especially if saturated conditions are maintained within the wetland. Results from baseline monitoring of the wetland (LANL 2014, 257590) and from monitoring in 2014 (LANL 2015, 600399) and 2015 (LANL 2016, 601432) show that the Sandia wetland system is chemically and physically stable, with stable to increasing wetland vegetation cover in different parts of the system. Most importantly, results of storm-water monitoring from gage station E123 have shown a reduction of PCBs and chromium post-GCS installation.

2.0 MONITORING PERFORMED DURING THE 2016 MONITORING PERIOD

Quarterly sampling of Sandia wetland surface water and alluvial water is coordinated with the Chromium Investigation monitoring group sampling conducted under the Interim Facility-Wide Groundwater Monitoring Plan. In 2016, performance sampling was conducted at 12 locations with a combination of piezometers and alluvial wells within the wetland (piezometers were gradually replaced with wells throughout the year [Table 1.5-2] as well as at surface water gaging stations E121 and E122 [above the wetland] and E123 [below the wetland]) (Figure 1.0-1).

2.1 Monitoring of Surface Water

Surface water gaging stations E121 and E122 are located in the upgradient western end of the Sandia Canyon watershed. Surface water gaging station E123 is located to the east immediately below the terminus of the wetland. Figure 1.0-1 shows the location of the gaging stations, outfalls, and the extent of the Sandia wetland. In 2016, gage station E121 measured discharge from Outfalls 001 and 03A027 and storm water runoff from approximately 50 acres from TA-03; however, with changes at SERF in September 2016, discharge from SCC cooling towers is primarily directed to Outfall 001, with Outfall 03A027 used only for maintenance and emergency discharge (section 1.4). Station E122 measures discharge from Outfall 03A199 and storm water runoff from approximately 50 acres from TA-03. Station E123 measures surface water flow below the wetland, including discharge from all outfalls and storm water runoff from approximately 185 acres, 100 acres of which are from E121 and E122.

Tables 2.1-1 and 2.1-2 detail surface water base flow sampling and field parameters, respectively, for samples collected in calendar year 2016 (section 1.5).

In 2016, ISCO 3700 automated samplers attempted to collect storm water samples when discharge was greater than 10 cfs at gaging stations E121 and E123. Until September 16, 2016, automated samples were collected at station E122 when discharge was greater than 5 cfs. Since September 14, 2016, the trip level at E122 was lowered to 0.5 cfs to collect samples because only one had been collected since the GCS was constructed. Storm water samples in 2016 were analyzed based on the suites presented in Table 1.5-3. Samplers at E121, E122, and E123 were activated on May 11, 2016, before the monsoon season and turned off for the winter on November 14, 2016. Stations E121 and E123 are equipped with a

Sutron 9210 data logger, an MDS 4710 radio transceiver, and a Sutron Accubar bubbler. Station E122 is equipped with a Sutron 9210 data logger, an MDS 4710 radio transceiver, and a Siemens Milltronics ultrasonic probe. On November 30, 2016, the probe at E122 was replaced with a VEGAPULS 61 radar sensor. Stage is recorded every 5 min and transmitted to a base station where it is archived in a database. All three stations are equipped with two automated ISCO samplers: one with a 24-bottle base for SSC analyses and one with a 12-bottle base for collection of chemistry samples.

For each sample-triggering storm event in 2016, Table 2.1-3 shows precipitation at rain gage RG121.9, storm water peak discharge and whether a sample was collected at E121, E122, and E123 (Figure 1.0-1). Storm water discharge at E121 equaled or exceeded the trip level (10 cfs) 10 times in 2016; samples were collected from 6 of these events and during 1 event when discharge was less than 10 cfs (8.4 cfs is within the stage measurement margin of error of ± 2 cfs). Samples could not be collected during 1 of the 10 events because it was within the stage measurement margin of error, and samples were also not collected during 3 of the 10 events because the sampler was full from a previous storm event. Discharge at E122 did not equal or exceed the trip level (5 cfs) throughout most of 2016; thus, the trip level was lowered to 0.5 cfs and samples were collected during 3 discharge events with peak discharges equal to or above 0.5 cfs. Samples were not collected during two events after the trip level was lowered because the sampler was full from a previous storm event. Discharge at E123 exceeded 10 cfs 8 times in 2016; samples were collected from 5 of these events and the other 3 events were within the stage measurement margin of error, thus the sampler did not attempt to collect.

2.2 Monitoring of Alluvial System

A summary of well performance is provided in Table 2.1-1 with the analytical suite listed in Table 1.5-3. The short holding time of 24 h for sulfide samples is often exceeded. These data are still useful for interpreting redox conditions in the wetland. Actual sulfide concentrations are expected to be higher than those measured outside the holding time, so measured sulfide concentrations are conservative in terms of assessing redox conditions (sulfide concentrations increase as reducing conditions increase). Cr(VI) was measured at all groundwater and surface water locations (base flow) quarterly. As(III) was measured for four rounds starting in February 2016, and Fe(II) was measured for three quarters starting in May 2016 at all sampled piezometer and alluvial well locations.

Full suites were collected and no problems were encountered when alluvial water was sampled this year because the piezometers had been replaced with alluvial wells. Alluvial wells were sampled as each was installed; piezometers were sampled until the installations of the collocated alluvial wells were completed (Table 2.1-1). Locations SWA-2-5 and SWA-2-6 were inaccessible during the May sampling round because a Sora (*Porzana carolina*) was nesting with nine eggs (Figure 2.2-1).

The alluvial wells provided the highest quality field parameter data (Table 2.1-2) because these wells produced sufficient water for accurate measurement of field parameters and had the best potential for reaching stability. For all sampled piezometers, priority was placed on obtaining sufficient volumes for sample collection versus achieving field parameter stability.

2.3 Water-Level Monitoring

Water-level and temperature data collected by sondes are discussed in section D-4.0 in Appendix D. It was determined that the sondes at locations within the channel would likely not freeze, and thus these sondes were left in place for the winter at locations SCPZ-1, SCPZ-5, SCPZ-8, SCPZ-11B, and SCPZ-12. Sondes were left in all the installed alluvial wells (SWA-1-2, SWA-2-6, SWA-3-8, and SWA-4-12) over winter as well. By mid-May 2016, sondes were reinstalled in all the piezometers outside a channel that

had not been replaced by alluvial wells. Sondes were installed about a month after the installation of each alluvial well when the well housing was in place.

2.4 Geomorphic Monitoring

A full description of the approach and results for geomorphic surveys is presented in Appendix B.

2.5 Vegetation Monitoring

A full description of the approach and results for vegetation surveys is presented in Appendix C.

2.7 Monitoring of the GCS

Inspection results from monitoring of the GCS are presented in Appendix E.

3.0 SUMMARY OF RESULTS FROM WETLAND PERFORMANCE METRICS

Detailed results of performance metrics are presented in Appendix D and are summarized here.

3.1 Key Monitoring Locations and Performance Metrics

It is important to note that deleterious changes in any one metric do not necessarily represent a detriment to the overall function of the wetland and will not necessarily lead to contaminant release from wetland sediments. The wetland should be evaluated in terms of total system performance over time with multiple lines of evidence used to determine if the system is stable.

Gaging station E121 is a good location to monitor the integrated impacts of changing input chemistry and decreasing effluent volumes from Outfalls 001 and 03A027 in base flow. Gaging station E123 is the key integrating location of total wetland performance in mitigating discharges of contaminants of concern. Monitoring of storm water at E123 will reveal if anomalously high levels of sediment and contaminants (e.g., chromium, PCBs, PAHs) are mobilized during floods because of a reduction in chemical and/or physical stability in the wetland. Monitoring during base flow conditions will indicate changes in outfall chemistry and changes associated with wetland biogeochemistry and function. The metric for identifying deleterious impacts monitored at this location would be increases in base flow or storm water contaminant concentrations that occur year after year following installation of the GCS.

The alluvial well array provides valuable water-level and alluvial-water chemistry data (Appendix D). These locations monitor potential changes associated with outfall volumes, evolving geomorphology, redistribution of reducing zones, and changes in chemistry of the outfall (in the case of more conservative constituents). The metrics for identifying deleterious impacts as monitored in the wells would be (1) persistent increases in contaminant concentrations [e.g., Cr(VI)] and/or increases in oxidizing conditions as indicated by redox-sensitive species (e.g., decreased sulfide, increased sulfate) and (2) persistent decreases in water levels that have deleterious effects on obligate wetland vegetation.

Geomorphic change detection using a combination of aerial LiDAR and ground-based field observations, coupled with thalweg monitoring using GPS ground-surveying techniques, has been implemented over the past 3 yr for monitoring changes in geomorphology in the wetland (Appendix B). Evaluation of these monitoring techniques has shown that ground-based field observations and thalweg monitoring are the best way to evaluate changes in the morphology of the cattail zone of the wetland. LiDAR cannot penetrate water or vegetation to obtain an elevation representing ground. LiDAR data representing ground surface within the cattail zone is prone to error. Therefore, field observation and thalweg surveys have proven the best method for evaluation of geomorphic change within the cattail zone. Evidence of

deleterious impacts includes widespread, persistent erosion over portions of the wetland that cannot be attributed to the wetland readjusting its grade in response to installation of the GCS or to incisions that have occurred in other parts of the wetland.

The quantitative vegetation cross-sections from previous years and perimeter mapping from 2016 (Appendix C) are used to monitor both the physical stability and the saturation state of the wetland, as indicated by changes in obligate and facultative wetland vegetation. Increases in upland vegetation within the current extent of the wetland would indicate deleterious impacts on wetland function.

After calendar year 2018, 5 yr of post-GSC monitoring will have been conducted. In the 2018 performance report, a robust conceptual model for overall system performance that captures interannual variability will be proposed. This conceptual model will evaluate the full 5 yr of records following the construction of the GCS and will capture the potential range of monitoring variability recorded in the Sandia wetland. During the annual monitoring periods from 2017 and 2018, the Laboratory will continue to refine and improve the monitoring plan in an effort to fully identify, and monitor for, key criteria that are reliable proxies for wetland stability (e.g., vegetation, spatial contaminant trends, geomorphic stability, and key redox indicators).

3.2 Spatial and Temporal Geochemical Patterns

In 2016, concentrations of PCBs, chromium, and PAHs in storm water were similar at gaging stations E121 and E123 (Figure D-2.0-7). Continued decreases of PCBs and chromium were observed at E123 over time compared with pre-GCS conditions (Figure D-2.0-7). In 2015, PAH concentrations downgradient of the wetland were slightly higher than upgradient of the wetland; however, in 2016, PAH concentrations downgradient of the wetland were lower than upgradient of wetland. Overall, the annual mass flux of sediment and contaminants of concern has decreased both spatially from E121 to E123 and temporally from 2014 to 2016 (Figures D-2.0-10 to D-2.0-13). These results indicate that, per volume of storm water, fewer contaminants are moving through the wetland. This steady reduction in mass flux corresponds to wetland vegetation expansion over the same time period and observed success of the GCS in stabilizing the terminus of the wetland. Therefore, the cause of the mass flux reduction may be multifaceted.

Indicators of base flow water quality show the impact of recent improvements in water quality because of the SERF upgrade (Appendix D-2.0). Redox indicators potentially show evidence of chemical reduction as surface water flows through the wetland (e.g., lower nitrate at gaging station E123 relative to E121). Base flow Cr(VI) concentrations at E121 and E122 are higher than at E123, indicating reduction occurring in the wetland (Figure D-2.0-5).

Low sulfate concentrations in alluvial waters relative to base flow, along with frequent detects of sulfide, emphasize the strong reducing nature of the wetland sediments. As sulfate reduction occurs at much lower redox potentials than the reduction of chromate, nitrate, iron, and so on, the wetland environment is highly favorable in terms of chemical stability of chromium as Cr(III). Several analytes clearly reflect reducing conditions in all alluvial locations throughout the wetland (sulfate, arsenic, iron, manganese, sulfide, and ammonium). For example, sulfide and ammonium are present at all locations and bound most of the redox ladder. Data indicate locations SWA-1-1, SWA-2-5, SWA-2-6, and SWA-2-8 seem to be the most reducing (based on alluvial arsenic, iron, manganese, and sulfate concentrations), while locations SWA-1-2, SWA-1-3, and perhaps SWA-2-4 are somewhat less reducing (based on alluvial manganese concentrations) (section D-3.2). While no preferential flow paths were identified in the alluvium, there do appear to be distinct geochemical domains in terms of redox conditions. It appears that the important easternmost transect is recovering from disturbance associated with installation of the GCS and is showing clear evidence of strongly reducing conditions (section D-3.0).

Only a few temporal trends are observed in the arsenic, iron, sulfate, and chromium species analyzed in the wetland (section D-3.1). Temporal decreases in arsenic and sulfate concentrations and increases in iron and manganese concentrations over the period of sampling may be the result of ongoing inputs of organic matter that continue to promote strong reducing conditions in the wetland. No temporal trends were observed in chromium concentrations.

3.2.1 Surface and Alluvial Water Exceedances

Base-flow and storm water analytical results from E121, E122, and E123 in 2016 were screened against the appropriate surface water–quality criteria (SWQC) (section D-2.1). The two main sources of surface water that enters the wetland are discharges from outfalls and storm water runoff from TA-03. This run-on source water is characterized by results from E121 and E122. Results from E123, characterize a mix of waters from E121, E122, runoff through the Sandia wetland, and runoff from the surrounding area that have Laboratory and Los Alamos County sources. The exceedances detected in 2016 include aluminum, benzo(a)anthracene, benzo(a)pyrene, benzo(b)fluoranthene, cadmium, copper, gross-alpha radioactivity, lead, zinc, and PCBs. Most of the exceedances occurred in storm water.

A comparison of the average and maximum results from E121 and E122 to E123 shows that the Sandia wetland is not a quantifiable source of the constituents that exceeded SWQC, with the exception of PCBs. The Sandia wetland probably contributed only PCBs to the list of analytes that exceed SWQC. Several constituents were not detected at station E123 (i.e., cadmium, PAHs, and zinc) but were detected at E121 or E122, indicating that the Sandia wetland is attenuating constituent concentrations as storm water flows through the wetland. The remainder of the constituents were either lower in average or maximum concentration at E123 or significantly equivalent to the concentrations detected at E121 or E122.

The alluvial system data from 2016 were screened to standards (section D-3.4 and Table D-3.4-1). Exceedances in alluvial water included iron, manganese, arsenic, chromium, lithium, and fluoride. High iron and manganese are expected in the reducing wetland conditions. The total measured iron in the wetland is in its reduced form, Fe(II); manganese, because it is close to iron on the redox ladder, is expected to be in its reduced form as well. Most of the total chromium concentration in alluvial water in the wetland is colloidal Cr(III), which creates the exceedance; the measured Cr(VI) at the locations of the exceedances is at or below the minimum detection limit. Lithium is present naturally in the regional aquifer and potentially concentrated in cooling towers that release water at stations E121 and E122 into the wetland; the highest concentrations of lithium were detected at E121 entering the wetland (Figure D-3.4-1). One exceedance of fluoride was detected at SWA-4-10, and the source of this exceedance is not known.

3.3 Temporal and Spatial Trends in Water Levels

Monitoring of water levels continues as a means to determine how operational effluent releases affect the overall wetland hydrology. Comparisons between the 2015 and 2016 water levels, shown in Figure D-4.0-2, indicate they have been relatively stable, even with changes in outfall volumes. Seasonal decreases in water levels are observed in a few wells in the easternmost transect, presumably as a result of high rates of evapotranspiration associated with warm temperatures and lower-magnitude precipitation events in the summers compared with those in the previous year (section D-2.0). The water levels in the alluvial system tend to stay stable because a relatively impermeable Bandelier Tuff bedrock base of the wetland, and an impermeable downgradient end (the GCS) keeps the water contained in the wetland. As such, as long as water inputs exceed wetland evapotranspiration, even significantly reduced outfall discharge may sustain water levels and sufficient saturation within wetland sediments. Decreased outfall discharge may manifest more in the surface water balance of the wetland than in alluvial water levels. A longer period of record will help to determine the overall impact to the wetland.

3.4 Geomorphic Trends in the Wetland

Geomorphic change detection studies (Appendix B) indicate minor geomorphic change occurred between 2015 and 2016. Interpretation of LiDAR survey results indicated there is greater likelihood that the wetland experienced net deposition when post-2015 monsoon with post-2016 monsoon season topographic data are compared, at least within the resolution of the technique. A small amount of erosion was detected through LiDAR survey of the small channel on the south side of reach S-2 that had previously contributed to the deposition of sediment, creating a fan, and is likely responsible for the eastward advancement of the fan along the southern edge of the wetland boundary. Field observations of this small side channel indicate that a small amount of sandy gravel continued to be deposited 3 to 5 ft farther into the wetland but has not resulted in the loss of any cattails during this monitoring period. Overall, the thalweg was stable between 2015 and 2016. The thalweg nick point observed in 2015 has not changed. The plunge pool at the head of the reach has also remained stable. Three alluvial fans entering the wetland from the north (drainage from the former Los Alamos County landfill) remained relatively stable.

3.5 Spatial and Temporal Trends in Vegetation

Between 2014 and 2015, the perimeter of the wetland vegetation had expanded by approximately 12% over the area of study (Appendix C of the “2015 Sandia Wetland Performance Report” [LANL 2016, 601432]). In 2016, robust growth of wetland vegetation has continued, with wetland vegetation expanding approximately 21% over the study area since 2015 (Appendix C). The most expansion occurred at the western part of the primary channel with willows growing northward, away from the channel, and at the upstream end of the reach where new cattails and willows expanded along the stream channel. Vegetation within the Sandia wetland continues to be stable or increasing.

Vegetation monitoring documented in this report does not constitute a formal wetland delineation. For example, the occurrence of hydric soils has not been determined. The combined approach of monitoring the saturation status of the wetland through water-level measurements and redox chemistry, along with spatial and temporal patterns in obligate wetland vegetation, however, is sufficiently robust to evaluate the performance of the wetland. For example, should the wetland begin to dewater as a result of operational changes associated with the SERF, these changes would be noted immediately in water-level data and subsequently in alluvial water chemistry and obligate wetland vegetation patterns.

3.6 Performance of GCS

Inspection results from monitoring of the GCS, presented in Appendix E, indicate the GCS is stable and does not require corrective or mitigative actions. In 2016, Los Alamos County completed field activities to support the design of a long-term solution to address run-off from the former landfill and associated erosion resulting from this runoff. As part of this effort, Los Alamos County removed sediment from behind the upper run-on defense cell and installed best management practices, including straw bales, farther upstream. The straw bales upstream of the run-on defense cells are trapping sediments from the landfill, preventing them from entering the wetland at the GCS. These best management practices continue to serve to prevent sediments from the former Los Alamos County landfill from reaching the GCS area. The GCS has prevented significant erosion associated with flood events over the last 3 yr. Alluvial sediments just above the GCS remain reducing and saturated. Storm water data indicate the GCS has had a positive impact on reducing contaminant mobility. Suspended sediment, PCBs, and chromium concentrations have decreased at gage E123 post-GCS, presumably as a result of the elimination of headcutting at the terminus of the wetland.

3.7 Proposed Changes to Monitoring Plan

In 2017, surface water base flow and alluvial wells will be sampled as proposed in Table 3.7-1. Changes for 2017 include the following:

- Alluvial wells will be sampled for arsenic and iron speciation during sampling to achieve four rounds of data from alluvial wells but will be discontinued after four total rounds of these analytes have been collected from each alluvial well.
- After the first round of sampling, the Laboratory will attempt to perform all analysis at an accredited off-site laboratory. The Laboratory will keep the NMED Hazardous Waste Bureau informed of progress in meeting this goal.
- Monitoring for nitrogen and oxygen (^{15}N and ^{18}O) isotopes in base flow will be discontinued. These constituents are no longer relevant in assessing the Sandia wetland performance because the conceptual model of nitrate sources and attenuation is well constrained (sections 3.1 and 3.2 of the "Sandia Wetland Performance Report, Baseline Conditions 2012–2014" [LANL 2014, 257590] and section 3.2 of the "Sandia Wetland Performance Report, Performance Period April 2014–December 2014" [LANL 2015, 600399]).

Storm water sampling and off-site analysis will continue as presented in Table 1.5-4. If four storm water runoff events have been sampled at a gaging station E121, E122, and E123 during the monitoring year, subsequent events with discharge less than the largest discharge of the sampled storm events will not be analyzed. This allows collection of representative data from each gage location and ensures the largest storm water runoff event of the season is analyzed.

Quantitative surveys of wetland vegetation along cross-sections will occur biennially, with the next surveys to be conducted in 2017. No other change in vegetation monitoring will occur.

In 2017, evaluation of geomorphic changes will rely on field observations to determine further actions. If storm water peak discharge at E123 is greater than 50 cfs, a visual inspection of the wetland will occur to document qualitative geomorphic changes. Following the summer monsoons, the thalweg survey will be conducted. Since minor geomorphic changes occurred from 2015 to 2016, this level of the changes can be used as a baseline for future evaluations. If the visual observations or thalweg survey indicate geomorphic changes that are not consistent with past year's observation, a LiDAR aerial flyover will be planned for the fall of 2017, and the processed data will be field-verified to ensure that geomorphic changes shown in a threshold DEM of difference comparison represent actual geomorphic changes. The installation and monitoring of erosion pins in the side channel south of the plunge pool above reach S-2 will be conducted to evaluate the impact and/or contribution of sediment into the expanding cattails at the western part of the reach.

4.0 CONCLUSIONS

This performance period covers the third year following baseline monitoring. The monitoring performed during the performance period indicates that the Sandia wetland is stable and expanding following the installation of the GCS. Year-over-year comparison of analytical results indicates the wetland is discharging lower concentrations of contaminants of concern in storm water. Even with periods of lower effluent volumes entering the wetland and periods of evapotranspiration, the alluvial system remains stable and wetland sediments remain highly reducing, with no detrimental temporal trends in chemistry noted. Even the upper portion of reach S-2 (the second reach down from the headwaters of Sandia Canyon and the reach that encompasses the Sandia wetland), which had been previously

dewatered and is outside the current footprint of the wetland, retains reducing conditions in alluvial groundwater at depth.

Despite overall reduced effluent volumes, water levels remain sufficiently high to sustain and promote the expansion of the obligate wetland vegetation. Continuing vegetation monitoring in future years will be valuable in assessing wetland performance, with abundant wetland vegetation promoting sediment stability and preserving reducing conditions. No large-scale systematic erosion has been noted in the wetland, and the system seems to be highly stable from a physical perspective. The GCS has arrested headcutting at the terminus of the wetland. Planted wetland vegetation has rapidly established around the GCS, and wetland vegetation is expanding in the upper portion of the system. Storm water data indicate that the GCS has had a positive impact on contaminant mobility. Suspended sediment, PCBs, and chromium concentrations have decreased at E123 post-GCS, presumably because of cessation of headcutting at the terminus of the wetland.

Ongoing monitoring will continue to allow the Laboratory to assess changes within the Sandia wetland related to the GCS, changes in effluent chemistry, and decreases in effluent volumes and discharge rates. The Laboratory will respond with an adaptive management strategy should adverse changes be noted.

5.0 REFERENCES AND MAP DATA SOURCES

5.1 References

The following list includes all documents cited in this report. Parenthetical information following each reference provides the author(s), publication date, and ER ID or ESH ID. This information is also included in text citations. ER IDs were assigned by the Environmental Programs Directorate's Records Processing Facility (IDs through 599999), and ESH IDs are assigned by the Environment, Safety, and Health (ESH) Directorate (IDs 600000 and above). IDs are used to locate documents in the Laboratory's Electronic Document Management System and, where applicable, in the master reference set.

Copies of the master reference set are maintained at the NMED Hazardous Waste Bureau and the ESH Directorate. The set was developed to ensure that the administrative authority has all material needed to review this document, and it is updated with every document submitted to the administrative authority. Documents previously submitted to the administrative authority are not included.

DOE (U.S. Department of Energy), August 24, 2010. "Final Environmental Assessment for the Expansion of the Sanitary Effluent Reclamation Facility and Environmental Restoration of Reach S-2 of Sandia Canyon at Los Alamos National Laboratory, Los Alamos, New Mexico," U.S. Department of Energy document DOE/EA-1736, Los Alamos Site Office, Los Alamos, New Mexico. (DOE 2010, 206433)

EPA (U.S. Environmental Protection Agency), June 8, 2007. "Authorization to Discharge under the National Pollutant Discharge Elimination System, NPDES Permit No. NM 0028355," Region 6, Dallas, Texas. (EPA 2007, 099009)

EPA (U.S. Environmental Protection Agency), August 12, 2014. "NPDES Permit No. NM0028355 Final Permit Decision," U.S. Environmental Protection Agency Region 6, Dallas, Texas. (EPA 2014, 600257)

LANL (Los Alamos National Laboratory), October 2009. "Investigation Report for Sandia Canyon," Los Alamos National Laboratory document LA-UR-09-6450, Los Alamos, New Mexico. (LANL 2009, 107453)

LANL (Los Alamos National Laboratory), May 2011. "Interim Measures Work Plan for Stabilization of the Sandia Canyon Wetland," Los Alamos National Laboratory document LA-UR-11-2186, Los Alamos, New Mexico. (LANL 2011, 203454)

LANL (Los Alamos National Laboratory), September 2011. "Work Plan and Final Design for Stabilization of the Sandia Canyon Wetland," Los Alamos National Laboratory document LA-UR-11-5337, Los Alamos, New Mexico. (LANL 2011, 207053)

LANL (Los Alamos National Laboratory), September 2012. "Phase II Investigation Report for Sandia Canyon," Los Alamos National Laboratory document LA-UR-12-24593, Los Alamos, New Mexico. (LANL 2012, 228624)

LANL (Los Alamos National Laboratory), December 2013. "Completion Report for Sandia Canyon Grade-Control Structure," Los Alamos National Laboratory document LA-UR-13-29285, Los Alamos, New Mexico. (LANL 2013, 251743)

LANL (Los Alamos National Laboratory), June 2014. "Sandia Wetland Performance Report, Baseline Conditions 2012–2014," Los Alamos National Laboratory document LA-UR-14-24271, Los Alamos, New Mexico. (LANL 2014, 257590)

LANL (Los Alamos National Laboratory), December 15, 2014. "2014 Annual Monitoring Report for Sandia Canyon Wetland Grade-Control Structure (SPA-2012-00050-ABQ)," Los Alamos National Laboratory letter and attachments (ENV-DO-14-0378) to K.E. Allen (USACE) from A.R. Grieggs (LANL), Los Alamos, New Mexico. (LANL 2014, 600083)

LANL (Los Alamos National Laboratory), April 2015. "Sandia Wetland Performance Report, Performance Period April 2014–December 2014," Los Alamos National Laboratory document LA-UR-15-22463, Los Alamos, New Mexico. (LANL 2015, 600399)

LANL (Los Alamos National Laboratory), April 2016. "2015 Sandia Wetland Performance Report," Los Alamos National Laboratory document LA-UR-16-22618, Los Alamos, New Mexico. (LANL 2016, 601432)

NMED (New Mexico Environment Department), June 9, 2011. "Approval with Modification, Interim Measures Work Plan for Stabilization of the Sandia Canyon Wetland," New Mexico Environment Department letter to G.J. Rael (DOE-LASO) and M.J. Graham (LANL) from J.E. Kieling (NMED-HWB), Santa Fe, New Mexico. (NMED 2011, 203806)

Rai, D., L.E. Eary, and J.M. Zachara, October 1989. "Environmental Chemistry of Chromium," *Science of the Total Environment,* Vol. 86, No. 1–2, pp. 15–23. (Rai et al. 1989, 249300)

5.2 Map Data Sources

Vegetation Monitoring Zones; Los Alamos National Laboratory; 2016.

Rain Gages; Los Alamos National Laboratory; ER-ES Surface Hydrology Group; 2017.

WQH NPDES Outfalls; Los Alamos National Laboratory, ENV Water Quality and Hydrology Group; Edition 2002.01; 01 September 2003.

Alluvial Well Locations; Los Alamos National Laboratory, Waste and Environmental Services Division; Locus EIM database pull; 2017

Paved Road Arcs; Los Alamos National Laboratory, FWO Site Support Services, Planning, Locating and Mapping Section; 06 January 2004; as published 29 November 2010.

Grade Control Structure and Cascade Pool; Los Alamos National Laboratory; ER-ES Engineering Services; As published, project 14-0015; 2017.

Structures; Los Alamos National Laboratory, FWO Site Support Services, Planning, Locating and Mapping Section; 06 January 2004; as published 29 November 2010.

Former Los Alamos County Landfill; Los Alamos National Laboratory; ER-ES Engineering Services; As published, project 14-0015; 2017.

Canyon Reaches; Los Alamos National Laboratory, ENV Environmental Remediation and Surveillance Program, ER2002-0592; 1:24,000 Scale Data; Unknown publication date.

Technical Area Boundaries; Los Alamos National Laboratory, Site Planning & Project Initiation Group, Infrastructure Planning Office; September 2007; as published 13 August 2010.

Orthophotography, Los Alamos National Laboratory Site, 2014; Los Alamos National Laboratory, Site Planning and Project Initiation Group, Space and Site Management Office; 2014.

Contours, 20 and 5-ft intervals; As generated from 2014 LiDAR elevation data; Los Alamos National Laboratory, ER-ES; As published, project 14-0015; 2017.

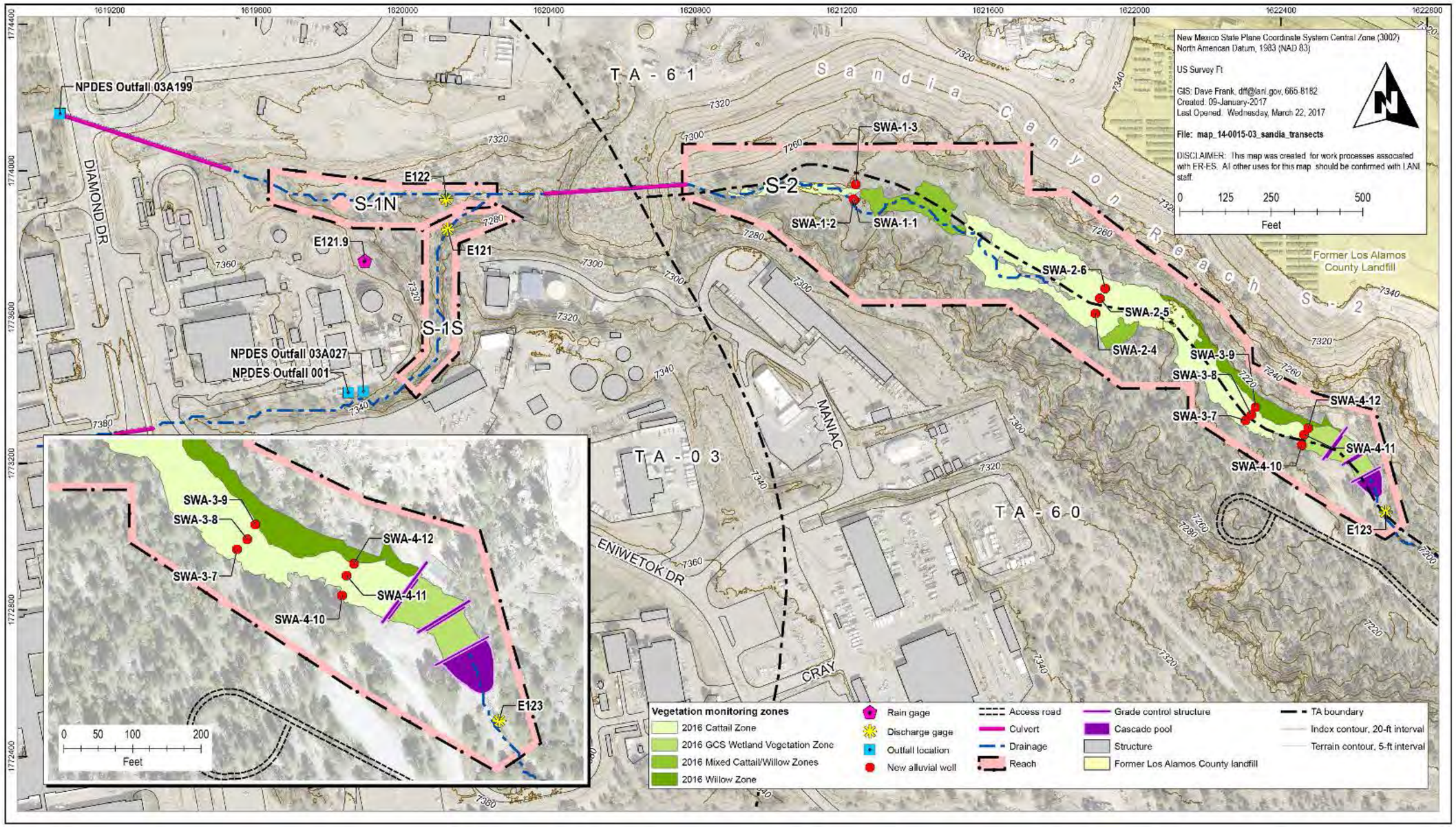

Figure 1.0-1 **Locations of the Sandia GCS (headcut was located at the upper most sheet pile at the terminus of the wetland), NPDES outfalls, precipitation gage E121.9, alluvial wells, surface and storm water gaging stations, former Los Alamos County landfill, surrounding TAs, and reaches S-1N, S-1S, and S-2; the vegetation monitoring zones outline the wetland proper**

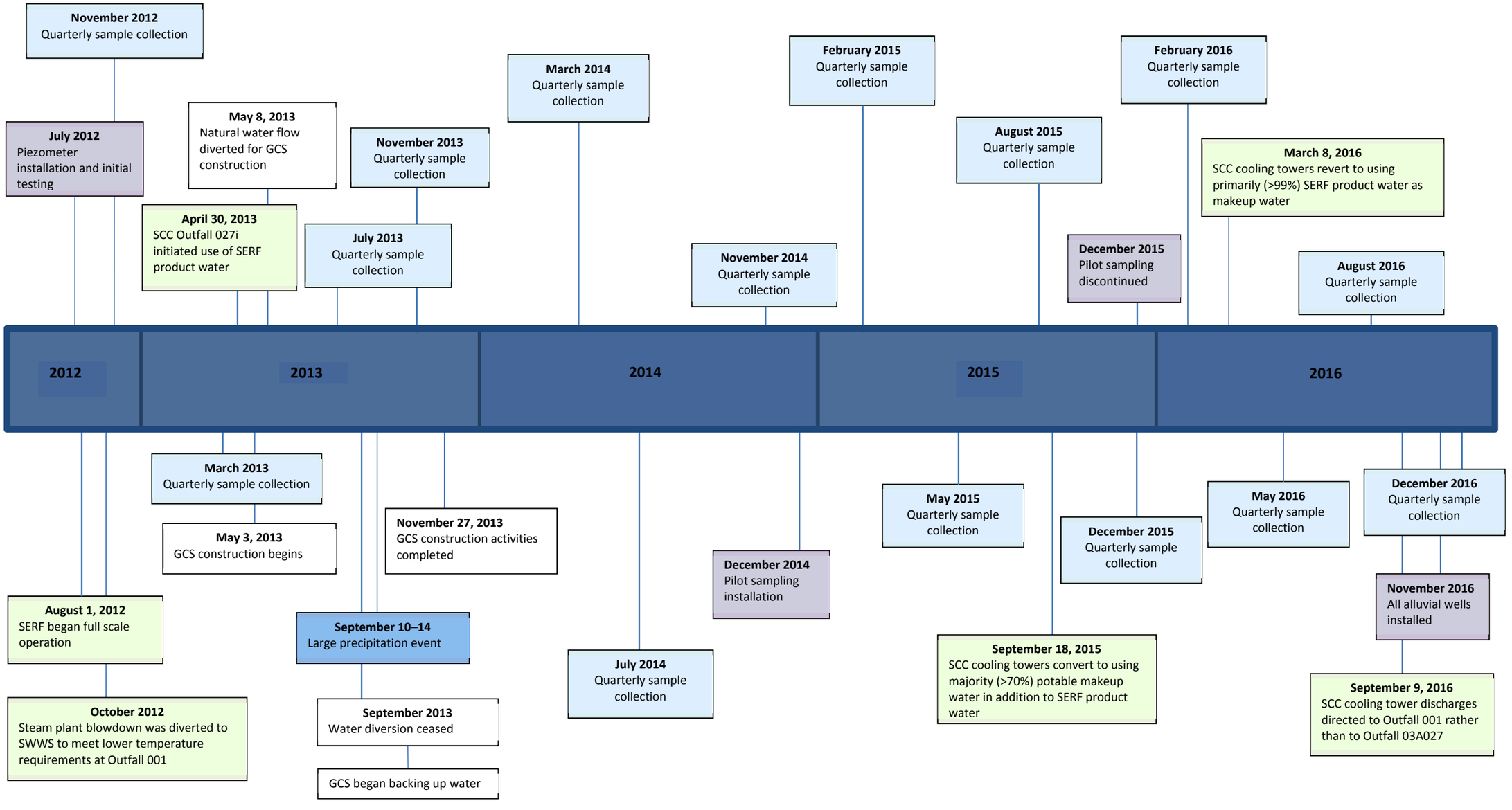

Figure 1.2-1 Sandia Canyon wetland timeline. Types of events are grouped by color.

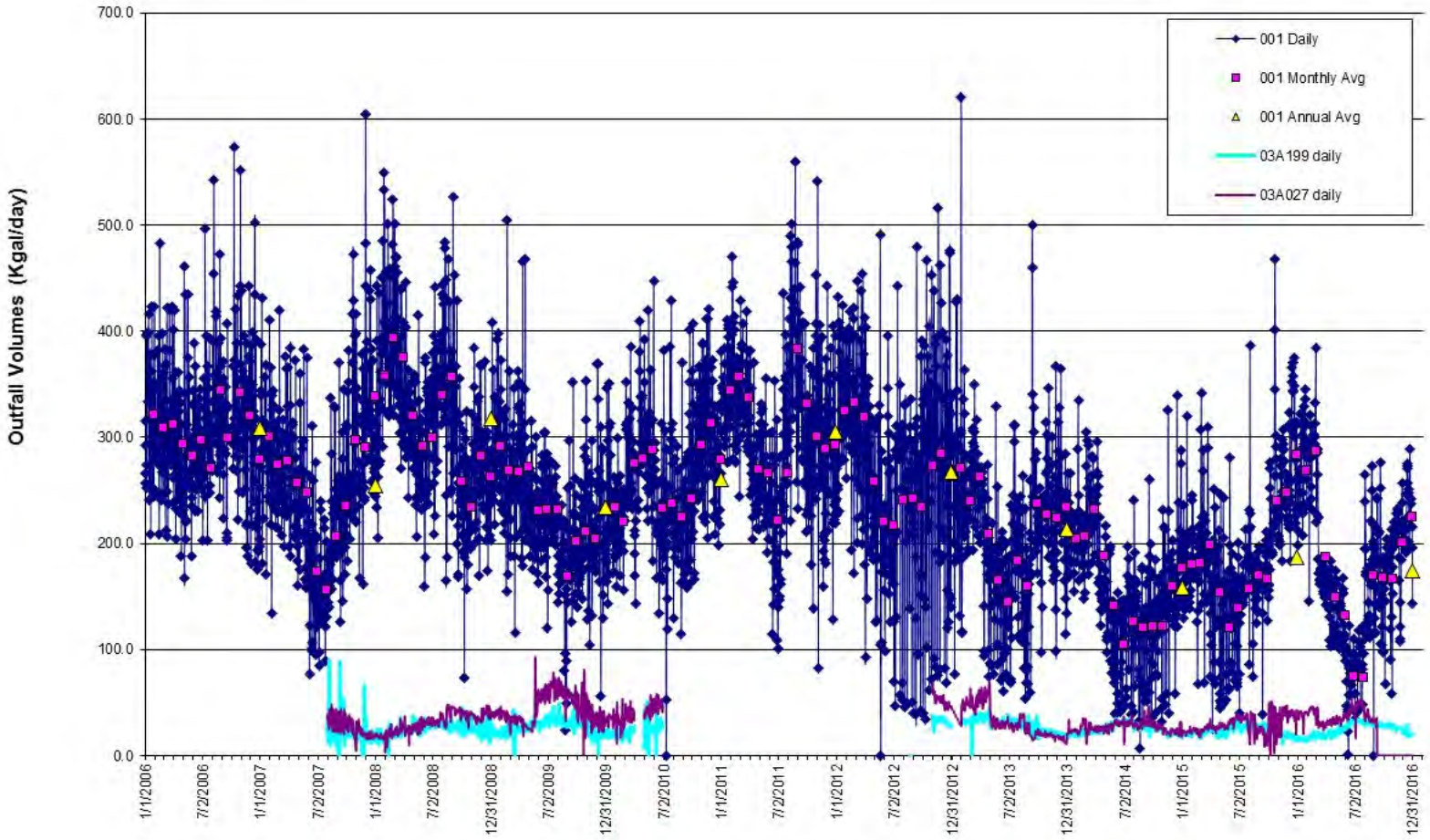

Figure 1.4-1 **Daily, monthly average, and yearly average effluent release volumes (expressed as Kgal./d) for Outfall 001 from 2006 to December 2016, and daily effluent releases for Outfalls 03A027 and 03A199 from August 2007 to January 2010 and from November 2012 to December 2016**

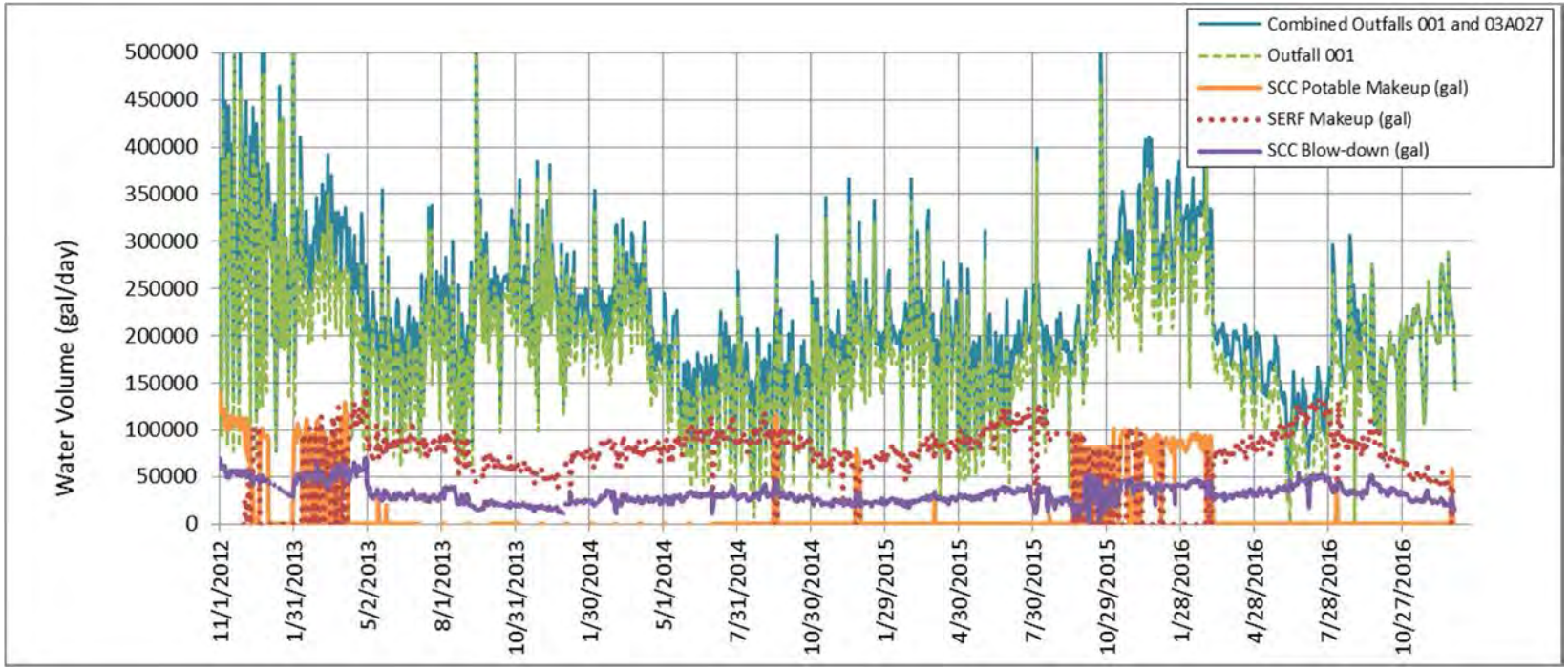

Figure 1.4-2 **Daily water volumes (gpd) from November 2012 to December 2016 for effluent released from combined Outfalls 001 and 03A027 and Outfall 001 only. Also included are effluent (blowdown) volumes from the SCC cooling towers and makeup water sources (potable or SERF-blended water) used at the SCC cooling towers. The SCC cooling tower blowdown was released to Outfall 03A027 until September 8, 2016; since September 9, 2016, the blowdown has been released to Outfall 001.**

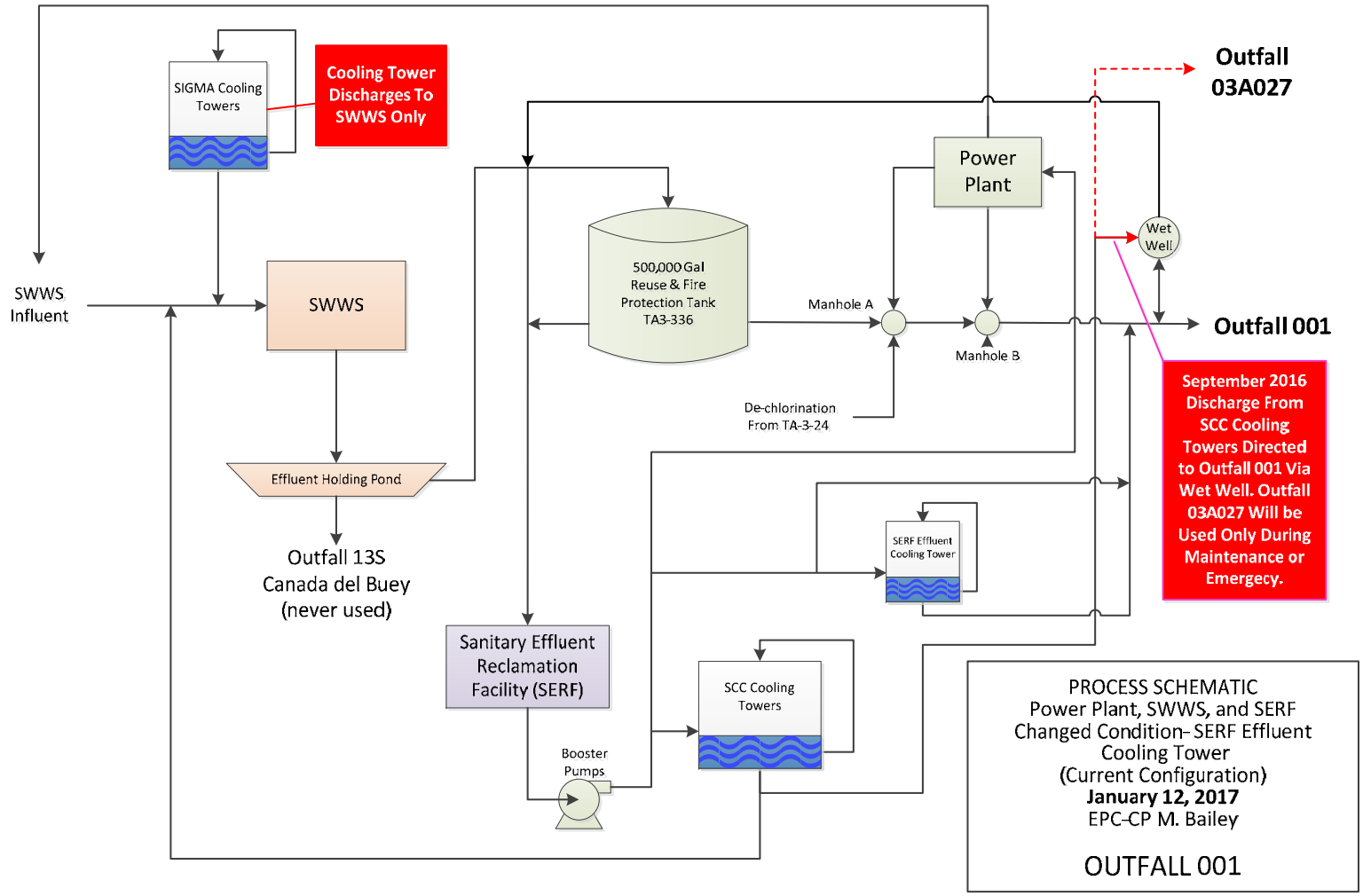

Figure 1.4-3 Updated process schematic for the power plant, SWWS, and SERF connections to Outfall 001 (current configuration)

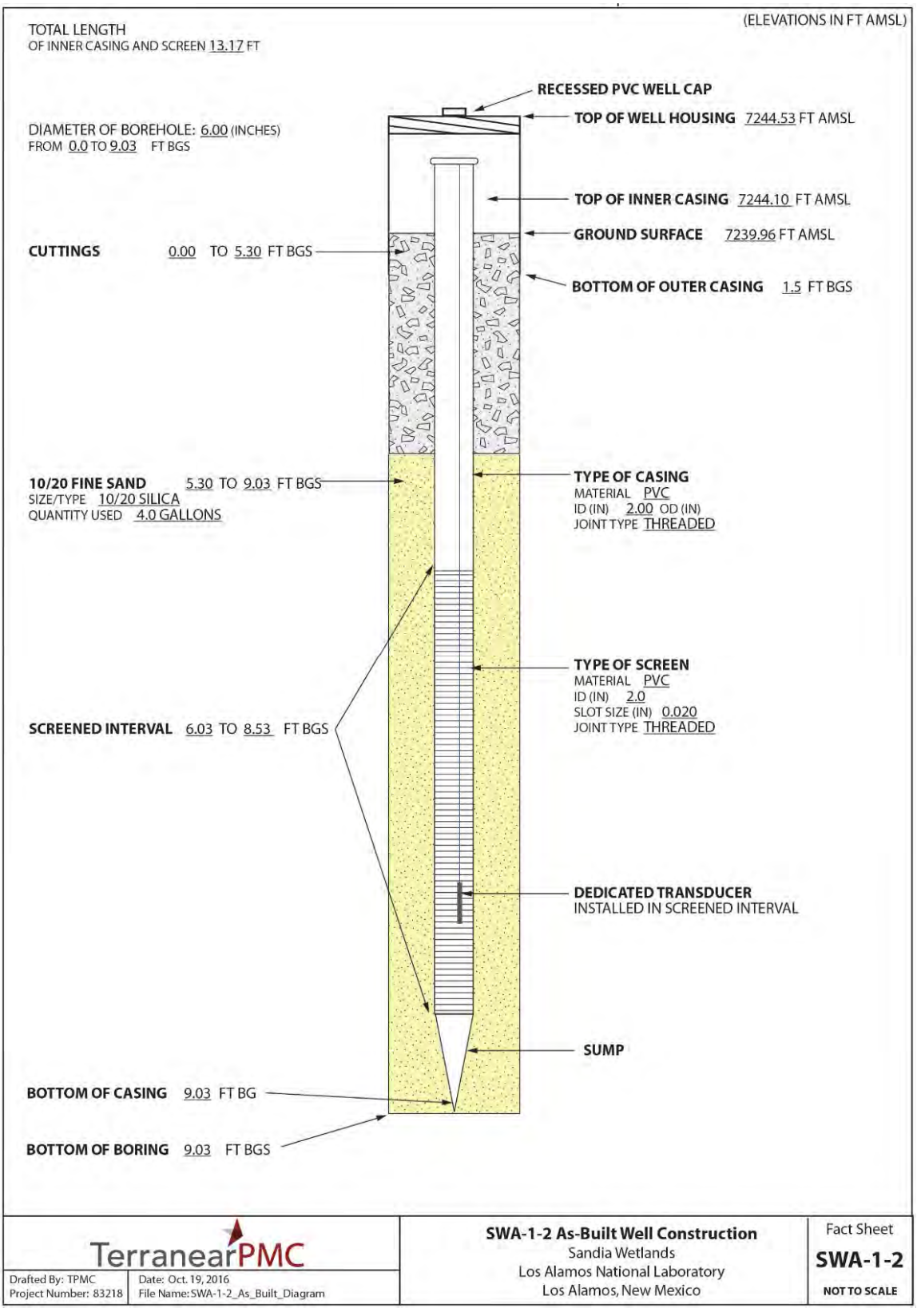

Figure 1.5.1 Example of the alluvial well completion diagram

Figure 2.2-1 Sora nest with nine eggs (left) and the adult Sora (right) between SWA-2-5 and SWA-2-6

Table 1.5-1
Completion Data for Alluvial Piezometers and Collocated Alluvial Wells

Piezometers													
	SCPZ-1	SCPZ-2	SCPZ-3	SCPZ-4	SCPZ-5	SCPZ-6	SCPZ-7	SCPZ-8	SCPZ-9	SCPZ-10	SCPZ-11(A)	SCPZ-11(B)	SCPZ-12
Total length (ft)	20.5	11.4	8.3	8.3	8.3	8.3	8.3	11.4	8.3	8.3	8.3	8.3	8.3
Stick up (ft)	4.36	3.26	3.19	3.16	2.64	3.18	4.32	4.78	3.35	4.01	3.8	4.48	3.77
Top of screen (ft bgs)	13.8	6.0	3	3	3	3	1.6	5.3	3	3	3	1	3
Total depth (ft bgs)	16.2	8.3	5.4	5.4	5.4	5.4	4.0	7.6	5.4	5.4	5.4	5.4	5.4
Alluvial Wells													
	SWA-1-1	SWA-1-2	SWA-1-3	SWA-2-4	SWA-2-5	SWA-2-6	SWA-3-7	SWA-3-8	SWA-3-9	SWA-4-10		SWA-4-11	SWA-4-12
Ground elevation (ft amsl*)	7239.9	7240.0	7239.2	7223.3	7223.0	7222.9	7212.7	7213.1	7212.9	7209.6		7210.8	7210.5
Total length (ft)	18.33	13.17	9.37	9.00	8.96	8.22	6.84	10.68	8.22	8.44		7.93	8.19
Stick up (ft)	2.33	4.14	3.02	3.00	2.96	2.1	3.24	2.88	3.02	3.94		1.93	2.2
Top of screen (ft bgs)	13.0	6.03	3.0	3.0	3.0	3.12	0.6	4.8	2.2	2.5		3	2.99
Bottom of screen (ft bgs)	15.5	8.53	5.5	5.5	5.5	5.62	3.1	7.3	4.7	5		5.5	5.49
Total depth (ft bgs)	16.0	9.03	6.0	6.0	6.0	6.12	3.6	7.8	5.2	5.5		6	5.99

Note: Alluvial wells shown below collocated piezometer.
*amsl = Above mean sea level.

Table 1.5-2
Schema Crosswalk: Past Piezometers and Current Alluvial Wells

Piezometer	To	Alluvial Well	Date of Alluvial Well Installation
SCPZ-1	→	SWA-1-1	8/19/2016
SCPZ-2	→	SWA-1 / SWA-1-2*	12/18/2014
SCPZ-3	→	SWA-1-3	7/21/2016
SCPZ-4	→	SWA-2-4	7/20/2016
SCPZ-5	→	SWA-2-5	7/20/2016
SCPZ-6	→	SWA-2 / SWA-2-6*	12/16/2014
SCPZ-7	→	SWA-3-7	4/27/2016
SCPZ-8	→	SWA-3 / SWA-3-8*	12/16/2014
SCPZ-9	→	SWA-3-9	4/28/2016
SCPZ-10	→	SWA-4-10	4/27/2016
SCPZ-11B	→	SWA-4-11	7/19/2016
SCPZ-12	→	SWA-4 / SWA-4-12*	12/15/2014

* SWA-1, SWA-2, SWA-3, and SWA-4 were pilot wells installed in December 2016; SWA-1-2, SWA-2-6, SWA-3-8, SWA-4-12 are the same wells relabeled in 2015.

Table 1.5-3
Alluvial Groundwater Sampling and Analysis
Plan for 2016 Sandia Wetland Stabilization Monitoring

Suite	Frequency	Comment
EES Metals[a] (filtered)	Quarterly	Includes redox-sensitive metals Fe, Mn, Cr, As. Samples filtered at 0.45 µm.
EES Anions[b] (filtered)	Quarterly	Includes redox-sensitive anions, sulfate and nitrate; nitrate is a wetland vegetation nutrient
Sulfide (unfiltered)	Quarterly	Redox indicator (reduction of sulfate)
Alkalinity/pH (unfiltered)	Quarterly	Organic matter degradation
Ammonia (unfiltered)	Quarterly	Indicator of organic matter degradation; wetland vegetation nutrient
DOC[c] (filtered)	Annually	Organic matter degradation (collected in August 2016)
Fe(II) (filtered)	Quarterly	Indicator of Fe(III) reducing to Fe(II); Collected in May, August and November 2016
As(III) (filtered	Quarterly	Indicator of As(V) reducing to As(III); Collected in February, May, August and November 2016
Cr(VI) (unfiltered)	Quarterly	Indicator of Cr(III) oxidizing to Cr(VI); Dropped microfiltration of metals and replaced with quarterly analysis of Cr(VI) after February 2015 sample event.

[a] EES metals refers to metals analyses conducted at the Laboratory's Earth and Environmental Sciences (EES) analytical laboratory and consists of the following suite: Ag, Al, As, B, Ba, Be, Cd, Co, Cr, Cs, Cu, Fe, K, Li, Mg, Mn, Na, Ni, Pb, Rb, Se, Si, Sr, Ti, Tl, U, V, Zn, Hg, Mo, Sb, Sn, Th.

[b] EES anions refers to anion analyses conducted at the Laboratory's EES analytical laboratory and consists of the following suite: Br, F, Cl, NO_2, NO_3, PO_4, SO_4, $C_2O_4H_2$ (oxalic acid).

[c] DOC = Dissolved organic carbon.

Table 1.5-4
ISCO Bottle Configurations and Analytical Suites Calendar Year 2016 Storm Water Sampling Plan

Bottle No.	Storm/Delay 0-1×4@1min/Delay 40-2×4@1min			Storm/Delay 0-6×1@5min/Delay 30-18×1@20min	
	Sample Collection Time (min)	Sandia E121, E122, E123		Sandia E121, E122, E123	
		Bottle Type	Analytical Suite	Sample Collection Time (min)	Analytical Suite 24 Bottle ISCO 1-L Poly Wedge
1	Max + 10	1-L Glass	PCB congener (UF[a])	Trigger + 0	SSC
2	Max + 10	1-L Glass	PAH (UF)	Trigger + 5	SSC
3	Max + 10	1-L Glass	SVOC[b] (UF)	Trigger + 10	SSC, Particle size
4	Max + 10	1-L Poly	TAL[c] metals (F[d]/UF)	Trigger + 15	Cl + SO4
5	Max + 50	1-L Glass	PCB congener (UF)	Trigger + 20	SSC
6	Max + 50	1-L Glass	PAH (UF)	Trigger + 25	DOC
7	Max + 50	1-L Glass	SVOC (UF)	Trigger + 30	Alk+pH
8	Max + 50	1-L Poly	TAL metals (F/UF)	Trigger + 50	SSC, Particle size
9	Max + 90	1-L Glass	PCB congener (UF)	Trigger + 70	SSC
10	Max + 90	1-L Glass	PAH (UF)	Trigger + 90	SSC, Particle size
11	Max + 90	1-L Glass	SVOC (UF)	Trigger + 110	SSC
12	Max + 90	1-L Poly	TAL metals (F/UF)	Trigger + 130	SSC
13	—[e]	—	—	Trigger + 150	SSC
14	—	—	—	Trigger + 170	SSC
15	—	—	—	Trigger + 190	SSC
16	—	—	—	Trigger + 210	SSC
17	—	—	—	Trigger + 230	SSC
18	—	—	—	Trigger + 250	SSC
19	—	—	—	Trigger + 270	SSC
20	—	—	—	Trigger + 290	SSC
21	—	—	—	Trigger + 310	SSC
22	—	—	—	Trigger + 330	SSC
23	—	—	—	Trigger + 350	SSC
24	—	—	—	Trigger + 370	SSC

Notes: E121 = Sandia right fork at Pwr Plant, E122 = Sandia left fork at Asph Plant or South fork of Sandia at E122, E123 = Sandia below Wetlands.

[a] UF = Unfiltered.

[b] SVOC = Semivolatile organic compound.

[c] TAL = Target analyte list (EPA).

[d] F = Filtered.

[e] — = None.

Table 2.1-1
Summary of Analytical Samples Collected during Calendar Year 2016

Location	MY2016Q2 Feb 2016	MY2016Q3 May–Jun 2015	MY2016Q4 Aug 2015	MY2017Q1 Nov 16
Transect 1 (West)				
SCPZ-1	Y[a]	Y	Y	NS
SWA-1-1 (installed Oct 16)	NS[b]	NS	NS	Y
SWA-1\SWA-1-2 (installed Dec 14)	Y	Y	Y	Y
SCPZ-3	Y	Y	NS	NS
SWA-1-3 (installed Jul 16)	NS	NS	Y	Y
Transect 2				
SCPZ-4	Y	Y	NS	NS
SWA-2-4 (installed Jul 16)	NS	NS	Y	Y
SCPZ-5	Y	NS	NS	NS
SWA-2-5 (installed Jul 16)	NS	AI[c]	Y	Y
SWA-2 \ SWA-2-6 (installed Dec 14)	Y	AI	Y	Y
Transect 3				
SCPZ-7	Y	NS	NS	NS
SWA-3-7 (installed Apr 16)	NS	Y	Y	Y
SWA-3 \ SWA-3-8 (installed Dec 14)	Y	Y	Y	Y
SCPZ-9	Y	NS	NS	NS
SWA-3-9 (installed Apr 16)	NS	Y	Y	Y
Transect 4 (East)				
SCPZ-10	Y	NS	NS	NS
SWA-4-10 (installed Apr 16)	NS	Y	Y	Y
SCPZ-11B	Y	Y	NS	NS
SWA-4-11 (installed Jul 16)	NS	NS	Y	Y
SWA-4 / SWA-4-12 (installed Dec 14)	Y	Y	Y	Y
Surface water at base flow				
Sandia Right Fork at Power Plant (E121)	Y	Y	Y	Y
South fork of Sandia at E122 (E122)	Y	Y	Y	F[d]
Sandia below Wetlands (E123)	Y	Y	Y	Y

Note: Adjacently located piezometers and alluvial wells that were sampled are shaded the same color.

[a] Y = Full analytical suite collected.

[b] NS= Not sampled: piezometers removed or well not installed yet.

[c] AI = Area inaccessible: protected species in sampling area.

[d] F = Base flow frozen: sample not collected.

Table 2.1-2
Field Data for Alluvial Locations and Surface Water Stations 2016 Sampling Events

Location Name	Date	Dissolved Oxygen (mg/L)	Oxidation-Reduction Potential (mV)	pH	Specific Conductance (µS/cm)	Temperature (°C)	Turbidity (NTU[a])
Surface Water Stations							
E121	2/19/2016	8.48	NR[b]	8.16	488	13.68	1.6
E121	5/25/2016	7.19	NR	8.44	433	19.65	0.2
E121	8/8/2016	7.04	NR	7.94	294.2	21.01	5.39
E121	12/1/2016	8.68	NR	8.8	510	11.1	0.2
E122	2/19/2016	10.6	NR	8.54	730	13.1	4.4
E122	5/25/2016	8.34	NR	8.64	528	19.52	2.2
E122	8/9/2016	6.97	NR	8.37	575	19.95	3.61
E123	2/19/2016	10.02	NR	7.78	567	5.8	0.8
E123	8/8/2016	6.26	NR	7.97	161.2	18.26	37.81
E123	12/1/2016	10.23	NR	7.92	429.6	0.1	0.1
Piezometers and Alluvial Wells							
SCPZ-1	2/24/2016	0.92	-9.7	7	532	11.87	9.1
SCPZ-1	5/25/2016	1.13	-141.5	7.17	674	12.68	0.3
SCPZ-1	8/11/2016	0.86	-147.1	7.25	589.6	17.7	2.5
SWA-1-1	12/1/2016	0.62	-136.7	6.91	571	13.5	0.9
SWA-1	2/24/2016	0.88	4.1	7.09	822	7.43	2.9
SWA-1	5/25/2016	1.89	-118.3	7.6	473	13.46	7.6
SWA-1-2	8/11/2016	0.72	-144.5	7.49	589.1	19.3	6.2
SWA-1-2	11/29/2016	0.58	-120.4	7.39	431.6	11.3	9.2
SCPZ-3	2/24/2016	2.46	55	7.01	429	5.9	0.2
SCPZ-3	5/25/2016	3.63	-120.9	7.12	506	15.08	5.1
SWA-1-3	8/11/2016	0.71	-129.3	6.97	589.6	19.2	5.9
SWA-1-3	11/29/2016	0.87	-100.7	6.63	455.6	7.6	11.2
SCPZ-4	2/25/2016	0.94	29.2	6.92	768	5.63	1.3
SCPZ-4	5/23/2016	1.81	-16.6	4.96	501	10.71	1.6
SWA-2-4	8/11/2016	0.23	-181.5	6.83	503	16.1	1.1
SWA-2-4	11/30/2016	0.76	-70.1	6.79	458.3	8.4	2.5
SCPZ-5	2/26/2016	2.19	-140.1	7.09	514	11.67	3
SWA-2-5	8/11/2016	0.14	-181.3	7.19	584	10.8	31.8
SWA-2-5	11/30/2016	0.4	-149.7	7.01	537	10.9	6.8
SWA-2	2/26/2016	1.12	-137.9	7.07	509	8.74	141.4
SWA-2-6	8/11/2016	0.44	-163.3	7.22	588.8	12	3.9
SWA-2-6	11/30/2016	0.52	-144.7	6.94	541	9	15.6

Table 2.1-2 (continued)

Location Name	Date	Dissolved Oxygen (mg/L)	Oxidation-Reduction Potential (mV)	pH	Specific Conductance (µS/cm)	Temperature (°C)	Turbidity (NTU[a])
Piezometers and Alluvial Wells							
SCPZ-7	2/22/2016	3.89	-57.8	6.32	693	5.28	683.5
SWA-3-7	5/25/2016	0.57	-75.2	6.4	712	9.26	65.6
SWA-3-7	8/10/2016	0.8	-23.5	6.34	674.2	15.84	3.52
SWA-3-7	11/30/2016	1.05	-61.2	6.13	758	4.7	2.9
SWA-3	2/22/2016	1.05	-101.9	6.68	578	4.94	1.1
SWA-3-8	5/25/2016	0.4	-106.8	6.78	594	7.26	3.3
SWA-3-8	8/10/2016	0.51	-94.9	6.85	620.9	12.25	1.93
SWA-3-8	11/30/2016	0.73	-112.8	6.82	597	7.6	9.5
SCPZ-9	2/22/2016	3.89	-85.7	6.77	577	5.45	14
SWA-3-9	5/25/2016	0.36	-69.2	5.66	644	7.19	3.4
SWA-3-9	8/10/2016	0.63	-107.1	6.9	613.2	12.96	0.49
SWA-3-9	11/30/2016	0.9	-126.6	6.87	584	6.9	4.6
SCPZ-10	2/22/2016	3.93	422.2	6.05	790	7.16	25.1
SWA-4-10	5/24/2016	1.58	-14.1	4.93	997	11.34	13
SWA-4-10	8/10/2016	1.2	-116.9	6.42	902.2	16.62	11.9
SWA-4-10	11/29/2016	1.21	-11.9	6.27	613	8.4	9.2
SCPZ-11(B)	2/22/2016	4.77	664.1	5.87	500	2.9	38.4
SCPZ-11(B)	5/24/2016	2.48	-120.1	7.11	468	15.95	11.4
SWA-4-11	8/10/2016	0.69	-139	6.63	474.9	17.79	2.87
SWA-4-11	11/29/2016	0.75	-105.3	6.58	410	5.7	19.7
SWA-4	2/25/2016	1.24	44.5	5.72	761	3.8	5.6
SWA-4	5/24/2016	0.67	-79.7	6.18	502	12.07	1.6
SWA-4-12	8/10/2016	0.55	-124	6.49	626.4	16.65	1.45
SWA-4-12	11/29/2016	0.91	-74.8	6.5	488.2	6.9	4.9

[a] NTU = Nephelometric turbidity unit.

[b] NR = Not recorded.

Table 2.1-3
Precipitation, Storm Water Peak Discharge, and Samples Collected at Gaging Stations E121, E122, and E123 for Each Sample-Triggering Storm Event in 2016

Storm Event Date	RG121.9 Total Precipitation (in.)	E121 Peak Discharge (cfs)	E122 Peak Discharge (cfs)	E123 Peak Discharge (cfs)
7/1/2016	0.3	22 S[a]	1.9 BT[b]	9.1 BT
7/15/2016	0.3	22 S	1.9 BT	11 CT[c]
7/31/2016	1.0	47 S	2.0 BT	46 S
8/3/2016	0.6	37 S	1.6 BT	13 S
8/4/2016	0.3	15 NS[d]	1.1 BT	9.0 BT
8/8/2016	0.4	44 NS	1.3 BT	12 CT
8/19/2016	0.2	10 CT	1.0 BT	9.3 BT
8/27/2016	0.9	51 S	2.3 BT	28 S
9/6/2016	0.5	40 S	2.6 BT	18 S
10/3/2016	0.1	1.7 BT	0.4 S[e]	2.2 BT
10/8/2016	0.1	1.5 BT	0.3 S[e]	1.8 BT
11/4/2016 (earlier)	0.7	2.3 BT	0.6 S[e]	2.5 BT
11/4/2016 (later)	0.7	8.4 S	2.0 NS	12 CT
11/5–11/6/2016	0.7	17 NS	2.0 NS	15 S

[a] S = Sample was collected. These discharge levels are shaded in green to emphasize those events for which discharge exceeded the trip level and samples were collected.

[b] BT = Below 10-cfs trip level, no sample collected.

[c] CT = Close to 10-cfs trip level, no sample collected. Stage measurement sensors can have inaccuracies ±2 cfs.

[d] NS = No sample collected, but discharge was above 10-cfs trip level. These discharge levels are shaded in yellow to highlight those events where discharge was above the trip level, but no samples were collected.

[e] Trip level at E122 was lowered to collect samples because only one sample has been collected at E122 since the GCS was constructed.

Table 3.7-1
Proposed Sampling and Preservation Requirements for Sandia Wetland

Analytical Suite	Analytical Code	Analytical Method	Sample Type[a]	Frequency	Filtered[b]	Preservation	Field Storage	Holding Time	Ideal Volume	Minimum Volume	Comment
Alluvial Wells											
EES Cr(VI) Speciation	WSP-EES-Cr(VI)	EPA:218.7	W	Qtrly	N	$NH_4OH/(NH_4)_2SO_4$ (liquid) buffer 1 mL to 100 mL of sample	<4°C	14 d	100 mL	100 mL	—[c]
EES As(III) Speciation	WSP-EES6-As(III)	EPA:200.8	W	Qtrly	Y	Nitric acid AFTER filtration through cartridge	<4°C	6 mo	60 mL	20 mL	Use As speciation kit
EES Fe(II) and Fe(III) Speciation	WSP-EES-Fe Speciation	SM:3500	W	Qtrly	Y	15 mL tube preloaded with 5-mL Ferrozine reagent	<4°C	2 wk	5 mL	5 mL	Use Fe speciation kit; keep out of sun
Target Analyte List (TAL) Metals	WSP-All Metals	EPA:200.7 EPA:200.8 EPA:245.2 SM:A2340B	W	Qtrly	Y	Nitric acid	<4°C	6 mo 28 d for Hg	1 L	300 mL	—
Anions	Anions	EPA:300	W	Qtrly	Y	None	<4°C	28 d	125 mL	50 mL	—
Ammonium, Nitrate-Nitrite, Phosphorus	NH3+PO4+ NO3NO2	EPA:350.1 EPA:353.2 EPA:365.4	W	Qtrly	Y	H_2SO_4	<4°C	28 d	250 mL	100 mL	—
Alkalinity/pH	SW-ALK+pH	EPA:150.1 EPA:310.1	W	Qtrly	N	None	<4°C	ASAP	125 mL	125 mL	—
DOC	WSP-DOC	EPA:415.1	W	Annually	Y	None	<4°C	28 d	40 mL	40 mL	Collect during August sample event
EES Sulfide	WSP-EES6-SULFIDE	EPA:376.2	W	Qtrly	N	Sulfide buffer pH 12	<4°C	24 h	15 mL	15 mL	—
Surface Water Base Flow at Gages E121, E122, and E123											
PCB Congeners	SW-PCB-1668A-MDL	EPA:1668A	WS	Qtrly	N	None	<4°C	1 yr	3 L	1L	Amber glass with Teflon lid (EPA Method 1668A)
PAHs	SW-625_SIM	EPA:625	WS	Qtrly	N	$Na_2O_3S_2$ if residual Cl is present	<4°C	7 d	3 L	1 L	—
TAL Metals	WSP-All Metals	EPA:200.7 EPA:200.8 EPA:245.2 SM:A2340B	WS	Qtrly	Y	Nitric acid	<4°C	6 mo 28 d for Hg	1 L	300 mL	Filtered metals
TAL Metals	WSP-All Metals	EPA:200.7 EPA:200.8 EPA:245.2 SM:A2340B	WS	Qtrly	N	Nitric acid	<4°C	6 mo 28 d for Hg	1 L	300 mL	Nonfiltered metals

Table 3.7-1 (continued)

Surface Water Base Flow at Gages E121, E122, and E123											
Analytical Suite	Analytical Code	Analytical Method	Sample Type	Frequency[a]	Filtered[b]	Preservation	Field Storage	Holding Time	Ideal Volume	Minimum Volume	Comment
EES Cr(VI) Speciation	WSP-EES-Cr(IV)	EPA:218.7	WS	Qtrly	N	$NH_4OH/(NH_4)_2SO_4$ (liquid) buffer 1 mL to 100 mL of sample	<4°C	14 d	100 mL	100 mL	—
EES Sulfide	WSP-EES6-Sulfide	EPA:376.2	WS	Qtrly	N	Sulfide buffer pH 12	<4°C	24 h	15 mL	15 mL	—
Anions	Anions	EPA:300	WS	Qtrly	Y	None	<4°C	28 d	125 mL	50 mL	—
Ammonium, Nitrate-Nitrite, Phosphorus	NH_3+PO_4+ NO_3NO_2	EPA:350.1 EPA:353.2 EPA:365.4	WS	Qtrly	Y	H_2SO_4	<4°C	28 d	250 mL	100 mL	—
Alkalinity/pH	SW-ALK+pH	EPA:150.1 EPA:310.1	WS	Qtrly	N	None	<4°C	As soon as possible	125 mL	125 mL	—
SSC	SW-SSC	ASTM:D3977-97	WS	Qtrly	N	None	No requirement	NA[d]	1 L	1 L	—
DOC	WSP- DOC	EPA:415.1	WS	Annually	Y	None	<4°C	28 d	40 mL	40 mL	August sample event

[a] W = Alluvial water samples; WS = base flow water samples.

[b] Y= Filtered using 0.45-µm pore size; N= nonfiltered.

[c] — = None.

[d] NA = not applicable.

Appendix A

Acronyms and Abbreviations,
Metric Conversion Table, and Data Qualifier Definitions

A-1.0 ACRONYMS AND ABBREVIATIONS

3-D	three-dimensional
amsl	above mean sea level
bgs	below ground surface
cfs	cubic foot per second
DC	direct current
DEM	digital elevation model
DGPS	differentially corrected global positioning system
DOC	dissolved organic carbon
DoD	DEM of difference
EES	Earth and Environmental Sciences (Laboratory group)
EPA	Environmental Protection Agency (U.S.)
ESH	Environment, Safety, and Health
F	filtered
FAC	facultative plant
FACU	facultative upland plant
FACW	facultative wetland plant
FIS	fuzzy inference system
GCD	geomorphic change detection
GCS	grade-control structure
gpd	gallons per day
gpm	gallons per minute
GPS	global positioning system
HH-OO	human health-organism only
IR	investigation report
LANL	Los Alamos National Laboratory
LiDAR	light detection and ranging
MCL	maximum contaminant level
MDL	method detection limit
MF	membership function
MY	monitoring year
NI	no indicator status
NMED	New Mexico Environment Department

NMWQCC	New Mexico Water Quality Control Commission
NPDES	National Pollutant Discharge Elimination System
NTU	nephelometric turbidity unit
OBL	obligate wetland plant
PAH	polycyclic aromatic hydrocarbon
PCB	polychlorinated biphenyl
PVC	polyvinyl chloride
RMSE	root-mean-square error
RPD	relative percent difference
SCC	Strategic Computing Complex
SERF	Sanitary Effluent Reclamation Facility
SOM	solid organic matter
SSC	suspended sediment concentration
SVOC	semivolatile organic compound
SWMU	solid waste management unit
SWQC	surface water–quality criteria
SWWS	Sanitary Waste Water System
TA	technical area
TAL	target analyte list
TDS	total dissolved solids
TKN	total Kjeldahl nitrogen
TOC	total organic compound
TSS	total suspended sediment
UF	unfiltered
UPL	upland plant
VE	vertical exaggeration

A-2.0 METRIC CONVERSION TABLE

Multiply SI (Metric) Unit	by	To Obtain U.S. Customary Unit
kilometers (km)	0.622	miles (mi)
kilometers (km)	3281	feet (ft)
meters (m)	3.281	feet (ft)
meters (m)	39.37	inches (in.)
centimeters (cm)	0.03281	feet (ft)
centimeters (cm)	0.394	inches (in.)
millimeters (mm)	0.0394	inches (in.)
micrometers or microns (µm)	0.0000394	inches (in.)
square kilometers (km^2)	0.3861	square miles (mi^2)
hectares (ha)	2.5	acres
square meters (m^2)	10.764	square feet (ft^2)
cubic meters (m^3)	35.31	cubic feet (ft^3)
kilograms (kg)	2.2046	pounds (lb)
grams (g)	0.0353	ounces (oz)
grams per cubic centimeter (g/cm^3)	62.422	pounds per cubic foot (lb/ft^3)
milligrams per kilogram (mg/kg)	1	parts per million (ppm)
micrograms per gram (µg/g)	1	parts per million (ppm)
liters (L)	0.26	gallons (gal.)
milligrams per liter (mg/L)	1	parts per million (ppm)
degrees Celsius (°C)	9/5 + 32	degrees Fahrenheit (°F)

A-3.0 DATA QUALIFIER DEFINITIONS

Data Qualifier	Definition
U	The analyte was analyzed for but not detected.
J	The analyte was positively identified, and the associated numerical value is estimated to be more uncertain than would normally be expected for that analysis.
J+	The analyte was positively identified, and the result is likely to be biased high.
J-	The analyte was positively identified, and the result is likely to be biased low.
UJ	The analyte was not positively identified in the sample, and the associated value is an estimate of the sample-specific detection or quantitation limit.
R	The data are rejected as a result of major problems with quality assurance/quality control (QA/QC) parameters.

Appendix B

2015–2016 Geomorphic Changes in Sandia Canyon Reach S-2

CONTENTS

Figures

Tables

Attachments

B-1.0 INTRODUCTION

This report evaluates geomorphic changes that occurred in 2015 and 2016 in reach S-2, above the Sandia Canyon grade-control structure (GCS) within the Los Alamos National Laboratory (LANL or the Laboratory). Geomorphic change was evaluated using aerial light detection and ranging (LiDAR) data collected in June 2014 before the 2014 northern New Mexico monsoon season and in November 2015, and October 2016 after the northern New Mexico monsoon seasons. This report compares LiDAR surveys encompassing accumulated change over two monsoon seasons: 2015 and 2016. Additionally, post-monsoon ground-based surveys of the thalweg, channel banks, plunge pool, and alluvial fans are presented, representing change over the 2016 monsoon season. Figure B-1.0-1 shows site locations discussed in this appendix. Attachment B-1 contains photographs of areas of erosion and deposition in Sandia Canyon reach S-2.

B-2.0 HYDROLOGIC EVENTS DURING THE 2016 MONSOON SEASON

Fourteen 2016 sample-triggering storm events are presented in Table B-2.0-1. The two largest runoff-producing events in 2016 at stream gages E121 and E122 (upstream of reach S-2) and E123 (downstream of the wetland and GCS, Figure B-1.0-1) occurred following heavy rains that fell on the Pajarito Plateau, Los Alamos townsite, and the Sierra de los Valles on July 31 and August 27, 2016 (section 2.0 in the report presents additional details). Twenty-four-hour rainfall totals measured by the E121.9 rain gage in Sandia Canyon (upstream of reach S-2) on July 31 and August 27 were 1.0 in. and 0.9 in., respectively. The maximum measured discharge at each gage occurred on August 27 at E121 (51 cubic feet per second [cfs]); on September 6 at E122 (2.6 cfs); and on July 31 at E123 (46 cfs, Table B-2.0-1). The 2016 peak discharge was similar to the previous year's discharge at all gage stations and near (E121) or well below (E122 and E123) the mean for the 10-yr period of record (Table B-2.0-2).

B-3.0 AERIAL AND GROUND-BASED SURVEY METHODS OF THE SANDIA WETLAND

LiDAR surveying is a process by which laser beams are directed at a surface and the resulting reflections are used to calculate the distance to the surface. Aerial LiDAR surveying involves mounting the LiDAR equipment in an airplane and flying a known course while directing lasers at the ground surface to generate a three-dimensional (3-D) point cloud of the surface. Aerial LiDAR surveys were flown over the Laboratory in June 2014 before the annual New Mexico monsoon season, in November 2015, and in October 2016 following the New Mexico monsoon season.

Two known disadvantages of the aerial LiDAR compared with the ground-based transect surveys are that (1) dense vegetation can result in misclassification of some LiDAR points as "ground" that should actually be "nonground," resulting in elevation discrepancies, and (2) water is opaque to LiDAR, so sediment erosion/deposition features that are submerged at the time of the survey are not captured. As a result, the ground survey of the thalweg and plunge pool is critical to capture these submerged sediment changes, particularly in areas of dense vegetation.

B-3.1 Aerial LiDAR Survey Data Collection and Processing

Aerial LiDAR data were collected in 2014 for the entire Laboratory and in 2015 and 2016 with a specific focus on canyon-bottom areas of interest, including Sandia Canyon reach S-2. The LiDAR surveys were accompanied by ground-based global positioning system (GPS) surveys of check points, which were used to further constrain the spatial position and accuracy of the LiDAR point cloud. The LiDAR points were then classified as ground points or nonground points (e.g., vegetation) using appropriate software and filtering methodologies, along with manual editing.

B-3.2 Digital Elevation Model Generation and Geomorphic Change Estimation Procedures

When surveys of an area are repeated, elevation changes will be observed. Actual elevation changes can occur from a variety of geomorphic processes (herein defined strictly as sediment erosion or deposition) as well as other nongeomorphic processes. However, apparent elevation changes can also occur as a result of error inherent to the survey data acquisition and classification methods. In this appendix, nongeomorphic processes encompass vegetation changes, burrowing by animals, road blading or slope stabilization efforts, differences in soil saturation or compaction between measurements, and any other processes not directly related to downslope sediment transport.

Reasonable error assessment of the survey methods yields thresholds above which all detected change is assumed to be actual elevation change of the surface—although this elevation change includes those caused by geomorphic and nongeomorphic processes. However, some small-magnitude actual elevation changes (e.g., deposition of a very thin sediment layer) may also fall below the threshold and thus be discounted from change detection calculations, even if physically observed. Above the threshold, field observations and vegetation maps can provide context to distinguish between geomorphic (sediment erosion or deposition) and nongeomorphic elevation changes (e.g., elevation increase from cattail mound development between surveys).

The points designated as “ground” in the aerial LiDAR data set from each survey year were used to generate digital elevation models (DEMs) that were clipped to the geographic boundaries of the study reach before further analysis. The 2015 DEM was then subtracted from the 2016 DEM to create a DEM of Difference (DoD) using the geomorphic change detection (GCD) plug-in for ArcGIS (Wheaton et al. 2010, 601298). Positive values of the DoD indicate deposition between the 2015 and 2016 surveys, and negative values indicate erosion over the same time period. A range of red pixels designate annual negative change (erosion); similarly a range of blue pixels identify annual positive change (deposition) at a given pixel. Grid resolution for the DEMs and DoD output are both 1 × 1 ft. Areas of DoD predicted geomorphic change were confirmed with field observations. Maximum detected positive and negative changes in elevation are specifically evaluated in the field to confirm whether they are the result of geomorphic or nongeomorphic processes.

In previous iterations of this report, error was estimated by simply comparing agreement of the predicted surface (the DEM) with a more accurate measurement of the actual surface (GPS-surveyed points). Computing the root-mean-square error (RMSE) of the difference in measured (GPS) versus predicted DEM values supplies an estimate of the error in values of the modeled surface. This value was previously applied in a uniform fashion to the calculations. However, not all surfaces will reflect this uniformly applied error value and may in fact have less, or more, inherent error. This is in part from the limitations of aerial LiDAR to accurately capture data on a variable surface.

Precision of the data collected during an aerial LiDAR survey is affected by variation of the ground surface which, in turn, influences the accuracy of any surface interpolated from a point cloud of elevation values. Primary among these attributes are slope, point density, and surface roughness.

- Slope: Measurements collected on an inclined surface have a higher inherent error than those collected on a relatively level one. In general, the greater the incline, the less accurate the elevation (Z) values derived by LiDAR will be, resulting in a higher uncertainty.
- Point Density: Only ground-classified points are used to build the DEM; therefore, it is expected that high point density will yield a more realistic representation of ground surface. When points are sparse, the modelling of ground surface is less realistic. An indicator of low-point density in a DEM surface is the presence of irregular polygons on the DEM surface. The presence of these

polygons indicates that the low-point density resulted in an over-interpolated model of the actual surface. Low point density areas have inherently higher error because their representation of actual ground surface is less accurate.

- Surface Roughness: Measurement of local differences in elevation between individual neighboring points gives an assessment of surface roughness. A surface with high local variability in Z values is less well represented by LiDAR than a smooth, continuous surface. Therefore, a high degree of surface roughness results in an inherent decrease of elevation accuracy. In general, smooth surfaces are represented well and rougher, or more variable surfaces, less well.

To compute the spatially variable error of a DEM surface, raster models of the previously mentioned point cloud derived attributes are required. A set of rules defining a fuzzy inference system (FIS) determines the amount of error applied to any given pixel involved in a DoD calculation. The FIS is structured with a set of membership functions (MFs) that categorize individual point cloud attributes into discrete groups based on the distribution of values the surface represents (e.g., slope is grouped into low [0–20], medium [20–45], and high [45–90]). After the surfaces have been analyzed and grouped, the rules that determine the pixel's individual value of error are processed. Below is an example of how a level, relatively well-represented surface would be assigned an appropriate low error value:

Properties of the pixel: 1. Slope = 03 degrees 2. Point Density = 2.0 pts/ft^2 3. Roughness = 0.3 ft

MF grouping: 1. Low slope 2. High point density 3. Low roughness

After the group into which the pixel falls is assessed, the pixel is assigned an appropriate error value based on the rule sets. The first rule set states that if the slope is low, then it should fall in the low error MF. The second rule states that if point density is high, then the pixel should again be assigned a low error. The third rule states that if roughness is low, a low error is applied. The range of values applied to the best-case scenario error is assigned to the low error MF, and therefore, this pixel would be represented by an error value within that best-case scenario range.

For the purposes of calculating sediment deposition, all elevation changes above the threshold defined in this appendix are assumed to represent sediment erosion or deposition. This assumption necessarily excluded small, but real, changes that occurred below the threshold and included elevation changes that occurred above the threshold because of nongeomorphic processes. Nongeomorphic elevation changes are often represented by a mottling on the DoD of both positive and negative detects in areas of steep terrain and dense tree canopy that do not represent actual geomorphic changes. These detects can often be attributed to misclassification of point cloud data.

B-3.3 Ground-based Survey of Thalweg, Channel Bank, Plunge Pool, and Alluvial Fans

The 2016 post-monsoon channel thalweg, channel banks, plunge pool, and downslope extent of the southern alluvial fan were surveyed using ground-based methods to document change. These features were surveyed using real-time kinematic differentially corrected GPS surveying equipment rather than LiDAR because of interference caused by dense vegetation and standing water in the LiDAR data acquisition. The alluvial fans on the northern edge of the wetland were also monitored via erosion pins during the 2016 monsoon season.

As in 2015, the 2016 longitudinal channel thalweg profile was surveyed for the entire study reach (Figure B-1.0-1). While the thalweg location is challenging to define in some areas (e.g., dense cattail vegetation) of the reach because of channel branching, a best-estimate location was determined for comparison with the 2015 data. For each thalweg survey point, the distance along the thalweg was calculated as the straight-line distance between the plunge pool and that point. This distance is referred to

as the “canyon distance.” Data tables of thalweg survey points and distances and ArcGIS shape files are included in Attachment B-2. The 2016 thalweg gradient and map-view location were compared with 2015 data for all reach sections where data were available.

Channel banks were surveyed in 2015 to document baseline conditions. Channel bank surveys were repeated in 2016 at the western end of reach S-2. In the central portion of the reach, where flow is diffused and there is standing water, there are no prominent channel banks. Data tables of channel survey points and ArcGIS shape files are included in Attachment B-2.

The plunge pool perimeter was surveyed at the lateral extent of the ponded area. The 2016 results are compared with the 2015 survey of the same area. Data tables of plunge pool survey points and ArcGIS shape files are included in Attachment B-2.

Three alluvial fan deposits on the north side and one on the south side of the reach S-2 were monitored in 2016. Alluvial fans on the northern edge of the wetland were monitored via erosion pins during the 2016 monsoon season. The lateral extent of the southern alluvial fan deposit was surveyed for comparison with the 2015 survey in the same area.

B-4.0 RESULTS AND DISCUSSION

Two complications arise when interpreting the LiDAR DEM for reach-scale calculations. First, some LiDAR points were likely misclassified as ground points that do not represent the actual ground surface. In areas of dense vegetation (i.e., cattails or dense tree canopy), the improper assignment of vegetation points as ground-classified points is more likely than in areas of sparse vegetation cover. When these “ground” (actually vegetation) points are used as part of the 3-D point cloud to generate the ground-surface DEM, they contribute to elevation-change anomalies. The DoD calculations will therefore identify some elevation changes that are in fact from changes in vegetation height rather than changes in the ground surface caused by sediment erosion or deposition.

The second complication arises because the edges of the reach are characterized by cliffs, steep embankments, and large boulders. These steep areas are not captured particularly well within the LiDAR data sets, and therefore, more extensive elevation may be apparent in the DoD even if no real topographic change has occurred at the canyon edges. Related to this complication is the fact that DoD detects on the steeply inclined and dense canopied edges of the study area generally show a positive “change” on the north side of the canyon and a negative “change” on the south side of the canyon. It is generally not understood how this result is achieved, but it is thought that the flight pattern of the plane collecting the LiDAR data may be responsible.

B-4.1 LiDAR DEM Error Assessment

It is important to recognize that certain areas are better represented by LiDAR data than others as presented in Table 3.2-1. The best-represented surfaces fall within the low-error grouping and are more likely to show lower-amplitude geomorphic change. However, it is also important to recognize that some areas, no matter how well defined within the FIS, will still result in a detected change. These detects are typically the result of either misclassified or poorly classified vegetation (e.g., primarily tree canopy) or of features (e.g., boulders) that were not previously classified as ground.

An estimate of the 95% confidence interval (2 standard deviations) of the RMSE for the DEM elevations was obtained by comparing a subset of aerial LiDAR-derived point elevations with ground-surveyed GPS point elevations (vertical accuracy for these GPS points is better than 0.1 ft). Data tables of surveyed checkpoints are included in Attachment B-2. Vegetation within mapped cattail zones of the Sandia

wetland is so dense that accurate assessment of ground surface by LiDAR methods has proven difficult. Comparison of check points to the DEM within the vegetated areas yields higher error values than check points collected on open, less vegetated surfaces. In general, error values for the DEM surface within the cattail vegetated zones are much higher than those outside of the zone. Therefore, a uniform error surface was computed to account for the high degree of error in the DEM within the cattail vegetated areas. A separate, spatially variable error value was generated for the area outside of the vegetated zone within reach S-2. For the DEM representing 2016, the 2 standard deviation RMSE values are ±3.65 ft and ±0.42 ft for within and outside of the heavily vegetated area respectively (Figure B-4.1-1). For the DEM representing 2015, the 2 standard deviation RMSE values are ±7.72 ft and ±0.38 ft for within and outside the heavily vegetated area, respectively (Figure B-4.1-2). The uniform RMSE error values of any pixel outside of the cattail area are then further subject to the FIS model to compute the spatially variable error of the DEM surface.

For the DoD calculations, standard error propagation in addition/subtraction operations yields a 2 standard deviation RMSE value of ±8.53 ft within the cattail vegetated zone and ±0.57 ft outside the vegetation zone. The propagated error values provide the threshold above/below which any values in the DoD are assumed to represent actual elevation change. The variable error surfaces were calibrated to the 95% confidence interval RMSE values calculated for respective monsoon year DEMs and propagated through the DoD calculations. Net changes for the study reach are then calculated by summing the DoD over areas of erosion/deposition above or below the error threshold. As discussed above, DoD values above the threshold are assumed to represent geomorphic erosion or deposition. These identified elevation changes were field-verified using visual inspection methods to determine if geomophoric change occurred. Areas of confirmed geomorphic change are identified and documented in this appendix. Regardless of field verification confirmation, all DoD values were used to calculate net volume changes as discussed below.

B-4.2 LiDAR DEM Characterization

The DoD was calculated using the 2015 and 2016 LiDAR-based DEMs for the study reach; elevation change values larger than the spatially variable thresholds are shown in Figure B-4.2-1. The net volume change for the study reach over the 2015 and 2016 monsoon seasons is 921 ft^3 ± 1057 ft^3 (28 m^3 ± 30 m^3). The net positive value of the DEM comparison indicates deposition has occurred at the reach scale between the 2015 and 2016 LiDAR surveys.

Erosion (negative elevation change) contributed to a calculated 438 ft^3 ± 372 ft^3 (12 m^3 ± 11 m^3) of volume difference since 2015. Deposition (positive elevation change) contributed to a calculated 1429 ft^3 ± 989 ft^3 (40 m^3 ± 28 m^3) of volume difference since 2015. Areas within the densely vegetated cattail zone did not show geomorphic change because error propagation thresholds out all possible changes. DoD results are apparent in areas defined by (1) boulder-covered surfaces, specifically the steep north side of the canyon and southeastern end of the reach; (2) in areas where vegetation height changed either because of new vegetation growth or changes in vegetation height from the LiDAR flight occurring at a slightly different time of year in 2015 and 2016; and (3) where lower water levels expose surfaces that were previously submerged. These detection areas were field-verified and determined to be not attributable to geomorphic processes.

Maximum detected erosion of −0.72 ft was identified by the DoD and verified by field observation to be attributed to geomorphic processes within the small side channel located on the south side of reach S-2 (Figure B-4.2-1 and Photos B1-1 and B1-2, Attachment B1). The incision and remobilization of previously deposited sediment on the fan is likely responsible for the eastward advancement of the fan along the edge of the wetland boundary.

Maximum detected deposition of +1.62 ft was identified by the DoD and verified by field observation to be attributed to geomorphic processes within the channel below gage station E123 (Figure B-4.2-1, inset map B). An additional area of smaller magnitude of deposition of +0.62 ft was also detected and confirmed within this channel (Figure B-4.2-1, inset map B). Moderately sized (3–5 ft long) swaths of bank material slumping into the main channel (Photo B1-3, Attachment B1) are evident and responsible for the positive elevation changes within the channel. Alternatively, the positive elevation change may be from a lower water level in 2016 than in 2015, resulting in the exposed banks being surveyed in 2016 and contributing to a DEM that more accurately represents the channel surface. This change in water level is plausible because bank collapse may have occurred in 2015. Nongeomorphic elevation change detections in this area are attributed to either a more accurate classification of ground points in 2016 versus 2015 or lower water level in the channel during the 2016 survey than during the 2015 survey.

The smaller amount of deposition of +0.62 ft was identified by the DoD and verified by field observation in a side channel fed by a storm drain located in the parking area due south of the plunge pool (Figure B-4.2-1 and Photo B1-4, Attachment B1). Field observations confirm the contribution of sandy sediment from this side channel depositing into the main channel during 2016.

The maximum detected elevation change of +5.5 ft was identified by the DoD and verified by field observation to be attributed to nongeomorphic processes at the far eastern part of reach S-2 (Figure B-4.2-1 and Photo B1-5, Attachment B1). This detection is the result of a point misclassification where the area was more poorly defined in 2015 than in 2016, resulting in a DEM in 2016 that more accurately represented the surface and when subtracted from the 2015 DEM resulted in a positive elevation change that cannot be attributed to geomorphic processes.

B-4.3 Thalweg Characterization

In 2016, as in 2015, the channel thalweg profile was surveyed as continuous from the plunge pool to gage station E123. In the central cattail zone, the thalweg remains challenging to identify as a distinct channel because of diffuse flow and channel branching within the active wetland. Where a main channel was not distinct, the thalweg of the most established channel branch was surveyed. Channel thalweg surveys in 2013 and 2014 did not include this central portion of the reach. Therefore, the channel thalweg survey of the central portion of the reach from 2015 constitutes a baseline for comparison with the 2016 and future surveys.

The channel thalweg profile (Figure B-4.3-1) compares 2015 and 2016 post-monsoon survey data displayed with a vertical exaggeration (VE) of 7 times. Overall, the 2016 thalweg profile closely matched the 2015 thalweg profile, indicating continued stability of the reach (LANL 2016, 601432). Between 2015 and 2016, the greatest difference in elevation along the thalweg profile is 1.3 ft and is located between sheet pile 2 and sheet pile 3. This difference in elevation is attributed to the movement of the thalweg to the south. There was no observed erosion or incision associated with the shift in thalweg position between sheet pile 2 and sheet pile 3.

Between 2015 and 2016, only minor lateral changes occurred in the thalweg position in the western and eastern ends of the study reach (Figure B-4.2-1). At the western part of reach S-2, the dominant flow of the 2016 thalweg was slightly south of the thalweg position surveyed in 2015. The shift to the south in 2016 could be attributed to the establishment of stable thalweg position in response to the continued vegetation growth, specifically the expansion of the cattail/willow zone to the south near this area (Appendix C).

At the eastern end of the reach, between the nick point and the GCS, the thalweg has shifted south, returning to its 2014 position (LANL 2016, 601432, Figure B-4.1-3). This lateral shift is related to the

elevation shift and is attributed to the response to the continued growth of cattails within the northern part of the GCS area. The nick point has remained stable in profile and map view since 2014 (Figure B-4.1-3; LANL 2016, 601432).

B-4.4 Plunge Pool Characterization

The shape and areal extent of the plunge pool in 2016 were not notably different from 2015 (Figure B-4.4-1). The 2016 perimeter survey shows expansion of less than 1 ft on the western side of the plunge pool, south of the culvert, and the reduction of a small peninsula to the northeast likely caused by the expansion of the western cattail zone (Appendix C). Additionally, comparison of 2015 and 2016 data indicate that a 2-ft expansion of the plunge pool to the south in 2015 (LANL 2016, 601432) has not continued.

B-4.5 Channel Bank Characterization

Stream banks below the plunge pool area show minimal change between surveys (Figures B-4.0-1 and B-4.2-1). Differences between the bank surveys may be attributed to different interpretations of what constituted the most important breaks in slope between surveys and may not reflect significant bank erosion or deposition. This observation is confirmed both in field observations and DoD analysis.

B-4.6 Alluvial Fan Characterization

Measurements recorded during 2016 indicate that the fans on the north side of the wetland (Figures B-4.0-1 and B-4.2-1) did not change significantly (< ±0.03 ft) and that the fans remained relatively stable throughout the year. However, sediments advanced eastward along a side channel that is spatially coincident with the edge of the central cattail zone (Figure B-4.2-1). The fan on the south side of reach S-2 that had previously impacted cattail growth (LANL 2016, 601432) has advanced approximately 3–5 ft farther north into the wetland but has not resulted in the destruction of any cattails. Based on the vegetation perimeter mapping presented in Appendix C, the cattails of the central cattail zone began revegetating the 2015 sand/gravel lobe (see Figure C-1.0-1 in Appendix C). The lobe of sediment on the downstream (easternmost) end of the fan has extended approximately 5 ft past the previous extent mapped in 2015 (Figure B-4.2-1).

B-5.0 CONCLUSIONS AND RECOMMENDATIONS

The 2015 to 2016 DoD analysis produced a net volume change result of 28 m^3 ± 30 m^3, indicating net deposition may have occurred in Sandia Canyon reach S-2. Field observations confirmed that most of the DoD results outside of the heavily vegetated cattail area are not depicting actual geomorphic change but are attributable to inconsistent point cloud classification for bare ground and vegetation in the two LiDAR surveys. Field verification of the changes greater than the spatially variable threshold DoD were conducted, and supplemental surveying has confirmed which of these detected changes are geomorphic. Specifically, a small amount of erosion was detected within the small side channel located on the south side of reach S-2. The incision and remobilization of previously deposited sediment on the fan is likely responsible for the eastward advancement of the fan along the edge of the wetland boundary. Also, deposition was detected within the channel below the GCS and gage station E123 that was likely the result of redistribution of collapsed bank material into the channel. Additionally, aggradation of sandy material was detected in a small side channel due south of the plunge pool. This deposition was likely the result of storm water runoff from a storm drain located in the parking area above the plunge pool. Otherwise, field observation in conjunction with the spatially variable thresholded DoD results indicate that between 2015 and 2016 no significant geomorphic change occurred at the Sandia wetland.

Repeat surveys of the channel thalweg indicate a few minor changes (largely in map-view position) between the 2015 and 2016 surveys and overall suggest thalweg stability over the past 2 yr. GPS surveying indicates that the plunge pool remained similarly stable from 2015 to 2016. Channel bank surveys were conducted at the western part of the study area (the only areas in the reach with prominent channel banks). The channel surveys below the plunge pool area show minimal change between surveys. Based on 2015 GPS surveying and 2016 erosion pin monitoring, the downslope extent of alluvial fan deposits on the northern side of the reach below the former Los Alamos County landfill has remained relatively stable. On the south side of the canyon, a side channel entering reach S-2 has continued to redistribute sandy gravel within the alluvial fan and into the wetland. Unlike in 2015, this advancement has not resulted in any vegetation (cattail) loss, and in fact cattails have revegetated the sand/gravel lobe deposited in 2015.

Future LiDAR surveys should be planned to obtain points at the same density or greater than in the 2016 LiDAR data set. LiDAR point cloud classification efforts will also seek to better distinguish between ground and nonground points, particularly in areas where wetland vegetation exists. Additionally, the installation and monitoring of erosion pins in the side channel south of the plunge pool above reach S-2 is recommend to evaluate the impact and/or contribution of sediment into the expanding cattails at the western part of the reach.

B-6.0 REFERENCES AND MAP DATA SOURCES

B-6.1 References

The following list includes all documents cited in this appendix. Parenthetical information following each reference provides the author(s), publication date, and ER ID or ESH ID. This information is also included in text citations. ER IDs were assigned by the Environmental Programs Directorate's Records Processing Facility (IDs through 599999), and ESH IDs are assigned by the Environment, Safety, and Health (ESH) Directorate (IDs 600000 and above). IDs are used to locate documents in the Laboratory's Electronic Document Management System and, where applicable, in the master reference set.

Copies of the master reference set are maintained at the New Mexico Environment Department Hazardous Waste Bureau and the ESH Directorate. The set was developed to ensure that the administrative authority has all material needed to review this document, and it is updated with every document submitted to the administrative authority. Documents previously submitted to the administrative authority are not included.

LANL (Los Alamos National Laboratory), April 2016. "2015 Sandia Wetland Performance Report," Los Alamos National Laboratory document LA-UR-16-22618, Los Alamos, New Mexico. (LANL 2016, 601432)

Wheaton, J.M., J. Brasington, S.E. Darby, and D.A. Sear, February 2010. "Accounting for Uncertainty in DEMs from Repeat Topographic Surveys: Improved Sediment Budgets," *Earth Surface Processes and Landforms,* Vol. 35, No. 2, pp. 136-156. (Wheaton et al. 2010, 601298)

B-6.2 Map Data Sources

The following list provides data sources for maps included in this appendix.

Gaging stations; Los Alamos National Laboratory, Waste and Environmental Services Division; 1:2,500; March 19, 2011.

LANL area orthophoto; Los Alamos National Laboratory, 2014.

Geomorphic Reach Boundary, Los Alamos National Laboratory, Earth and Environmental Science, GISLab, 2009.

Geomorphology Units; Los Alamos National Laboratory, Earth and Environmental Sciences, GISLab, 2009.

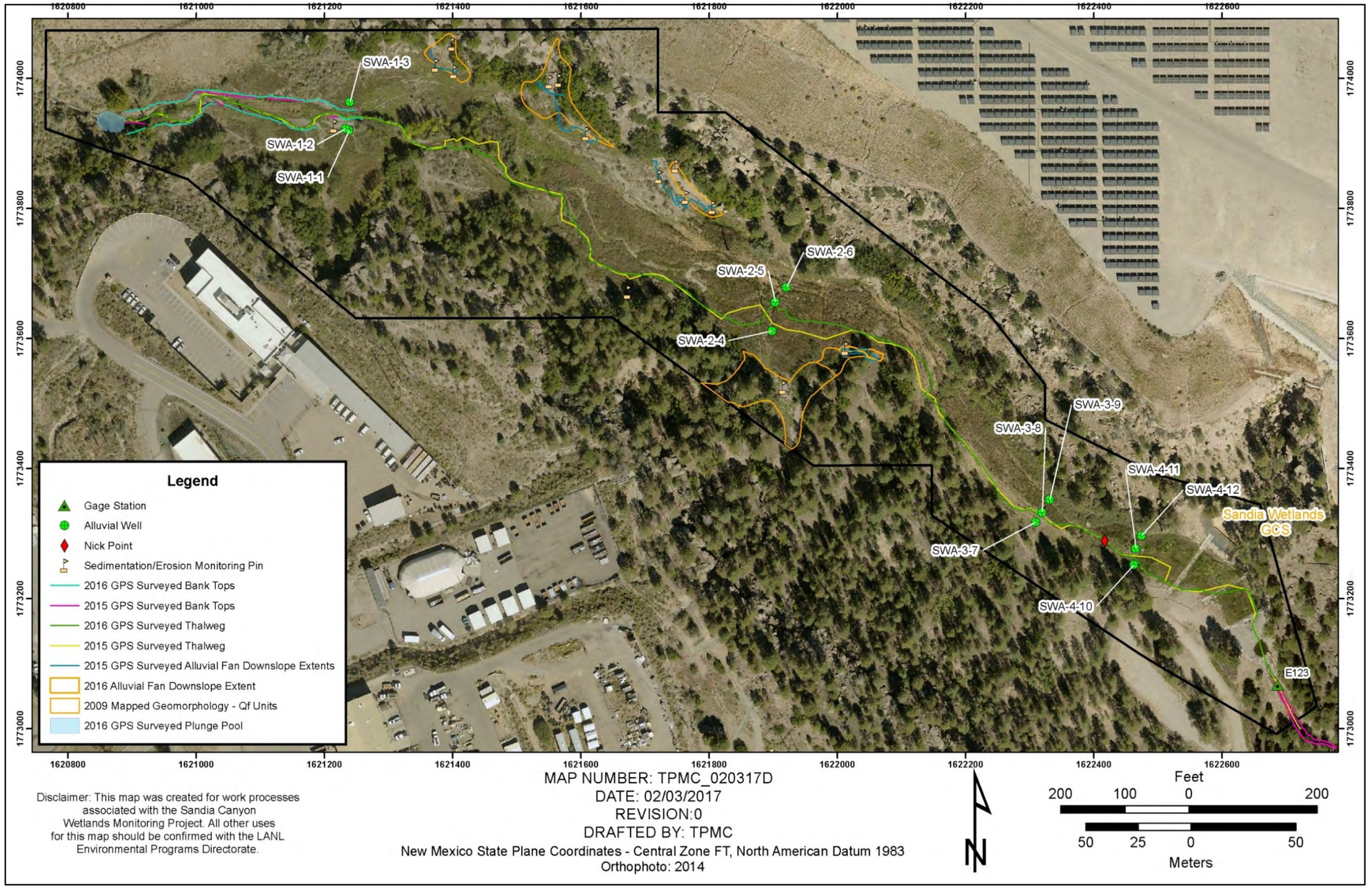

Note: Qf (alluvial fan) consists of relatively young sands, gravel, and cobbles made up of Bandelier Tuff and pumice fragments and quartzite gravels.

Figure B-1.0-1 Sandia Canyon reach S-2 orthophoto with gage station E123, alluvial wells, and survey locations mentioned in report, including channel banks, thalweg, alluvial fans, and the plunge pool

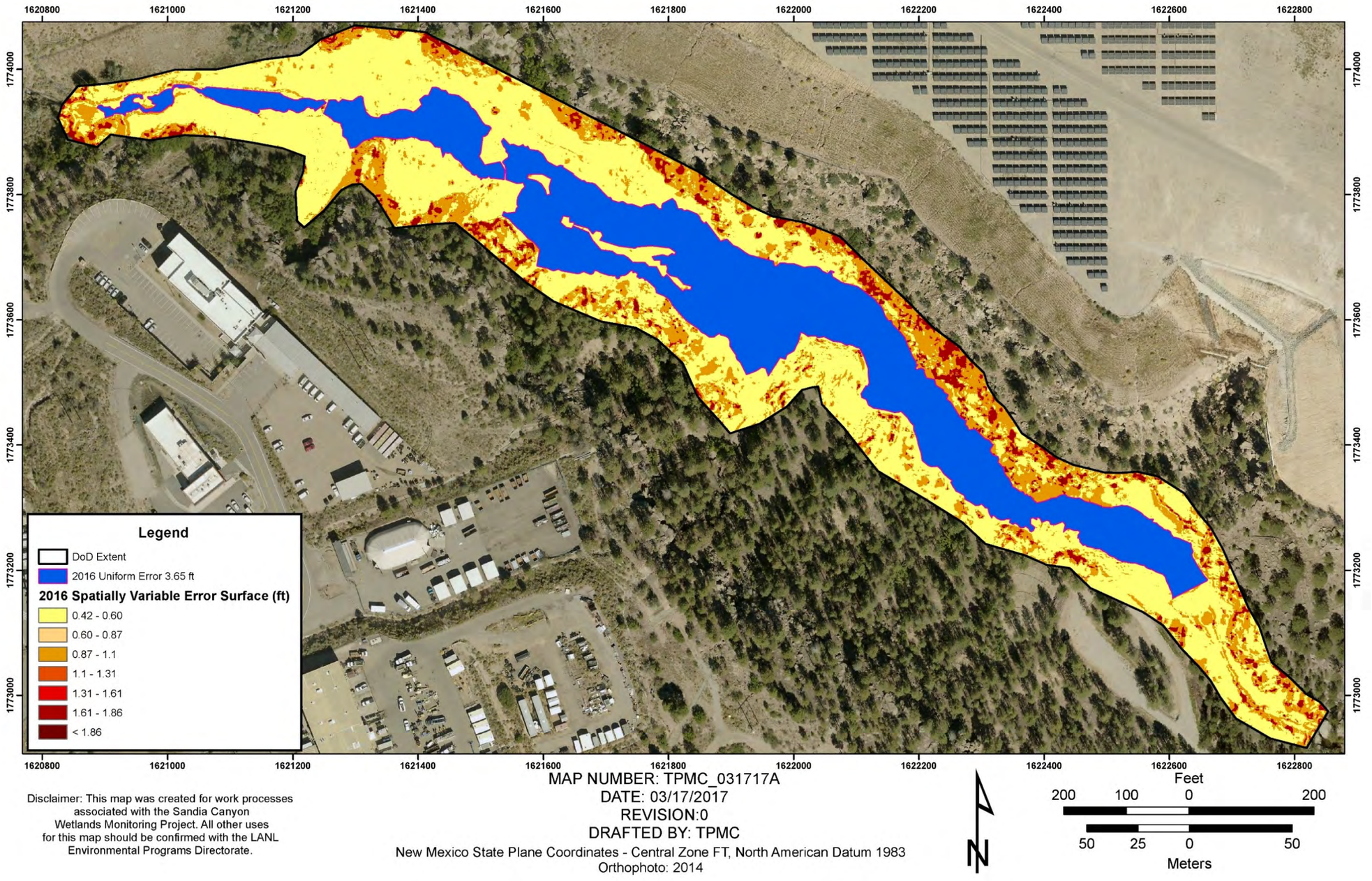

Figure B-4.1-1 Error surface calculated for 2016 Sandia Canyon reach S-2 GCD analysis

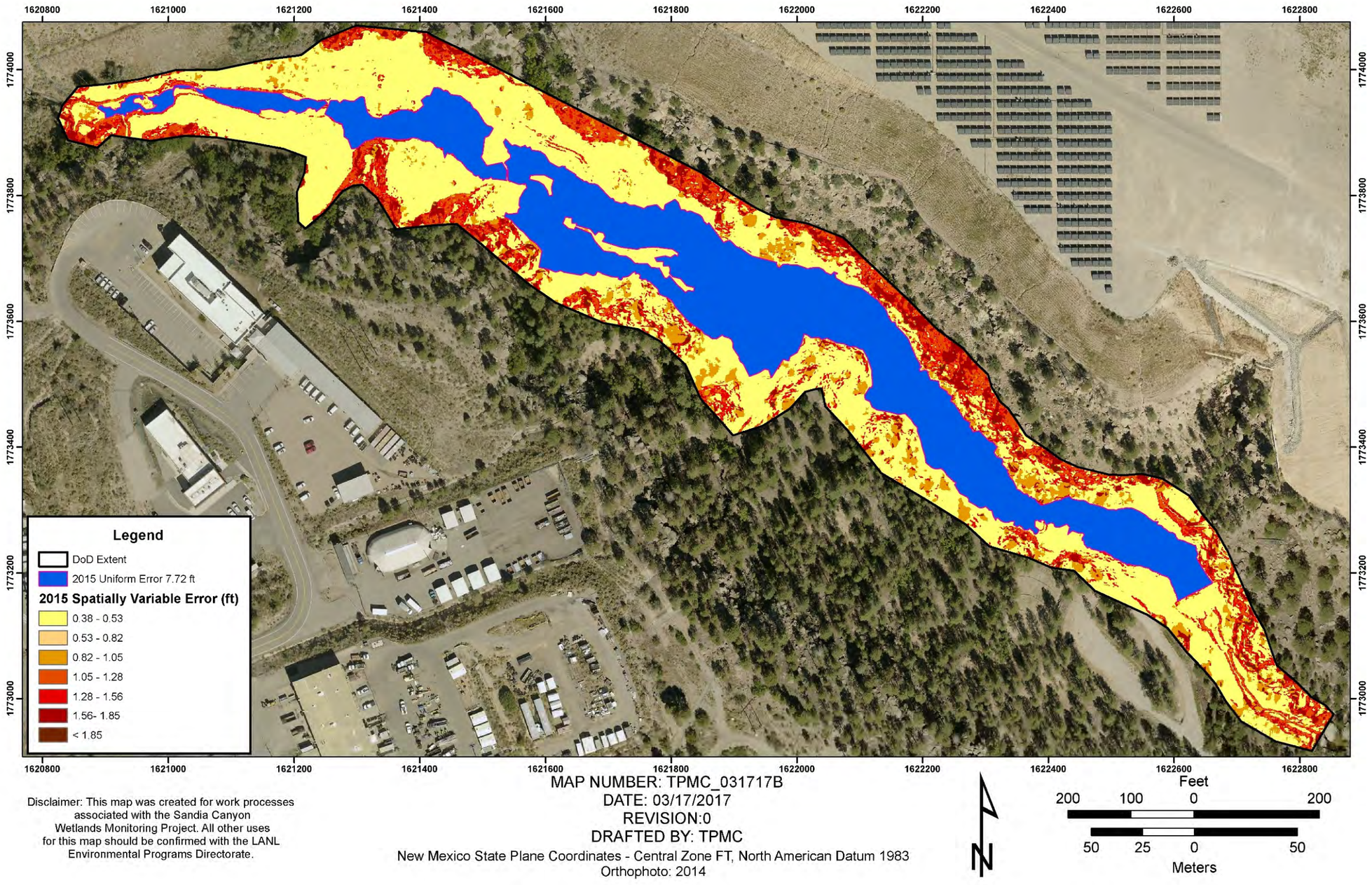

Figure B-4.1-2 Error surface calculated for 2015 Sandia Canyon reach S-2 GCD analysis

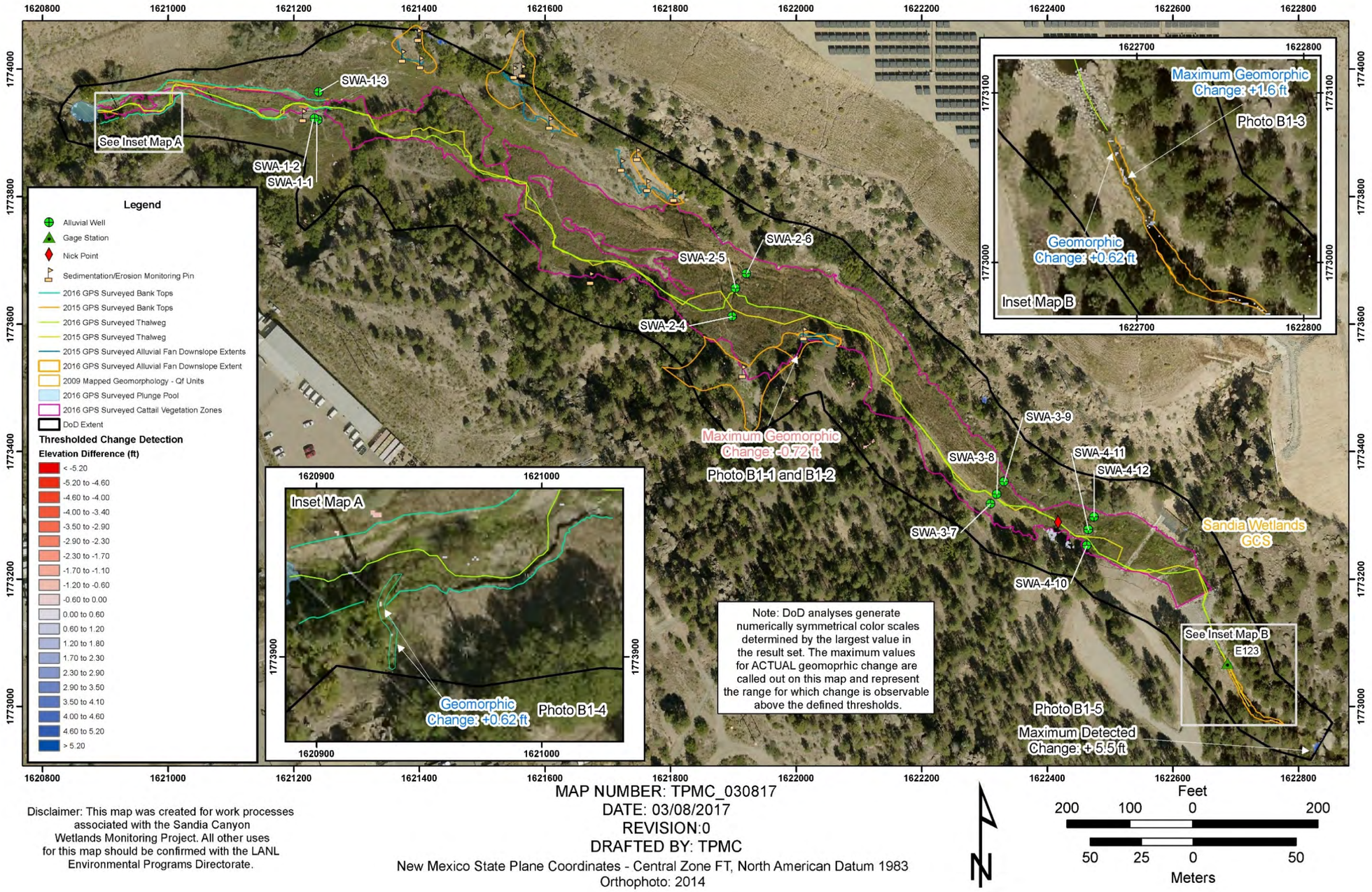

Disclaimer: This map was created for work processes associated with the Sandia Canyon Wetlands Monitoring Project. All other uses for this map should be confirmed with the LANL Environmental Programs Directorate.

MAP NUMBER: TPMC_030817
DATE: 03/08/2017
REVISION:0
DRAFTED BY: TPMC
New Mexico State Plane Coordinates - Central Zone FT, North American Datum 1983
Orthophoto: 2014

Figure B-4.2-1 Sandia Canyon reach S-2 DoD with central cattail vegetation perimeter map defining main wetland area

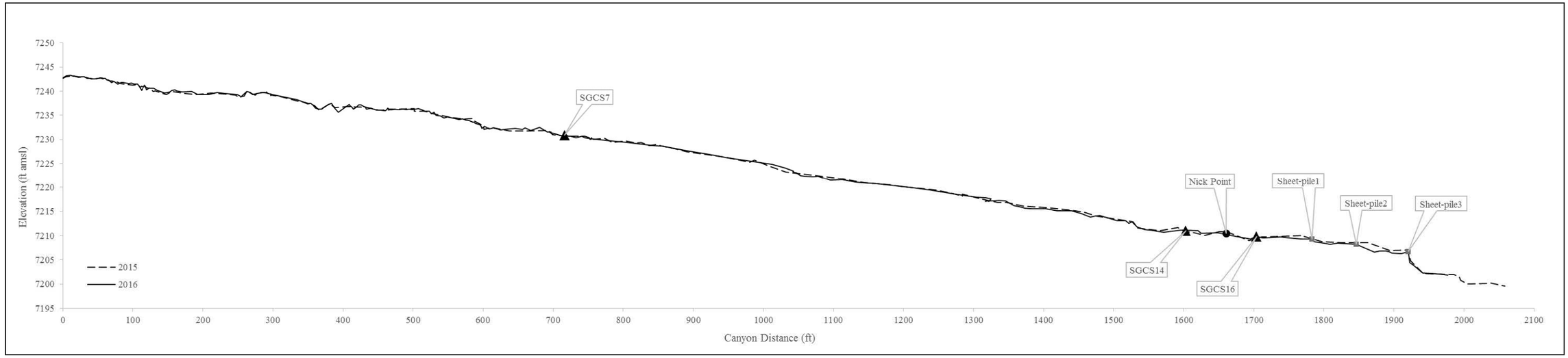

Notes: Vertical exaggeration is about 17 times. At the nick point, the thalweg elevation drops ~1.5 ft. Inset photo is the same as Photo B1-4, Attachment B-1.

Figure B-4.3-1 Thalweg profile in Sandia Canyon reach S-2

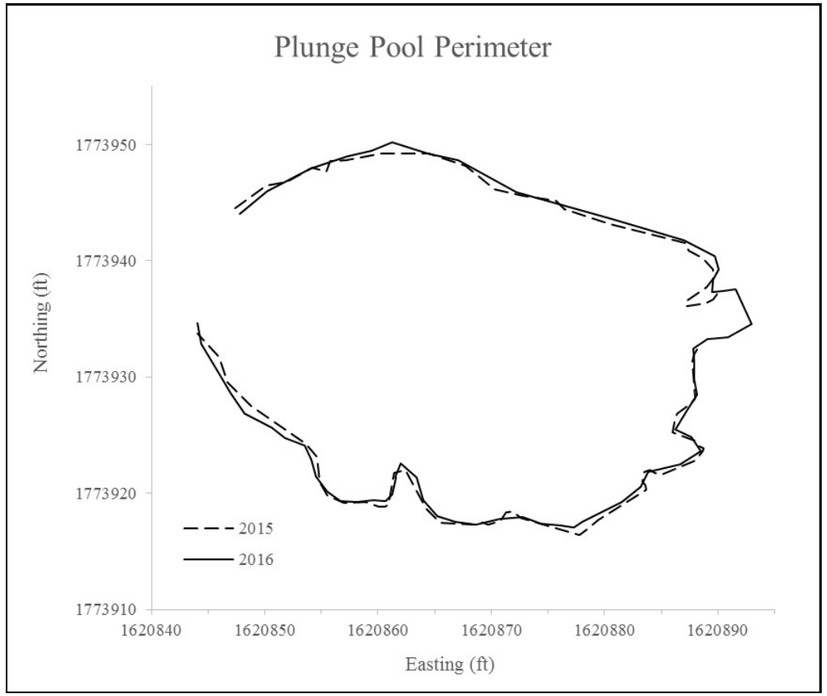

Figure B-4.4-1 Plan view of plunge pool in Sandia Canyon reach S-2

Table B-2.0-1
Rainfall Events at E121.9 and the Associated Peak Discharge at E121, E122, and E123

Storm Event Date	RG121.9 Total Precipitation (in.)	E121 Peak Discharge (cfs)	E122 Peak Discharge (cfs)	E123 Peak Discharge (cfs)
7/1/2016	0.3	22	1.9	9.1
7/15/2016	0.3	22	1.9	11
7/31/2016	1.0	47	2.0	46
8/3/2016	0.6	37	1.6	13
8/4/2016	0.3	15	1.1	9.0
8/8/2016	0.4	44	1.3	12
8/19/2016	0.2	10	1.0	9.3
8/27/2016	0.9	51	2.3	28
9/6/2016	0.5	40	2.6	18
10/3/2016	0.1	1.7	0.4	2.2
10/8/2016	0.1	1.5	0.3	1.8
11/4/2016 (earlier)	0.7	2.3	0.6	2.5
11/4/2016 (later)	0.7	8.4	2.0	12
11/5–11/6/2016	0.7	17	2.0	15

Table B-2.0-2
Peak Discharge at E121, E122, and E123

Year	Peak Discharge (cfs) Stream Gage E121	Peak Discharge (cfs) Stream Gage E122	Peak Discharge (cfs) Stream Gage E123
2006	86	9	73
2007	67	14	67
2008	70	16	81
2009	41	15	78
2010	22	10	74
2011	77	12	70
2012	28	19	34
2013	68	18	108
2014	66	19	110
2015	50	5	64
2016	51	3	46
Mean	**57**	**13**	**73**

Table B-3.2-1
DEM Elevation Error Estimates for 2015 and 2016

Typical Comparison Areas for DEM Elevation Error Estimation	2016 Z Error (ft)	2015 Z Error (ft)	Propagated Error (ft)
Relatively level ground with minor vegetation	0.42	0.38	0.57
Banks, or other inclined features	1.34	1.48	1.99
Heavily vegetated areas	3.65	7.72	8.53

Note: Values in table are calculated from comparisons to checkpoint data collected in 2016 and 2015. They are representative of actual surfaces in Sandia Canyon reach S-2.

Attachment B1

Photographs of Geomorphic Conditions
in Sandia Canyon Reach S-2

Photo B1-1 **Maximum detected negative change (erosion) in reach S-2. March 2017 photo looking to north of the channel incision of 0.7 ft into alluvial fan on southern edge of the reach.**

Photo B1-2 **Closeup of incised alluvial fan where maximum erosion was noted. March 2017 photo looking north.**

Photo B1-3 **Maximum detected and field confirmed positive geomorphic change (deposition) of +1.61 ft in reach S-2. Slumping of channel banks below gage station E123 resulted in deposition of large blocks of bank sediment on the channel surface. March 2017 photo looking northwest (upstream).**

Photo B1-4 **Deposition in side channel located approximately 50 ft downstream of plunge pool on south side of reach S-2. March 2017 photo looking south at storm drain outfall and cliff edge of Sandia Canyon.**

Photo B1-5 **Location of maximum elevation change (+5.5 ft) detected. No actual geomorphic change occurred. This boulder at the eastern end of reach S-2 was classified as ground in 2016 but not in 2015. March 2017 photo looking south.**

Attachment B2

2016 Geomorphic Changes in
Sandia Canyon Reach S-2 Survey Data
(on CD included with this document)

Appendix C

2016 Wetland Vegetation Monitoring
in Sandia Canyon Reach S-2

CONTENTS

Figures

Tables

Attachments

C-1.0 INTRODUCTION

This appendix evaluates vegetation changes that occurred in Sandia Canyon reach S-2 at Los Alamos National Laboratory (LANL or the Laboratory). The vegetation survey perimeter map and qualitative photographic comparisons for 2016 document vegetation conditions in reach S-2 to satisfy annual vegetation monitoring requirements (LANL 2016, 601432). This appendix compares the previous year's (2015) vegetation perimeter map and photographs with those prepared in fall 2016.

Vegetation surveys are performed because the vitality of wetland species is a good indicator of redox and saturation conditions over a spatial distribution that cannot be easily measured by other point data techniques such as alluvial well/piezometer monitoring. Specifically, the presence of obligate wetland vegetation implies persistent saturation. Persistent saturation and contribution of organic matter from wetland vegetation are highly favorable to producing and maintaining reducing conditions. Perimeter mapping of wetland vegetation is performed and is supplemented with annual photographic comparisons to help evaluate the extent of obligate wetland vegetation. Annual photographic comparisons also help evaluate the establishment of overbank vegetation and their ability to compete for any remaining bare ground. Figure C-1.0-1 shows the extent of perimeter mapped wetland species. Attachment C1 presents photographs taken in 2015 and 2016 that compare vegetation conditions in Sandia Canyon reach S-2. For a comprehensive species list, refer to Table C-3.1-1 of Appendix C of the "2015 Wetland Vegetation Monitoring in Sandia Canyon Reach S-2" (LANL 2016, 601432).

C-2.0 Vegetation Monitoring Methods

To evaluate vegetation success at Sandia Canyon reach S-2, vegetation perimeter mapping was used to document the spatial distribution and areal extent of targeted wetland species (Figure C-1.0-1). Through the comparison of annual perimeter maps, success of wetland zones can be quantified based on the areal extent of specific wetland obligate zones. Vegetation perimeter mapping documents targeted cattails, coyote willows, and grade-control structure (GCS) wetland species. These targeted areas are defined by wetland obligate species or species expected to occur almost always (estimated probability of >99%) in wetland systems. While these targeted species represent the majority of vegetation in their designated zone, many other species (both wetland obligate and nonobligate) species coexist within the same zones. In some instances (western end of reach S-2), targeted species were intermixed with other plant species and/or are discontinuous. When a gap in the targeted species was encountered along the length of the reach, the survey perimeter (i.e., polygon) was closed. While most of these targeted species were of sufficient concentration to be easily identified as a mappable unit, no spatial density interpretations of the interior of the mapped perimeters are implied. Surveys were conducted using a differentially corrected global positioning system (DGPS). Raw survey data (x and y coordinates using the New Mexico State Plane coordinate system and elevations of all survey points) for surveyed perimeters are included electronically as Attachment C2 (on CD included with this document).

Photograph points that were established at both the north and south ends of each vegetation transect (see Attachment C1 for photos) were used to qualitatively compare annual changes in vegetation. Vegetation growth (height) and species diversity can be analyzed qualitatively from these comparison photographs documenting changes from 2015 to 2016.

C-3.0 MONITORING RESULTS

Overall, this analysis indicates an expansion of vegetation and a corresponding increase in wetland obligate species competition among vegetative groups in the Sandia wetland. The increased area of

wetland species and changing spatial distribution in the Sandia wetland signify a complex vegetative environment that continues to change on an annual basis.

C-3.1 Wetland Vegetation Area

The perimeter of wetland vegetation was surveyed using DGPS. Five distinct zone types were mapped and are labelled in Figure C-1.0-1: (1) Central Cattail Zone, (2) West Cattail Zone, (3) Mixed Cattail/Willow Zones, (4) Willow Zone, and (5) GCS Wetland Vegetation Zone. The area encompassed by each zone and percent change are provided in Table C-3.1-1.

The West Cattail Zone is a narrow strip of cattails with few willows that parallels the open channel at the head of the study area and encompasses an area of 646 m^2. The West Cattail Zone perimeter has expanded 6% since 2015 (Table C-3.1-1). The increase is from the expansion of cattails along the continuously flowing channel. As a result, cattails inhabit the channel all the way upstream to the plunge pool (Figure C-1.0-1). During 2016 vegetation perimeter surveying, five new populations of cattails were identified at the plunge pool and in the field of giant redtop grass south of the Western Cattail Zone (Figure C-3.1-1). The total areal extent of these newly observed populations is approximately 10 m^2.

The Northern Willow Zone, located along the northern extent of the Central Cattail Zone, encompasses 1474 m^2, an expansion of 281% since 2015 (Table C-3.1-1). The Northern Willow Zone perimeter expanded since 2015, moving both upslope along the northern slope of the wetland and into the Central Cattail Zone. This increase is from the growth of wetland obligate species (coyote willow) into upland areas previously absent of wetland species. Additionally, the perimeter expanded into the established Central Cattail Zone because of the competitive advancement of willow communities.

There are two Mixed Cattail/Willow Zones: one (Central Mixed Cattail/Willow Zone) located on the south central edge and the second (Upper Mixed Cattail/Willow Zone) located on the northwestern extent of the Central Cattail Zone. Together they encompass 2023 m^2 in 2016 (Figure C-1.0-1). These zones are primarily dominated by coyote willows with several lanceleaf cottonwood trees as well as stands of cattails along the stream channel and vegetative boundaries. These areas in reach S-2 show significant changes in areal extent from that of 2015.

The Upper Mixed Cattail/Willow Zone perimeter near SGCS-4 and SGCS-3B has expanded by 56% since 2015, largely from willow growth to the south of the stream channel (Figures C-1.0-1 and C-3.1-1 and Table C-3.1-1). Compared with 2014, this perimeter has continued annual expansion (LANL 2016, 601432) as a result of new willow growth west and south of the 2014 zone of mixed cattails and willows (Figure C-3.1-2).

The Central Mixed Cattail/ Willow Zone was originally mapped on the south side of the Central Cattail Zone in 2015 (Figure C-1.0-1). This area, including the inner boundary, was surveyed again in 2016 (Figure C-1.0-1). The mixed area is dominated by willows on the south and has a gradational contact into strictly cattails to the north. This interior contact of the mixed zone with the Central Cattail Zone was surveyed in 2016 using new benchmarks that allowed for stronger GPS signal in this area (LANL 2016, 601432). Any apparent change from in this area is probably from the estimated 2015 boundary.

The Central Cattail Zone encompassed 10,892 m^2, an increase of 8% since 2016 and is the dominant vegetation feature of the study area (Table C-3.1-1). The Central Cattail Zone continued to thrive as a stable vegetative unit in 2016 and exhibits minor growth expanding its outer boundary (Figure C-1.0-1). This zone remains a stable and homogenous stand of broad-leafed cattails in 2016. A small side channel on the south side of the Central Cattail Zone has deposited a small amount of sandy gravel into the wetland, burying a small patch of cattails in 2015 (Figure C-1.0-1). Monitoring of this feature in 2016

included installing erosion pins on the established channel to determine if alluvium was advancing farther out into the Central Cattail Zone perimeter. Results from the erosion pins show the fan is stable, but sediments are advancing eastward along channel, which is spatially coincident with the edge of the central cattail zone. Continued advancement of the alluvium eastward may impact the southern boundary of the central cattail zone much as it had in 2015. However, cattails have revegetated the sand-gravel deposits along the southern edge of the wetland in 2016 (Figure C-1.0-1).

Additional alluvial fans on the northern edge of the wetland were also monitored via erosion pins during the 2016 monsoon season. Measurements recorded in 2016 indicate the fans on the north side of the wetland did not significantly change (< ±0.03 ft) and have remained relatively stable throughout the year.

Gravel bars devoid of wetland vegetation were surveyed in the middle of the Central Cattail Zone in 2015 (Figure C-1.0-1). These gravel bars were approximately 1–2 ft above the water surface in the wetland at the time of survey and were populated with grasses and small shrubs such as rubber rabbitbrush (LANL 2016, 601432). Observations from the fall of 2016 of previously mapped gravel bars indicate they are still populated with gramminoid species, rubber rabbitbrush, and thistle species. A very narrow trail exists on the top of the gravel bars with no vegetation; otherwise, the gravel bars are revegetating with primarily nonobligate wetland species.

The GCS Wetland Vegetation Zone surrounding the GCS encompasses 1298 m^2, an expansion of 13% from 2015, primarily to the west into an area previously mapped as the Central Cattail Zone (Figure C-1.0-1). There is no longer a distinct boundary separating the western edge of the GCS vegetation area from the eastern edge of the established wetland of the Central Cattail Zone, indicating growth and areal expansion of the GCS wetland between 2015 and 2016 (Figure C-1.0-1).

C-3.2 Wetland Vegetation Photograph Comparisons

Representative photos from 2015 and 2016 of each transect are presented in Attachment C1 and are consistent with the results of the vegetation surveys and indicate an expansion of vegetation and a corresponding increase in wetland obligate species competition among vegetative groups in the Sandia wetland (LANL 2016, 601432, Table C-3.1-1, includes a comprehensive list of species). Photo C1-1 in Attachment C1 shows an overall increase in cattails along transect SGCS-3A within the Western Cattail Zone. While there is no observable change in vegetation expansion in this photograph, it indicates an environment suitable for an established stand of cattails to thrive. Photos C1-2 through C1-6 in Attachment C1 show no observable change to the wetland vegetation in the Mixed Cattail/Willow Zone and upper part of the Central Cattail Zone, indicating stable conditions. Photo C1-7 in Attachment C1 exhibits an absence of yellow sweetclover (shrub) in 2016, whereas in 2015 it was prevalent throughout the southern edge of the wetland. This indicates yellow sweetclover is being outcompeted by blue grama, giant redtop, and other gramminoid species. Photos C1-8 and C1-9 in Attachment C1 show no observable change to the wetland vegetation in the central and lower parts of the Central Cattail Zone, indicating stable conditions. Photo C1-10 shows the absence of yellow sweetclover in 2016 and an increase in thistle species along the southern bank and slightly to the west of transect SGCS-16. Field observations verified that thistle species are outcompeting native vegetation and expanding west along the Central Cattail Zone perimeter.

Photos C1-11 and C1-12 in Attachment C1 show the expansion of wetland obligate species hardstem bulrush, softstem bulrush and water sedge within the already established broad-leafed cattail zone, resulting in an increase in species diversity at the GCS. Similar to Photo C1-7, Photos C1-11 and C1-13 in Attachment C1 indicate the same progression of yellow sweetclover being outcompeted by blue grama. This process shows a strong state of competition in the upland overbank plant community between

already established native populations. Competition between native species indicates the upland plant community is in a dynamic yet stable condition. All three GCS transect photo groups (Photo C1-11 through C1-13) show the establishment and expansion of the broad-leafed cattail zone within the GCS area.

Expansion of a dense and homogenous stand of thistle species along the southern bank of the Central Cattail Zone is observed in Photo C1-14. It is unlikely thistle species will successfully establish a population within the saturated wetland area and out compete obligate species, however, they could limit obligate species expansion at the fringe of the saturated zone. Field observations suggest that the expansion of thistle species has reduced the presence of upland species and competing native plant communities (Photo C1-14 in Attachment C1). Continued monitoring of this thistle stand in 2017 is recommended.

Photo C1-15 in Attachment C1 shows the newly observed cattail populations in 2016 discussed in the Western Cattail part of section C-3.1 and displayed in Figure C-3.1-1.

Overall, this qualitative photograph analysis indicates the vegetation in the wetland is either in a state of expansion around the GCS, transition from shrub to gramminoid species, or stability with little noticeable change in 2016.

C-4.0 CONCLUSIONS AND RECOMMENDATIONS

This appendix presents the annual vegetation monitoring surveys of Sandia Canyon reach S-2. Vegetation perimeter mapping was conducted and repeat photographs were taken at established locations throughout all 13 vegetation transects in the fall of 2016. Moving west to east in reach S-2, the areal extent of the wetland system is initially confined to a narrow zone within a defined channel and gradually expands moving eastward across a much wider area into the Central Cattail Zone and terminates downstream of the GCS. Between 2015 and 2016, wetland vegetation area has expanded by about 21% over the whole study area. Growth is attributed to expansion of new willow and mixed willow communities along the western part of the primary channel (Western Cattail Zone) and along the northern bank (Northern Willow Zone) within the eastern half of the wetland. Repeat photos and perimeter mapping suggest that the wetland is stable and restoration has been successful during the two years of measurable change at the Sandia Wetland GCS.

Quantitative surveys of wetland vegetation along cross-sections will continue to occur biennially, with the next surveys to be conducted in 2017. Significant storm events (resulting in flow greater than 50 cubic feet per second) will trigger a visual inspection of the wetland. If the storm event physically disrupts large areas of wetland vegetation, detailed characterization of wetland vegetation cross-sections in years in which such surveys were not scheduled will be conducted. Perimeter surveys of the wetland cattails, willows and GCS species and qualitative photographic surveys of the wetland will continue annually.

C-5.0 REFERENCES AND MAP DATA SOURCES

C-5.1 References

The following list includes all documents cited in this appendix. Parenthetical information following each reference provides the author(s), publication date, and ER ID or ESH ID. This information is also included in text citations. ER IDs were assigned by the Environmental Programs Directorate's Records Processing Facility (IDs through 599999), and ESH IDs are assigned by the Environment, Safety, and Health (ESH)

Directorate (IDs 600000 and above). IDs are used to locate documents in the Laboratory's Electronic Document Management System and, where applicable, in the master reference set.

Copies of the master reference set are maintained at the New Mexico Environment Department Hazardous Waste Bureau and the ESH Directorate. The set was developed to ensure that the administrative authority has all material needed to review this document, and it is updated with every document submitted to the administrative authority. Documents previously submitted to the administrative authority are not included.

LANL (Los Alamos National Laboratory), April 2016. "2015 Sandia Wetland Performance Report," Los Alamos National Laboratory document LA-UR-16-22618, Los Alamos, New Mexico. (LANL 2016, 601432)

C-5.2 Map Data Sources

The following list provides data sources for maps included in this appendix.

Gaging stations; Los Alamos National Laboratory, Waste and Environmental Services Division; 1:2,500; March 19, 2011.

LANL area orthophoto; Los Alamos National Laboratory, 2014.

Geomorphic Reach Boundary, Los Alamos National Laboratory, Earth and Environmental Science, GISLab, 2009.

Geomorphology Units; Los Alamos National Laboratory, Earth and Environmental Sciences, GISLab, 2009.

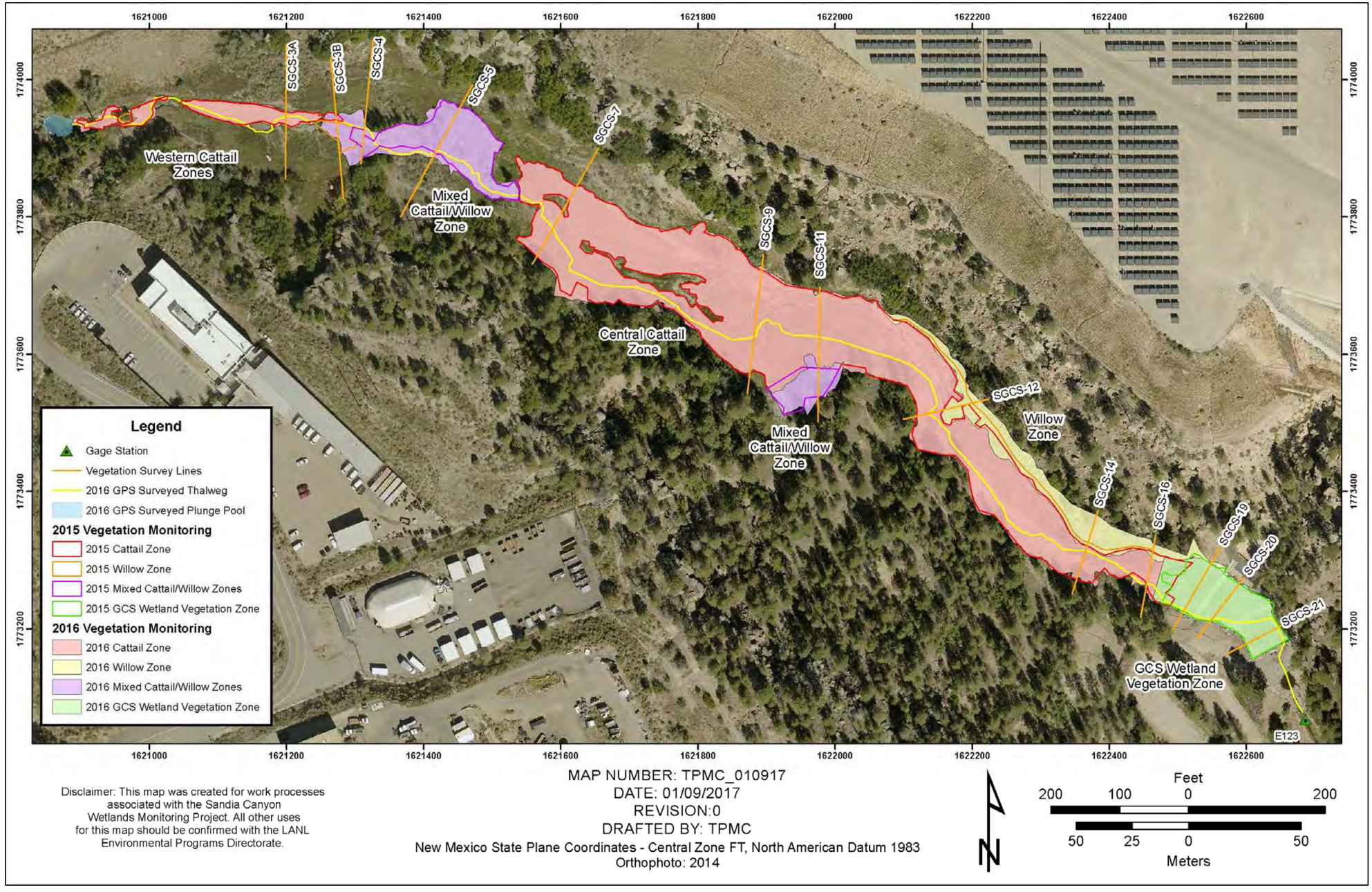

Figure C-1.0-1 Mapping comparison results of 2015 and 2016 vegetation perimeter at Sandia Canyon reach S-2

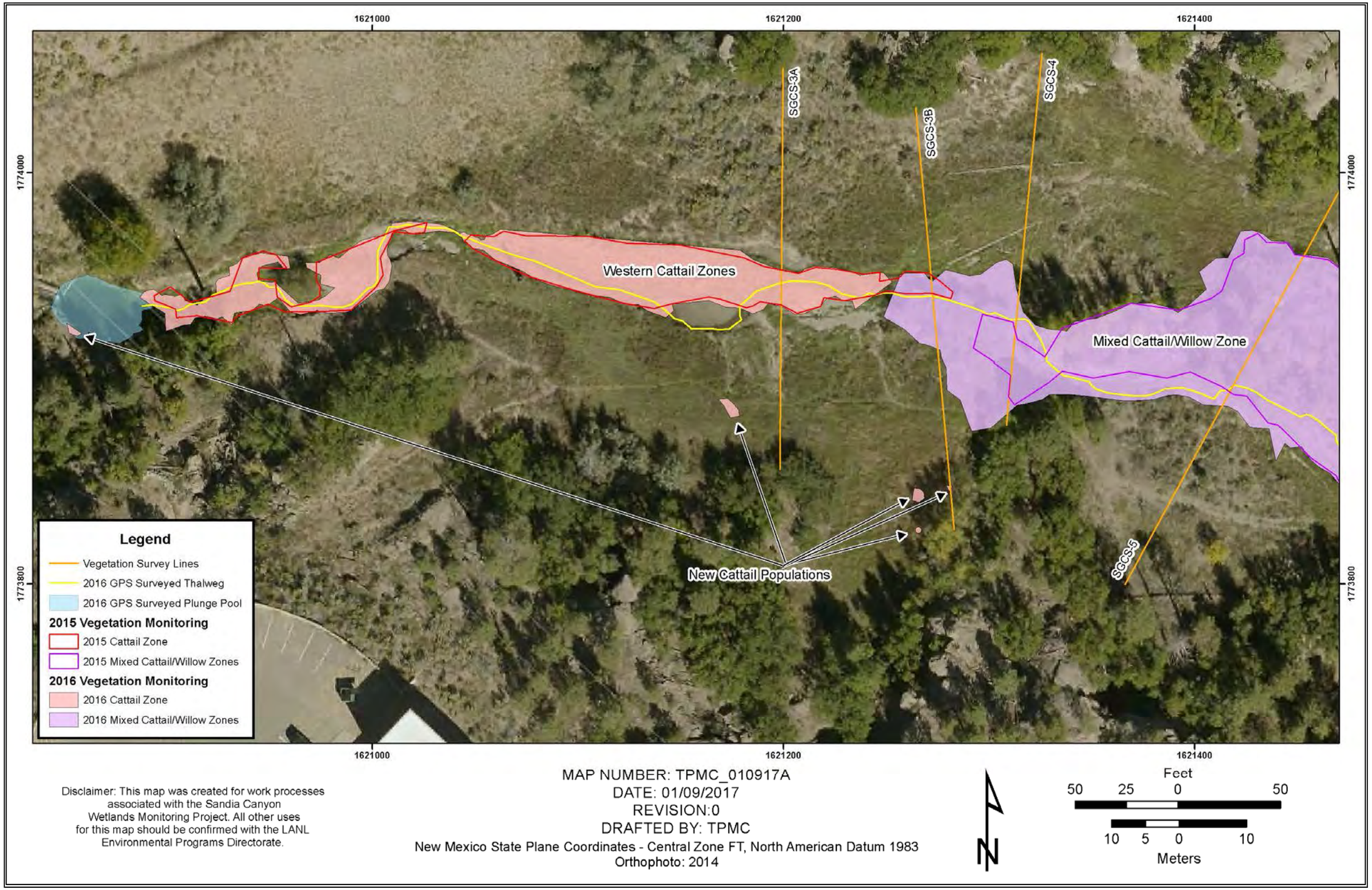

Figure C-3.1-1 Upper wetland area highlighting new cattail populations

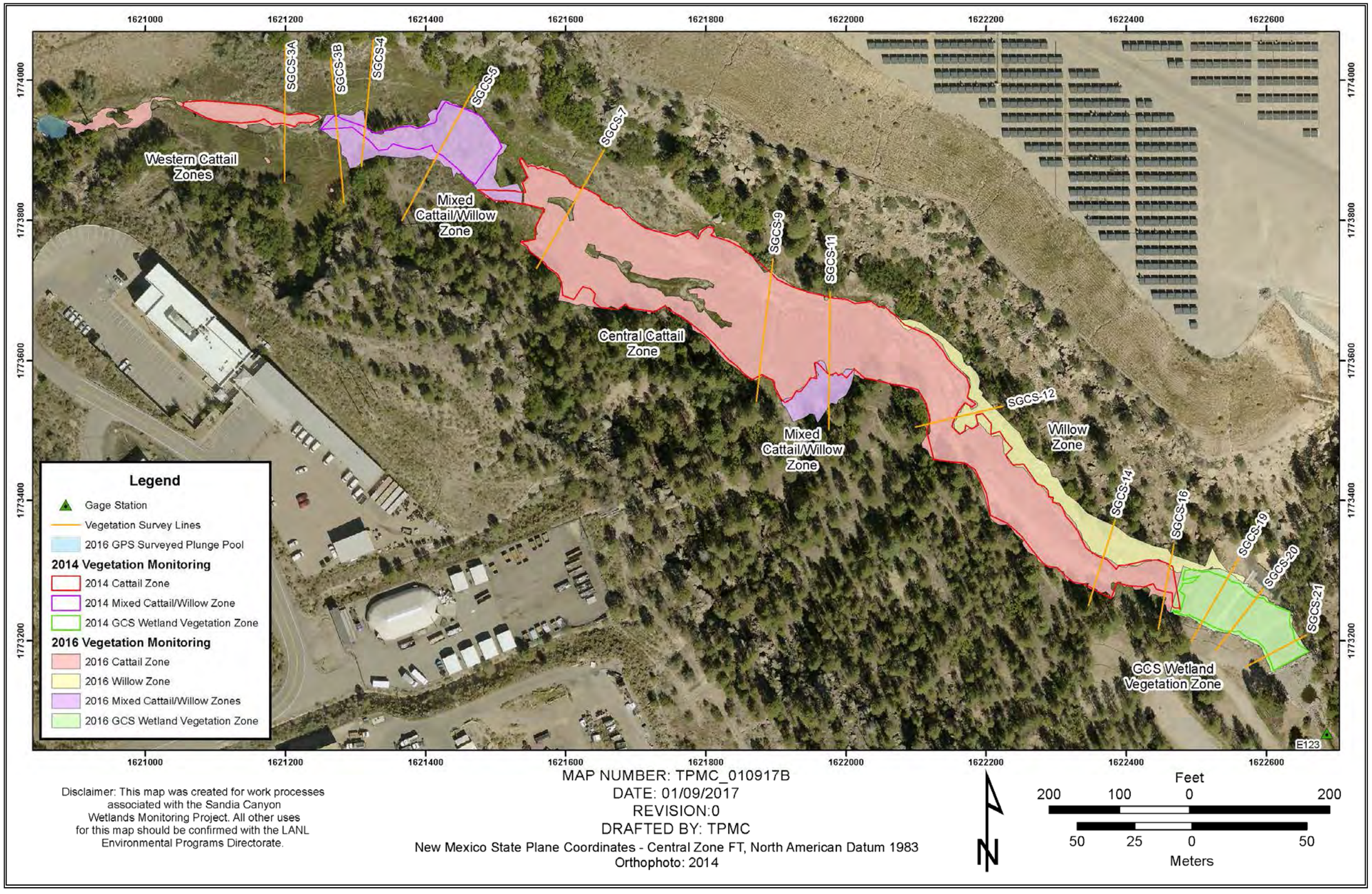

Figure C-3.1-2 Two-year (2014–2016) comparison of wetland vegetation perimeters

Table C-3.1-1
Wetland Vegetation Area Totals

Zone Name	2015 Area (m^2)	2016 Area (m^2)	% Change	Comments
West Cattail Zone	608	646	+6%	Cattail expansion upstream to the plunge pool
Mixed Cattail/Willow Zone	1293	2023	+56%	Willow expansion south of the channel
Central Cattail Zone	10,095	10,892	+8%	Stable with minor growth along outer boundary
GCS Vegetation Zone	1146	1298	+13%	Expansion westward reducing previous gaps between GCS Vegetation Zone and Central Cattail Zone
North Willow Zone	387	1474	+281%	Growth along northern bank that was previously absent of wetland species and encroachment on north side of Central Cattail Zone
Total	**13,529**	**16,333**	**+21%**	

Attachment C-1

2015–2016 Comparison Photographs of Sandia Wetland Vegetation Monitoring

Photo C1-1 SGCS-3A looking north: September 2015 (left) and September 2016 (right)

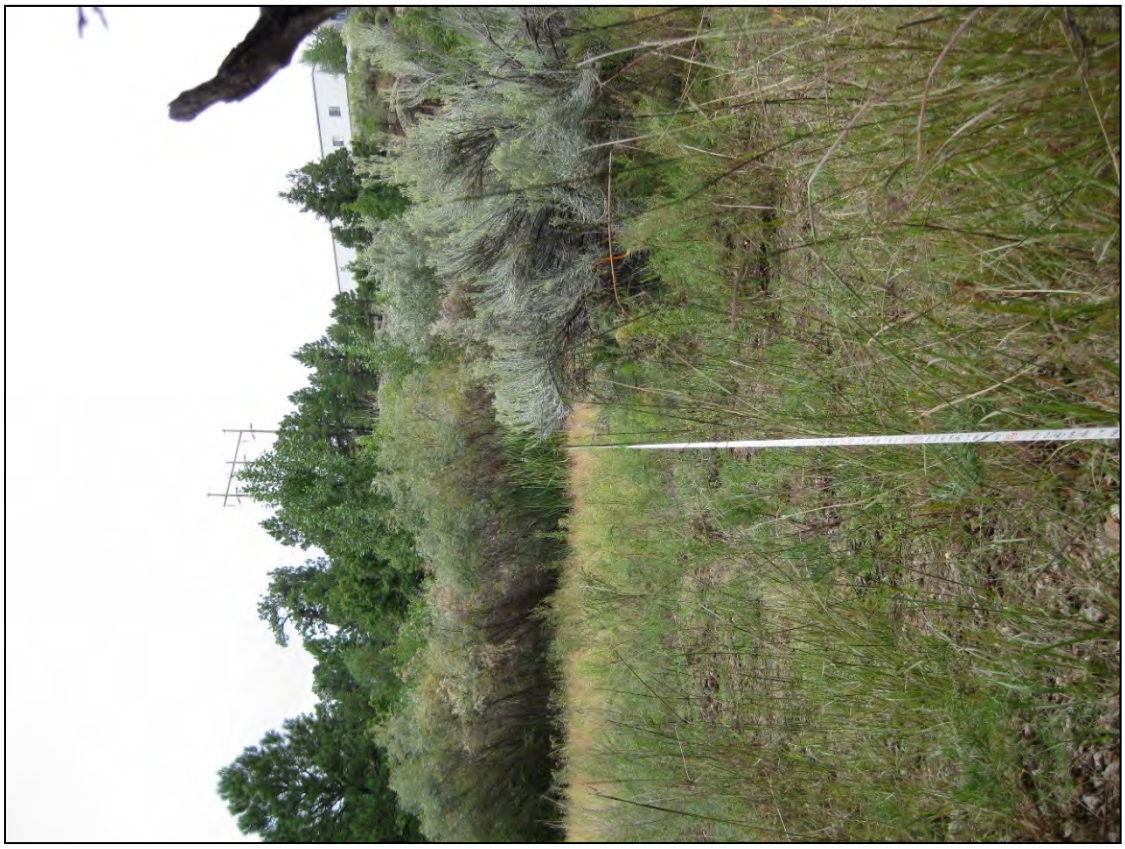

Photo C1-2 SGCS-3B looking south: September 2015 (left) and September 2016 (right)

Photo C1-3 SGCS-4 looking north: September 2015 (left) and September 2016 (right)

Photo C1-4 SGCS-5 looking north: September 2015 (left) and September 2016 (right)

Photo C1-5 SGCS-7 looking south: September 2015 (left) and September 2016 (right)

Photo C1-6 SGCS-9 looking north: September 2015 (left) and September 2016 (right)

Photo C1-7 SGCS-11 looking north: September 2015 (left) and September 2016 (right)

Photo C1-8 SGCS-12 looking north: September 2015 (left) and September 2016 (right)

Photo C1-9 SGCS-14 looking north: September 2015 (left) and September 2016 (right)

Photo C1-10 SGCS-16 looking north: September 2015 (left) and September 2016 (right)

Photo C1-11 SGCS-19 looking north, upstream of sheet pile 1: September 2015 (left) and September 2016 (right)

Photo C1-12 SGCS-20 looking north, between sheet pile 1 and 2: September 2015 (left) and September 2016 (right)

Photo C1-13 SGCS-21 looking north, upstream of sheet pile 3: September 2015 (left) and September 2016 (right)

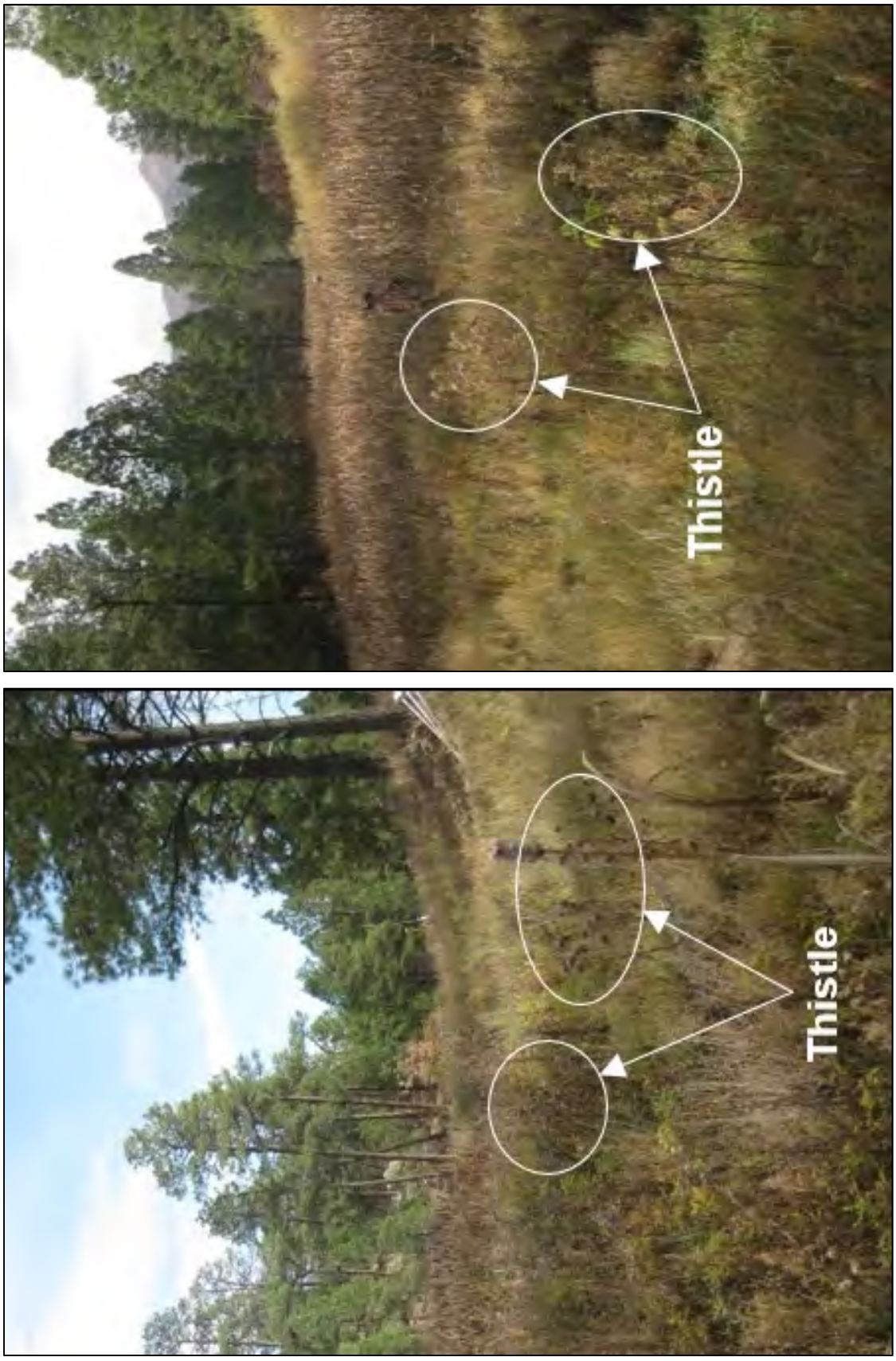

Photo C1-14 **Observed thistle species expansion (2016) between southern end of transects SGCS-14 and -16: looking east toward grade-control structure (left) and looking west from south end of SGCS-16 (right)**

Photo C1-15 **Newly observed cattail populations in 2016: discrete populations living within giant redtop grass along southern end of SGCS-3A and -3B (left) and new population on southwestern bank of plunge pool (right)**

Attachment C2

2016 Vegetation Changes in Sandia Canyon
ReachS-2 Survey Data
(on CD included with this document)

Appendix D

Geochemical and Hydrologic Monitoring in Sandia Canyon

CONTENTS

Figures

Tables

D-1.0 INTRODUCTION

The geochemical and hydrologic analytical results from performance monitoring of the Sandia wetland are presented and evaluated herein. Construction and subsequent revegetation of the Sandia grade-control structure (GCS) and the implementation of monitoring were undertaken by Los Alamos National Laboratory (LANL or the Laboratory) not with the objective of reducing concentrations of contaminants in water to specific values; therefore, the comparison between analytical results and water-quality standards or other criteria presented in sections D-2.1 and D-3.4 are not for the purpose of evaluating compliance with regulatory requirements.

D-2.0 ANALYTICAL RESULTS FROM SURFACE WATER GAGING STATIONS E121, E122, AND E123

As noted in the baseline performance report (LANL 2014, 257590), similar base flow chemistry for many constituents between upgradient and downgradient locations indicates a relatively short residence time for surface water and little interaction (exchange) with alluvial groundwater. This finding is evident for chloride, nitrate plus nitrite, and silica, which are indicators of water quality in outfall discharge in the context of chemistry from Outfall 001 (Figures D-2.0-1 to D-2.0-3). Improvements in water chemistry discharged from Outfall 001 are obvious for chloride and silica (as inferred from concentrations at E121) and also for total dissolved solids (TDS), a general indicator of water quality in outfall discharge (Figures D-2.0-1 to D-2.0-3). Manganese, a sensitive redox indicator, is discussed because this base-flow constituent shows some evidence for temporal trends (Figure D-2.0-4). Hexavalent chromium, also a contaminant of concern along with total chromium, is also discussed (Figures D-2.0-5). Base flow and storm flow data for three key contaminants associated with wetland sediments, polychlorinated biphenyls (PCBs), chromium, and polycyclic aromatic hydrocarbons (PAHs) are discussed below.

In terms of indicators of improved water quality associated with the Sanitary Effluent Reclamation Facility (SERF) expansion, no strong base flow temporal concentration trends exist for filtered chloride and nitrate (Figures D-2.0-1 and D-2.0-2, respectively). However, the patterns observed post-SERF expansion (August 2012) are similar at both gaging stations and Outfall 001 (Figures D-2.0-1 and D-2.0-2). Interestingly, nitrate has consistently lower concentrations at gaging station E123 relative to station E121 (Figure D-2.0-2). This finding is expected because nitrate is not only a water-quality indicator, it is also a plant nutrient and a redox-sensitive species that may be reduced and assimilated during surface water transport through the wetland. The most recent data show peak increases in nitrate at the Outfall 001 that are reflected in base flow nitrate concentrations (Figure D-2.0-2). These increases are likely related to an increase in Sanitary Waste Water System (SWWS) nitrate-containing effluent in Outfall 001 water until March 2016. More data are needed to determine how operational changes, including switching back to the reuse of SERF-blended water, since 2016 will affect discharge at Outfall 001 (section 1.4). Surface water base flow silicon dioxide concentrations are plotted in Figure D-2.0-3. TDS is also plotted as a general indicator of water quality associated with outfall discharge. The effect of the SERF expansion on both parameters is clear (Figure D-2.0-3).

Among redox-sensitive species, dissolved manganese in base flow at gaging station E123 appears to be showing overall improvement in water quality through time (Figure D-2.0-4). The cause of periodic spikes in manganese concentrations at E123 is not clear. Following completion of the GCS, manganese concentrations have remained generally lower. Manganese at E123 could represent either colloidal Mn(IV) and/or dissolved Mn(II). Manganese in alluvial waters will tend to be present as mobile Mn(II) and, given the slow oxidation kinetics, may not fully oxidize to less soluble Mn(IV) in the time between alluvial waters surfacing (at the headcut pre-GCS or at the upper impermeable wall post-GCS) and reaching

gage E123 immediately downstream. Generally lower manganese concentrations post-GCS are likely the result of some combination of cessation of headcutting at the terminus of the wetland, which would reduce colloidal transport of Mn(IV), and altered alluvial water dynamics, which could affect Mn(II) concentrations and oxidation kinetics. Because most of the wetland is still saturated (section D-4.0), it is unlikely that trends in manganese concentrations at downstream gage E123 reflect changes in redox conditions within the wetland. Further monitoring may explain the cause of the overall decrease through time. Dissolved concentrations of manganese are consistently higher at gaging station E123 relative to E121 because alluvial waters in the wetland have high manganese concentrations, probably as Mn(II) and possibly because of colloidal transport of Mn(IV). Greater mobilization of Mn(IV) colloids during construction of the GCS could account for the large spike in manganese concentration before the GCS was completed (Figure D-2.0-4).

Background concentrations of approximately 5–6 µg/L Cr(VI) occur in regional aquifer waters (LANL 2007, 095817). Because potable water is derived from the regional aquifer, it provides a starting point for expected concentrations of Cr(VI) in sanitary waste water before modifications occur at SWWS, SERF, or the cooling towers where potable water is used. Water from Outfall 03A027 analyzed for Cr(VI) in September 2015 showed a concentration of 6.41 µg/L (unfiltered), and the result falls within expected values for potable water. Cr(VI) has been detected in unfiltered samples at gage E121 with values up to 7.76 µg/L in May 2016. At E123, most values of Cr(VI) have been below or at the detection limit, with the highest measured value of 1.33 µg/L with a detection limit at 1 µg/L. Hexavalent chromium shows evidence of attenuation as it is transported through the wetland; multiple detections of Cr(VI) at E121 tend to become nondetections by the time they reach gaging station E123 (Figure D-2.0-5).

Surface water at gaging stations E121, E122, and E123 is perennial; thus, the results for primary contaminants PCBs, chromium, and PAHs are separated into base-flow and storm-flow components. Figure D-2.0-6 shows the discharge measured at E121, E122, and E123 from 2010 to 2016 and the varying base flow at each station during this period. This figure also shows the total discharge from the three outfalls and the influence of discharge on each gaging station, particularly E121 and E123. For both base flow and storm flow, box-and-whisker plots of peak discharge, suspended sediment concentration (SSC)/total suspended sediments (TSS), PCBs, chromium, and PAHs are presented in Figure D-2.0-7.

SSC, PCBs, chromium, and PAHs are discussed in the context of peak discharge and are used as key parameters to track the performance of the GCS. Results from gaging stations E121 and E122, which monitor most of the surface water flow into the wetland, and gaging station E123, which monitors surface water flow out of the wetland, are plotted together to show changes in surface water discharge and chemistry from upgradient to downgradient of the wetland (Figure D-2.0-7). These plots show the range of concentrations and represent a historical baseline before GCS construction (pre-GCS), during the first year of performance monitoring after GCS construction (post-GCS), and in 2015 and 2016. Multiple years of data are needed to fully delineate the performance metrics for the GCS.

In Figure D-2.0-7, storm-flow discharge is expectedly greater than base-flow discharge for all the gaging stations. At E121 and E123, base-flow discharge is highly dependent on the outfall effluent discharge rate (Figure D-2.0-6); thus, the reduction in this rate from pre- to post-GCS and the increase in this rate in 2015 and 2016 is reflected in the base-flow discharge, more so at E121 than at E123. Gaging station E122 base-flow discharge is fairly stable throughout the years. One of the objectives of the GCS is to reduce the peak discharge of the storm flow, which can cause erosion and thus movement of contaminants. The storm-flow peak discharge from upstream (E121 and E122) to downstream (E123) of the GCS was reduced post-GCS, in 2015 and 2016. It is also important to note that precipitation in 2015 and 2016 was less intense than in 2013 and 2014, thus possibly attributing to the reduction in storm-flow

peak discharge. However, the wetland alone attenuates the storm-flow peak discharge, as can be noted during pre-GCS conditions.

Hydrographs for the 12 sample-triggering storm events recorded at E121, E122, and E123 from July 1 to November 5, 2016, are presented in Figure D-2.0-8. During these storm events, tributaries downstream of E121 and E122 can contribute significant flow. Table D-2.0-1 presents the timing of the transmission of flood bore, or peak, from E121 and E122 downstream to E123. In 2016, the average time of transmission from E121 to E123 and from E122 to E123 is approximately 88 min. This finding indicates storm water from both upgradient stations flows through the wetland in approximately the same amount of time and quite rapidly, although not as rapidly as during the post-GCS period (approximately 40-min average travel time between E121 and E122 to E123) when precipitation events were more intense.

In Figure D-2.0-7, the sediment content in base flow is lower than storm flow, significantly so for TSS (compare pre-GCS TSS for base flow and storm flow) and slightly so for SSC. This is typical for storm water because of the greater erosive energy of the increased peak discharge. Note that base flow was sampled for TSS pre-GCS and SSC in 2016, and storm flow was sampled for TSS pre-GCS and SSC post-GCS in 2015 and in 2016. As expected, storm flow SSC at E121 and E122 is not significantly different pre- to post-GCS; however, at E123, storm flow SSC is significantly reduced after construction of the GCS and continues to remain low through 2016, possibly because of a cessation of headcutting at the terminus of the wetland. This reduction is noteworthy because contaminants in the wetland are strongly sorbed to sediments, and a reduction in SSC should be associated with a reduction in contaminant migration. In 2015 and 2016, SSC at E121 and E122 is less than that measured during the post-GCS period. At E123, the reduction in sediment content is significant pre- to post-GCS, and then continues to remain stable in 2015 and 2016. Again, this result is most likely because of the lack of more intense precipitation and erosive runoff in 2015 and 2016.

The box-and-whisker plots in Figure D-2.0-7 indicate that PCB and total chromium concentrations in storm flow at E123 are significantly reduced since the GCS was constructed. While PCB concentrations in storm flow were significantly higher downgradient of the wetland (relative to upgradient locations E121 and E122) before the GCS was built, the concentrations are closer in magnitude upgradient and downgradient of the wetland since the GCS was constructed. In 2015 and 2016, PCB concentrations downgradient of the wetland were slightly higher than upgradient of the wetland, but the temporal trend shows a reduction in PCBs at all gaging stations. In general, total chromium concentrations are higher downgradient of the wetland, suggesting surface water is transporting measurable concentrations of Cr(III) associated with colloids from the wetland. However, a temporal trend also shows reductions in total chromium at all gaging stations. The trends in PCBs and total chromium may be a result of continued growth of GCS vegetation, corresponding to the stabilization of sediments (Appendixes B and C).

Total PAH was computed using the 18 most prominent PAHs, and nondetections were considered zero. PAHs were not analyzed in base flow or storm flow before the GCS was built. In base flow, all results were nondetections, with the exception of one sample collected at E123 in 2016. In storm flow during the post-GCS period, PAH concentrations were similar upgradient and downgradient of the wetland. In 2015, PAH concentrations downgradient of the wetland were slightly higher than upgradient of the wetland. In 2016, the reverse is true: PAH concentrations downgradient of the wetland are slightly lower than upgradient of the wetland. Overall, higher concentrations of PAHs were detected at E122 than at E121 and E123, suggesting the influence of the former asphalt batch plant near the northern fork of upper Sandia Canyon is still evident and is the most likely source of PAHs at the downstream gaging station, E123, because the low concentrations of PAHs at E121 do not indicate a source.

Fairly consistent correlations exist between SSC, PCBs, chromium, PAHs, and discharge as presented in Figure D-2.0-9. Correlations show that as discharge increases, the concentrations of these constituents

increase. There are exceptions to this regular correlation (e.g., E121 for SSC and E122 for chromium); however, in general, these relationships show that discharge is a good indicator of sediment and associated contaminant transport. The relationships shown in Figure D-2.0-9 were obtained after removing data points when the ISCO sampler malfunctioned and removing outliers using the standardized residual outlier method. These relationships were used to calculate the mass flux as follows. The line of best fit was used to calculate the approximate concentrations of sediment, total PCBs, and total chromium every 5 min using the following discharge measurements:

$$y_{n,i} = m_n x_i + b_n \qquad \textbf{Equation D-3.1-1}$$

where $y_{n,i}$ is the calculated concentration of each constituent n every 5 min or time step i; n = SSC, total PCBs, or total chromium; x_i is the discharge at each time step i; and m_n and b_n are each constituent's linear equation parameters (slope and y-intercept, respectively). The annual mass flux was then computed as the area under the 5-min concentration curve multiplied by the discharge:

$$\text{mass flux}_n = \sum_{i=1}^{I} \left(\frac{y_{n,i+1} + y_{n,i}}{2} \right) * (t_{i+1} - t_i) * x_i \qquad \textbf{Equation D-3.1-2}$$

where t_i is the time of the discharge measurement at time step i and the annual mass flux was computed as the sum of the mass for calendar years 2014, 2015, and 2016.

Figures D-2.0-10 through D-2.0-13 show the estimated annual mass flux from 2014 to 2016 at each gaging station for sediment, total PCBs, total chromium, and total PAHs, respectively. Also shown in these figures is the annual mass flux normalized by annual runoff volume for each constituent. Sediment flux into the wetland is greater than the sediment flux out, which was also observed in the SSC box plots in Figure D-2.0-7, and indicates sediment is no longer being moved near the headcut and the GCS is performing well. According to the normalized plots, storm water runoff from the E121 watershed is more sediment-laden than runoff from the E122 or E123 watersheds, again indicating a reduction in sediment load through the wetland.

PCB flux out of the wetland is slightly greater than the PCB flux into the wetland in 2014 and 2015, suggesting a small amount of PCBs is being entrained in the surface water through the wetland. In 2016, this trend was reversed. Increases in PCB concentrations through the wetland were also observed in the total PCB box plots in Figure D-2.0-7, where the concentrations of PCBs in storm flow and base flow at E123 are greater than at E121 and E122. From 2014 to 2016, a slight reduction occurred over time in total PCB flux at all the gaging stations. However, when the normalized PCB flux is examined, E122 is stable over time and a reduction occurs at E121 and E123. There was less runoff volume in 2015 and 2016 than in 2014, most likely because of the less intense storm events in 2015 and 2016 possibly contributing to the reduction in normalized PCB flux over time. The total PCBs wetland inventory [the sum of 5.5 kg, 3.3 kg, 31.1 kg, and 24.4 kg for Aroclor-1242, Aroclor-1248, Aroclor-1254, and Aroclor-1260, respectively (LANL 2009, 107453), see section 1.1] is plotted in Figure D-2.0-11. Note that Aroclors were used to compute the total PCBs inventory, while congeners were used to compute the annual mass flux, and thus they are not directly comparable, but the wetland inventory provides perspective on the magnitude of annual flux of PCBs into and out of the wetland.

Chromium flux out of the wetland is slightly greater than the chromium flux into the wetland in 2014 and 2015, suggesting a small amount of chromium is being entrained in the surface water through the wetland. In 2016, this trend is reversed: increases in chromium concentrations through the wetland were also observed in the total chromium box plots in Figure D-2.0-7, where the concentration of total chromium in storm flow and base flow at E123 were greater than at E121 and E122. From 2014 to 2016, there is a slight reduction over time in total chromium flux at E123, while the flux at E121 and E122 remained fairly stable. The less intense storm events in 2015 and 2016 than in 2014 possibly contributed

to the reduction in normalized chromium flux over time at all of the gaging stations. The total chromium wetland inventory (approximately 15,000 kg of chromium as Cr(III) [LANL 2009, 107453], see section 1.1) is plotted in Figure D-2.0-12. Note that the inventory is computed for Cr(III) while the total chromium concentrations were used to compute the annual mass flux, and thus they are not directly comparable, but the wetland inventory provides perspective on the magnitude of annual flux of chromium into and out of the wetland. Also, most of the chromium in the wetland exists as Cr(III) (section 1.6.3); thus, this comparison is reasonable.

PAH flux out of the wetland is slightly greater than the PAH flux into the wetland, indicating a small amount of PAHs is being entrained in the surface water through the wetland. Note that the relationships between total PAHs and discharge, which is the foundation of the mass flux calculations, are not very good for E121 or E123; thus; there is significant uncertainty associated with the flux.

In addition to using the relationship between SSC and discharge to estimate annual sediment flux, the actual sediment flux for each sampled storm event was also computed (Table D-2.0-2). The relationship between sediment volume and runoff volume for storm water tends to be a stronger relationship than sediment volume and peak discharge, and for all of upper Sandia Canyon this relationship is R^2=0.52:

$$\text{sediment volume} = 0.1728 * \text{runoff volume}^{1.044} \qquad \textbf{Equation D-3.1-3}$$

D-2.1 Screening Surface and Storm Water to Surface Water Quality Criteria

Base flow and storm water collected at gaging stations E121, E122, and E123 and analyzed in 2016 were screened against the appropriate surface water–quality criteria (SWQC) in 20.6.4.900 New Mexico Administrative Code. Chronic aquatic life criteria for hardness-dependent metals (i.e., aluminum, cadmium, copper, lead, and zinc) were calculated using hardness values for samples collected for storm water and average hardness values for base flow.

Sample results that exceed SWQC are presented in Table D-2.1-1. Base flow exceedances were observed for aluminum, copper, and PCBs. Exceedances in storm water were observed primarily for aluminum, copper, lead, PCBs, and zinc. A few additional storm water exceedances occurred for benzo(a)anthracene, benzo(a)pyrene, benzo(b)fluoranthene, cadmium, and gross alpha.

The Sandia wetland receives run-on water from developed areas within Technical Area 03 (TA-03) at the Laboratory, which is characterized by water-quality results from E121 and E122. Developed areas in and around the Laboratory are documented sources of contaminants exceeding SWQC, including aluminum, copper, lead, zinc, and PCBs, as determined by storm water runoff monitoring (LANL 2012, 219767; LANL 2013, 239557). Therefore, exceedances of SWQC for these constituents at E121 and E122 are likely sourced from developed areas within TA-03. In addition, E121 and E122 may be influenced by historical releases from solid waste management units (SWMUs) upgradient of these monitoring locations. Since the Sandia wetland is downgradient of E121 and E122, contaminants from the Sandia wetland do not influence the sample results.

Gage station E123 is downgradient of the Sandia wetland. Base flow water that constitutes E123 water includes outfall water upgradient of E121 and E122 and any alluvial recharge water from the Sandia wetland. Storm water that constitutes E123 water includes run-on from E121 and E122 and areas that drain to the E123 watershed surrounding the Sandia wetland (such as the former Los Alamos County landfill). This storm water flows through the Sandia wetland where potential contaminants sourced from the Sandia wetland may be entrained and may contribute to the discharge at E123. Comparing results from E121/E122 with E123 is useful in evaluating exceedances to determine if the Sandia wetland may

be a source of constituents exceeding SWQC. Table D-2.1-2 provides summary statistics for each analyte exceeding SWQC for E121, E122, and E123 in 2016 for base flow and storm water.

Table D-2.1-2 shows that the average, and maximum results for aluminum at E123 are greater than E121 and E122 for base flow and storm water. Aluminum is not a contaminant of concern associated with the Sandia wetland (LANL 2011, 203454). Laboratory studies of storm water runoff of reference watersheds have shown that aluminum frequently exceeds SWQC and is known to be sourced from natural landscapes underlain by Bandelier Tuff on the Pajarito Plateau (LANL 2013, 239557). On the Pajarito Plateau, much of the sediment-bound aluminum is associated with poorly crystalline silica-rich glass of Bandelier Tuff. As the tuff weathers, the glass particles and associated aluminum-form sediment that accumulate are entrained and transported by runoff of storm water. Aluminum exceedances observed at E123 indicate a source of Bandelier Tuff sediments in water samples from undeveloped hillslopes and side drainages surrounding the Sandia wetland.

For base flow, copper is the only metal that exceeded SWQC, except for aluminum. For copper the average of the SWQC exceedances at E121, E122, and E123 were approximately equivalent, ranging from 3.93 µg/L at E121 to 4.02 µg/L at E123. Gage station E121 reported the highest maximum concentration and the most samples exceeding SWQC for copper. This finding indicates the Sandia wetland is not a quantifiable source of the copper in the SWQC exceedances at E123.

Copper, lead, and zinc are common constituents in storm water discharging from developed environments. For copper, lead, and zinc exceedances of SWQC in storm water, the average and maximum concentrations at E123 are less than at E121 and E122. Thus, the Sandia wetland is not a quantifiable source of the copper, lead, and zinc in the SWQC exceedances at E123. Zinc, which exceeded SWQC at E121 and E122 but did not exceed SWQC at E123, indicating the wetland is not a source of zinc but actually attenuates zinc as storm water flows through the wetland.

PCBs, historically used in hundreds of industrial and commercial applications in developed environments in the United States, are a common constituent in storm water discharging from developed environments. However the average and maximum concentrations of PCBs at E121 and E122 are less than E123 for base flow and storm water, indicating the Sandia wetland may be a source of PCBs. The Sandia wetland contains a known inventory of PCBs within the sediments as a result of spills at SWMU 03-056(c), a former transformer storage area. SWMU 03-056(c) is located just upgradient of E121, and PCB sediments from the SWMU may still be influencing the concentrations of PCBs at E121. Figure D-2.0-7 shows box plots of PCBs concentrations in storm water at E121, E122, and E123 for 2016 and the previous 4 yr. The plots show a decreasing trend of PCB concentrations through time at all three gage locations. The box plots also show that E121 and E123 annually have a comparative range of PCB values.

One sample from E122 exceeded SWQC for benzo(a)anthracene, benzo(a)pyrene, benzo(b)fluoranthene, and benzo(k)fluoranthene. These compounds are PAHs. Asphalt and coal tar sealants are common sources of PAHs and they are widely distributed in developed environments with asphalt roads, roofing materials, and coal tar sealants (Rogge et al. 1993, 602276; Yunker et al. 2002, 602278; Wang and Mulligan 2006, 602277; Mahler et al. 2012, 602275). However, since one sample exceeded SWQC the source of the exceedance is difficult to determine. No PAH exceedances were detected at E123 during 2016.

One sample exceeded SWQC for gross alpha at E121 and one sample for cadmium at E122 on November 4 and October 3, 2016, respectively; the source of these exceedances is not known. However, gross alpha in storm water is known to be sourced from undeveloped landscapes underlain by Bandelier Tuff (LANL 2013, 239557).

D-3.0 ANALYTICAL RESULTS FROM ALLUVIAL SYSTEM

Selected analytical results for water chemistry time-series data (filtered) from the alluvial sampling array are presented in Figures D-3.0-1 to D-3.0-10. Time-series plots are presented in the relative spatial distribution of the wells in the wetland (i.e., the upper plots are from the most northerly wells in each transect, ordered from west to east; the middle set of plots are from wells in the center of each transect, again ordered from west to east; and bottom plots are from the southernmost wells in each transect, in the same orientation) making up four transects running north to south along through the wetland. Additionally surface water entering the wetland at gage station E121 and exiting the wetland at gage station E123 is plotted at the western and easternmost parts of the wetland, respectively, serving as a comparison of input and output base flow chemistry. Differences between base flow data and alluvial water data may indicate subsurface processes (e.g., reduction) and provide information about residence times in the alluvial system. Key analytes plotted include a major cation (magnesium); a major conservative anion (chloride); a species that reflects changes in outfall chemistry (silicon dioxide); key contaminants (dissolved arsenic and chromium); and redox-sensitive species (sulfate, iron, manganese, ammonium, and sulfide) (Figures D-3.0-1 to D-3.0-10). As(III), Cr(VI), and Fe(II) speciated data were collected and are plotted along with the total arsenic, chromium, and iron, respectively (Figures D-3.0-4, D-3.0-5, and D-3.0-8).

D-3.1 Temporal Trends

Although no significant temporal trends are observed for most of the species and locations, over the last 3 yr a general decrease in arsenic and sulfate concentrations and an increase in iron and manganese concentrations have been observed in certain locations sampled in the wetland.

A decrease in arsenic, a contaminant of concern, has been observed in most wells, suggesting a reduction of mobility of the arsenic species as the reducing environment continues to persist with new inputs of organic matter that potentially bind the arsenic (Wang and Mulligan 2006, 602277) (Figure D-3.0-4). Whether this decrease of arsenic is related to the minor decrease in wetland surface water input concentrations, as suggested at surface water flow monitoring location E121, is not clear. Favorable temporal decreases in sulfate concentrations have been observed in the easternmost transect (Figure D-3.0-6). Lower values of sulfate, a redox-sensitive species, indicate an increase in sediment reduction capacity. This area was drier and more channelized before the GCS was constructed. Since the recovery from disturbance associated with the GCS, this transect has become more saturated with the proliferation of vegetation and less channelization, reflected in the observed decreases of sulfate, especially at SWA-4-10. Both these trends show some signs of leveling out since 2015 (Figures D-3.0-4 and D-3.0-6), indicating further stabilization of subsurface wetland conditions.

A steady increase in iron concentrations is observed in SWA-1-3, SWA-2-5, SWA-2-6, SWA-3-7, and SWA-3-9. As confirmed by the speciation data, most of this iron is Fe(II), the reduced form (section D-3.3 and Figure D-3.0-8). Increases in reduced iron suggest increases in reducing conditions. Likewise, small increasing trends of manganese were observed at SWA-3-7, SWA-3-8, and SWA-3-9 (Figure D-3.0-9). Most of the manganese is believed to be in its reduced form as well, with increases indicating increasing reducing conditions in alluvial sediment.

D-3.2 Spatial Trends

Concentrations at E121 and E123 are approximately the same for all species, other than Cr(VI) whose concentrations are lower at E123 (section D-3.3), indicating short residence times for surface water compared with the alluvial system. In general, the concentrations in the wetland alluvial waters are about equal to the concentrations in surface water for chloride, magnesium, and silicon dioxide, species that are not redox sensitive. Concentrations of arsenic, manganese, iron, sulfide, and ammonium tend to be

higher in the alluvial system than in surface water, indicating reducing conditions in the alluvial system. Conversely, sulfate concentrations tend to be lower in the wetland than in surface water, also suggesting more reducing conditions in the alluvial system. The high concentrations of total chromium primarily represent colloidal Cr(III) (section D-3.3).

Spatial trend evaluation of the alluvial well transects indicates the wells in the westernmost transect, with the exception of SWA-1-1 where the screen is deeper, seem to have somewhat lower reducing conditions compared with the other transects. As discussed in Appendix C, the western transect is drier at the surface and composed of coarse-grained and organically poor sediment. The easternmost transect has had a lot of variability in concentrations of redox-sensitive species in the past as a result of channelization before the GCS was constructed and disturbances during its construction; however, after installation of the GCS, the concentrations of most species appear to be leveling out. Additional monitoring should confirm this observation.

As silica reflects the changes in outfall chemistry, the variation in concentrations is indicative of changes in the incoming water at E121 (Figure D-3.0-3). Changes in silica concentrations are observed at E121 with a 3- to 6-mo delayed signal present in most of the alluvial sampling locations, suggesting slow connectivity of the surface and alluvial water is present. Locations SWA-1-1, SWA-2-5, SWA-2-6, and SWA-3-8 show more constant concentrations of silica, reflecting less connectivity with the surface water; lower sulfate values detected in these locations imply a more reducing environment.

Most alluvial locations have lower sulfate concentrations than surface water input to the wetland, reflecting the strong reducing conditions in wetland sediments (Figure D-3.0-6). Locations with historically higher values of sulfate include SWA-1-2, which has coarse-grained and organically poor sediment; SWA-3-7 for unknown reasons; and SWA-4-10, SWA-4-11, and SWA-4-12, which have been disturbed by the construction of the GCS. However, in the past year, all locations, with exception of SWA-3-7, have observed a decrease in concentrations of sulfate, indicating increasingly reducing alluvial sediment conditions reflecting the expansion of wetland vegetation and resaturation occurring at the head and terminus of the wetland. Locations SWA-2-5 and SWA-2-6 are particularly reducing based on lower sulfate concentrations relative to other locations. Location SWA-2-6 is in a very stagnant area based on observations of limited standing water with no apparent flow. Wells SWA-2-5 and SWA-3-8 are in or next to the central surface water flow path in the wetland but may be completed in tighter, more reducing sediments.

Sulfide has been detected throughout the wetland, further confirming the overall reducing nature of the system (Figure D-3.0-7). This is particularly clear when comparing sulfide concentrations in alluvial locations with those found in base flow where sulfide has not been detected. With sulfide near the bottom of the redox ladder, other species, including arsenic, iron, and chromium, are expected to be present primarily in their reduced forms, as observed in the speciated data (section D-3.3).

Location SWA-2-5 and wells in the easternmost transect have the highest concentrations of iron (Figure D-3.0-8). A relative decrease and stabilization of iron concentrations were observed in the easternmost downgradient transect. The historically higher values are believed to be of colloidal iron, which has decreased as a result of the recovery from disturbance caused by the installation of the GCS, as suggested by other constituents.

Alluvial manganese concentrations are typically higher than concentrations in surface water at E121 (Figure D-3.0-9). All the locations appear to be strongly reducing with respect to manganese at the depth of screen completion. Locations SWA-1-2 and SWA-1-3 have somewhat lower manganese concentrations, consistent with their shallow completion depths in sands and gravels. Location SWA-2-4 also has somewhat lower concentrations of manganese.

Dissolved total chromium concentrations in the wetland alluvial system are quite high (the New Mexico Environment Department [NMED] groundwater standard for exceedance of chromium is 50 ppb [section D-3.4]) with significant spatial variation in chromium distribution (Figure D-3.0-5), but predominantly reflects colloidal Cr(III) (section D-3.3 and Figure D-3.0-5). Given the colloidal nature of chromium, it is difficult to make meaningful spatial comparisons of total chromium, but locations SWA-1-2, SWA-1-3, SWA-4-10, and SWA-4-11 have higher concentrations on average, with the latter two, perhaps resulting from disturbance associated with GCS construction in the easternmost transect. The reason for higher colloidal Cr(III) in the westernmost transect is not clear.

As identified by the speciation data (section D-3.3), the arsenic detected in the wetland is in the reduced form, As(III) (Figure D-3.0-4). Locations SWA-1-1, SWA-2-5, and SWA-2-6 have higher concentrations of arsenic than in surface water, suggesting these locations are most reducing. An increase in arsenic at SWA-1-2 indicates an increase in the reducing conditions of this location, perhaps as a result of the expansion of cattails in this area.

Ammonium concentrations are generally nondetections in surface waters but are frequently detected in the alluvial system, confirming the reducing nature of wetland sediments (Figure D-3.0-10). Ammonium is stable under reducing conditions in the wetland and likely derives from mineralization of organic matter (e.g., dead cattail fronds). High concentrations of ammonium are not necessarily expected in the subsurface because of potential nutritive uptake by wetland plants.

D-3.3 Speciation Results

Arsenic can exist as As(III) or As(V). As(III) is relatively mobile and should predominate under reducing conditions. As expected, within the range of analytical error, most of the total arsenic detected in analytical results from alluvial wells is As(III), confirming the reducing conditions of the wetland (Figure D-3.0-4).

As with arsenic, Fe(II), the reduced form of iron, is the predominant form present in alluvial waters of the wetland (Figure D-3.0-8). The Fe(II) results plotted above, or just slightly below, total iron concentrations, suggesting most of the iron in solution is Fe(II). Total iron concentrations higher than Fe(II) are believed to be samples with colloidal Fe(III).

The concentrations of Cr(VI) measured in the alluvial system over the past 2 yr were nearly all nondetections (Figure D-3.0-5), with the exceptions of detections at SWA-3-7 and at SWA-3-9. These detections of Cr(VI) are only slightly above the minimum detection limit for Cr(VI) and are similar to or less than those detected in base flow (Figure D-3.0-5), suggesting the total chromium analysis is sampling mostly colloidal Cr(III) in the alluvial waters. The overall lack of Cr(VI) detections reflects the strongly reducing conditions in the wetland. The highest detections of Cr(VI) concentration are at E121 and E122 with concentrations up to 11.5 µg/L in May 2015 at E122. These higher concentrations of Cr(VI) entering the wetland are believed to be from potable water derived from the regional aquifer and concentrated in the cooling towers (section D-2.0). Knowing that these incoming concentrations of Cr(VI) at E121 and E122 are reduced at E123, it can be confirmed that exchange and reduction are occurring in the wetland.

D-3.4 Screening Alluvial Water Results to Groundwater Standards

The alluvial system data from 2016 were screened to the screening standard in the 2016 Compliance Order on Consent. Alluvial data were evaluated using the following screening process:

- Groundwater data are screened in accordance to Section IX of the Consent Order. For an individual substance, the lower of the New Mexico Water Quality Control Commission (NMWQCC) groundwater

standard or U.S. Environmental Protection Agency (EPA) maximum contaminant level (MCL) is used as the screening value.

- If an NMWQCC groundwater standard or an MCL has not been established for a specific substance for which toxicological information is published, the NMED screening level for tap water is used as the groundwater screening value. The NMED screening levels are for either a cancer- or noncancer-risk type. For the cancer-risk type, the screening levels are based on a 10^{-5} excess cancer risk. This appendix was prepared using the July 2015 NMED screening levels for tap water.
- If an NMED screening level for tap water has not been established for a specific substance for which toxicological information is published, the EPA regional screening level for tap water is used as the groundwater screening value. The EPA screening levels are for either a cancer- or noncancer-risk type. For the cancer-risk type, the Consent Order specifies screening at a 10^{-5} excess cancer risk. The EPA screening levels for tap water are for 10^{-6} excess cancer risk, so 10 times the EPA 10^{-6} screening levels is used in the screening process. This report was prepared using the May 2016 EPA regional screening levels for tap water.

The screening standard exceedances for the alluvial system, including the screening value and screening value type, are presented in Table D-3.4-1.

Exceedances of iron and manganese concentrations are observed at most of the wells during most sampling events. These exceedances are expected because the wetland is a reducing environment, and speciated Fe(II) data indicate that most, if not all, the iron in the alluvial system within the wetland is in its reduced form (section D-3.3). With manganese at nearly the same location on the redox ladder as iron, most of this manganese is expected to be in its reduced state as well. Location SWA-2-6 had two exceedances of 10.288 µg/L and 10.611 µg/L in August and November 2016, respectively, slightly above the screening value of 10 µg/L.

The speciated arsenic data indicate that all the aqueous arsenic in the alluvial system is As(III), the reduced mobile form, and is present as an exceedance only because alluvial wells, which are in subsurface-reducing conditions, were sampled. Once exposed to oxygen, this As(III) would likely convert to As(V) and be immobilized in a mineral phase.

As discussed in section D-3.3, most of the total chromium is colloidal Cr(III), the nontoxic form. Exceedances of chromium occurred in wells SWA-1-2, SWA-4-10, and SWA-4-12 during the August 2016 sampling round. The Cr(VI) for these events in both SWA-4-10 and SWA-4-12 are nondetections, and only SWA-1-4 had a detection of Cr(VI), which is probably from the higher detected concentration of Cr(VI) at E121 entering the wetland during this same event.

Exceedances of lithium values are observed throughout the wetland. As Figure D-3.4-1 shows, however, the highest values of lithium are observed at E121, entering the wetland. Lithium is a relatively conservative species. Lithium concentrations are present and vary naturally through the regional aquifer (Blake et al. 1995, 049931). Because the regional aquifer water is used as potable water throughout the Laboratory and is part of SWWS discharge blended with SERF water, it is released into the wetland. As observed with the elevated incoming concentrations of Cr(VI) at E121 and E122, elevated lithium entering the wetland is believed to be concentrated from the natural source of lithium in regional aquifer waters.

D-4.0 WATER-LEVEL RESULTS FROM ALLUVIAL SYSTEM

Water-level data were continuously recorded in alluvial wells SWA-1-2, SWA-2-6, SWA-3-8, and SWA 4-12 in 2016 and in piezometers SCPZ-1, SCPZ-5, SCPZ-8, SCPZ-11B, and SCPZ-12 before they were replaced by alluvial wells. Sondes were reinstalled in SWA-3-9 at the end of May and at all other

2016 installed alluvial wells by end of September 2016. The delay in transducer installment and well completion is because of the additional installation of the outer casing that occurred about a month after the installation of the well.

Water-level data are presented in Figure D-4.0-1 for calendar years 2015 and 2016. The plots are arranged within the figures to represent the spatial distribution of the alluvial locations throughout the wetland. Daily flows at gaging station E121 and precipitation data from the weather station at E121.9 are plotted along with the alluvial water-level data. The E121 data include inputs from Outfalls 001 and 03A027 from January 2015 to September 2016 and only from Outfall 001 from September 2016 to December 2016; surface-water flow from precipitation and runoff is included in the data.

Overall, minimal changes in water level were observed between the piezometers and alluvial wells for most locations, with larger variation when the wells were farther from the original piezometer location. Temperatures were consistent with those of previous years, showing temporal changes with seasons and with less variation in wells located in the channel (SCPZ-1, SCPZ-5, and SCPZ-5) (Figure D-3.0-2).

- *SWA-1-1 (SCPZ-1), SWA-1-2 (SCPZ-2), and SWA-1-3 (SCPZ-3):* The 2016 data showed continued rapid responses to changes in water levels as noted in previous years for this transect (top plot in Figure D-4.0-1). Water levels responded almost immediately to precipitation events (tenths of feet to 1.5 ft, depending on the size of the event). In addition, water levels responded quickly, but to a much lesser extent, to changes in base flow (driven by effluent releases at Outfalls 001 and 03A027), confirming the aquifer material in this narrow transect is relatively transmissive and storage is minimal. The changes in water level between alluvial wells and piezometers seem to be less than 0.2 ft, with the exception of SWA-1-1 and SCPZ-1 where the difference is 0.5 ft because SWA-1-1 is located farther from SCPZ-1.
- *SWA-2-4 (SCPZ-4), SWA-2-5 (SCPZ-5), and SWA-2-6 (SCPZ-6):* In 2016, water levels at the second transect (second plot from top in Figure D-4.0-1) also responded almost immediately to precipitation and showed much lower responses to variations in flow at gage E121. The variations are generally only a few tenths of a foot and are short-lived. The stability of water levels in this transect reflects the saturated conditions that occur in this part of the wetland. Surface flow spreads across a broad area in this well-vegetated transect. The fine-grained alluvial material has a lower hydraulic conductivity such that it neither drains nor fills rapidly, resulting in extremely flat water-level data. The changes in water level between alluvial wells and piezometers seem to be less than 0.2 ft.
- *SWA-3-7, SWA-3-8 (SCPZ-8), and SWA-3-9 (SCPZ-9):* In 2016, water levels at the third transect (third plot from top in Figure D-4.0-1) showed similar responses to those observed in the past. Water levels show rapid responses to both precipitation events and to outfall-driven changes in base flow. The near-instantaneous response to precipitation events and variations in base flow imply a strong connection to flowing surface waters. The changes in water level between alluvial wells and piezometers seem to be less than 0.2 ft.
- *SWA-4-10 (SCPZ-10), SWA-4-11 (SCPZ-11B), and SWA-4-12 (SCPZ-12):* Again, water levels in 2016 (bottom plot in Figure D-4.0-1) responded quickly to both precipitation events and to variations in outfall flows (as measured by gage E121). The drops in water level have been observed in this transect during the summers. It appears the drop in water levels occurs after the monsoon season has ended and little precipitation occurs. This drop in precipitation coincides with the highest annual temperatures recorded in wetland waters (Figure D-4.0-2) and is hypothesized to result from increased evapotranspiration from vegetation. The changes in water level between alluvial wells and piezometers seem to be less than 0.2 ft, with the exception of SWA-4-12 and SCPZ-12 where the difference in water levels is approximately 1 ft.

D-5.0 REFERENCES

The following list includes all documents cited in this appendix. Parenthetical information following each reference provides the author(s), publication date, and ERID or ESHID. This information is also included in text citations. ERIDs were assigned by the Environmental Programs Directorate's Records Processing Facility (IDs through 599999), and ESHIDs are assigned by the Environment, Safety, and Health (ESH) Directorate (IDs 600000 and above). IDs are used to locate documents in the Laboratory's Electronic Document Management System and, where applicable, in the master reference set.

Copies of the master reference set are maintained at the NMED Hazardous Waste Bureau and the ESH Directorate. The set was developed to ensure that the administrative authority has all material needed to review this document, and it is updated with every document submitted to the administrative authority. Documents previously submitted to the administrative authority are not included.

Blake, W.D., F.E. Goff, A.I. Adams, and D. Counce, May 1, 1995. "Environmental Geochemistry for Surface and Subsurface Waters in the Pajarito Plateau and Outlying Areas, New Mexico," Los Alamos National Laboratory report LA-12912-MS, Los Alamos, New Mexico. (Blake et al. 1995, 049931)

LANL (Los Alamos National Laboratory), May 2007. "Groundwater Background Investigation Report, Revision 3," Los Alamos National Laboratory document LA-UR-07-2853, Los Alamos, New Mexico. (LANL 2007, 095817)

LANL (Los Alamos National Laboratory), October 2009. "Investigation Report for Sandia Canyon," Los Alamos National Laboratory document LA-UR-09-6450, Los Alamos, New Mexico. (LANL 2009, 107453)

LANL (Los Alamos National Laboratory), May 2011. "Interim Measures Work Plan for Stabilization of the Sandia Canyon Wetland," Los Alamos National Laboratory document LA-UR-11-2186, Los Alamos, New Mexico. (LANL 2011, 203454)

LANL (Los Alamos National Laboratory), May 2012. "Polychlorinated Biphenyls in Precipitation and Stormwater within the Upper Rio Grande Watershed," Los Alamos National Laboratory document LA-UR-12-1081, Los Alamos, New Mexico. (LANL 2012, 219767)

LANL (Los Alamos National Laboratory), April 2013. "Background Metals Concentrations and Radioactivity in Storm Water on the Pajarito Plateau, Northern New Mexico," Los Alamos National Laboratory document LA-UR-13-22841, Los Alamos, New Mexico. (LANL 2013, 239557)

LANL (Los Alamos National Laboratory), June 2014. "Sandia Wetland Performance Report, Baseline Conditions 2012–2014," Los Alamos National Laboratory document LA-UR-14-24271, Los Alamos, New Mexico. (LANL 2014, 257590)

Mahler, B.J., P.C. Van Metre, J.L. Crane, A.W. Watts, M. Scoggins, and E.S. Williams, 2012. "Coal-Tar-Based Pavement Sealcoat and PAHs: Implications for the Environment, Human Health, and Stormwater Management," *Environmental Science & Technology,* Vol. 46, pp. 3039-3045. (Mahler et al. 2012, 602275)

Rogge, W.F., L.M. Hildemann, M.A. Mazurek, and G.R. Cass, 1993. "Sources of Fine Organic Aerosol. 3. Road Dust, Tire Debris, and Organometallic Brake Lining Dust: Roads as Sources and Sinks," *Environmental Science & Technology,* Vol. 27, pp. 1892-1904. (Wolfgang et al. 1993, 602276)

Wang, S., and C.N. Mulligan, 2006. "Effect of Natural Organic Matter on Arsenic Release from Soils and Sediments into Groundwater," *Environmental Geochemistry and Health,* Vol. 28, pp. 197-214. (Wang and Mulligan 2006, 602277)

Yunker, M.B., R.W. Macdonald, R. Vingarzan, R.H. Mitchell, D. Goyette, and S. Sylvestre, 2002. "PAHs in the Fraser River Basin: A Critical Appraisal of PAH Ratios as Indicators of PAH Source and Composition," *Organic Chemistry,* Vol. 33, pp. 489-515. (Yunker et al. 2002, 602278)

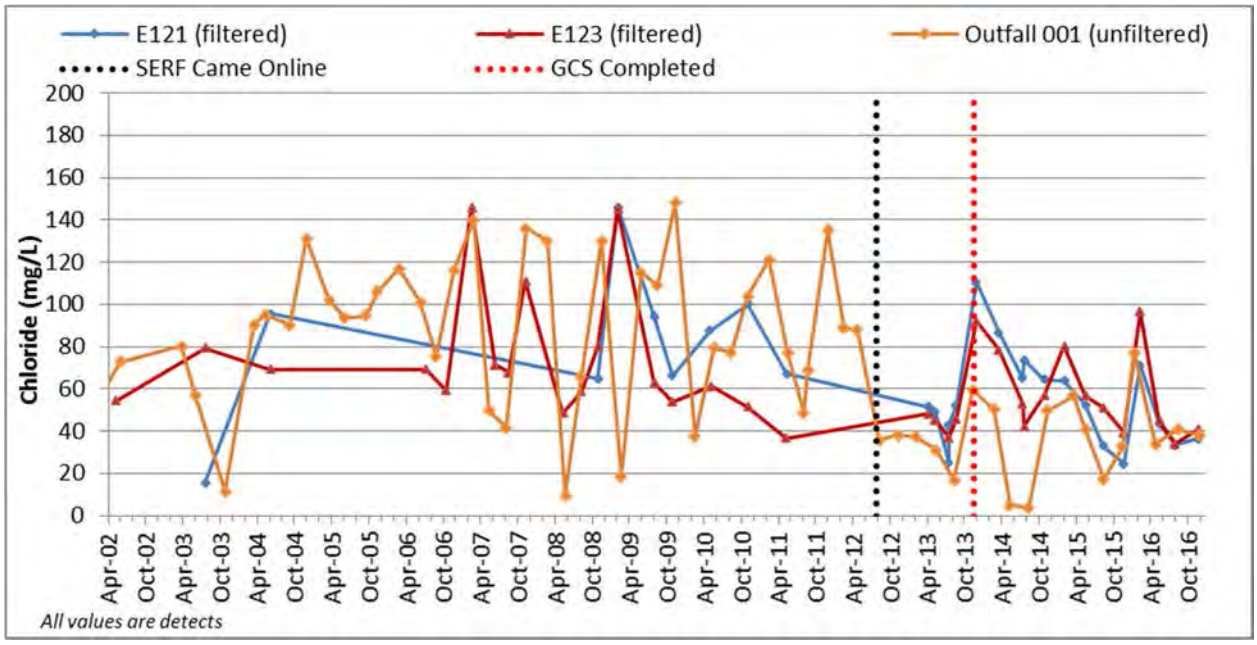

Figure D-2.0-1 Time-series plot showing chloride concentrations at gaging stations E121 and E123 and National Pollutant Discharge Elimination System– (NPDES-) permitted Outfall 001

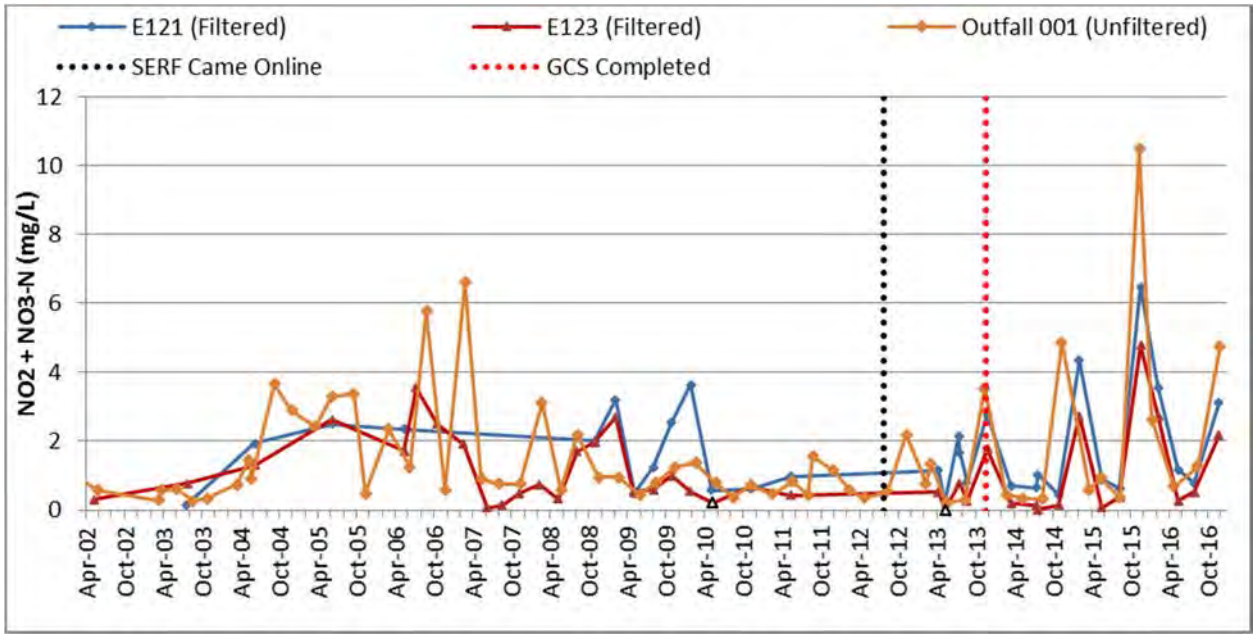

Notes: Final values for nitrate from Outfall 001 from 11/23/15 include initial analysis at 10.5 mg/L and reanalysis at 8.99 mg/L. The reanalysis exceeded the holding time. All open symbols are non-detects. Nondetect values are estimates when above the MDL; otherwise values equal to half the MDL are used.

Figure D-2.0-2 Time-series plot showing nitrate plus nitrite as nitrogen concentrations at gaging stations E121 and E123 and NPDES Outfall 001

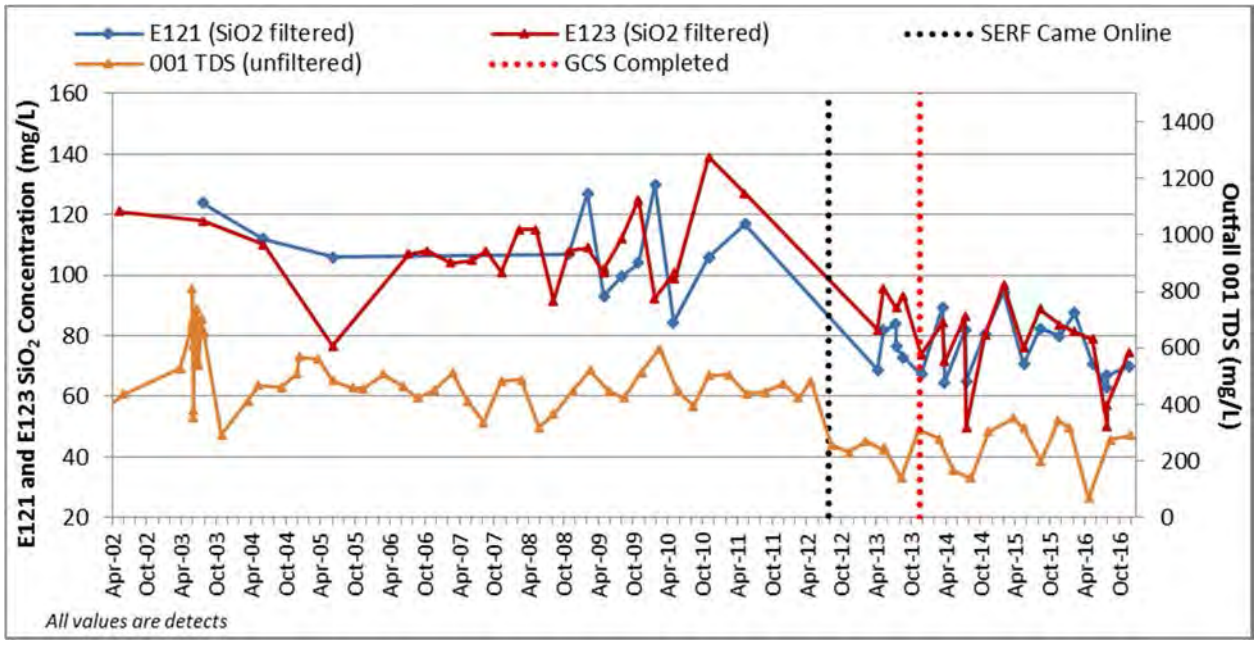

Figure D-2.0-3 Time-series plot showing silicon dioxide concentrations and TDS at gaging stations E121 and E123 and NPDES Outfall 001

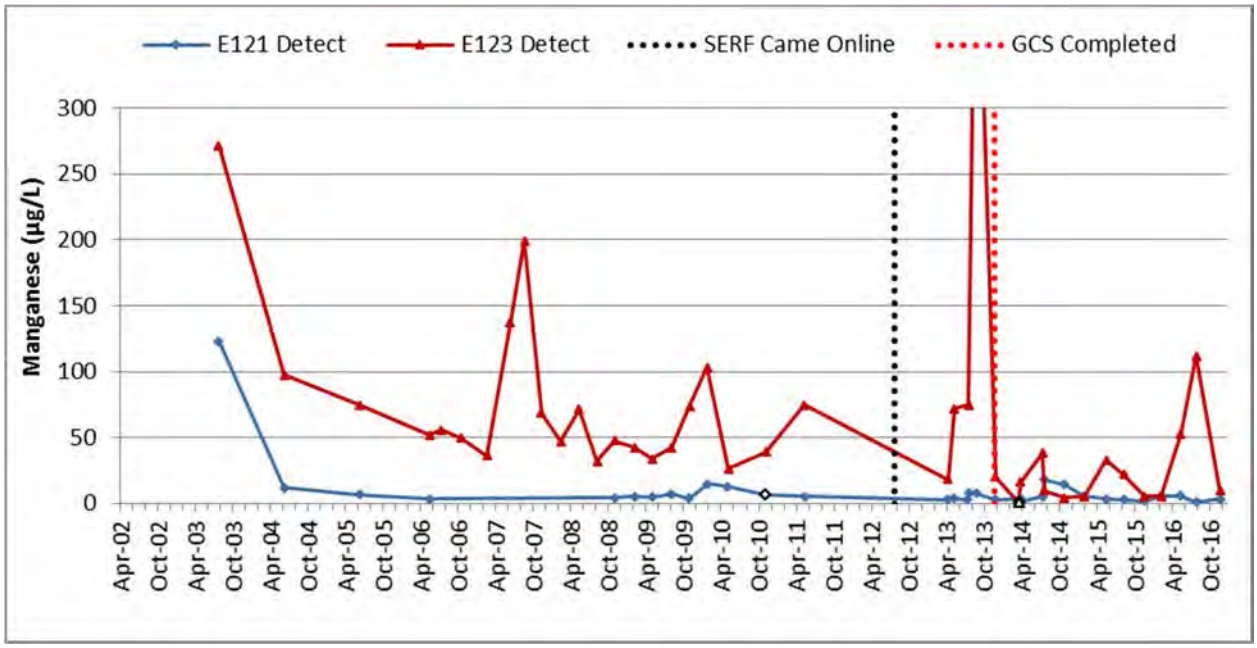

Note: The highest concentration of manganese plots off the scale of the chart and was 495.5 µg/L on August 30, 2013. All open symbols are nondetections.

Figure D-2.0-4 Time-series plot showing manganese concentrations at gaging stations E121 and E123

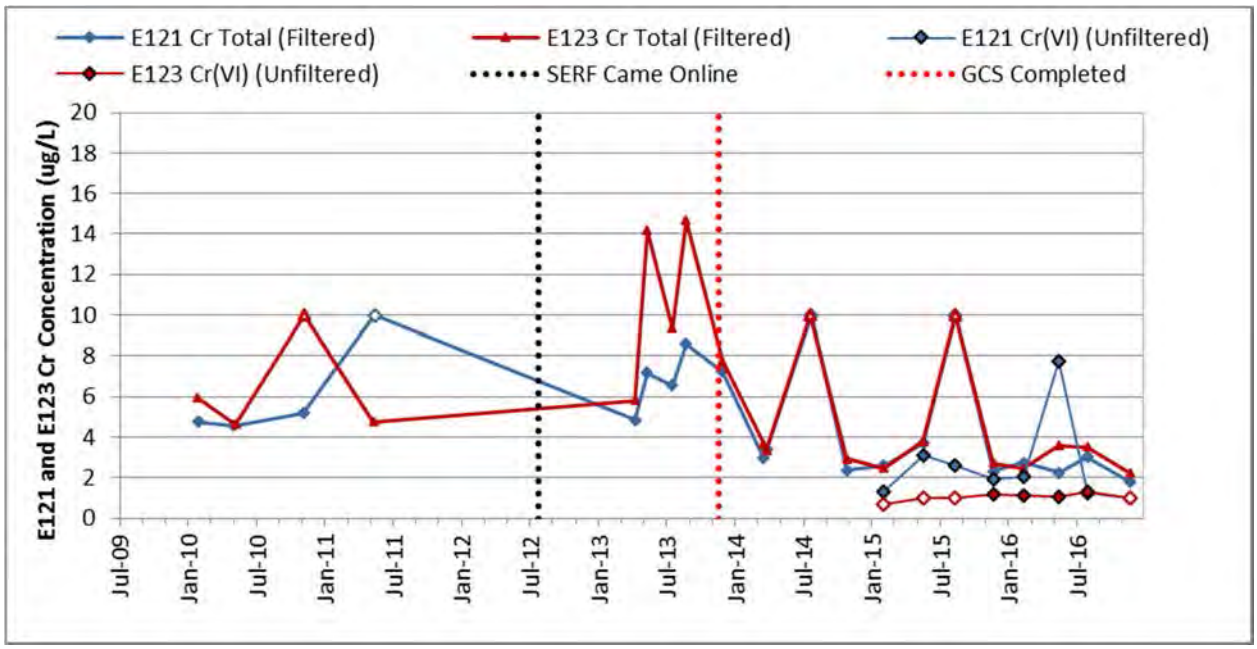

Notes: The small concentrations of Cr(VI) versus total chromium illustrate that most of the chromium within the wetland is colloidal Cr(III). Cr(VI) shows multiple detects in base flow into the wetland but is largely attenuated within the wetland with only a few detects near the detection limit at E123. Method detection limit at gaging stations is 1 µg/L. Cr(VI) at NPDES Outfall 001 was a nondetection with an method detection limit (MDL) of 3 µg/L (not shown on plot). All open symbols are nondetections.

Figure D-2.0-5 Time-series plot showing total chromium and Cr(VI) concentrations at gaging stations E121 and E123.

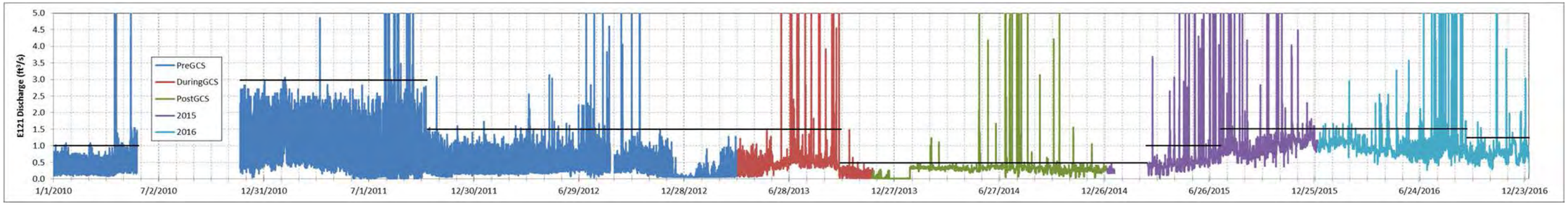

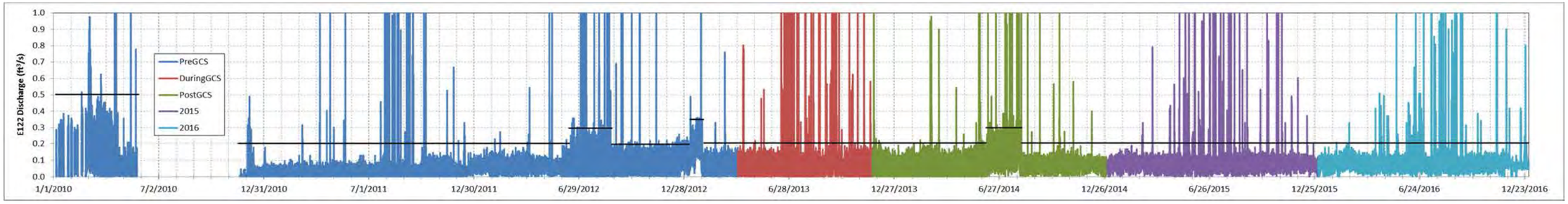

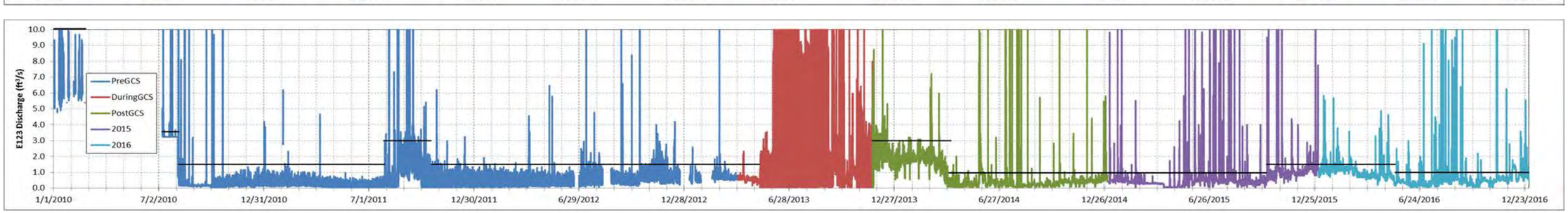

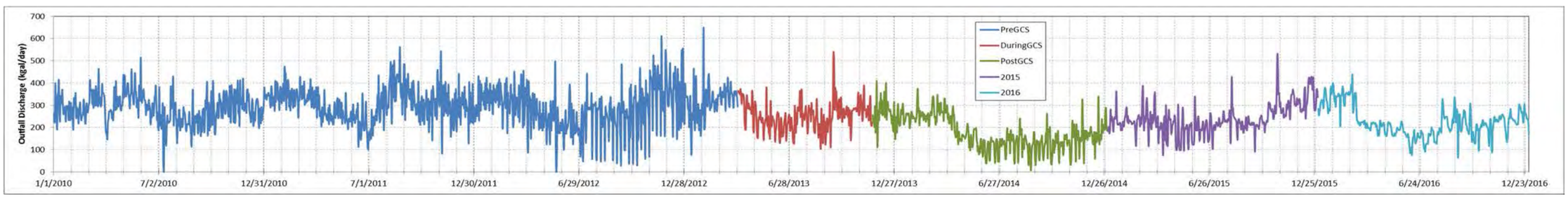

Figure D-2.0-6 **Time-series plots from 2010 to 2016 showing discharge at E121, E122, and E123 and total discharge from Outfalls 001, 03A027, and 03A199; solid black horizontal lines indicate approximate base-flow discharge at the surface-water gaging stations, which vary throughout the 7-yr period**

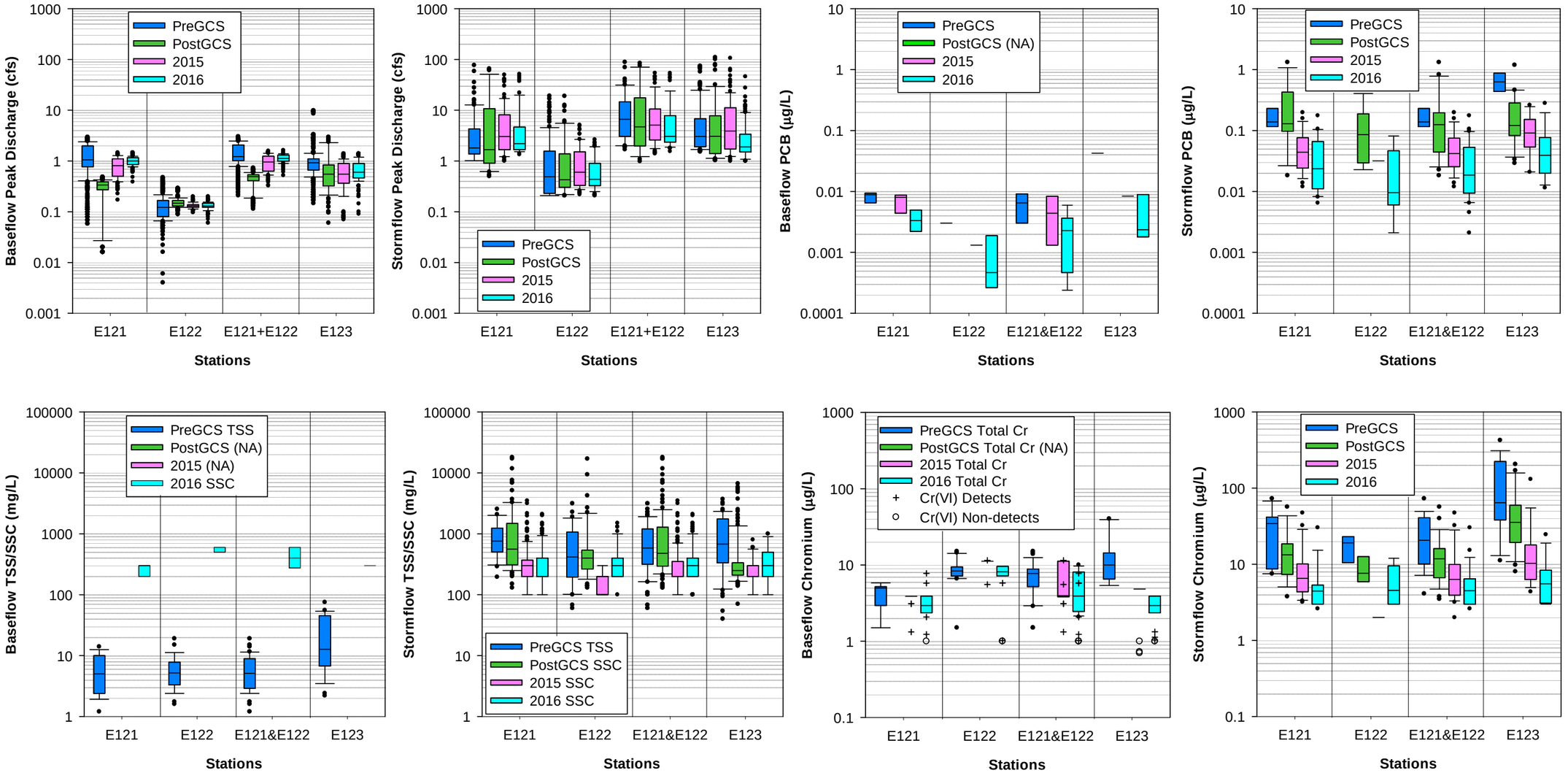

Figure D-2.0-7 **Box-and-whisker plots of peak discharge, TSS/SSC, PCBs, unfiltered chromium and Cr(VI), and PAHs for base flow and storm flow at gaging stations E121, E122, and E123, pre- and post-construction of the GCS, respectively, in 2015 and 2016. (NA = Not analyzed.)**

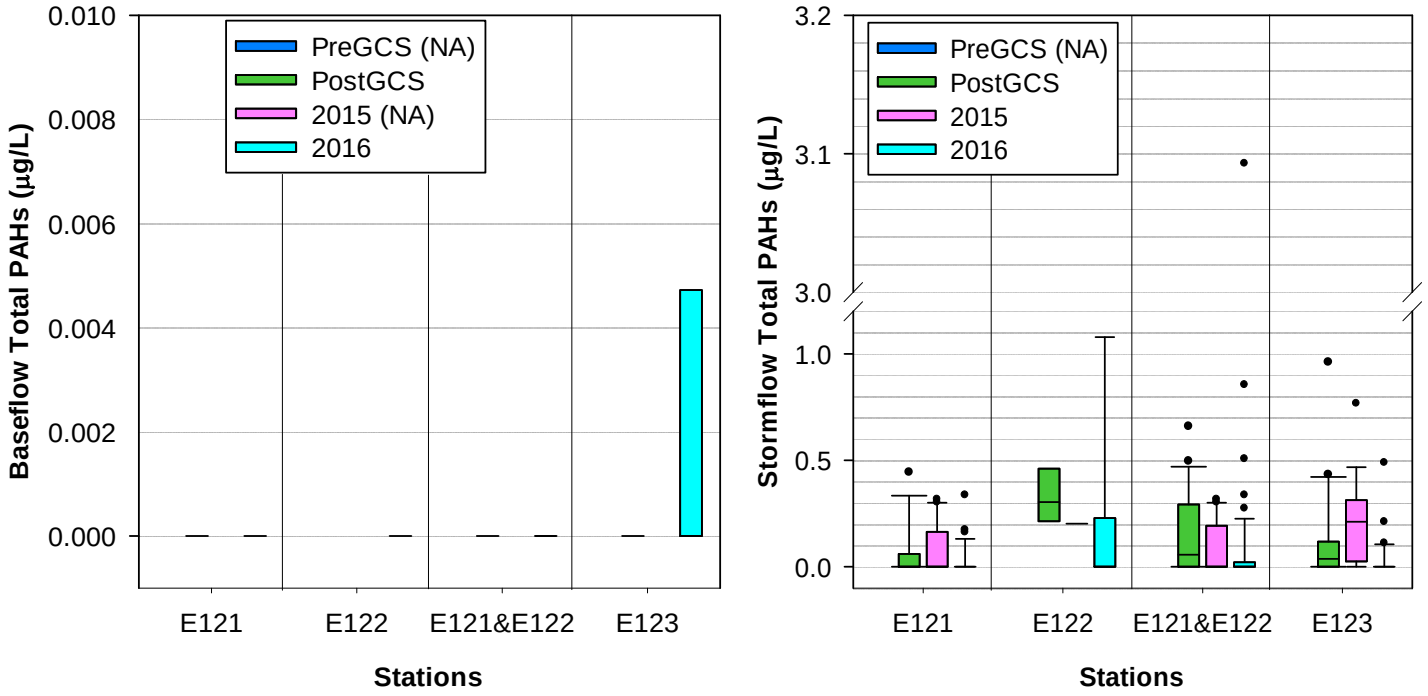

Figure D-2.0-7 (continued) **Box-and-whisker plots of peak discharge TSS/SSC, total PCBs, unfiltered chromium and Cr(VI), and total PAHs for base flow and storm flow at gaging stations E121, E122, and E123, pre- and post-construction of the GCS, respectively, in 2015 and 2016. (NA = Not analyzed.)**

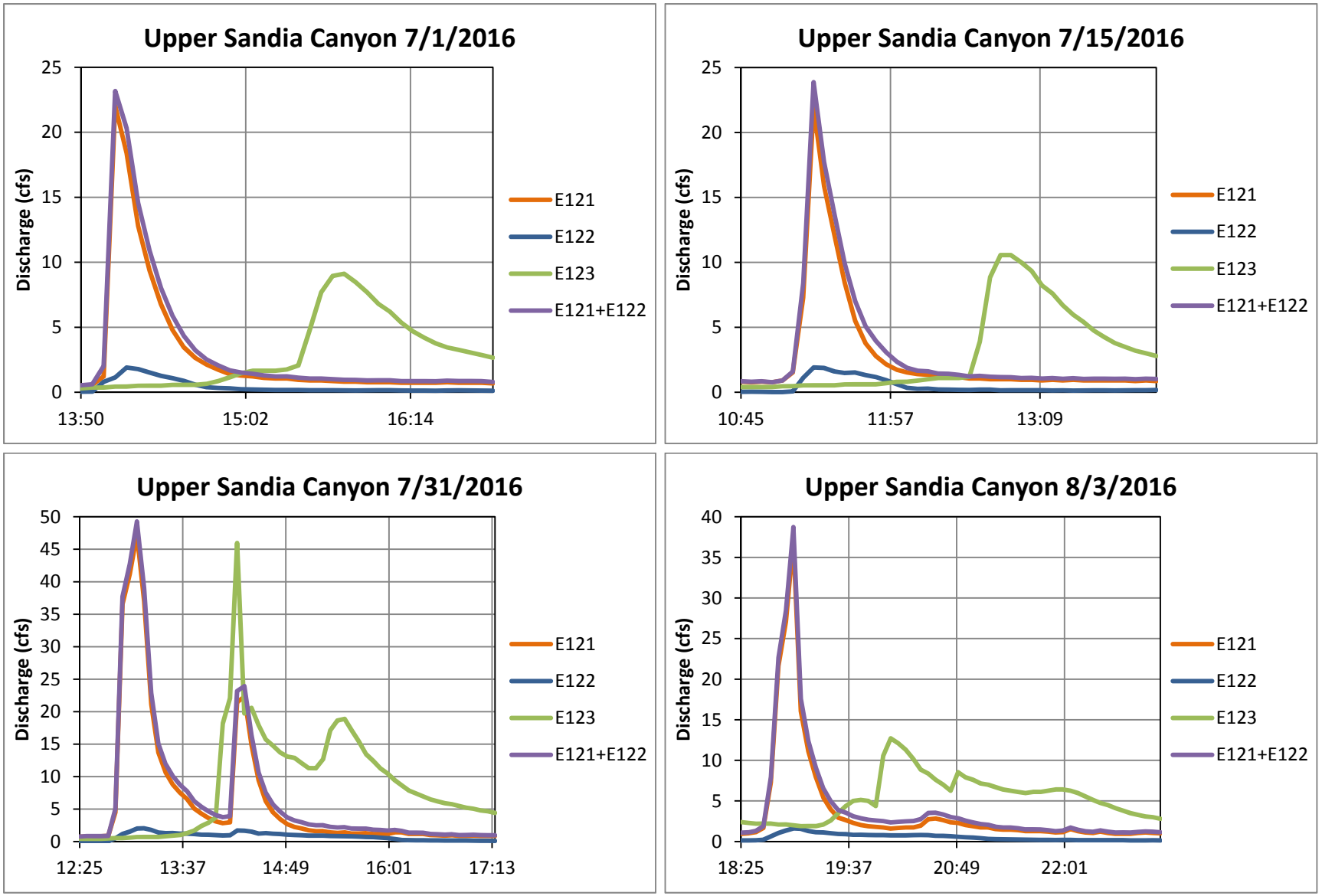

Figure D-2.0-8 Hydrographs of storm-water discharge at E121, E122, and E123 during each sample-triggering storm event in 2016

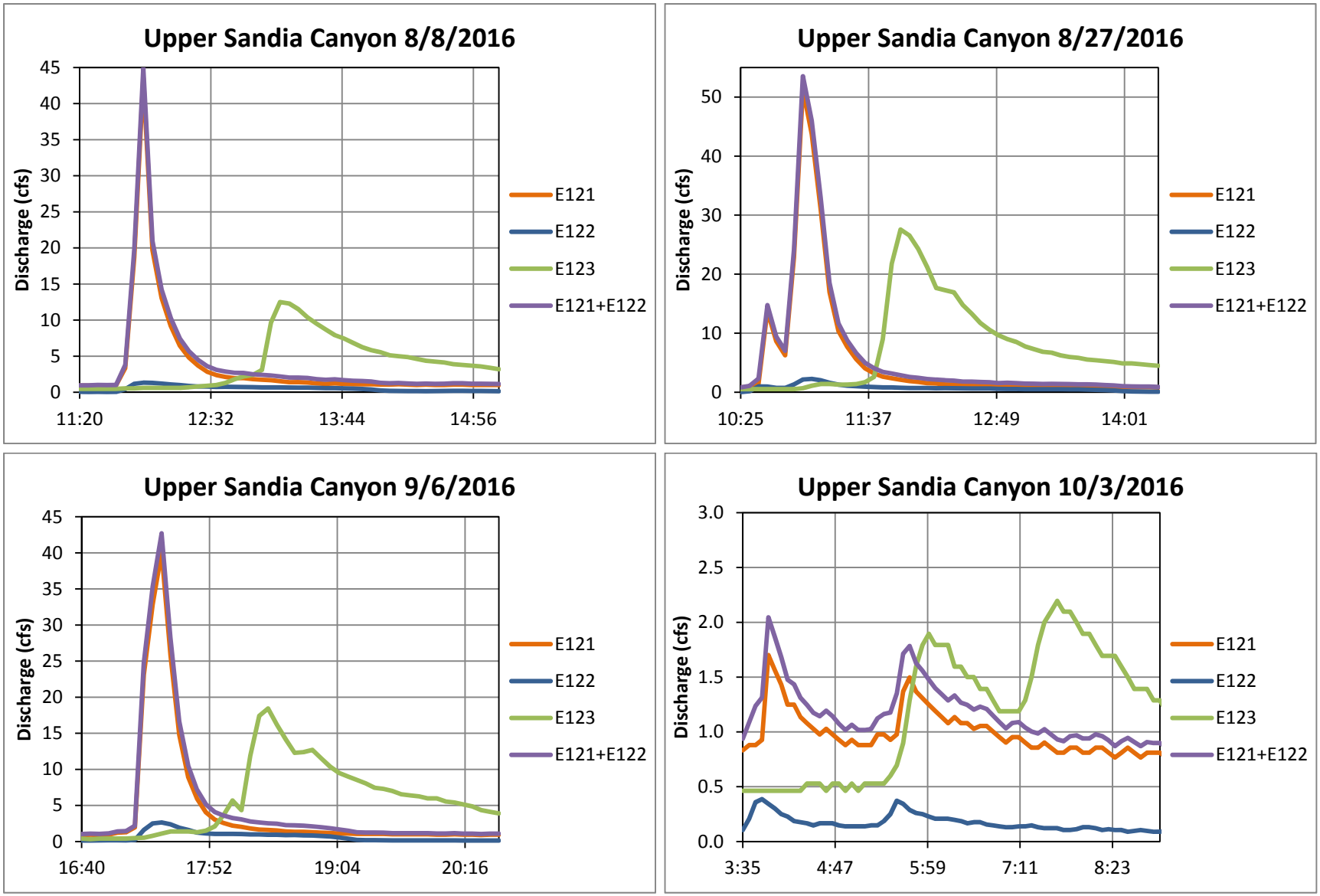

Figure D-2.0-8 (continued) **Hydrographs of storm-water discharge at E121, E122, and E123 during each sample-triggering storm event in 2016**

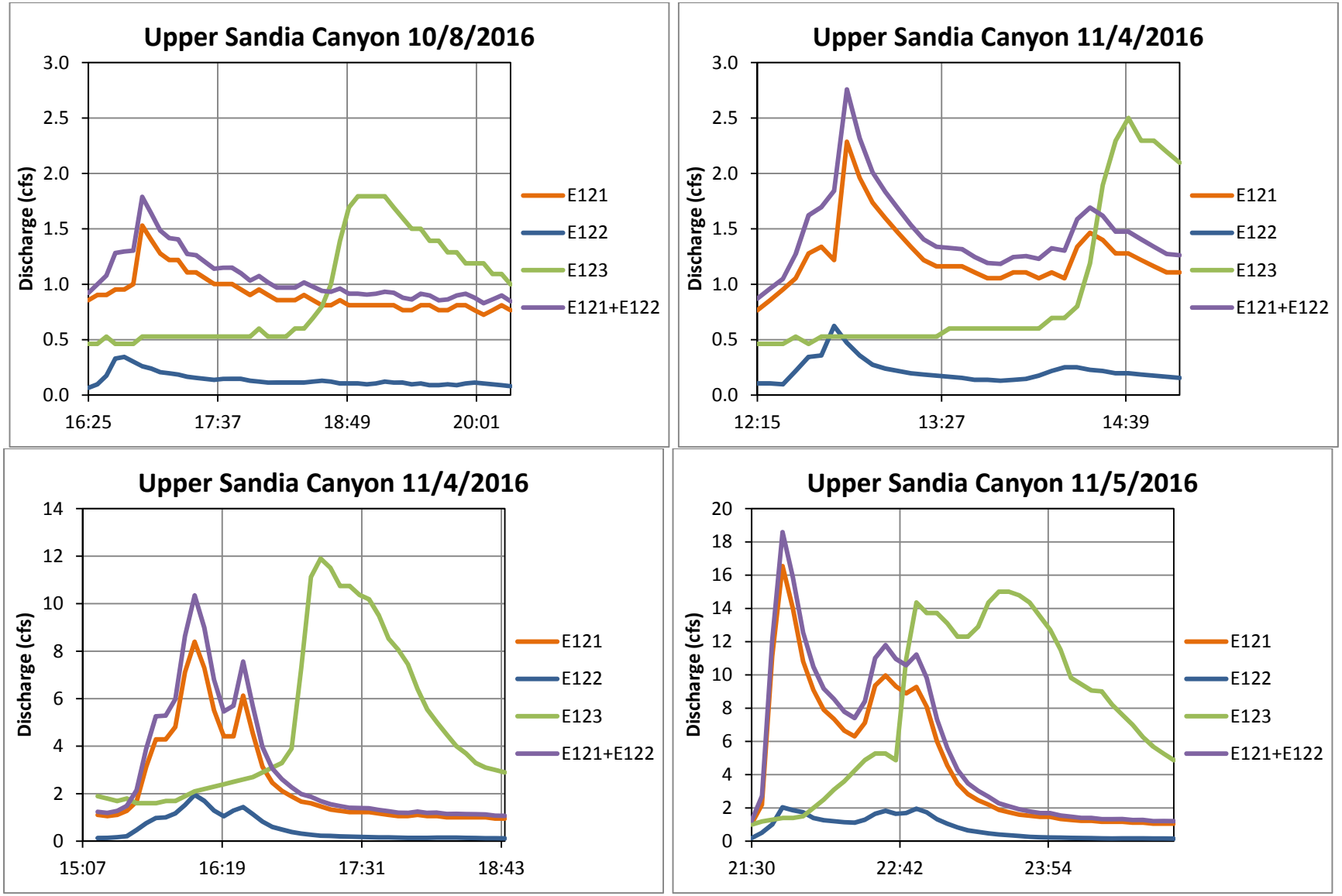

Figure D-2.0-8 (continued) **Hydrographs of storm water discharge at E121, E122, and E123 during each sample-triggering storm event in 2016**

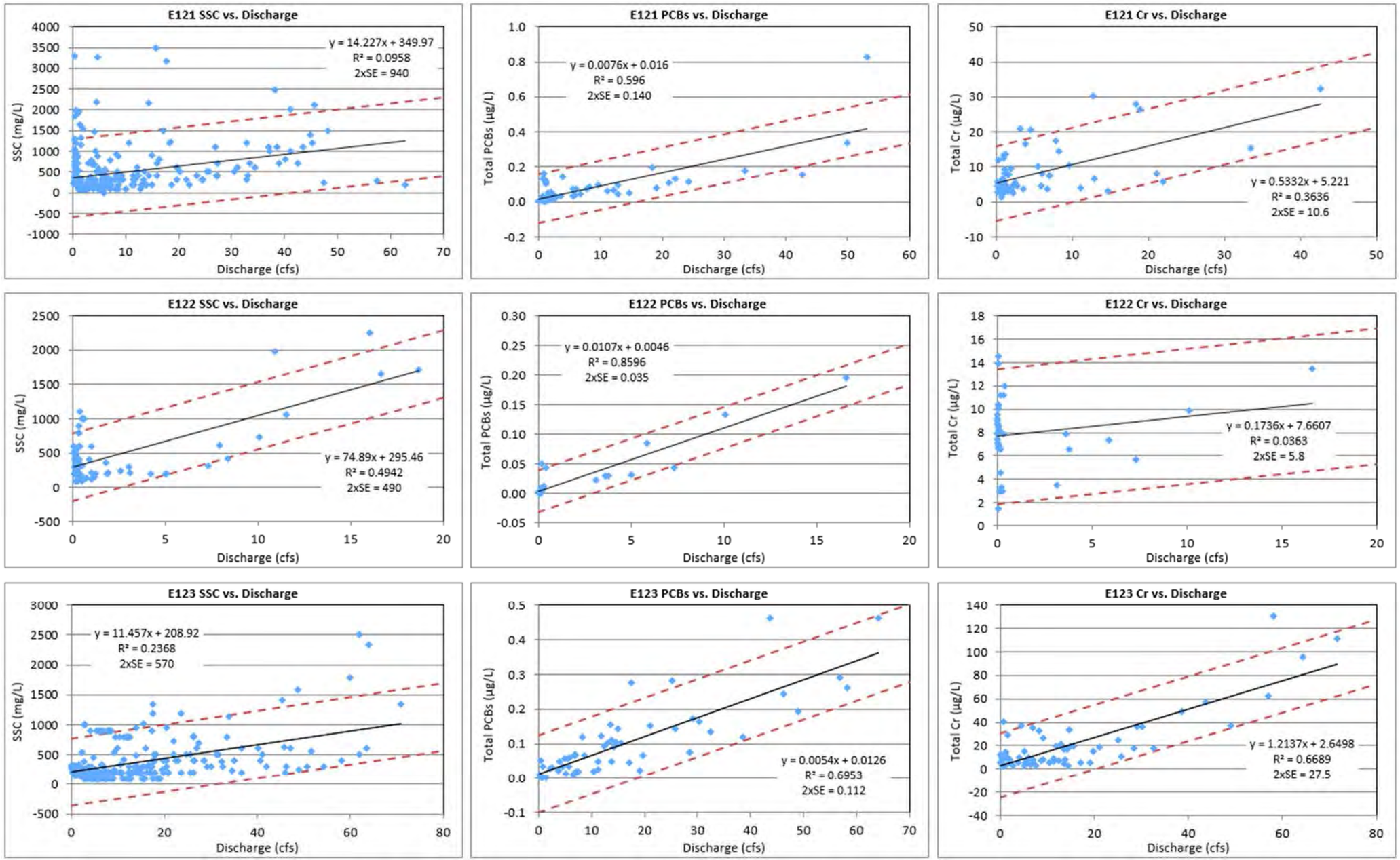

Figure D-2.0-9 Storm- and base-flow discharge correlations with SSC, total PCBs, unfiltered chromium, and total PAHs from 2014 to 2016 at E121, E122, and E123 with standardized residual outliers removed; the red dashed lines are 2 times the standard error (2×SE) of the estimate, as noted with the equation of the line and the Pearson's correlation coefficient (R^2)

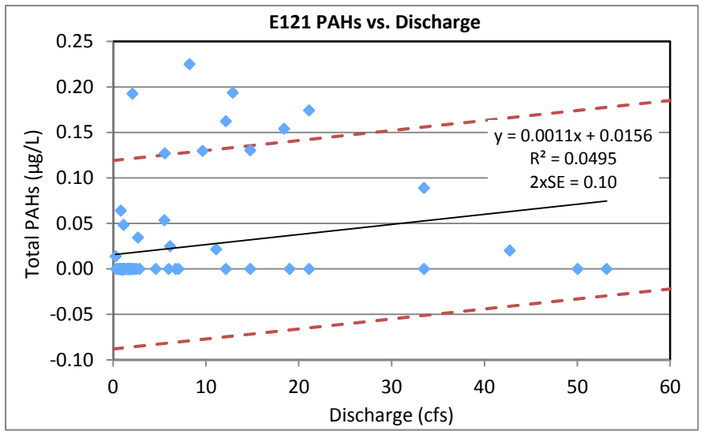

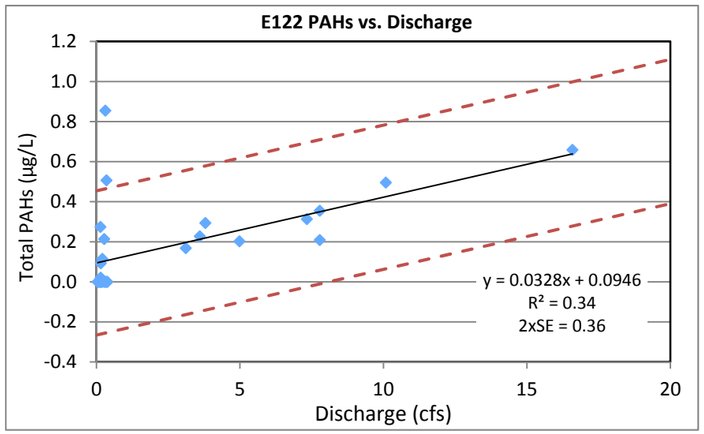

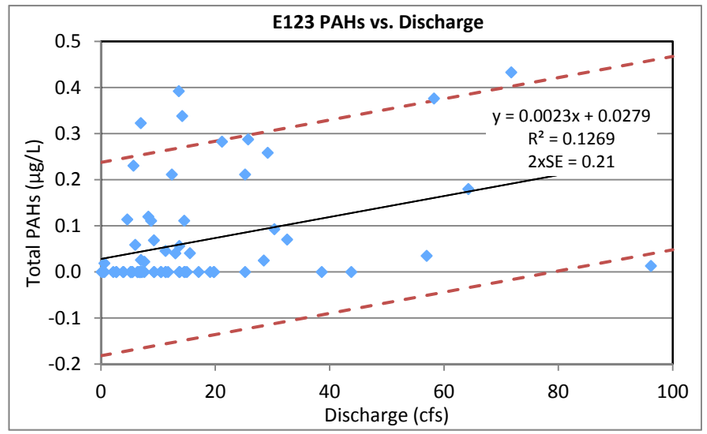

Figure D-2.0-9 (continued) **Storm- and base-flow discharge correlations with SSC, total PCBs, unfiltered chromium, and total PAHs from 2014 to 2016 at E121, E122, and E123 with standardized residual outliers removed; the red dashed lines are 2 times the standard error (2×SE) of the estimate, as noted with the equation of the line and the Pearson's correlation coefficient (R^2)**

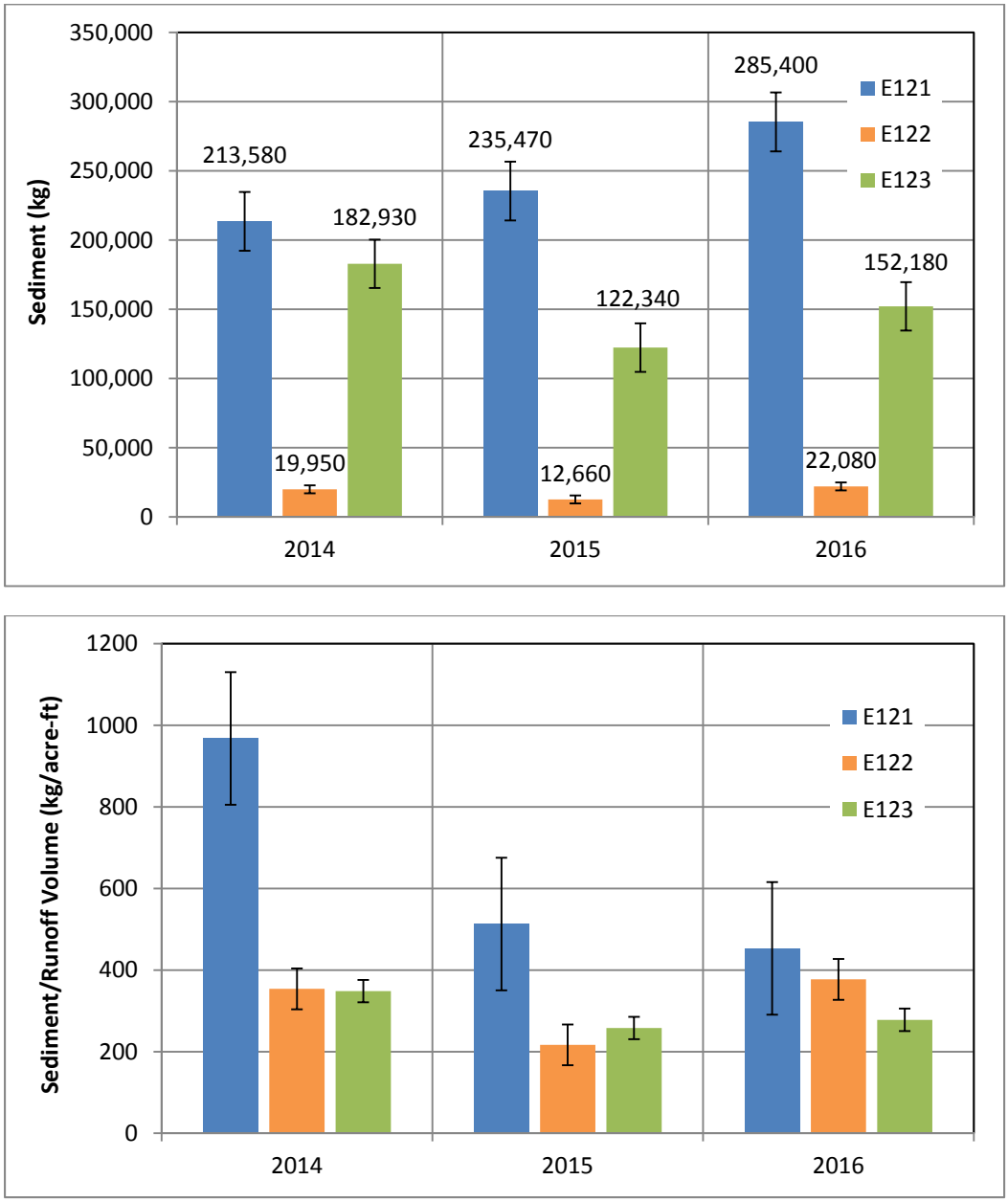

Figure D-2.0-10 **Annual mass flux (top) and annual mass flux normalized by runoff volume (bottom) for sediment at gaging stations E121 (blue), E122 (orange), and E123 (green) from 2014 to 2016. Gaging stations E121 and E122 represent inputs into the wetland, and E123 represents output from the wetland. Error bars represent the standard error of the mean.**

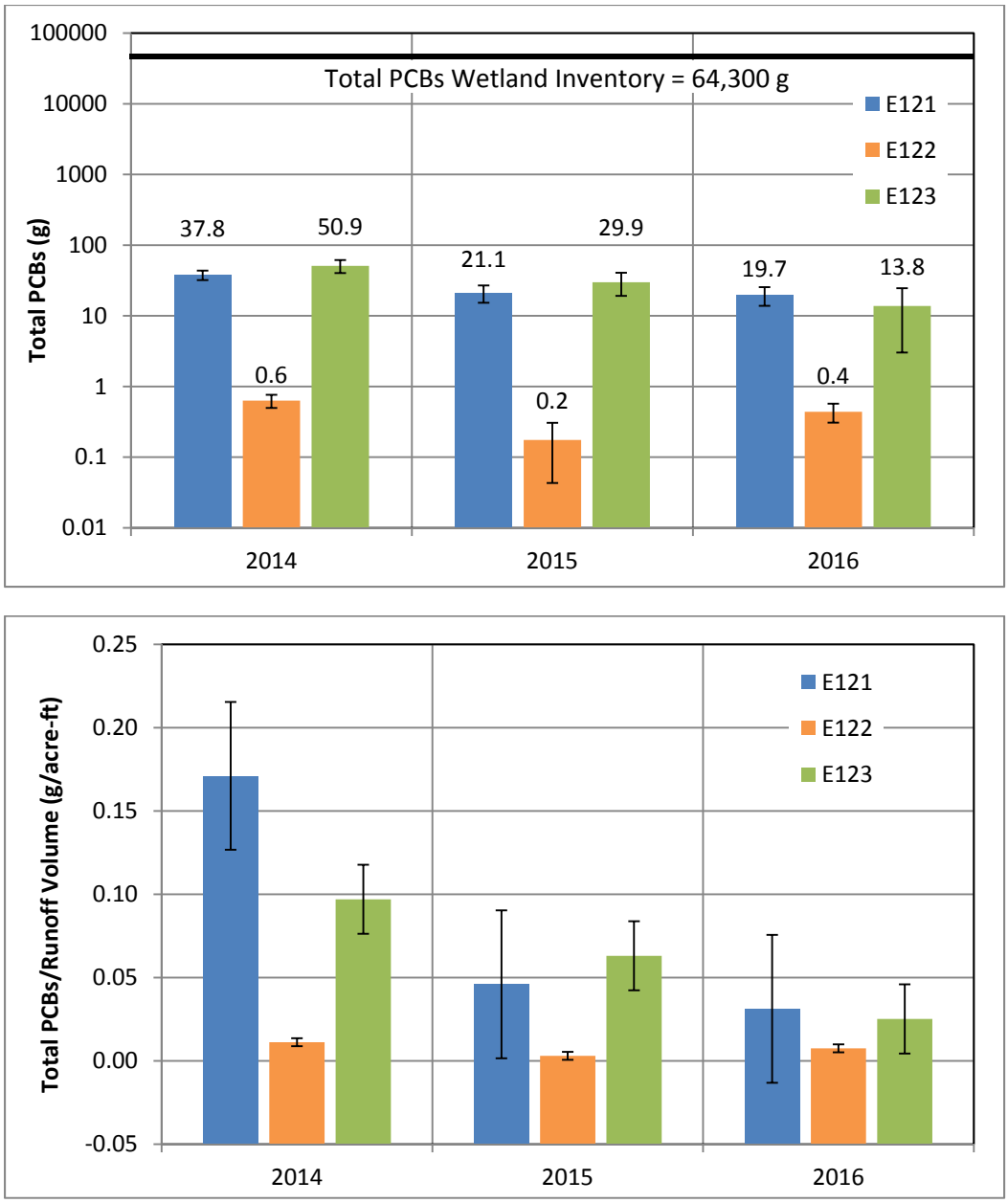

Figure D-2.0-11 **Annual mass flux (top) and annual mass flux normalized by runoff volume (bottom) for total PCBs at gaging stations E121 (blue), E122 (orange), and E123 (green) from 2014 to 2016. Gaging stations E121 and E122 represent inputs into the wetland, and E123 represents output from the wetland. Error bars represent the standard error of the mean.**

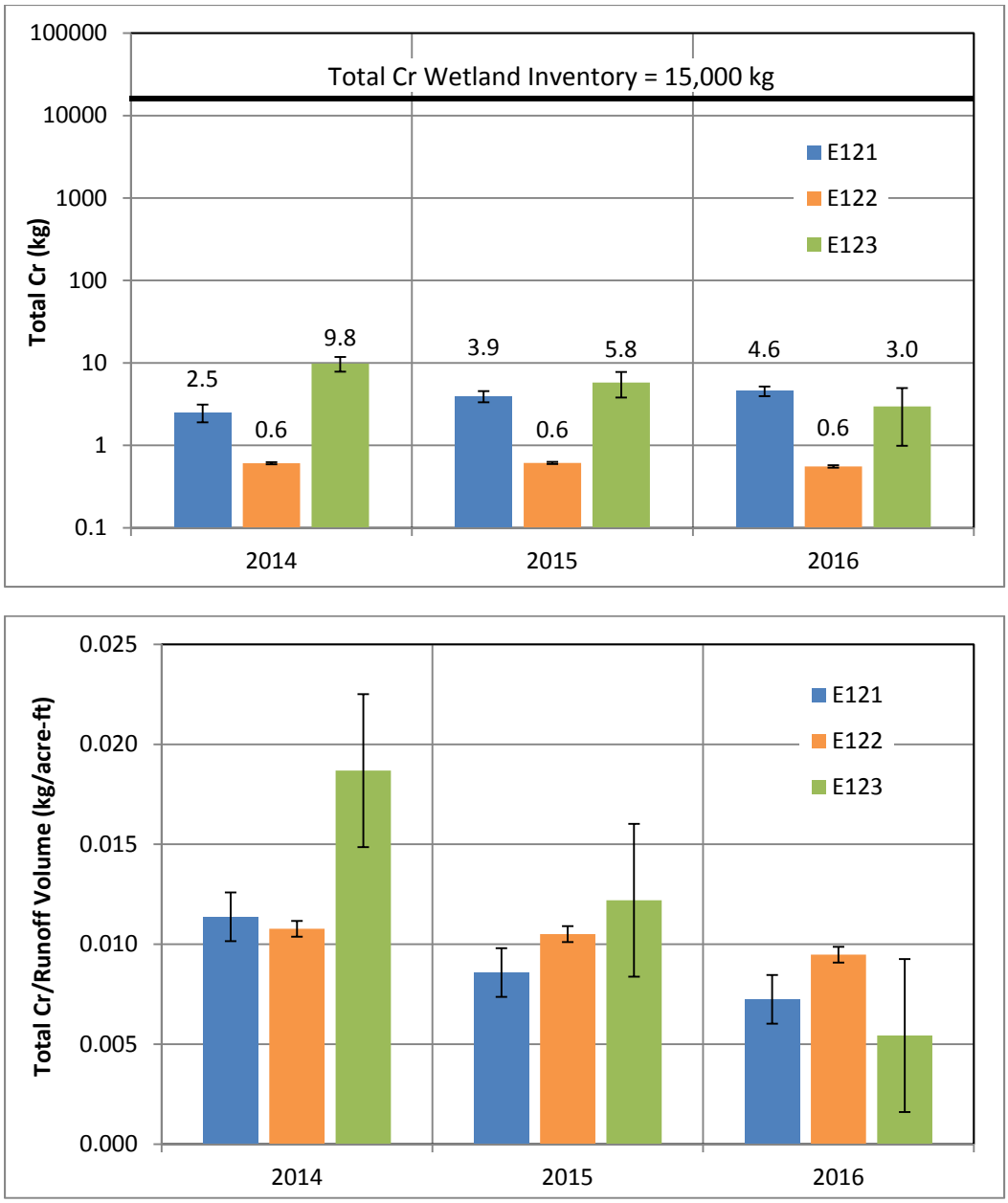

Figure D-2.0-12 Annual mass flux (top) and annual mass flux normalized by runoff volume (bottom) for total chromium at gaging stations E121 (blue), E122 (orange), and E123 (green) from 2014 to 2016. Gaging stations E121 and E122 represent inputs into the wetland, and E123 represents output from the wetland. Error bars represent the standard error of the mean.

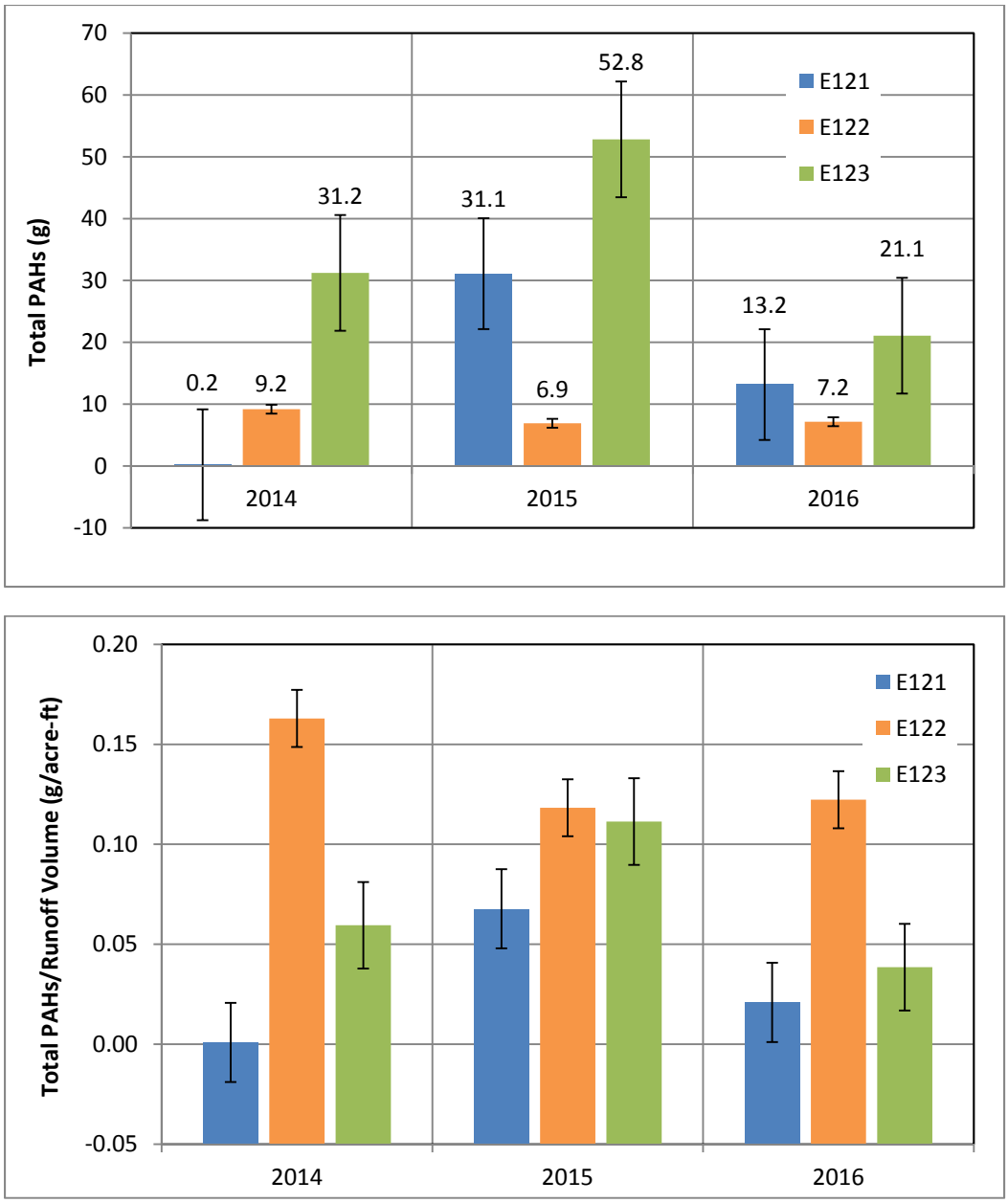

Figure D-2.0-13 **Annual mass flux (top) and annual mass flux normalized by runoff volume (bottom) for total PAHs at gaging stations E121 (blue), E122 (orange), and E123 (green) from 2014 to 2016. Gaging stations E121 and E122 represent inputs into the wetland, and E123 represents output from the wetland. Error bars represent the standard error of the mean.**

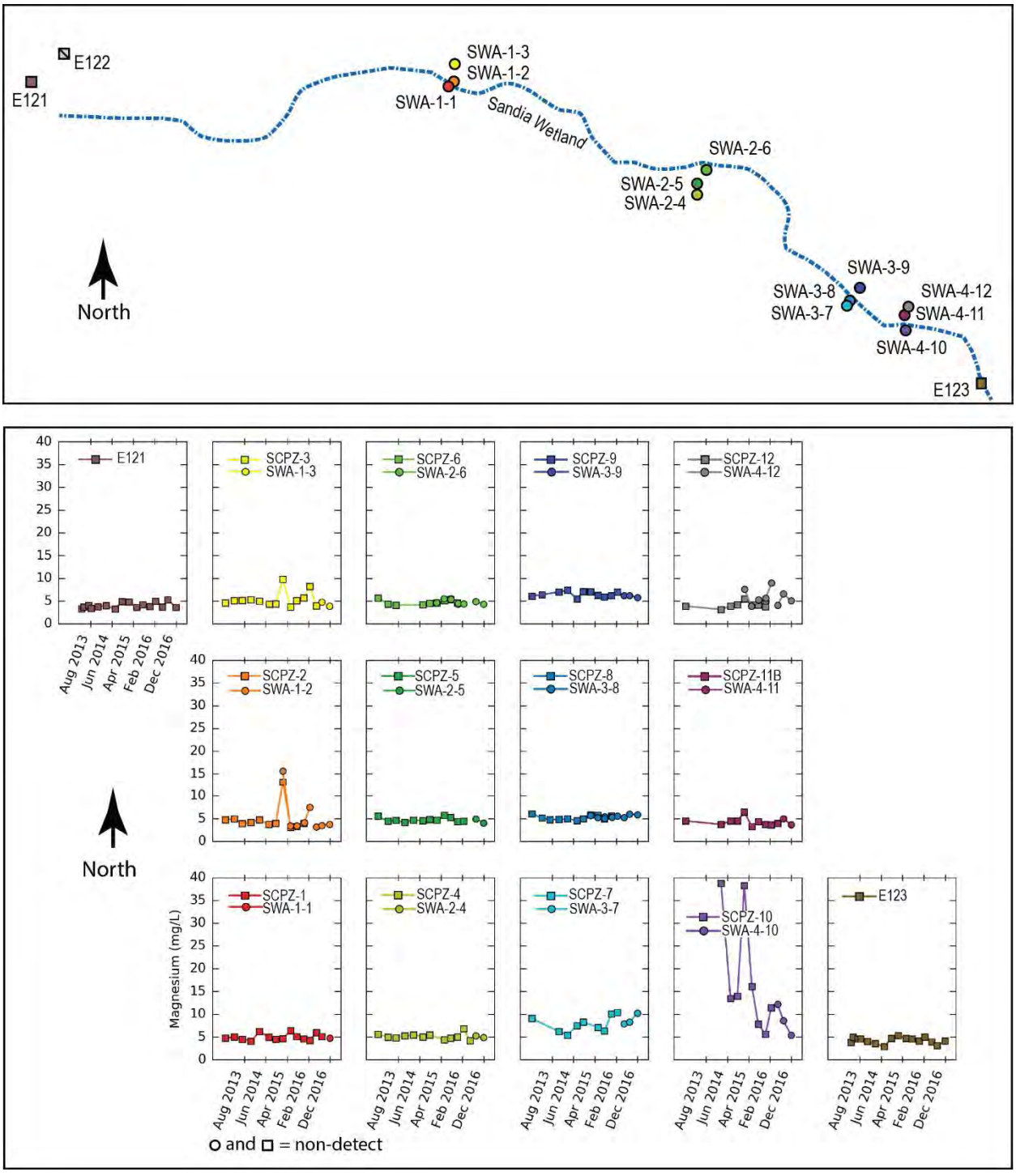

Notes: Surface water stations include E121, E122 (plot not shown), and E123. Piezometers are labeled with the prefix SCPZ (square symbols), and alluvial wells are labeled with the prefix SWA (circle symbols). The plots are arranged in four transects from west to east. Data are plotted for the full period of wetland monitoring. Nondetects are plotted as the MDL with open symbols. The map above is not to scale but shows approximate sampling locations in relation to the approximate thalweg (blue dashed line).

Figure D-3.0-1 Magnesium concentrations in Sandia wetland surface water and alluvial system

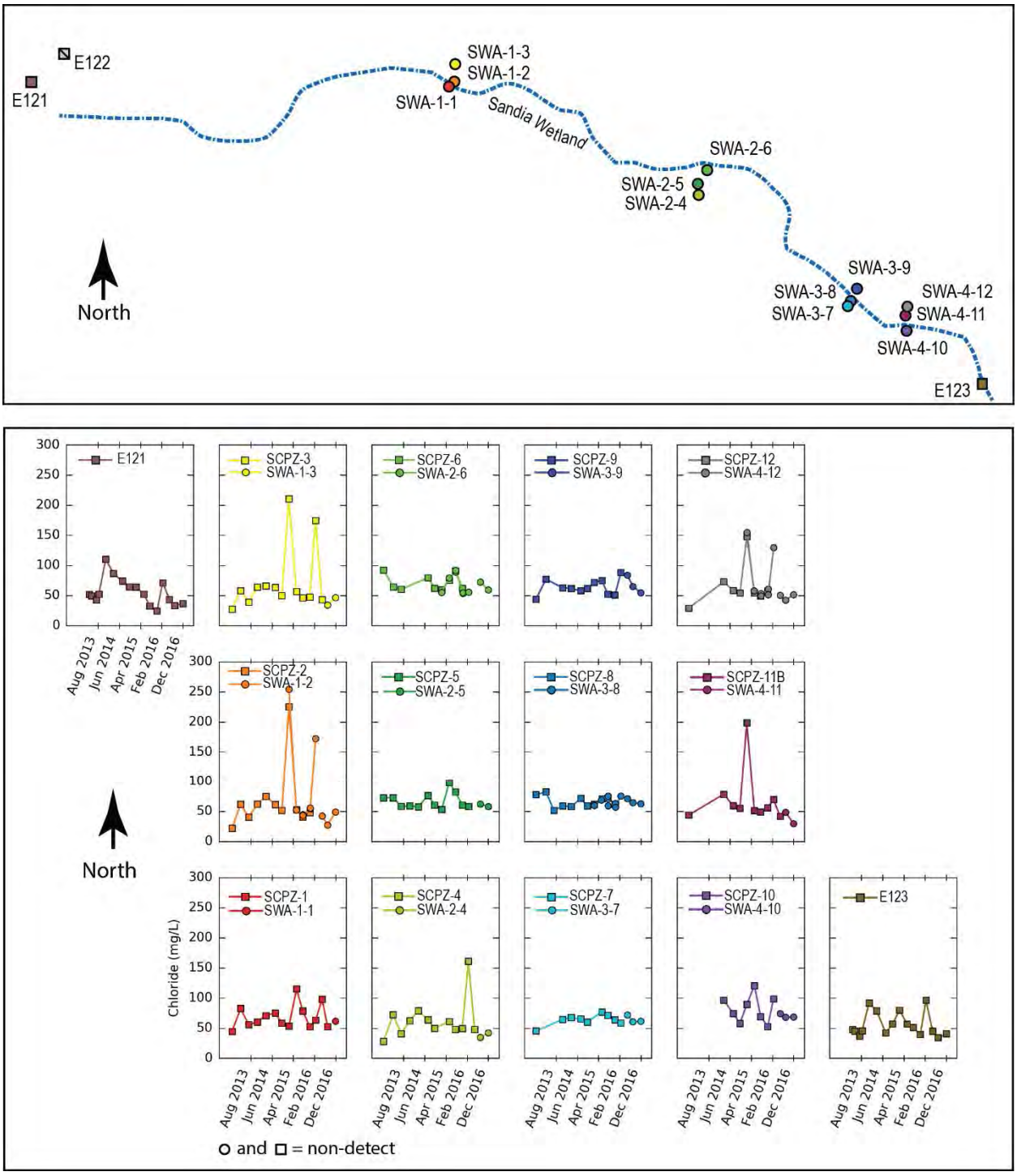

Notes: Surface water stations include E121, E122 (plot not shown), and E123. Piezometers are labeled with the prefix SCPZ (square symbols), and alluvial wells are labeled with the prefix SWA (circle symbols). The plots are arranged in four transects from west to east. Data are plotted for the full period of wetland monitoring. Nondetects are plotted as the MDL with open symbols. The map above is not to scale, but shows approximate sampling locations in relation to the approximate thalweg (blue dashed line).

Figure D-3.0-2 Chloride concentrations in Sandia wetland surface water and alluvial system

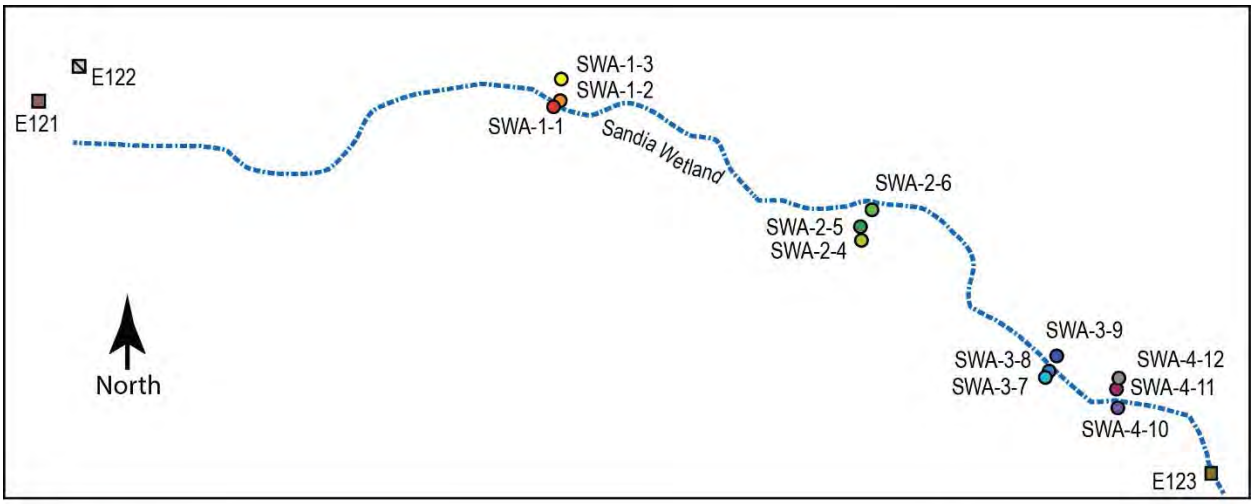

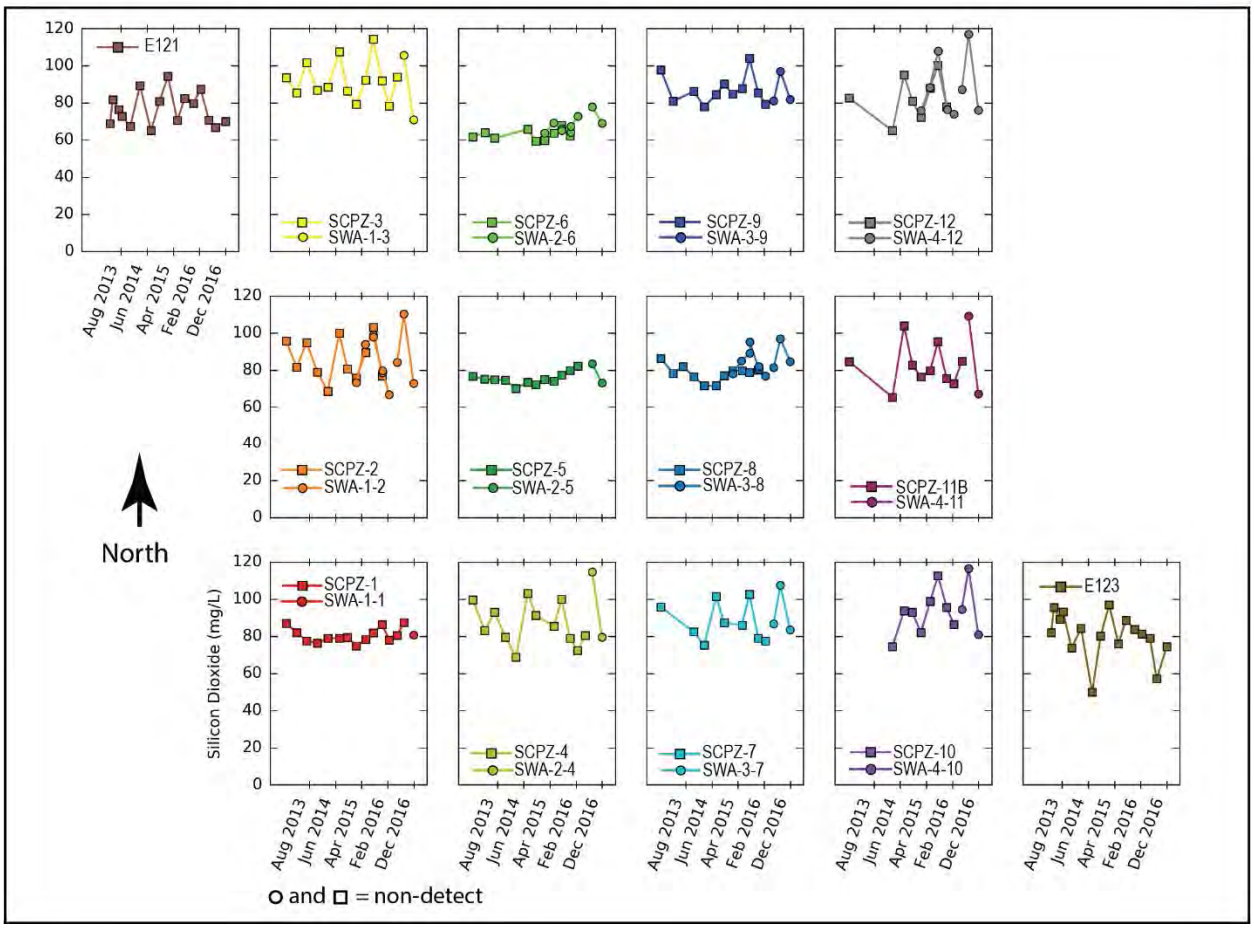

Notes: Surface water stations include E121, E122 (plot not shown), and E123. Piezometers are labeled with the prefix SCPZ (square symbols), and alluvial wells are labeled with the prefix SWA (circle symbols). The plots are arranged in four transects from west to east. Data are plotted for the full period of wetland monitoring. Nondetects are plotted as the MDL with open symbols. The map above is not to scale but shows approximate sampling locations in relation to the approximate thalweg (blue dashed line).

Figure D-3.0-3 Silicon dioxide concentrations in Sandia wetland surface water and alluvial system

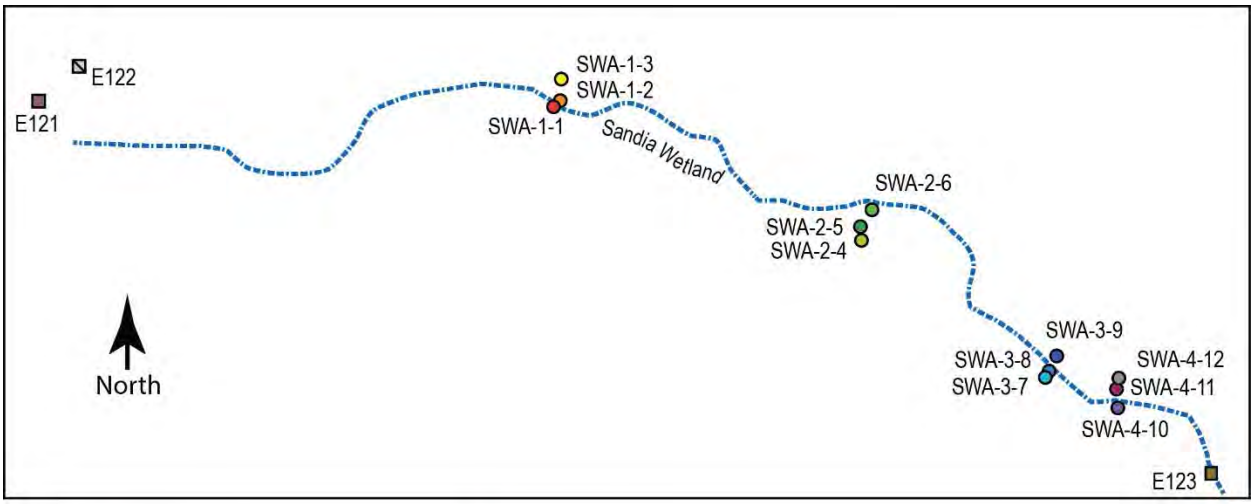

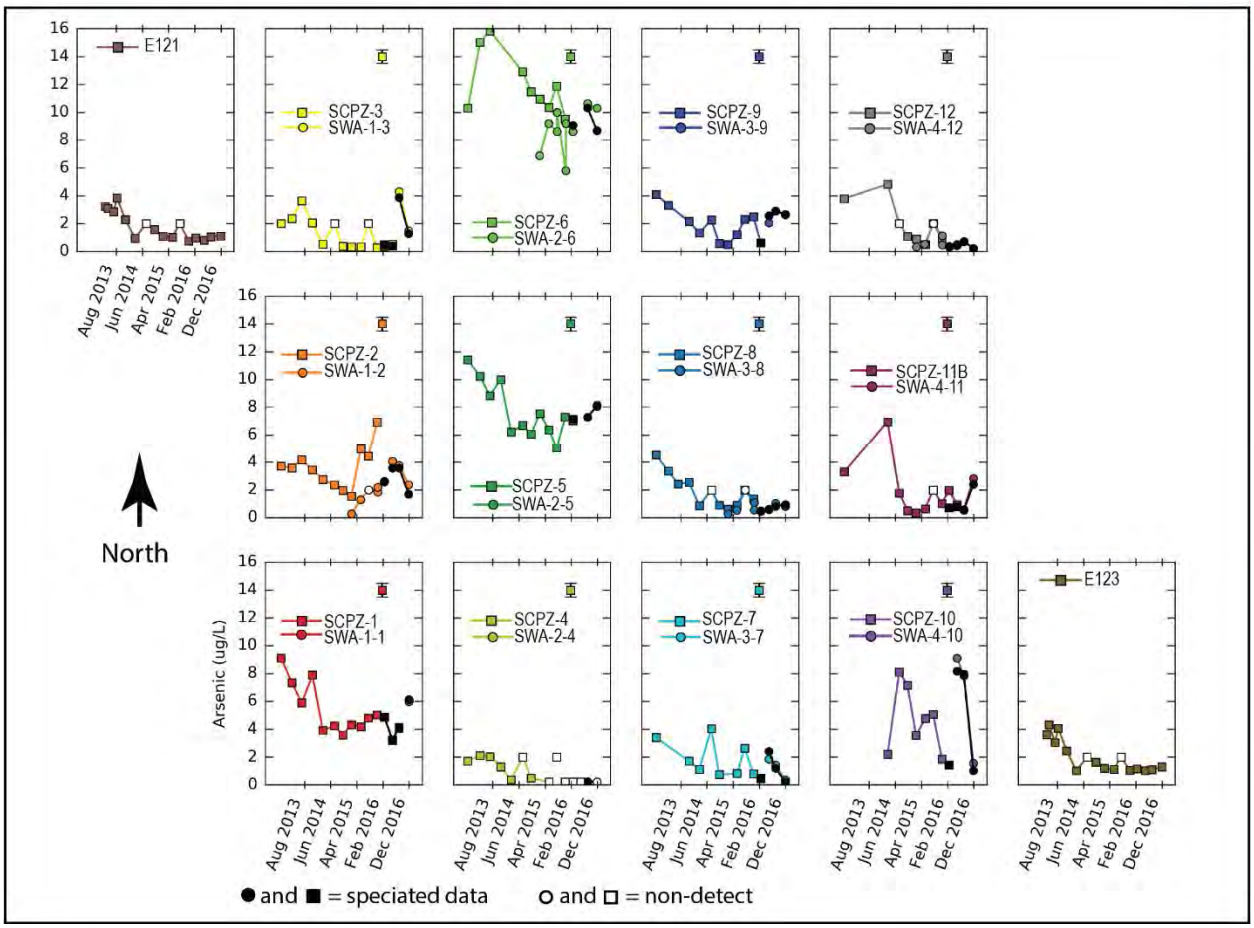

Notes: Surface water stations include E121, E122 (plot not shown), and E123. Piezometers are labeled with the prefix SCPZ (square symbols), and alluvial wells are labeled with the prefix SWA (circle symbols). The plots are arranged in four transects from west to east. Data are plotted for the full period of wetland monitoring. Nondetects are plotted as the MDL with open symbols. Total arsenic is represented with the colored symbols and As(III) with black symbols. The symbol with deviation in the upper right corners of the alluvial location plots shows the analytical error between total and speciated arsenic. The map above is not to scale but shows approximate sampling locations in relation to the approximate thalweg (blue dashed line).

Figure D-3.0-4 Arsenic concentrations in Sandia wetland surface water and alluvial system

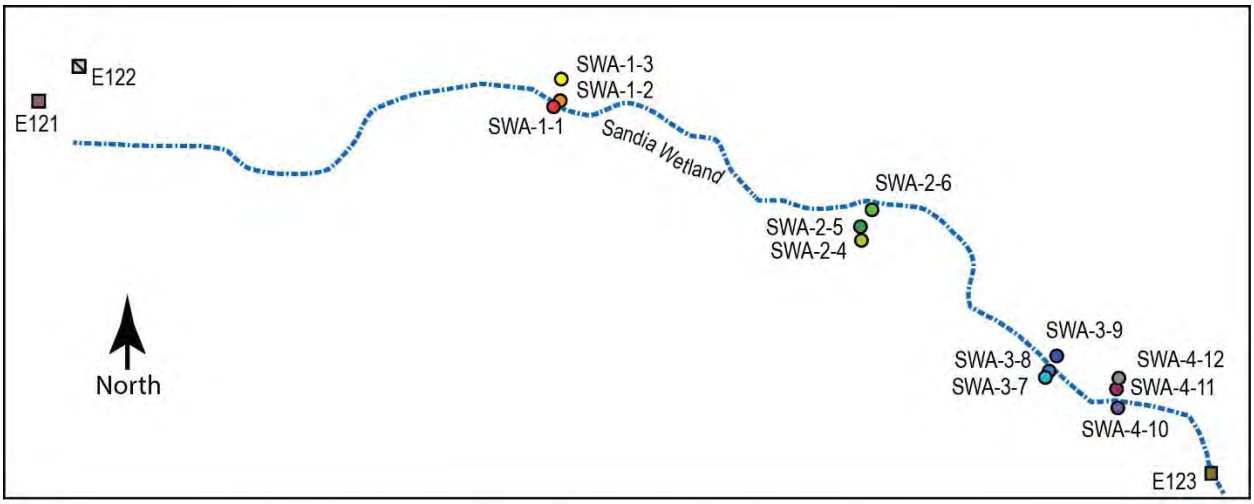

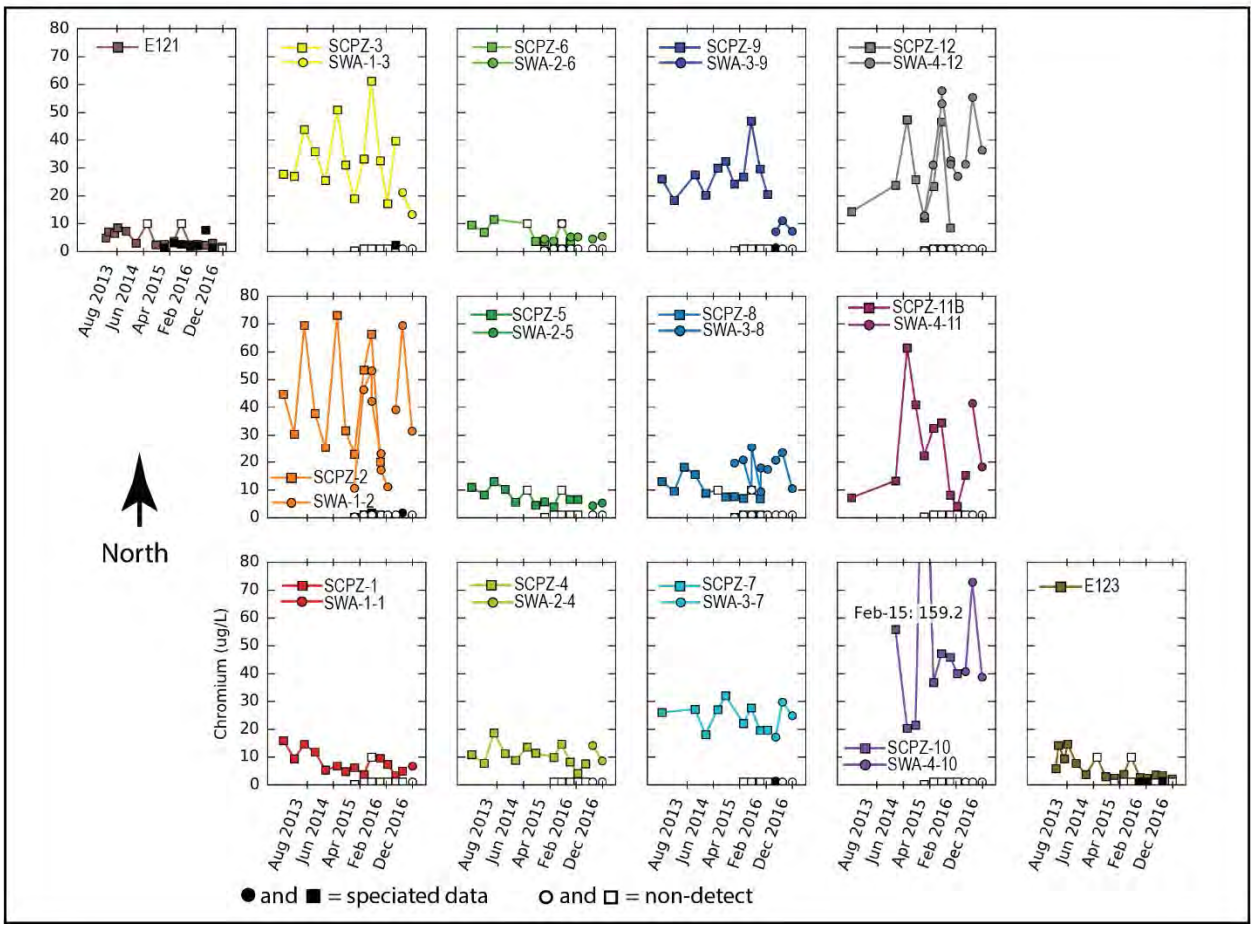

Notes: Surface water stations include E121, E122 (plot not shown), and E123. Piezometers are labeled with the prefix SCPZ (square symbols), and alluvial wells are labeled with the prefix SWA (circle symbols). The plots are arranged in four transects from west to east. Data are plotted for the full period of wetland monitoring. Nondetects are plotted as the MDL with open symbols. Total chromium is represented with the colored symbols and Cr(VI) with black symbols. The map above is not to scale but shows approximate sampling locations in relation to the approximate thalweg (blue dashed line).

Figure D-3.0-5 Chromium concentrations in Sandia wetland surface water and alluvial system

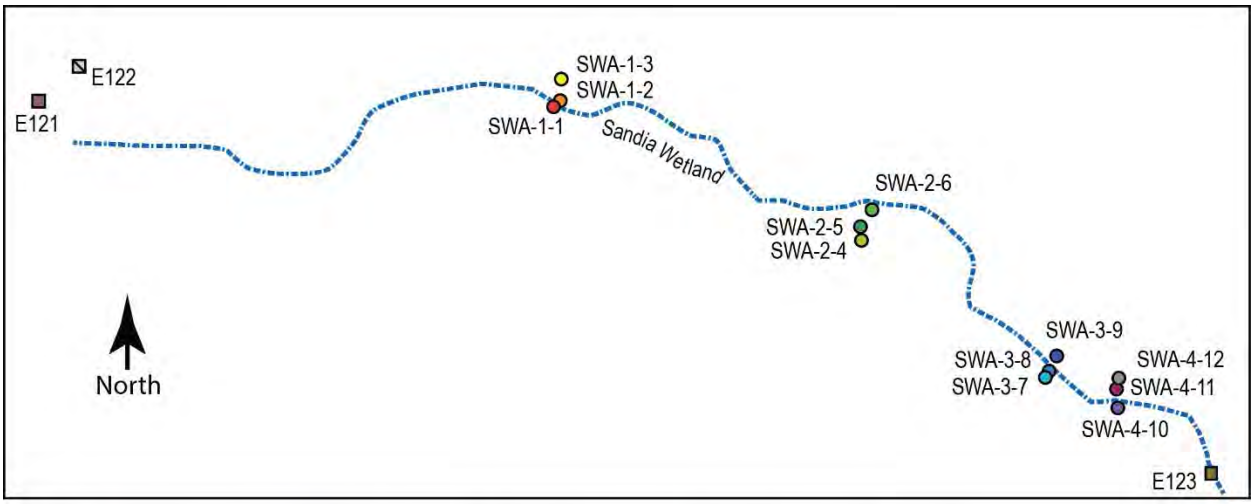

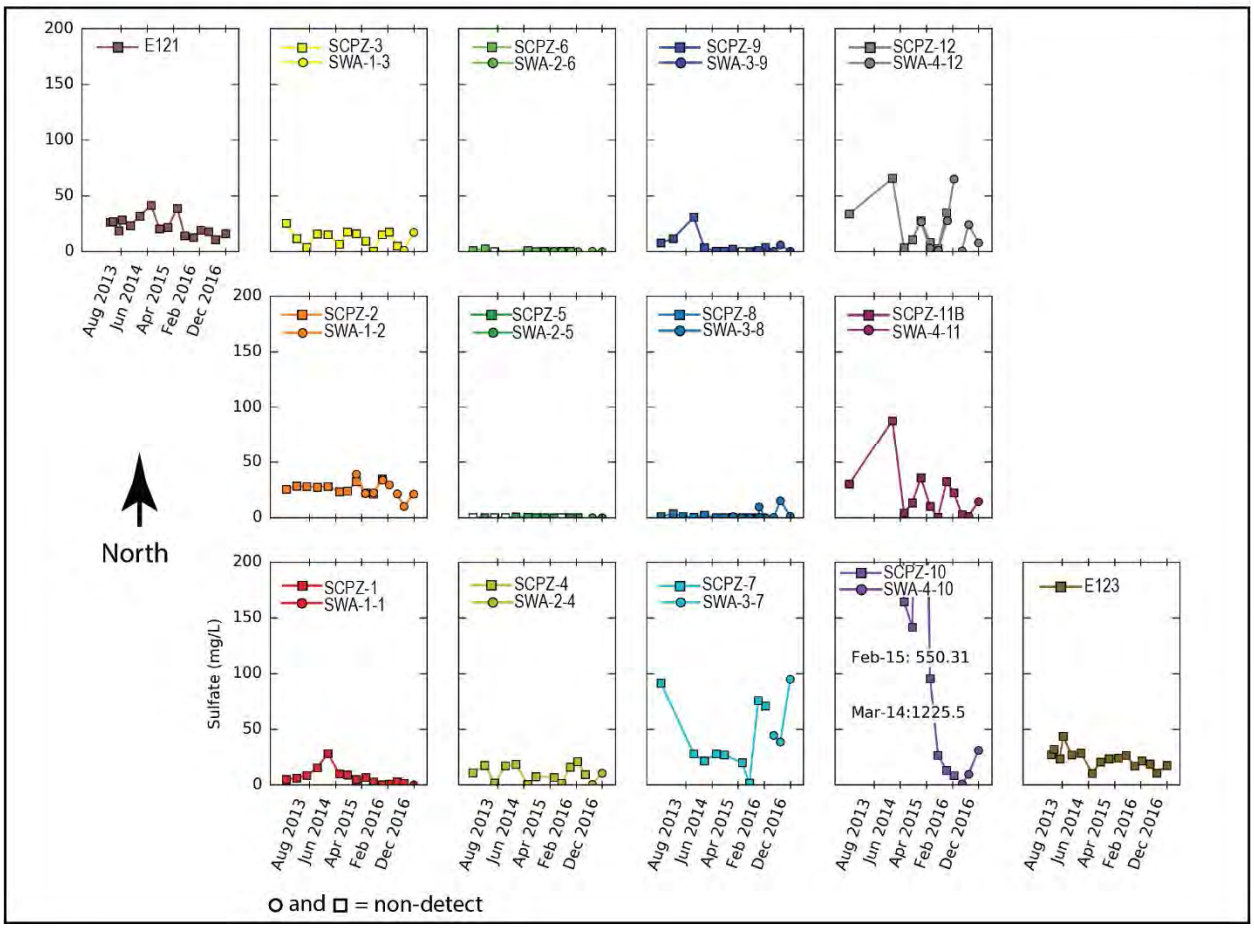

Notes: Surface water stations include E121, E122 (plot not shown), and E123. Piezometers are labeled with the prefix SCPZ (square symbols), and alluvial wells are labeled with the prefix SWA (circle symbols). The plots are arranged in four transects from west to east. Data are plotted for the full period of wetland monitoring. Nondetects are plotted as the MDL with open symbols. The map above is not to scale but shows approximate sampling locations in relation to the approximate thalweg (blue dashed line).

Figure D-3.0-6 Sulfate concentrations in Sandia wetland surface water and alluvial system

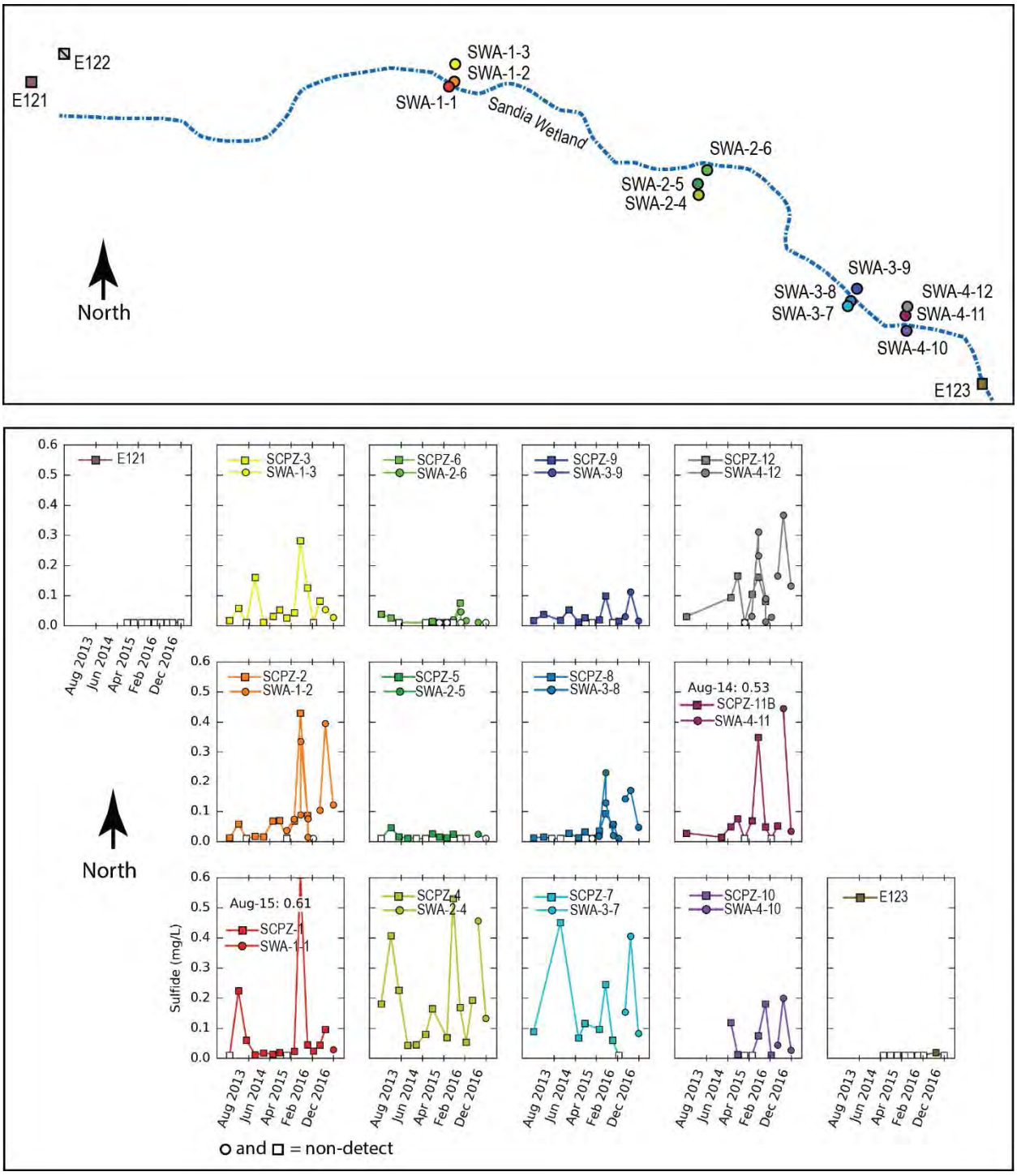

Notes: Surface water stations include E121, E122 (plot not shown), and E123. Piezometers are labeled with the prefix SCPZ (square symbols), and alluvial wells are labeled with the prefix SWA (circle symbols). The plots are arranged in four transects from west to east. Data are plotted for the full period of wetland monitoring. Nondetects are plotted as the MDL with open symbols. The map above is not to scale but shows approximate sampling locations in relation to the approximate thalweg (blue dashed line).

Figure D-3.0-7 Sulfide concentrations in Sandia wetland surface water and alluvial system

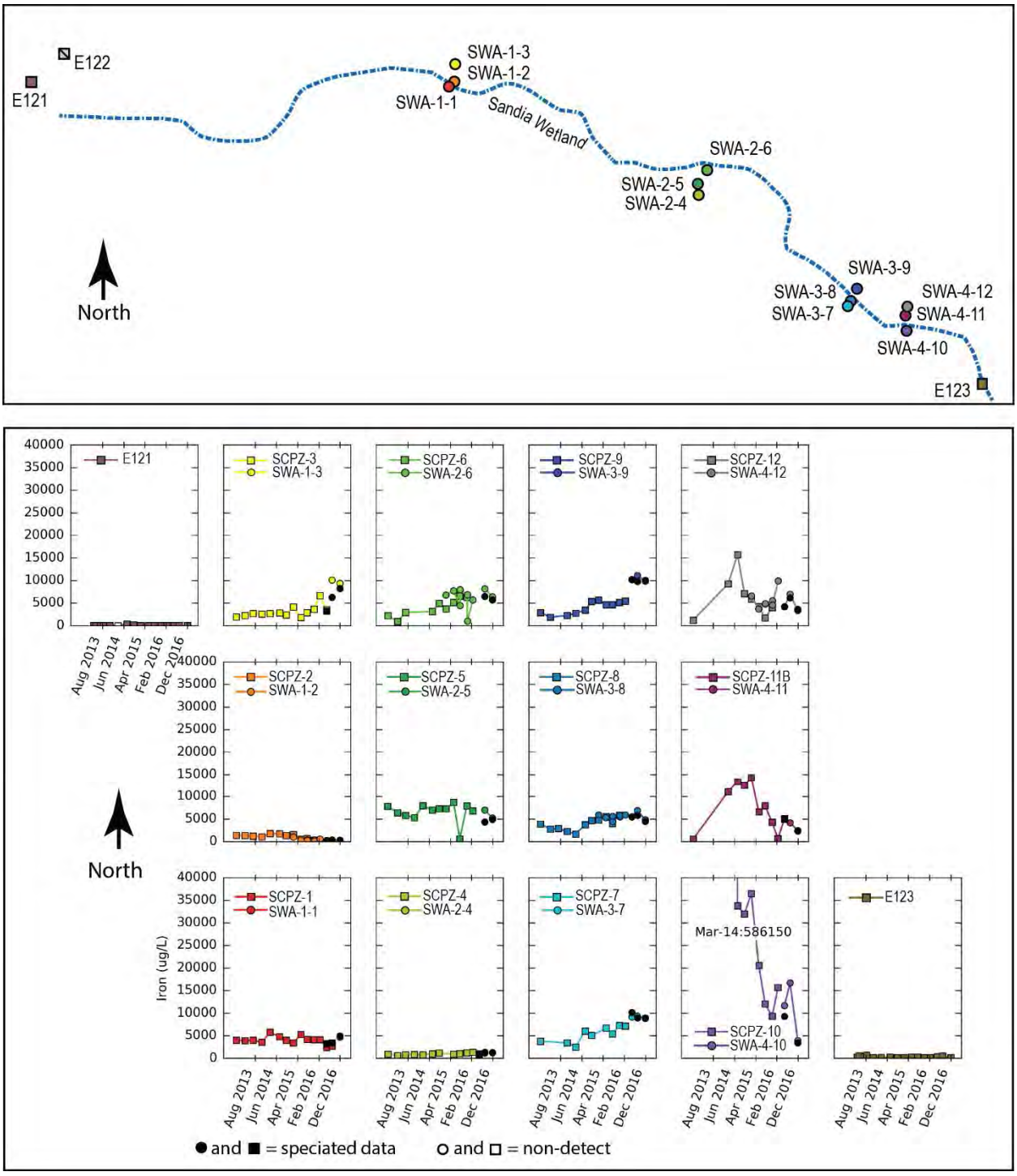

Notes: Surface water stations include E121, E122 (plot not shown), and E123. Piezometers are labeled with the prefix SCPZ (square symbols), and alluvial wells are labeled with the prefix SWA (circle symbols). The plots are arranged in four transects from west to east. Data are plotted for the full period of wetland monitoring. Nondetects are plotted as the MDL with open symbols. Total iron is represented with colored symbols and Fe(11) with black symbols. The map above is not to scale but shows approximate sampling locations in relation to the approximate thalweg (blue dashed line).

Figure D-3.0-8 Iron concentrations in Sandia wetland surface water and alluvial system

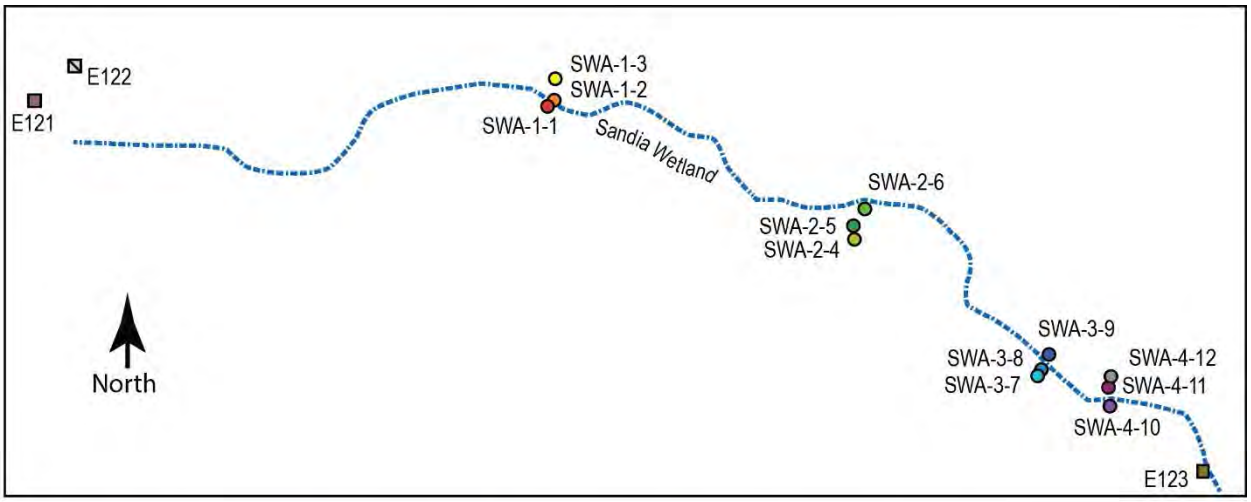

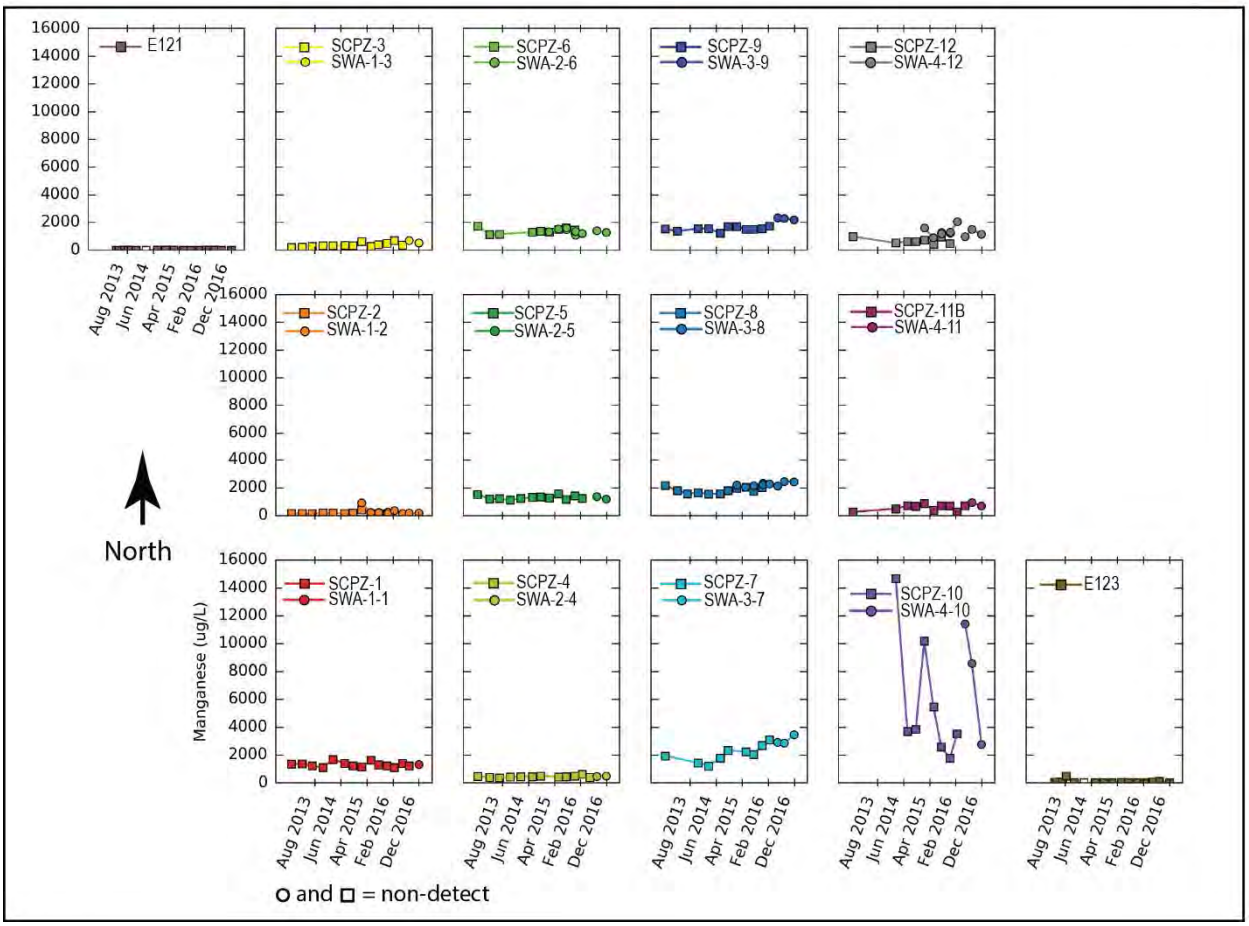

Notes: Surface water stations include E121, E122 (plot not shown), and E123. Piezometers are labeled with the prefix SCPZ (square symbols), and alluvial wells are labeled with the prefix SWA (circle symbols). The plots are arranged in four transects from west to east. Data are plotted for the full period of wetland monitoring. Nondetects are plotted as the MDL with open symbols. The map above is not to scale but shows approximate sampling locations in relation to the approximate thalweg (blue dashed line).

Figure D-3.0-9 Manganese concentrations in Sandia wetland surface water and alluvial system

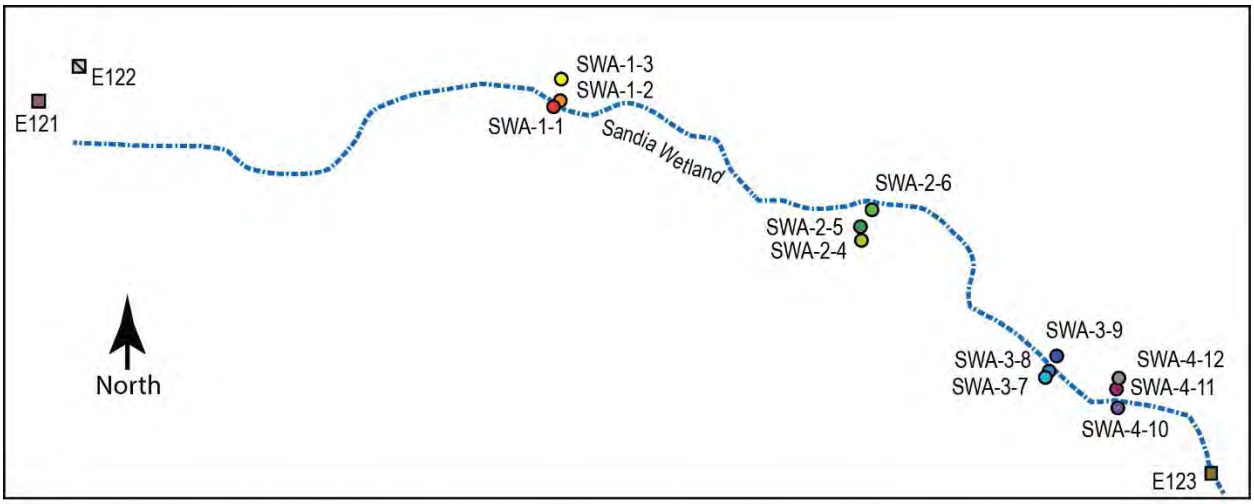

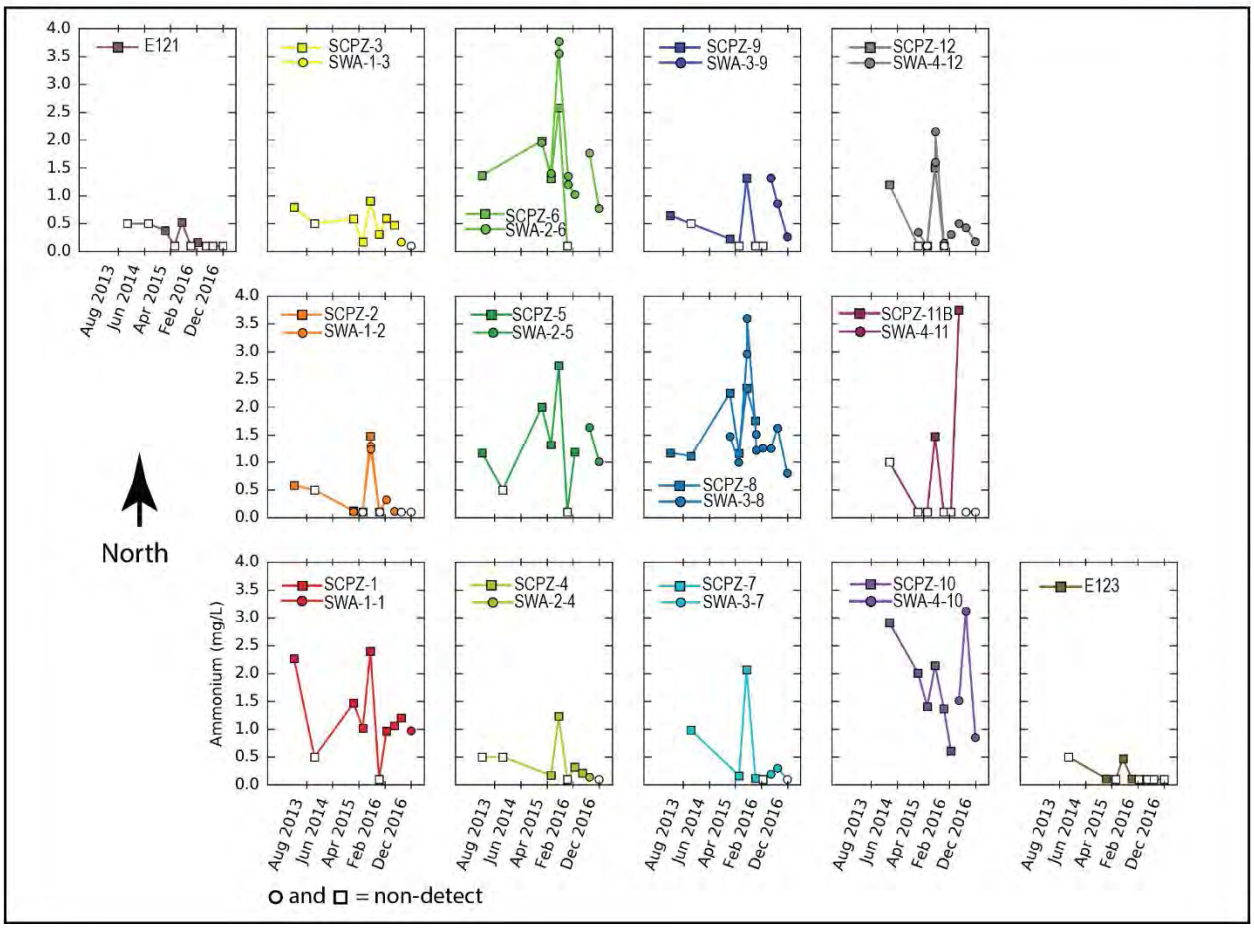

Notes: Surface water stations include E121, E122 (plot not shown), and E123. Piezometers are labeled with the prefix SCPZ (square symbols), and alluvial wells are labeled with the prefix SWA (circle symbols). The plots are arranged in four transects from west to east. Data are plotted for the full period of wetland monitoring. Nondetects are plotted as the MDL with open symbols. The map above is not to scale but shows approximate sampling locations in relation to the approximate thalweg (blue dashed line).

Figure D-3.0-10 Ammonium concentrations in Sandia wetland surface water and alluvial system

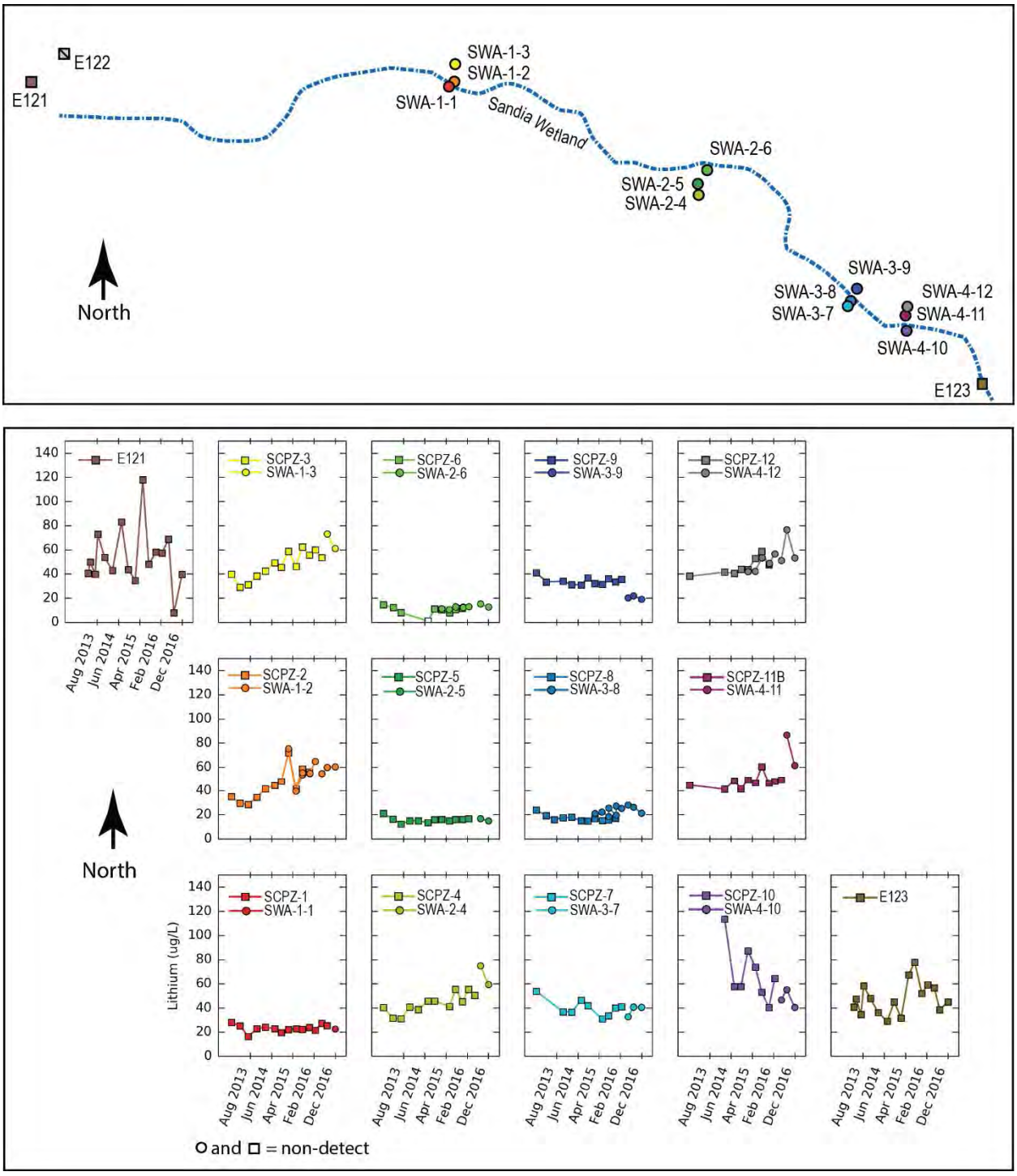

Notes: Surface water stations include E121, E122 (plot not shown), and E123. Piezometers are labeled with the prefix SCPZ (square symbols), and alluvial wells are labeled with the prefix SWA (circle symbols). The plots are arranged in four transects from west to east. Data are plotted for the full period of wetland monitoring. Nondetects are plotted as the MDL with open symbols. The map above is not to scale but shows approximate sampling locations in relation to the approximate thalweg (blue dashed line).

Figure D-3.4-1 Lithium concentrations in Sandia wetland surface water and alluvial system

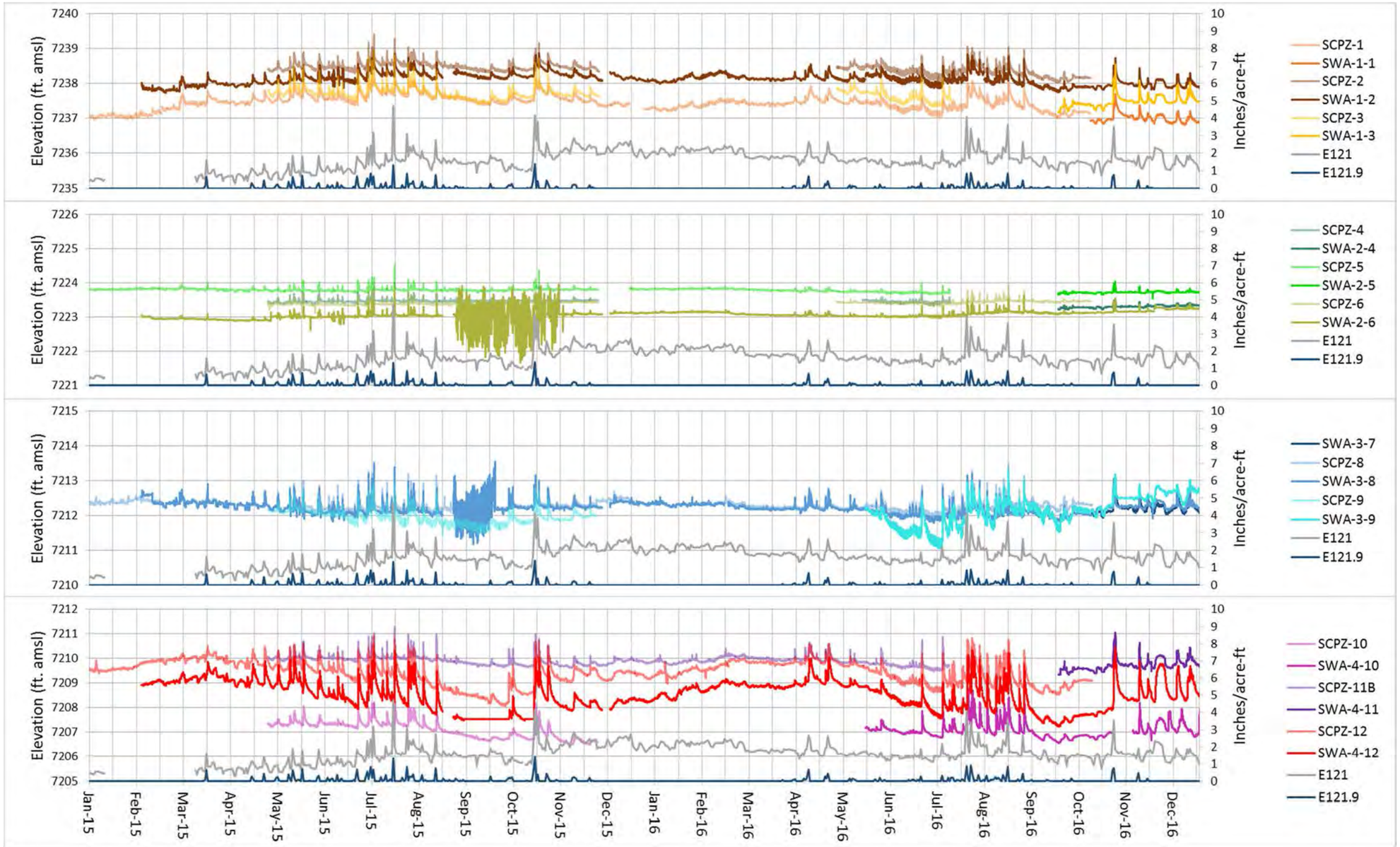

Notes: Water levels collected in the Sandia wetland were at times adjusted for reference value calculation errors and then checked against manual measurements taken in the field during sampling events. Most adjustments were made in response to inaccurate values of the wells inner/outer casing elevations and calculation errors when defining the new reference level. All changes made were made following standard operating procedure ER-SOP-20231, "Groundwater-Level Data Processing, Review, and Validation".

Figure D-4.0-1 Water levels recorded by sondes located in the alluvial system plotted with precipitation data from the E121.9 weather station and total daily volume of flow in surface water gage E121 in 2015 and 2016

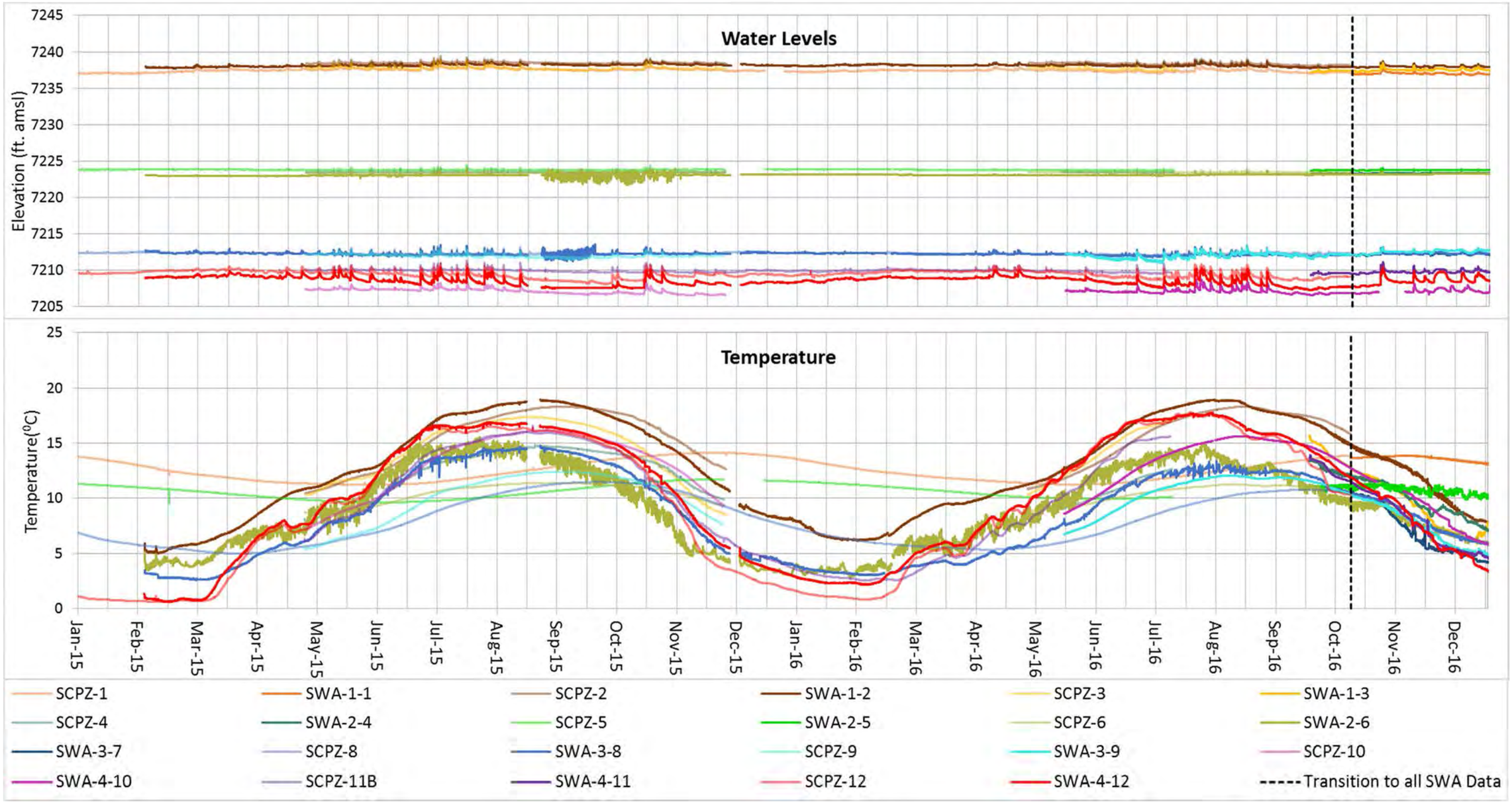

Notes: Total daily volumes of flow in surface water gage E121 are also shown on the water-level plot. The spike in conductance at SCPZ-12 in January 2015 may be because of freezing conditions (see correlation with lowest temperatures).
The sonde in SCPZ-1 has errors from reinstallation at various depths in 2014. No specific conductance data were collected at SCPZ-2, SCPZ-3, SCPZ-4, SCPZ-6, SCPZ-9, SCPZ-10, SCPZ-11A, and SCPZ-11B in 2015.

Figure D-4.0-2 Time series of water level and temperature in alluvial system in 2015 and 2016

Table D-2.0-1
Travel Time of Flood Bore, Peak Discharge, Increase or Decrease in Peak Discharge, and Percent Change in Peak Discharge from Upgradient to Downgradient of the Wetland for Each Sample-Triggering Storm Event in 2016

Date	Travel Time from E121 to E123 (min)	Peak Discharge (cfs)		+/–[a]	%[b]	Travel Time from E122 to E123 (min)	Peak Discharge (cfs)		+/–	%
		E121	E123				E122	E123		
7/1	100	22	9.1	-	59	95	1.9	9.1	+	79
7/15	95	22	11	-	50	95	1.9	11	+	83
7/31	70	47	46	-	2	65	2.0	46	+	96
8/3	65	37	13	-	65	65	1.6	13	+	88
8/4	85	15	9.0	-	40	85	1.1	9.0	+	88
8/8	75	44	12	-	73	75	1.3	12	+	89
8/19	100	10	9.3	-	7	100	1.0	9.3	+	89
8/27	55	51	28	-	45	50	2.3	28	+	92
9/6	60	40	18	-	55	60	2.6	18	+	86
10/3	125	1.7	2.2	+	23	130	0.4	2.2	+	82
10/8	120	1.5	1.8	+	15	130	0.3	1.8	+	81
7/1	110	2.3	2.5	+	9	115	0.6	2.5	+	75
7/15	65	8.4	12	+	29	65	2.0	12	+	83
7/31	105	17	15	-	9	105	2.0	15	+	87
11/4	100	22	9.1	-	59	95	1.9	9.1	+	79
	95	22	11	-	50	95	1.9	11	+	83
11/5–11/6	70	47	46	-	2	65	2.0	46	+	96
Min	55	1.5	1.8	---[c]	2	50	0.3	1.8	---	75
Mean	88	23	13	---	34	88	1.5	13	---	85
Max	125	51	46	---	73	130	2.6	46	---	96

[a] + = Increase; – = decrease.

[b] % = Percent change in peak discharge.

[c] — = Result is not applicable.

Table D-2.0-2
Calculated Sediment Yield and Runoff Volume at Gaging Stations
E121, E122, and E123 for Each Sample-Triggering Storm Event from 2014 to 2016

Station	Date	Sediment Yield (ton)	Sediment Volume (yd^3)	Runoff Volume (acre-feet)	Peak Discharge (cfs)
2016					
E121	7/1/2016	0.36	0.16	0.8	22
E121	7/15/2016	0.26	0.12	1.2	22
E121	7/31/2016	1.80	0.81	2.7	47
E121	8/3/2016	0.34	0.15	1.6	37
E121	8/27/2016	1.57	0.70	1.9	51
E121	9/6/2016	0.75	0.34	1.5	40
E121	11/4/2016	0.15	0.07	0.8	8.4
E122	10/3/2016	0.02	0.01	0.1	22
E122	10/8/2016	0.01	0.01	0.1	22
E122	11/4/2016	0.03	0.01	0.1	47
E123	7/31/2016	0.34	0.15	4.0	46
E123	8/3/2016	2.10	0.94	2.9	13
E123	8/27/2016	0.54	0.24	3.3	28
E123	9/6/2016	0.15	0.07	3.1	18
E123	11/5–11/6/2016	0.16	0.07	3.4	15
2015					
E121	6/1/2015	0.45	0.20	1.7	20
E121	6/26/2015	3.88	1.74	1.3	18
E121	7/3/2015	0.71	0.32	1.6	30
E121	7/15–7/16/2015	0.50	0.22	1.3	39
E121	7/20–7/21/2015	1.62	0.73	4.0	50
E121	7/29–7/30/2015	0.38	0.17	2.2	14
E121	7/31/2015	0.27	0.12	1.1	9.2
E121	8/17/2015	0.45	0.20	1.6	36
E121	10/23–10/24/2015	0.38	0.17	2.0	28
E122	10/23–10/24/2015	0.07	0.03	0.4	5.1
E123	7/3/2015	1.26	0.56	3.9	35
E123	7/20–7/21/2015	2.58	1.16	10.6	64
E123	7/29–7/30/2015	0.84	0.37	5.8	29
E123	8/8/2015	0.15	0.07	1.8	16
E123	8/17/2015	1.06	0.47	3.2	38
E123	10/20/2015	0.25	0.11	1.9	16
E123	10/23/2015	1.19	0.53	4.6	48
2014					
E121	7/7/2014	0.84	0.38	2.3	63
E121	7/14–7/15/2014	0.19	0.09	0.7	4.8
E121	7/15–7/16/2014	1.64	0.73	0.6	10
E121	7/19/2014	3.22	1.44	0.6	11
E121	7/27–7/28/2014	0.57	0.26	0.9	29

Table D-2.0-2 (continued)

2014					
E121	7/31/2014	15.4	6.91	2.9	66
E122	7/8/2014	0.60	0.27	1.0	10
E122	7/27–7/28/2014	0.05	0.02	0.6	6.2
E122	7/29/2014	0.73	0.33	1.2	12
E122	7/31/2014	1.55	0.69	1.0	19
E123	5/23/2014	1.62	0.73	2.7	18
E123	7/7/2014	4.12	1.84	6.4	80
E123	7/8/2014	18.2	8.14	7.0	76
E123	7/15–7/16/2014	2.01	0.90	3.1	20
E123	7/19/2014	0.39	0.17	1.7	18
E123	7/29/2014	7.36	3.30	7.5	62
E123	7/31/2014	28.6	12.8	7.2	109

Table D-2.1-1
Analytical Exceedances in Surface Water at Gaging Stations E121, E122, and E123

Location	Location Alias	Date	Sample Time	Analyte	Sample Type[a]	Sample Purpose[b]	Field Prep Code[c]	Result	Unit	MDL[d]	PQL[e]	Screening Value	Screening Value Type	Comments
Sandia right fork at Pwr Plant	E121	5/25/2016	15:50	Copper	W	REG	F	4.456	µg/L	1	NA[f]	3.03	Aquatic Life Chronic[g]	Average hardness used
Sandia right fork at Pwr Plant	E121	5/25/2016	15:50	Copper	W	FD	F	4.6759	µg/L	1	NA	3.03	Aquatic Life Chronic	Average hardness used
Sandia right fork at Pwr Plant	E121	8/8/2016	15:40	Copper	WS	REG	F	3.3141	µg/L	1	NA	3.03	Aquatic Life Chronic	Average hardness used
Sandia right fork at Pwr Plant	E121	2/19/2016	12:00	Total PCB	W	REG	UF	0.00398	µg/L	NA	NA	0.00064	Aquatic Life HH-OO[h]	
Sandia right fork at Pwr Plant	E121	5/25/2016	15:50	Total PCB	W	FD	UF	0.00228	µg/L	NA	NA	0.00064	Aquatic Life HH-OO	
Sandia right fork at Pwr Plant	E121	5/25/2016	15:50	Total PCB	W	REG	UF	0.00213	µg/L	NA	NA	0.00064	Aquatic Life HH-OO	
Sandia right fork at Pwr Plant	E121	8/8/2016	15:40	Total PCB	WS	REG	UF	0.00593	µg/L	NA	NA	0.00064	Aquatic Life HH-OO	
Sandia right fork at Pwr Plant	E121	12/1/2016	13:55	Total PCB	WS	REG	UF	0.00332	µg/L	NA	NA	0.00064	Aquatic Life HH-OO	
Sandia right fork at Pwr Plant	E121	7/1/2016	14:15	Aluminum	WT	REG	F	181	µg/L	15	50	140	Aquatic Life Chronic	Measured hardness used
Sandia right fork at Pwr Plant	E121	7/1/2016	15:05	Aluminum	WT	REG	F	277	µg/L	15	50	144	Aquatic Life Chronic	Measured hardness used
Sandia right fork at Pwr Plant	E121	7/1/2016	15:55	Aluminum	WT	REG	F	326	µg/L	15	50	217	Aquatic Life Chronic	Measured hardness used
Sandia right fork at Pwr Plant	E121	7/15/2016	13:10	Aluminum	WT	REG	F	286	µg/L	15	50	221	Aquatic Life Chronic	Measured hardness used
Sandia right fork at Pwr Plant	E121	7/31/2016	13:15	Aluminum	WT	REG	F	338	µg/L	15	50	85.6	Aquatic Life Chronic	Measured hardness used
Sandia right fork at Pwr Plant	E121	7/31/2016	14:05	Aluminum	WT	REG	F	374	µg/L	15	50	157	Aquatic Life Chronic	Measured hardness used
Sandia right fork at Pwr Plant	E121	7/31/2016	14:55	Aluminum	WT	REG	F	424	µg/L	15	50	139	Aquatic Life Chronic	Measured hardness used
Sandia right fork at Pwr Plant	E121	8/3/2016	19:10	Aluminum	WT	REG	F	291	µg/L	15	50	53.4	Aquatic Life Chronic	Measured hardness used
Sandia right fork at Pwr Plant	E121	8/3/2016	20:00	Aluminum	WT	REG	F	375	µg/L	15	50	149	Aquatic Life Chronic	Measured hardness used
Sandia right fork at Pwr Plant	E121	8/3/2016	20:50	Aluminum	WT	REG	F	220	µg/L	15	50	134	Aquatic Life Chronic	Measured hardness used
Sandia right fork at Pwr Plant	E121	8/27/2016	11:09	Aluminum	WT	REG	F	539	µg/L	15	50	62.6	Aquatic Life Chronic	Measured hardness used
Sandia right fork at Pwr Plant	E121	8/27/2016	12:49	Aluminum	WT	REG	F	522	µg/L	15	50	120	Aquatic Life Chronic	Measured hardness used
Sandia right fork at Pwr Plant	E121	8/27/2016	12:49	Aluminum	WT	REG	F	444	µg/L	15	50	215	Aquatic Life Chronic	Measured hardness used
Sandia right fork at Pwr Plant	E121	9/6/2016	17:35	Aluminum	WT	REG	F	258	µg/L	15	50	44.2	Aquatic Life Chronic	Measured hardness used
Sandia right fork at Pwr Plant	E121	9/6/2016	18:25	Aluminum	WT	REG	F	307	µg/L	15	50	149	Aquatic Life Chronic	Measured hardness used
Sandia right fork at Pwr Plant	E121	11/4/2016	17:05	Aluminum	WT	REG	F	174	µg/L	15	50	112	Aquatic Life Chronic	Measured hardness used
Sandia right fork at Pwr Plant	E121	11/4/2016	17:55	Cadmium	WT	REG	F	0.86	µg/L	0.3	1	0.183	Aquatic Life Chronic	Measured hardness used
Sandia right fork at Pwr Plant	E121	7/1/2016	14:15	Copper	WT	REG	F	5.23	µg/L	0.35	1	2.16	Aquatic Life Chronic	Measured hardness used
Sandia right fork at Pwr Plant	E121	7/1/2016	15:05	Copper	WT	REG	F	5.71	µg/L	0.35	1	2.2	Aquatic Life Chronic	Measured hardness used
Sandia right fork at Pwr Plant	E121	7/1/2016	15:55	Copper	WT	REG	F	5.75	µg/L	0.35	1	2.83	Aquatic Life Chronic	Measured hardness used
Sandia right fork at Pwr Plant	E121	7/15/2016	12:20	Copper	WT	REG	F	5.86	µg/L	0.35	1	3.92	Aquatic Life Chronic	Measured hardness used
Sandia right fork at Pwr Plant	E121	7/15/2016	13:10	Copper	WT	REG	F	8.06	µg/L	0.35	1	2.87	Aquatic Life Chronic	Measured hardness used
Sandia right fork at Pwr Plant	E121	7/31/2016	13:15	Copper	WT	REG	F	4	µg/L	0.35	1	1.59	Aquatic Life Chronic	Measured hardness used
Sandia right fork at Pwr Plant	E121	7/31/2016	14:05	Copper	WT	REG	F	5.49	µg/L	0.35	1	2.32	Aquatic Life Chronic	Measured hardness used
Sandia right fork at Pwr Plant	E121	7/31/2016	14:55	Copper	WT	REG	F	5.12	µg/L	0.35	1	2.15	Aquatic Life Chronic	Measured hardness used
Sandia right fork at Pwr Plant	E121	8/3/2016	19:10	Copper	WT	REG	F	2.72	µg/L	0.35	NA	1.18	Aquatic Life Chronic	Measured hardness used
Sandia right fork at Pwr Plant	E121	8/3/2016	20:00	Copper	WT	REG	F	3.56	µg/L	0.35	1	2.24	Aquatic Life Chronic	Measured hardness used
Sandia right fork at Pwr Plant	E121	8/3/2016	20:50	Copper	WT	REG	F	3.58	µg/L	0.35	1	2.1	Aquatic Life Chronic	Measured hardness used

Table D-2.1-1 (continued)

Location	Location Alias	Date	Sample Time	Analyte	Sample Type	Sample Purpose	Field Prep Code	Result	Unit	MDL	PQL	Screening Value	Screening Value Type	Comments
Sandia right fork at Pwr Plant	E121	8/27/2016	11:09	Copper	WT	REG	F	2.92	µg/L	0.35	1	1.31	Aquatic Life Chronic	Measured hardness used
Sandia right fork at Pwr Plant	E121	8/27/2016	12:49	Copper	WT	REG	F	4.11	µg/L	0.35	1	1.96	Aquatic Life Chronic	Measured hardness used
Sandia right fork at Pwr Plant	E121	8/27/2016	12:49	Copper	WT	REG	F	4.15	µg/L	0.35	1	2.82	Aquatic Life Chronic	Measured hardness used
Sandia right fork at Pwr Plant	E121	9/6/2016	17:35	Copper	WT	REG	F	2.79	µg/L	0.35	1	1.05	Aquatic Life Chronic	Measured hardness used
Sandia right fork at Pwr Plant	E121	9/6/2016	18:25	Copper	WT	REG	F	4.65	µg/L	0.35	1	2.24	Aquatic Life Chronic	Measured hardness used
Sandia right fork at Pwr Plant	E121	9/6/2016	19:15	Copper	WT	REG	F	4.15	µg/L	0.35	1	3.17	Aquatic Life Chronic	Measured hardness used
Sandia right fork at Pwr Plant	E121	11/4/2016	17:05	Copper	WT	REG	F	3.38	µg/L	0.35	1	1.88	Aquatic Life Chronic	Measured hardness used
Sandia right fork at Pwr Plant	E121	11/4/2016	17:55	Copper	WT	REG	F	3.2	µg/L	0.35	1	3.05	Aquatic Life Chronic	Measured hardness used
Sandia right fork at Pwr Plant	E121	9/6/2016	17:35	Gross alpha	WT	REG	UF	18.7	pCi/L	1.66[e]	NA	15	LW[i]	
Sandia right fork at Pwr Plant	E121	7/1/2016	15:05	Lead	WT	REG	F	0.552	µg/L	0.5	2	0.404	Aquatic Life Chronic	Measured hardness used
Sandia right fork at Pwr Plant	E121	7/1/2016	15:55	Lead	WT	REG	F	0.658	µg/L	0.5	2	0.565	Aquatic Life Chronic	Measured hardness used
Sandia right fork at Pwr Plant	E121	7/31/2016	14:05	Lead	WT	REG	F	0.565	µg/L	0.5	2	0.435	Aquatic Life Chronic	Measured hardness used
Sandia right fork at Pwr Plant	E121	7/31/2016	14:55	Lead	WT	REG	F	0.566	µg/L	0.5	2	0.392	Aquatic Life Chronic	Measured hardness used
Sandia right fork at Pwr Plant	E121	8/3/2016	20:00	Lead	WT	REG	F	0.523	µg/L	0.5	2	0.416	Aquatic Life Chronic	Measured hardness used
Sandia right fork at Pwr Plant	E121	8/27/2016	11:09	Lead	WT	REG	F	0.878	µg/L	0.5	2	0.202	Aquatic Life Chronic	Measured hardness used
Sandia right fork at Pwr Plant	E121	8/27/2016	12:49	Lead	WT	REG	F	0.647	µg/L	0.5	2	0.348	Aquatic Life Chronic	Measured hardness used
Sandia right fork at Pwr Plant	E121	8/27/2016	12:49	Lead	WT	REG	F	0.627	µg/L	0.5	2	0.563	Aquatic Life Chronic	Measured hardness used
Sandia right fork at Pwr Plant	E121	9/6/2016	18:25	Lead	WT	REG	F	0.56	µg/L	0.5	2	0.416	Aquatic Life Chronic	Measured hardness used
Sandia right fork at Pwr Plant	E121	7/1/2016	14:15	Total PCB	WT	REG	UF	0.0979	µg/L	NA	NA	0.014	WH[j]	
Sandia right fork at Pwr Plant	E121	7/1/2016	14:15	Total PCB	WT	REG	UF	0.0979	µg/L	NA	NA	0.014	Aquatic Life Chronic	
Sandia right fork at Pwr Plant	E121	7/1/2016	14:15	Total PCB	WT	REG	UF	0.0979	µg/L	NA	NA	0.00064	Aquatic Life HH-OO	
Sandia right fork at Pwr Plant	E121	7/1/2016	15:05	Total PCB	WT	REG	UF	0.0158	µg/L	NA	NA	0.014	WH	
Sandia right fork at Pwr Plant	E121	7/1/2016	15:05	Total PCB	WT	REG	UF	0.0158	µg/L	NA	NA	0.014	Aquatic Life Chronic	
Sandia right fork at Pwr Plant	E121	7/1/2016	15:05	Total PCB	WT	REG	UF	0.0158	µg/L	NA	NA	0.00064	Aquatic Life HH-OO	
Sandia right fork at Pwr Plant	E121	7/1/2016	15:55	Total PCB	WT	REG	UF	0.00885	µg/L	NA	NA	0.00064	Aquatic Life HH-OO	
Sandia right fork at Pwr Plant	E121	7/15/2016	11:30	Total PCB	WT	REG	UF	0.0701	µg/L	NA	NA	0.014	WH	
Sandia right fork at Pwr Plant	E121	7/15/2016	11:30	Total PCB	WT	REG	UF	0.0701	µg/L	NA	NA	0.014	Aquatic Life Chronic	
Sandia right fork at Pwr Plant	E121	7/15/2016	11:30	Total PCB	WT	REG	UF	0.0701	µg/L	NA	NA	0.00064	Aquatic Life HH-OO	
Sandia right fork at Pwr Plant	E121	7/15/2016	12:20	Total PCB	WT	REG	UF	0.0115	µg/L	NA	NA	0.00064	Aquatic Life HH-OO	
Sandia right fork at Pwr Plant	E121	7/15/2016	13:10	Total PCB	WT	REG	UF	0.00646	µg/L	NA	NA	0.00064	Aquatic Life HH-OO	
Sandia right fork at Pwr Plant	E121	7/31/2016	13:15	Total PCB	WT	REG	UF	0.106	µg/L	NA	NA	0.014	WH	
Sandia right fork at Pwr Plant	E121	7/31/2016	13:15	Total PCB	WT	REG	UF	0.106	µg/L	NA	NA	0.014	Aquatic Life Chronic	
Sandia right fork at Pwr Plant	E121	7/31/2016	13:15	Total PCB	WT	REG	UF	0.106	µg/L	NA	NA	0.00064	Aquatic Life HH-OO	
Sandia right fork at Pwr Plant	E121	7/31/2016	14:05	Total PCB	WT	REG	UF	0.0291	µg/L	NA	NA	0.014	WH	
Sandia right fork at Pwr Plant	E121	7/31/2016	14:05	Total PCB	WT	REG	UF	0.0291	µg/L	NA	NA	0.014	Aquatic Life Chronic	
Sandia right fork at Pwr Plant	E121	7/31/2016	14:05	Total PCB	WT	REG	UF	0.0291	µg/L	NA	NA	0.00064	Aquatic Life HH-OO	
Sandia right fork at Pwr Plant	E121	7/31/2016	14:55	Total PCB	WT	REG	UF	0.0265	µg/L	NA	NA	0.014	WH	
Sandia right fork at Pwr Plant	E121	7/31/2016	14:55	Total PCB	WT	REG	UF	0.0265	µg/L	NA	NA	0.014	Aquatic Life Chronic	

Table D-2.1-1 (continued)

Location	Location alias	Date	Sample Time	Analyte	Sample Type	Sample Purpose	Field Prep Code	Result	Unit	MDL	PQL	Screening Value	Screening Value Type	Comments
Sandia right fork at Pwr Plant	E121	7/31/2016	14:55	Total PCB	WT	REG	UF	0.0265	µg/L	NA	NA	0.00064	Aquatic Life HH-OO	
Sandia right fork at Pwr Plant	E121	8/3/2016	19:10	Total PCB	WT	REG	UF	0.0625	µg/L	NA	NA	0.014	WH	
Sandia right fork at Pwr Plant	E121	8/3/2016	19:10	Total PCB	WT	REG	UF	0.0625	µg/L	NA	NA	0.014	Aquatic Life Chronic	
Sandia right fork at Pwr Plant	E121	8/3/2016	19:10	Total PCB	WT	REG	UF	0.0625	µg/L	NA	NA	0.00064	Aquatic Life HH-OO	
Sandia right fork at Pwr Plant	E121	8/3/2016	20:00	Total PCB	WT	REG	UF	0.0175	µg/L	NA	NA	0.014	WH	
Sandia right fork at Pwr Plant	E121	8/3/2016	20:00	Total PCB	WT	REG	UF	0.0175	µg/L	NA	NA	0.014	Aquatic Life Chronic	
Sandia right fork at Pwr Plant	E121	8/3/2016	20:00	Total PCB	WT	REG	UF	0.0175	µg/L	NA	NA	0.00064	Aquatic Life HH-OO	
Sandia right fork at Pwr Plant	E121	8/3/2016	20:50	Total PCB	WT	REG	UF	0.0096	µg/L	NA	NA	0.00064	Aquatic Life HH-OO	
Sandia right fork at Pwr Plant	E121	8/27/2016	11:09	Total PCB	WT	REG	UF	0.176	µg/L	NA	NA	0.014	WH	
Sandia right fork at Pwr Plant	E121	8/27/2016	11:09	Total PCB	WT	REG	UF	0.176	µg/L	NA	NA	0.014	Aquatic Life Chronic	
Sandia right fork at Pwr Plant	E121	8/27/2016	11:09	Total PCB	WT	REG	UF	0.176	µg/L	NA	NA	0.00064	Aquatic Life HH-OO	
Sandia right fork at Pwr Plant	E121	8/27/2016	11:59	Total PCB	WT	REG	UF	0.0467	µg/L	NA	NA	0.014	WH	
Sandia right fork at Pwr Plant	E121	8/27/2016	11:59	Total PCB	WT	REG	UF	0.0467	µg/L	NA	NA	0.014	Aquatic Life Chronic	
Sandia right fork at Pwr Plant	E121	8/27/2016	11:59	Total PCB	WT	REG	UF	0.0467	µg/L	NA	NA	0.00064	Aquatic Life HH-OO	
Sandia right fork at Pwr Plant	E121	8/27/2016	12:49	Total PCB	WT	REG	UF	0.0235	µg/L	NA	NA	0.014	WH	
Sandia right fork at Pwr Plant	E121	8/27/2016	12:49	Total PCB	WT	REG	UF	0.0235	µg/L	NA	NA	0.014	Aquatic Life Chronic	
Sandia right fork at Pwr Plant	E121	8/27/2016	12:49	Total PCB	WT	REG	UF	0.0235	µg/L	NA	NA	0.00064	Aquatic Life HH-OO	
Sandia right fork at Pwr Plant	E121	9/6/2016	17:35	Total PCB	WT	REG	UF	0.0478	µg/L	NA	NA	0.014	WH	
Sandia right fork at Pwr Plant	E121	9/6/2016	17:35	Total PCB	WT	REG	UF	0.0478	µg/L	NA	NA	0.014	Aquatic Life Chronic	
Sandia right fork at Pwr Plant	E121	9/6/2016	17:35	Total PCB	WT	REG	UF	0.0478	µg/L	NA	NA	0.00064	Aquatic Life HH-OO	
Sandia right fork at Pwr Plant	E121	9/6/2016	18:25	Total PCB	WT	REG	UF	0.0119	µg/L	NA	NA	0.00064	Aquatic Life HH-OO	
Sandia right fork at Pwr Plant	E121	9/6/2016	19:15	Total PCB	WT	REG	UF	0.0107	µg/L	NA	NA	0.00064	Aquatic Life HH-OO	
Sandia right fork at Pwr Plant	E121	11/4/2016	16:15	Total PCB	WT	REG	UF	0.0728	µg/L	NA	NA	0.014	WH	
Sandia right fork at Pwr Plant	E121	11/4/2016	16:15	Total PCB	WT	REG	UF	0.0728	µg/L	NA	NA	0.014	Aquatic Life Chronic	
Sandia right fork at Pwr Plant	E121	11/4/2016	16:15	Total PCB	WT	REG	UF	0.0728	µg/L	NA	NA	0.00064	Aquatic Life HH-OO	
Sandia right fork at Pwr Plant	E121	11/4/2016	17:05	Total PCB	WT	REG	UF	0.0197	µg/L	NA	NA	0.014	WH	
Sandia right fork at Pwr Plant	E121	11/4/2016	17:05	Total PCB	WT	REG	UF	0.0197	µg/L	NA	NA	0.014	Aquatic Life Chronic	
Sandia right fork at Pwr Plant	E121	11/4/2016	17:05	Total PCB	WT	REG	UF	0.0197	µg/L	NA	NA	0.00064	Aquatic Life HH-OO	
Sandia right fork at Pwr Plant	E121	11/4/2016	17:55	Total PCB	WT	REG	UF	0.00812	µg/L	NA	NA	0.00064	Aquatic Life HH-OO	
Sandia right fork at Pwr Plant	E121	7/1/2016	14:15	Zinc	WT	REG	F	50.4	µg/L	3.3	10	26.6	Aquatic Life Chronic	Measured hardness used
Sandia right fork at Pwr Plant	E121	7/1/2016	15:05	Zinc	WT	REG	F	33	µg/L	3.3	10	27.1	Aquatic Life Chronic	Measured hardness used
Sandia right fork at Pwr Plant	E121	7/31/2016	13:15	Zinc	WT	REG	F	19.6	µg/L	3.3	10	19.2	Aquatic Life Chronic	Measured hardness used
Sandia right fork at Pwr Plant	E121	8/27/2016	11:09	Zinc	WT	REG	F	20.1	µg/L	3.3	10	15.6	Aquatic Life Chronic	Measured hardness used
Sandia right fork at Pwr Plant	E121	9/6/2016	17:35	Zinc	WT	REG	F	19.2	µg/L	3.3	10	12.4	Aquatic Life Chronic	Measured hardness used
Sandia right fork at Pwr Plant	E121	9/6/2016	18:25	Zinc	WT	REG	F	29.8	µg/L	3.3	10	27.8	Aquatic Life Chronic	Measured hardness used
South Fork of Sandia at E122	E122	8/9/2016	13:29	Copper	WS	REG	F	4.1543	µg/L	1	NA	3.03	Aquatic Life Chronic	Average hardness used
South Fork of Sandia at E122	E122	8/9/2016	13:29	Copper	WS	FD	F	3.7971	µg/L	1	NA	3.03	Aquatic Life Chronic	Average hardness used
South Fork of Sandia at E122	E122	2/19/2016	12:45	Total PCB	W	REG	UF	0.00231	µg/L	NA	NA	0.00064	Aquatic Life HH-OO	

Table D-2.1-1 (continued)

Location	Location alias	Date	Sample Time	Analyte	Sample Type	Sample Purpose	Field Prep Code	Result	Unit	MDL	PQL	Screening Value	Screening Value Type	Comments
Sandia left fork at Asph Plant	E122	10/3/2016	5:39	Aluminum	WT	REG	F	253	µg/L	15	50	183	Aquatic Life Chronic	Measured hardness used
Sandia left fork at Asph Plant	E122	10/8/2016	18:34	Aluminum	WT	REG	F	369	µg/L	15	50	303	Aquatic Life Chronic	Measured hardness used
Sandia left fork at Asph Plant	E122	11/4/2016	12:54	Benzo(a)anthracene	WT	REG	UF	0.333	µg/L	0.0198	0.0617	0.18	Aquatic Life HH-OO	
Sandia left fork at Asph Plant	E122	11/4/2016	12:54	Benzo(a)pyrene	WT	REG	UF	0.296	µg/L	0.0198	0.0617	0.18	Aquatic Life HH-OO	
Sandia left fork at Asph Plant	E122	11/4/2016	12:54	Benzo(b)fluoranthene	WT	REG	UF	0.332	µg/L	0.0198	0.0617	0.18	Aquatic Life HH-OO	
Sandia left fork at Asph Plant	E122	11/4/2016	12:54	Benzo(k)fluoranthene	WT	REG	UF	0.225	µg/L	0.00988	0.0309	0.18	Aquatic Life HH-OO	
Sandia left fork at Asph Plant	E122	10/3/2016	5:39	Cadmium	WT	REG	F	0.805	µg/L	0.3	1	0.157	Aquatic Life Chronic	Measured hardness used
Sandia left fork at Asph Plant	E122	10/3/2016	3:59	Copper	WT	REG	F	20.3	µg/L	0.35	1	3.79	Aquatic Life Chronic	Measured hardness used
Sandia left fork at Asph Plant	E122	10/3/2016	4:49	Copper	WT	REG	F	17.6	µg/L	0.35	1	5.26	Aquatic Life Chronic	Measured hardness used
Sandia left fork at Asph Plant	E122	10/3/2016	5:39	Copper	WT	REG	F	14.1	µg/L	0.35	1	2.55	Aquatic Life Chronic	Measured hardness used
Sandia left fork at Asph Plant	E122	10/8/2016	16:54	Copper	WT	REG	F	25.5	µg/L	0.35	1	2.96	Aquatic Life Chronic	Measured hardness used
Sandia left fork at Asph Plant	E122	10/8/2016	17:44	Copper	WT	REG	F	21.3	µg/L	0.35	1	3.56	Aquatic Life Chronic	Measured hardness used
Sandia left fork at Asph Plant	E122	10/8/2016	18:34	Copper	WT	REG	F	22	µg/L	0.35	1	3.49	Aquatic Life Chronic	Measured hardness used
Sandia left fork at Asph Plant	E122	11/4/2016	12:54	Copper	WT	REG	F	38.5	µg/L	0.35	1	3.63	Aquatic Life Chronic	Measured hardness used
Sandia left fork at Asph Plant	E122	11/4/2016	13:44	Copper	WT	REG	F	29	µg/L	0.35	1	5.43	Aquatic Life Chronic	Measured hardness used
Sandia left fork at Asph Plant	E122	11/4/2016	14:34	Copper	WT	REG	F	46.3	µg/L	0.35	1	3.11	Aquatic Life Chronic	Measured hardness used
Sandia left fork at Asph Plant	E122	10/3/2016	3:59	Lead	WT	REG	F	0.87	µg/L	0.5	2	0.83	Aquatic Life Chronic	Measured hardness used
Sandia left fork at Asph Plant	E122	10/3/2016	5:39	Lead	WT	REG	F	0.637	µg/L	0.5	2	0.492	Aquatic Life Chronic	Measured hardness used
Sandia left fork at Asph Plant	E122	10/8/2016	16:54	Lead	WT	REG	F	1.04	µg/L	0.5	2	0.6	Aquatic Life Chronic	Measured hardness used
Sandia left fork at Asph Plant	E122	10/8/2016	18:34	Lead	WT	REG	F	0.929	µg/L	0.5	2	0.744	Aquatic Life Chronic	Measured hardness used
Sandia left fork at Asph Plant	E122	11/4/2016	12:54	Lead	WT	REG	F	1.1	µg/L	0.5	2	0.782	Aquatic Life Chronic	Measured hardness used
Sandia left fork at Asph Plant	E122	11/4/2016	14:34	Lead	WT	REG	F	1.19	µg/L	0.5	2	0.639	Aquatic Life Chronic	Measured hardness used
Sandia left fork at Asph Plant	E122	10/3/2016	3:59	Total PCB	WT	REG	UF	0.0814	µg/L	NA	NA	0.014	WH	
Sandia left fork at Asph Plant	E122	10/3/2016	3:59	Total PCB	WT	REG	UF	0.0814	µg/L	NA	NA	0.014	Aquatic Life Chronic	
Sandia left fork at Asph Plant	E122	10/3/2016	3:59	Total PCB	WT	REG	UF	0.0814	µg/L	NA	NA	0.00064	Aquatic Life HH-OO	
Sandia left fork at Asph Plant	E122	10/3/2016	4:49	Total PCB	WT	REG	UF	0.00746	µg/L	NA	NA	0.00064	Aquatic Life HH-OO	
Sandia left fork at Asph Plant	E122	10/3/2016	4:49	Total PCB	WT	REG	UF	0.0501	µg/L	NA	NA	0.014	WH	
Sandia left fork at Asph Plant	E122	10/3/2016	4:49	Total PCB	WT	REG	UF	0.0501	µg/L	NA	NA	0.014	Aquatic Life Chronic	
Sandia left fork at Asph Plant	E122	10/3/2016	4:49	Total PCB	WT	REG	UF	0.0501	µg/L	NA	NA	0.00064	Aquatic Life HH-OO	
Sandia left fork at Asph Plant	E122	10/8/2016	16:54	Total PCB	WT	REG	UF	0.0129	µg/L	NA	NA	0.00064	Aquatic Life HH-OO	
Sandia left fork at Asph Plant	E122	10/8/2016	17:44	Total PCB	WT	REG	UF	0.00453	µg/L	NA	NA	0.00064	Aquatic Life HH-OO	
Sandia left fork at Asph Plant	E122	10/8/2016	18:34	Total PCB	WT	REG	UF	0.00209	µg/L	NA	NA	0.00064	Aquatic Life HH-OO	
Sandia left fork at Asph Plant	E122	11/4/2016	12:54	Total PCB	WT	REG	UF	0.0435	µg/L	NA	NA	0.014	WH	
Sandia left fork at Asph Plant	E122	11/4/2016	12:54	Total PCB	WT	REG	UF	0.0435	µg/L	NA	NA	0.014	Aquatic Life Chronic	
Sandia left fork at Asph Plant	E122	11/4/2016	12:54	Total PCB	WT	REG	UF	0.0435	µg/L	NA	NA	0.00064	Aquatic Life HH-OO	
Sandia left fork at Asph Plant	E122	11/4/2016	13:44	Total PCB	WT	REG	UF	0.00958	µg/L	NA	NA	0.00064	Aquatic Life HH-OO	
Sandia left fork at Asph Plant	E122	11/4/2016	14:34	Total PCB	WT	REG	UF	0.00745	µg/L	NA	NA	0.00064	Aquatic Life HH-OO	
Sandia left fork at Asph Plant	E122	10/3/2016	3:59	Zinc	WT	REG	F	158	µg/L	3.3	10	48.6	Aquatic Life Chronic	Measured hardness used

Table D-2.1-1 (continued)

Location	Location alias	Date	Sample Time	Analyte	Sample Type	Sample Purpose	Field Prep Code	Result	Unit	MDL	PQL	Screening Value	Screening Value Type	Comments
Sandia left fork at Asph Plant	E122	10/3/2016	4:49	Zinc	WT	REG	F	81.7	µg/L	3.3	10	68.7	Aquatic Life Chronic	Measured hardness used
Sandia left fork at Asph Plant	E122	10/3/2016	5:39	Zinc	WT	REG	F	87.1	µg/L	3.3	10	31.8	Aquatic Life Chronic	Measured hardness used
Sandia left fork at Asph Plant	E122	10/8/2016	16:54	Zinc	WT	REG	F	124	µg/L	3.3	10	37.3	Aquatic Life Chronic	Measured hardness used
Sandia left fork at Asph Plant	E122	10/8/2016	17:44	Zinc	WT	REG	F	86.2	µg/L	3.3	10	45.4	Aquatic Life Chronic	Measured hardness used
Sandia left fork at Asph Plant	E122	10/8/2016	18:34	Zinc	WT	REG	F	71.8	µg/L	3.3	10	44.5	Aquatic Life Chronic	Measured hardness used
Sandia left fork at Asph Plant	E122	11/4/2016	12:54	Zinc	WT	REG	F	233	µg/L	3.3	10	46.3	Aquatic Life Chronic	Measured hardness used
Sandia left fork at Asph Plant	E122	11/4/2016	13:44	Zinc	WT	REG	F	110	µg/L	3.3	10	71.2	Aquatic Life Chronic	Measured hardness used
Sandia left fork at Asph Plant	E122	11/4/2016	14:34	Zinc	WT	REG	F	149	µg/L	3.3	10	39.3	Aquatic Life Chronic	Measured hardness used
Sandia below Wetlands	E123	2/19/2016	10:07	Copper	W	REG	F	4.06	µg/L	1	NA	3.03	Aquatic Life Chronic	Average hardness used
Sandia below Wetlands	E123	5/23/2016	14:20	Copper	W	REG	F	4.4137	µg/L	1	NA	3.03	Aquatic Life Chronic	Average hardness used
Sandia below Wetlands	E123	8/8/2016	13:50	Copper	WS	REG	F	4.2061	µg/L	1	NA	3.03	Aquatic Life Chronic	Average hardness used
Sandia below Wetlands	E123	2/19/2016	10:07	Total PCB	W	REG	UF	0.00235	µg/L	NA	NA	0.00064	Aquatic Life HH-OO	
Sandia below Wetlands	E123	5/23/2016	14:20	Total PCB	W	REG	UF	0.00401	µg/L	NA	NA	0.00064	Aquatic Life HH-OO	
Sandia below Wetlands	E123	8/8/2016	13:50	Total PCB	WS	REG	UF	0.0138	µg/L	NA	NA	0.00064	Aquatic Life HH-OO	
Sandia below Wetlands	E123	12/1/2016	10:05	Total PCB	WS	FD	UF	0.00162	µg/L	NA	NA	0.00064	Aquatic Life HH-OO	
Sandia below Wetlands	E123	12/1/2016	10:05	Total PCB	WS	REG	UF	0.00196	µg/L	NA	NA	0.00064	Aquatic Life HH-OO	
Sandia below Wetlands	E123	7/31/2016	14:20	Aluminum	WT	REG	F	313	µg/L	15	50	151	Aquatic Life Chronic	Measured hardness used
Sandia below Wetlands	E123	7/31/2016	15:10	Aluminum	WT	REG	F	480	µg/L	15	50	174	Aquatic Life Chronic	Measured hardness used
Sandia below Wetlands	E123	7/31/2016	16:00	Aluminum	WT	REG	F	395	µg/L	15	50	151	Aquatic Life Chronic	Measured hardness used
Sandia below Wetlands	E123	8/3/2016	20:15	Aluminum	WT	REG	F	533	µg/L	15	50	144	Aquatic Life Chronic	Measured hardness used
Sandia below Wetlands	E123	8/3/2016	21:05	Aluminum	WT	REG	F	577	µg/L	15	50	137	Aquatic Life Chronic	Measured hardness used
Sandia below Wetlands	E123	8/3/2016	21:55	Aluminum	WT	REG	F	566	µg/L	15	50	182	Aquatic Life Chronic	Measured hardness used
Sandia below Wetlands	E123	8/27/2016	12:03	Aluminum	WT	REG	F	538	µg/L	15	50	113	Aquatic Life Chronic	Measured hardness used
Sandia below Wetlands	E123	8/27/2016	12:53	Aluminum	WT	REG	F	675	µg/L	15	50	140	Aquatic Life Chronic	Measured hardness used
Sandia below Wetlands	E123	8/27/2016	13:43	Aluminum	WT	REG	F	582	µg/L	15	50	176	Aquatic Life Chronic	Measured hardness used
Sandia below Wetlands	E123	9/6/2016	18:34	Aluminum	WT	REG	F	340	µg/L	15	50	87.4	Aquatic Life Chronic	Measured hardness used
Sandia below Wetlands	E123	9/6/2016	19:24	Aluminum	WT	REG	F	387	µg/L	15	50	123	Aquatic Life Chronic	Measured hardness used
Sandia below Wetlands	E123	9/6/2016	20:14	Aluminum	WT	REG	F	181	µg/L	15	50	155	Aquatic Life Chronic	Measured hardness used
Sandia below Wetlands	E123	11/5/2016	00:39	Aluminum	WT	REG	F	470	µg/L	15	50	110	Aquatic Life Chronic	Measured hardness used
Sandia below Wetlands	E123	11/5/2016	22:59	Aluminum	WT	REG	F	446	µg/L	15	50	176	Aquatic Life Chronic	Measured hardness used
Sandia below Wetlands	E123	11/5/2016	23:49	Aluminum	WT	REG	F	423	µg/L	15	50	97.4	Aquatic Life Chronic	Measured hardness used
Sandia below Wetlands	E123	7/31/2016	14:20	Copper	WT	REG	F	5.17	µg/L	0.35	1	2.26	Aquatic Life Chronic	Measured hardness used
Sandia below Wetlands	E123	7/31/2016	15:10	Copper	WT	REG	F	5.44	µg/L	0.35	1	2.47	Aquatic Life Chronic	Measured hardness used
Sandia below Wetlands	E123	7/31/2016	16:00	Copper	WT	REG	F	4.96	µg/L	0.35	1	2.26	Aquatic Life Chronic	Measured hardness used
Sandia below Wetlands	E123	8/3/2016	20:15	Copper	WT	REG	F	4.3	µg/L	0.35	1	2.2	Aquatic Life Chronic	Measured hardness used
Sandia below Wetlands	E123	8/3/2016	21:05	Copper	WT	REG	F	3.76	µg/L	0.35	1	2.13	Aquatic Life Chronic	Measured hardness used
Sandia below Wetlands	E123	8/3/2016	21:55	Copper	WT	REG	F	4.23	µg/L	0.35	1	2.54	Aquatic Life Chronic	Measured hardness used
Sandia below Wetlands	E123	8/27/2016	12:03	Copper	WT	REG	F	3.57	µg/L	0.35	1	1.89	Aquatic Life Chronic	Measured hardness used

Table D-2.1-1 (continued)

Location	Location alias	Date	Sample Time	Analyte	Sample Type	Sample Purpose	Field Prep Code	Result	Unit	MDL	PQL	Screening Value	Screening Value Type	Comments
Sandia below Wetlands	E123	8/27/2016	12:03	Copper	WT	REG	F	3.57	µg/L	0.35	1	2.16	Aquatic Life Chronic	Measured hardness used
Sandia below Wetlands	E123	8/27/2016	13:43	Copper	WT	REG	F	4.41	µg/L	0.35	1	2.48	Aquatic Life Chronic	Measured hardness used
Sandia below Wetlands	E123	9/6/2016	18:34	Copper	WT	REG	F	3.98	µg/L	0.35	1	1.61	Aquatic Life Chronic	Measured hardness used
Sandia below Wetlands	E123	9/6/2016	19:24	Copper	WT	REG	F	4.38	µg/L	0.35	1	1.99	Aquatic Life Chronic	Measured hardness used
Sandia below Wetlands	E123	9/6/2016	20:14	Copper	WT	REG	F	3.8	µg/L	0.35	1	2.3	Aquatic Life Chronic	Measured hardness used
Sandia below Wetlands	E123	11/5/2016	00:39	Copper	WT	REG	F	3.07	µg/L	0.35	1	1.86	Aquatic Life Chronic	Measured hardness used
Sandia below Wetlands	E123	11/5/2016	22:59	Copper	WT	REG	F	3.96	µg/L	0.35	1	2.48	Aquatic Life Chronic	Measured hardness used
Sandia below Wetlands	E123	11/5/2016	23:49	Copper	WT	REG	F	2.97	µg/L	0.35	1	1.72	Aquatic Life Chronic	Measured hardness used
Sandia below Wetlands	E123	7/31/2016	14:20	Lead	WT	REG	F	0.557	µg/L	0.5	2	0.421	Aquatic Life Chronic	Measured hardness used
Sandia below Wetlands	E123	7/31/2016	15:10	Lead	WT	REG	F	0.552	µg/L	0.5	2	0.473	Aquatic Life Chronic	Measured hardness used
Sandia below Wetlands	E123	8/3/2016	20:15	Lead	WT	REG	F	0.617	µg/L	0.5	2	0.404	Aquatic Life Chronic	Measured hardness used
Sandia below Wetlands	E123	8/3/2016	21:05	Lead	WT	REG	F	0.594	µg/L	0.5	2	0.387	Aquatic Life Chronic	Measured hardness used
Sandia below Wetlands	E123	8/3/2016	21:55	Lead	WT	REG	F	0.638	µg/L	0.5	2	0.49	Aquatic Life Chronic	Measured hardness used
Sandia below Wetlands	E123	8/27/2016	12:03	Lead	WT	REG	F	0.636	µg/L	0.5	2	0.331	Aquatic Life Chronic	Measured hardness used
Sandia below Wetlands	E123	8/27/2016	12:53	Lead	WT	REG	F	0.756	µg/L	0.5	2	0.394	Aquatic Life Chronic	Measured hardness used
Sandia below Wetlands	E123	8/27/2016	13:43	Lead	WT	REG	F	0.689	µg/L	0.5	2	0.476	Aquatic Life Chronic	Measured hardness used
Sandia below Wetlands	E123	9/6/2016	19:24	Lead	WT	REG	F	0.536	µg/L	0.5	2	0.355	Aquatic Life Chronic	Measured hardness used
Sandia below Wetlands	E123	11/5/2016	00:39	Lead	WT	REG	F	0.501	µg/L	0.5	2	0.324	Aquatic Life Chronic	Measured hardness used
Sandia below Wetlands	E123	11/5/2016	22:59	Lead	WT	REG	F	0.562	µg/L	0.5	2	0.476	Aquatic Life Chronic	Measured hardness used
Sandia below Wetlands	E123	7/31/2016	14:20	Total PCB	WT	REG	UF	0.067	µg/L	NA	NA	0.014	WH	
Sandia below Wetlands	E123	7/31/2016	14:20	Total PCB	WT	REG	UF	0.067	µg/L	NA	NA	0.014	Aquatic Life Chronic	
Sandia below Wetlands	E123	7/31/2016	14:20	Total PCB	WT	REG	UF	0.067	µg/L	NA	NA	0.00064	Aquatic Life HH-OO	
Sandia below Wetlands	E123	7/31/2016	15:10	Total PCB	WT	REG	UF	0.0258	µg/L	NA	NA	0.014	WH	
Sandia below Wetlands	E123	7/31/2016	15:10	Total PCB	WT	REG	UF	0.0258	µg/L	NA	NA	0.014	Aquatic Life Chronic	
Sandia below Wetlands	E123	7/31/2016	15:10	Total PCB	WT	REG	UF	0.0258	µg/L	NA	NA	0.00064	Aquatic Life HH-OO	
Sandia below Wetlands	E123	7/31/2016	16:00	Total PCB	WT	REG	UF	0.0187	µg/L	NA	NA	0.014	WH	
Sandia below Wetlands	E123	7/31/2016	16:00	Total PCB	WT	REG	UF	0.0187	µg/L	NA	NA	0.014	Aquatic Life Chronic	
Sandia below Wetlands	E123	7/31/2016	16:00	Total PCB	WT	REG	UF	0.0187	µg/L	NA	NA	0.00064	Aquatic Life HH-OO	
Sandia below Wetlands	E123	8/3/2016	20:15	Total PCB	WT	REG	UF	0.0482	µg/L	NA	NA	0.014	WH	
Sandia below Wetlands	E123	8/3/2016	20:15	Total PCB	WT	REG	UF	0.0482	µg/L	NA	NA	0.014	Aquatic Life Chronic	
Sandia below Wetlands	E123	8/3/2016	20:15	Total PCB	WT	REG	UF	0.0482	µg/L	NA	NA	0.00064	Aquatic Life HH-OO	
Sandia below Wetlands	E123	8/3/2016	21:05	Total PCB	WT	REG	UF	0.0204	µg/L	NA	NA	0.014	WH	
Sandia below Wetlands	E123	8/3/2016	21:05	Total PCB	WT	REG	UF	0.0204	µg/L	NA	NA	0.014	Aquatic Life Chronic	
Sandia below Wetlands	E123	8/3/2016	21:05	Total PCB	WT	REG	UF	0.0204	µg/L	NA	NA	0.00064	Aquatic Life HH-OO	
Sandia below Wetlands	E123	8/3/2016	21:55	Total PCB	WT	REG	UF	0.0115	µg/L	NA	NA	0.00064	Aquatic Life HH-OO	
Sandia below Wetlands	E123	8/27/2016	12:03	Total PCB	WT	REG	UF	0.281	µg/L	NA	NA	0.014	WH	
Sandia below Wetlands	E123	8/27/2016	12:03	Total PCB	WT	REG	UF	0.281	µg/L	NA	NA	0.014	Aquatic Life Chronic	
Sandia below Wetlands	E123	8/27/2016	12:03	Total PCB	WT	REG	UF	0.281	µg/L	NA	NA	0.00064	Aquatic Life HH-OO	

Table D-2.1-1 (continued)

Location	Location alias	Date	Sample Time	Analyte	Sample Type	Sample Purpose	Field Prep Code	Result	Unit	MDL	PQL	Screening Value	Screening Value Type	Comments
Sandia below Wetlands	E123	8/27/2016	13:43	Total PCB	WT	REG	UF	0.0571	µg/L	NA	NA	0.014	WH	
Sandia below Wetlands	E123	8/27/2016	13:43	Total PCB	WT	REG	UF	0.0571	µg/L	NA	NA	0.014	Aquatic Life Chronic	
Sandia below Wetlands	E123	8/27/2016	13:43	Total PCB	WT	REG	UF	0.0571	µg/L	NA	NA	0.00064	Aquatic Life HH-OO	
Sandia below Wetlands	E123	9/6/2016	18:34	Total PCB	WT	REG	UF	0.106	µg/L	NA	NA	0.014	WH	
Sandia below Wetlands	E123	9/6/2016	18:34	Total PCB	WT	REG	UF	0.106	µg/L	NA	NA	0.014	Aquatic Life Chronic	
Sandia below Wetlands	E123	9/6/2016	18:34	Total PCB	WT	REG	UF	0.106	µg/L	NA	NA	0.00064	Aquatic Life HH-OO	
Sandia below Wetlands	E123	9/6/2016	19:24	Total PCB	WT	REG	UF	0.0204	µg/L	NA	NA	0.014	WH	
Sandia below Wetlands	E123	9/6/2016	19:24	Total PCB	WT	REG	UF	0.0204	µg/L	NA	NA	0.014	Aquatic Life Chronic	
Sandia below Wetlands	E123	9/6/2016	19:24	Total PCB	WT	REG	UF	0.0204	µg/L	NA	NA	0.00064	Aquatic Life HH-OO	
Sandia below Wetlands	E123	9/6/2016	20:14	Total PCB	WT	REG	UF	0.014	µg/L	NA	NA	0.014	WH	
Sandia below Wetlands	E123	9/6/2016	20:14	Total PCB	WT	REG	UF	0.014	µg/L	NA	NA	0.014	Aquatic Life Chronic	
Sandia below Wetlands	E123	9/6/2016	20:14	Total PCB	WT	REG	UF	0.014	µg/L	NA	NA	0.00064	Aquatic Life HH-OO	
Sandia below Wetlands	E123	11/5/2016	00:39	Total PCB	WT	REG	UF	0.0312	µg/L	NA	NA	0.014	WH	
Sandia below Wetlands	E123	11/5/2016	00:39	Total PCB	WT	REG	UF	0.0312	µg/L	NA	NA	0.014	Aquatic Life Chronic	
Sandia below Wetlands	E123	11/5/2016	00:39	Total PCB	WT	REG	UF	0.0312	µg/L	NA	NA	0.00064	Aquatic Life HH-OO	
Sandia below Wetlands	E123	11/5/2016	22:59	Total PCB	WT	REG	UF	0.112	µg/L	NA	NA	0.014	WH	
Sandia below Wetlands	E123	11/5/2016	22:59	Total PCB	WT	REG	UF	0.112	µg/L	NA	NA	0.014	Aquatic Life Chronic	
Sandia below Wetlands	E123	11/5/2016	22:59	Total PCB	WT	REG	UF	0.112	µg/L	NA	NA	0.00064	Aquatic Life HH-OO	
Sandia below Wetlands	E123	11/5/2016	23:49	Total PCB	WT	REG	UF	0.0473	µg/L	NA	NA	0.014	WH	
Sandia below Wetlands	E123	11/5/2016	23:49	Total PCB	WT	REG	UF	0.0473	µg/L	NA	NA	0.014	Aquatic Life Chronic	
Sandia below Wetlands	E123	11/5/2016	23:49	Total PCB	WT	REG	UF	0.0473	µg/L	NA	N/A	0.00064	Aquatic Life HH-OO	

Note: Shaded rows indicate base flow, unshaded rows indicate storm flow.

[a] W and WS = Base flow water; WT = storm water.

[b] REG = Regular investigative sample; FD = field duplicate.

[c] F = Filtered using 0.45-µm pore size; UF = nonfiltered.

[d] MDL = Method detection limit.

[e] PQL = Practical quantitation limit.

[f] NA = Not available.

[g] Aquatic Life Chronic = NMWQCC Aquatic Life Standards Chronic.

[h] Aquatic Life HH-OO = Human Health Organism Only Aquatic Life Standard.

[i] WL = Livestock Watering Standard.

[j] WH = Wildlife Habitat Standard.

Table D-2.1-2
Summary of 2016 Base Flow and Storm Water SWQC Exceedances

Location	Media Type	Filtration	Analyte	Total Samples	Number of Samples Exceeding SWQC	Average of Sample Results Exceeding SWQC	Maximum Sample Results Exceeding SWQC	Unit
E121	Base flow	UF[a]	Aluminum	7	3	486.52	511.00	µg/L
E122	Base flow	UF	Aluminum	4	2	378.19	393.20	µg/L
E123	Base flow	UF	Aluminum	6	2	1377.70	1695.40	µg/L
E121	Base flow	F[b]	Copper	7	5	3.93	4.68	µg/L
E122	Base flow	F	Copper	4	2	3.98	4.15	µg/L
E123	Base flow	F	Copper	6	4	4.02	4.41	µg/L
E121	Base flow	UF	Total PCB	5	5	0.0035	0.0059	µg/L
E122	Base flow	UF	Total PCB	4	1	0.0023	0.0023	µg/L
E123	Base flow	UF	Total PCB	5	5	0.0047	0.0138	µg/L
E121	Storm water	F	Aluminum	19	19	313.00	539.00	µg/L
E122	Storm water	F	Aluminum	9	1	369.00	369.00	µg/L
E123	Storm water	F	Aluminum	15	15	460.40	675.00	µg/L
E122	Storm water	UF	Benzo(a)anthracene	18	1	0.33	0.33	µg/L
E122	Storm water	UF	Benzo(a)pyrene	18	1	0.30	0.30	µg/L
E122	Storm water	UF	Benzo(b)fluoranthene	18	1	0.33	0.33	µg/L
E122	Storm water	UF	Benzo(k)fluoranthene	18	1	0.23	0.23	µg/L
E121	Storm water	F	Cadmium	19	2	0.51	0.86	µg/L
E122	Storm water	F	Cadmium	9	1	0.81	0.81	µg/L
E121	Storm water	F	Copper	19	19	4.44	8.06	µg/L
E122	Storm water	F	Copper	9	9	26.07	46.30	µg/L
E123	Storm water	F	Copper	15	15	4.10	5.44	µg/L
E121	Storm water	UF	Gross alpha	7	1	18.70	18.70	pCi/L
E121	Storm water	F	Lead	19	10	0.61	0.88	µg/L
E122	Storm water	F	Lead	9	6	1.04	1.19	µg/L
E123	Storm water	F	Lead	15	11	0.60	0.76	µg/L
E121	Storm water	UF	Total PCB	21	21	0.0419	0.1760	µg/L
E122	Storm water	UF	Total PCB	9	9	0.0243	0.0814	µg/L
E123	Storm water	UF	Total PCB	14	14	0.0615	0.2810	µg/L
E121	Storm water	F	Zinc	19	18	27.47	50.40	µg/L
E122	Storm water	F	Zinc	9	9	122.31	233.00	µg/L

[a] UF = Non-filtered.

[b] F = Filtration using 0.45-µm pore size.

Table D-3.4-1
Analytical Exceedances in the Alluvial System

Location	Date	Analyte	Field Prep Code[a]	Result	Unit	MDL[b]	Screening Value	Screening-Value Type
SCPZ-1	2/24/2016	Iron	F	4111.4	µg/L	10	1000	NMWQCC
SCPZ-1	5/25/2016	Iron	F	2410.5	µg/L	10	1000	NMWQCC
SCPZ-1	8/11/2016	Iron	F	2749.8	µg/L	10	1000	NMWQCC
SCPZ-1	2/24/2016	Manganese	F	1093.5	µg/L	1	200	NMWQCC
SCPZ-1	5/25/2016	Manganese	F	1384.3	µg/L	1	200	NMWQCC
SCPZ-1	8/11/2016	Manganese	F	1223.5	µg/L	1	200	NMWQCC
SWA-1-1	12/1/2016	Iron	F	4695.8	µg/L	10	1000	NMWQCC
SWA-1-1	12/1/2016	Manganese	F	1325.4	µg/L	1	200	NMWQCC
SWA-1-2	8/11/2016	Chromium	F	69.392	µg/L	1	50	NMWQCC
SWA-1-2	5/25/2016	Lithium	F	54.545	µg/L	1	40	EPA Regional[c]
SWA-1-2	8/11/2016	Lithium	F	59.795	µg/L	1	40	EPA Regional
SWA-1-2	11/29/2016	Lithium	F	60.306	µg/L	1	40	EPA Regional
SCPZ-3	2/24/2016	Iron	F	6665.7	µg/L	10	1000	NMWQCC
SCPZ-3	5/25/2016	Iron	F	3578.2	µg/L	10	1000	NMWQCC
SCPZ-3	2/24/2016	Lithium	F	60.006	µg/L	1	40	EPA Regional
SCPZ-3	5/25/2016	Lithium	F	53.631	µg/L	1	40	EPA Regional
SCPZ-3	2/24/2016	Manganese	F	707.85	µg/L	1	200	NMWQCC
SCPZ-3	5/25/2016	Manganese	F	368.26	µg/L	1	200	NMWQCC
SWA-1-3	8/11/2016	Iron	F	10132	µg/L	10	1000	NMWQCC
SWA-1-3	11/29/2016	Iron	F	9334	µg/L	10	1000	NMWQCC
SWA-1-3	8/11/2016	Lithium	F	73.208	µg/L	1	40	EPA Regional
SWA-1-3	11/29/2016	Lithium	F	61.01	µg/L	1	40	EPA Regional
SWA-1-3	8/11/2016	Manganese	F	702.85	µg/L	1	200	NMWQCC
SWA-1-3	11/29/2016	Manganese	F	520.51	µg/L	1	200	NMWQCC
SCPZ-4	2/25/2016	Iron	F	1329.7	µg/L	10	1000	NMWQCC
SCPZ-4	2/25/2016	Lithium	F	55.311	µg/L	1	40	EPA Regional
SCPZ-4	5/23/2016	Lithium	F	50.401	µg/L	1	40	EPA Regional
SCPZ-4	2/25/2016	Manganese	F	610.84	µg/L	1	200	NMWQCC
SCPZ-4	5/23/2016	Manganese	F	380.56	µg/L	1	200	NMWQCC
SWA-2-4	8/11/2016	Iron	F	1347.6	µg/L	10	1000	NMWQCC
SWA-2-4	11/30/2016	Iron	F	1300.2	µg/L	10	1000	NMWQCC
SWA-2-4	8/11/2016	Lithium	F	74.847	µg/L	1	40	EPA Regional
SWA-2-4	11/30/2016	Lithium	F	59.251	µg/L	1	40	EPA Regional
SWA-2-4	8/11/2016	Manganese	F	470.59	µg/L	1	200	NMWQCC
SWA-2-4	11/30/2016	Manganese	F	489.42	µg/L	1	200	NMWQCC
SCPZ-5	2/26/2016	Iron	F	6786.2	µg/L	10	1000	NMWQCC

Table D-3.4-1 (continued)

Location	Date	Analyte	Field Prep Code	Result	Unit	MDL	Screening Value	Screening-Value Type
SCPZ-5	2/26/2016	Manganese	F	1234.9	µg/L	1	200	NMWQCC
SWA-2-5	8/11/2016	Iron	F	7008.7	µg/L	10	1000	NMWQCC
SWA-2-5	11/30/2016	Iron	F	5213.9	µg/L	10	1000	NMWQCC
SWA-2-5	8/11/2016	Manganese	F	1371.6	µg/L	1	200	NMWQCC
SWA-2-5	11/30/2016	Manganese	F	1172.9	µg/L	1	200	NMWQCC
SWA-2-6	8/11/2016	Arsenic	F	10.611	µg/L	0.2	10	MCL
SWA-2-6	11/30/2016	Arsenic	F	10.288	µg/L	0.2	10	MCL
SWA-2-6	8/11/2016	Iron	F	8137.2	µg/L	10	1000	NMWQCC
SWA-2-6	11/30/2016	Iron	F	6385.2	µg/L	10	1000	NMWQCC
SWA-2-6	8/11/2016	Manganese	F	1390.1	µg/L	1	200	NMWQCC
SWA-2-6	11/30/2016	Manganese	F	1285.6	µg/L	1	200	NMWQCC
SCPZ-7	2/22/2016	Iron	F	7157.9	µg/L	10	1000	NMWQCC
SCPZ-7	2/22/2016	Lithium	F	40.827	µg/L	1	40	EPA Regional
SCPZ-7	2/22/2016	Manganese	F	3078.9	µg/L	1	200	NMWQCC
SWA-3-7	5/25/2016	Iron	F	9168.6	µg/L	100	1000	NMWQCC
SWA-3-7	8/10/2016	Iron	F	9327.5	µg/L	10	1000	NMWQCC
SWA-3-7	11/30/2016	Iron	F	8813.6	µg/L	10	1000	NMWQCC
SWA-3-7	8/10/2016	Lithium	F	40.605	µg/L	1	40	EPA Regional
SWA-3-7	11/30/2016	Lithium	F	40.391	µg/L	1	40	EPA Regional
SWA-3-7	5/25/2016	Manganese	F	2897.5	µg/L	10	200	NMWQCC
SWA-3-7	8/10/2016	Manganese	F	2843.5	µg/L	1	200	NMWQCC
SWA-3-7	11/30/2016	Manganese	F	3456.5	µg/L	1	200	NMWQCC
SWA-3-8	5/25/2016	Iron	F	5499.3	µg/L	10	1000	NMWQCC
SWA-3-8	8/10/2016	Iron	F	6884.5	µg/L	10	1000	NMWQCC
SWA-3-8	11/30/2016	Iron	F	4855.2	µg/L	10	1000	NMWQCC
SWA-3-8	5/25/2016	Manganese	F	2123.8	µg/L	1	200	NMWQCC
SWA-3-8	8/10/2016	Manganese	F	2449.3	µg/L	1	200	NMWQCC
SWA-3-8	11/30/2016	Manganese	F	2431.3	µg/L	1	200	NMWQCC
SCPZ-9	2/22/2016	Iron	F	5477.5	µg/L	10	1000	NMWQCC
SCPZ-9	2/22/2016	Manganese	F	1725.7	µg/L	1	200	NMWQCC
SWA-3-9	5/25/2016	Iron	F	10225	µg/L	10	1000	NMWQCC
SWA-3-9	8/10/2016	Iron	F	11143	µg/L	10	1000	NMWQCC
SWA-3-9	11/30/2016	Iron	F	9887.6	µg/L	10	1000	NMWQCC
SWA-3-9	5/25/2016	Manganese	F	2338.1	µg/L	10	200	NMWQCC
SWA-3-9	8/10/2016	Manganese	F	2288.6	µg/L	1	200	NMWQCC
SWA-3-9	11/30/2016	Manganese	F	2180.9	µg/L	1	200	NMWQCC
SCPZ-10	2/22/2016	Iron	F	15675	µg/L	10	1000	NMWQCC

Table D-3.4-1 (continued)

Location	Date	Analyte	Field Prep Code	Result	Unit	MDL	Screening Value	Screening-Value Type
SCPZ-10	2/22/2016	Lithium	F	64.204	µg/L	1	40	EPA Regional
SCPZ-10	2/22/2016	Manganese	F	3499	µg/L	1	200	NMWQCC
SWA-4-10	8/10/2016	Chromium	F	72.853	µg/L	10	50	NMWQCC
SWA-4-10	5/24/2016	Fluoride	F	1.6811	mg/L	0.01	1.6	NMWQCC
SWA-4-10	5/24/2016	Iron	F	11649	µg/L	100	1000	NMWQCC
SWA-4-10	8/10/2016	Iron	F	16711	µg/L	10	1000	NMWQCC
SWA-4-10	11/29/2016	Iron	F	3921.6	µg/L	10	1000	NMWQCC
SWA-4-10	5/24/2016	Lithium	F	46.711	µg/L	1	40	EPA Regional
SWA-4-10	8/10/2016	Lithium	F	55.116	µg/L	1	40	EPA Regional
SWA-4-10	11/29/2016	Lithium	F	40.455	µg/L	1	40	EPA Regional
SWA-4-10	5/24/2016	Manganese	F	11409	µg/L	10	200	NMWQCC
SWA-4-10	8/10/2016	Manganese	F	8584	µg/L	1	200	NMWQCC
SWA-4-10	11/29/2016	Manganese	F	2764.7	µg/L	1	200	NMWQCC
SCPZ-11(B)	5/24/2016	Iron	F	5093.7	µg/L	10	1000	NMWQCC
SCPZ-11(B)	2/22/2016	Lithium	F	47.848	µg/L	1	40	EPA Regional
SCPZ-11(B)	5/24/2016	Lithium	F	49.229	µg/L	1	40	EPA Regional
SCPZ-11(B)	2/22/2016	Manganese	F	248.43	µg/L	1	200	NMWQCC
SCPZ-11(B)	5/24/2016	Manganese	F	707.08	µg/L	1	200	NMWQCC
SWA-4-11	8/10/2016	Iron	F	4161.9	µg/L	10	1000	NMWQCC
SWA-4-11	11/29/2016	Iron	F	2464.5	µg/L	10	1000	NMWQCC
SWA-4-11	8/10/2016	Lithium	F	86.598	µg/L	1	40	EPA Regional
SWA-4-11	11/29/2016	Lithium	F	61.454	µg/L	1	40	EPA Regional
SWA-4-11	8/10/2016	Manganese	F	937.17	µg/L	1	200	NMWQCC
SWA-4-11	11/29/2016	Manganese	F	682.72	µg/L	1	200	NMWQCC
SWA-1	2/24/2016	Lithium	F	64.777	µg/L	1	40	EPA Regional
SWA-1	2/24/2016	Manganese	F	364.78	µg/L	1	200	NMWQCC
SWA-2	2/26/2016	Iron	F	5714.3	µg/L	10	1000	NMWQCC
SWA-2	2/26/2016	Manganese	F	1194.2	µg/L	1	200	NMWQCC
SWA-3	2/22/2016	Iron	F	5904.6	µg/L	10	1000	NMWQCC
SWA-3	2/22/2016	Manganese	F	2265.6	µg/L	1	200	NMWQCC
SWA-4	2/25/2016	Iron	F	9940.5	µg/L	10	1000	NMWQCC
SWA-4	2/25/2016	Lithium	F	56.65	µg/L	1	40	EPA Regional
SWA-4	2/25/2016	Manganese	F	2051.4	µg/L	1	200	NMWQCC
SWA-4-12	8/10/2016	Chromium	F	55.409	µg/L	10	50	NMWQCC
SWA-4-12	5/24/2016	Iron	F	4191.6	µg/L	10	1000	NMWQCC
SWA-4-12	8/10/2016	Iron	F	6986.3	µg/L	10	1000	NMWQCC
SWA-4-12	11/29/2016	Iron	F	3368.8	µg/L	10	1000	NMWQCC

Table D-3.4-1 (continued)

Location	Date	Analyte	Field Prep Code	Result	Unit	MDL	Screening Value	Screening-Value Type
SWA-4-12	5/24/2016	Lithium	F	51.242	µg/L	1	40	EPA Regional
SWA-4-12	8/10/2016	Lithium	F	76.706	µg/L	1	40	EPA Regional
SWA-4-12	11/29/2016	Lithium	F	53.387	µg/L	1	40	EPA Regional
SWA-4-12	5/24/2016	Manganese	F	962.11	µg/L	1	200	NMWQCC
SWA-4-12	8/10/2016	Manganese	F	1498.9	µg/L	1	200	NMWQCC
SWA-4-12	11/29/2016	Manganese	F	1156.1	µg/L	1	200	NMWQCC

[a] F = Filtered using 0.45-µm pore size.

[b] MDL = Method detection limit.

[c] EPA regional screening levels for tap water.

Appendix E

2016 Watershed Mitigations Inspections

E-1.0 INTRODUCTION

Watershed storm water controls and grade-control structures (GCSs) are inspected twice a year and after significant flow events (greater than 50 cubic feet per second at locations with gaging stations). These inspections are completed to ensure watershed mitigations are functioning properly and to determine if maintenance is required. Examples of items evaluated during inspections include the following:

- debris/sediment accumulation that could impede operation
- water levels behind retention structures
- physical damage of structure, or failure of structural components
- undermining, piping, flanking, settling, movement, or breeching of structure
- vegetation establishment and vegetation that may negatively impact structural components
- rodent damage
- vandalism
- erosion

The photographs in this appendix show the 2016 March, June, and November inspections of watershed mitigations in Sandia Canyon. Each group of photographs is associated with a specific feature (e.g., standpipe, weir, upstream, downstream, vegetated cover) that has could develop issues. The photographs are in chronological order and depict the feature throughout 2016. Photographs of features were taken to mirror previous inspection photos as closely as possible. Certain findings were discovered as the year progressed, and thus appear later during the year.

In 2016, Sandia GCS downstream gage did not record significant flow events. Therefore, two regular inspections as well as a mid-year inspection were conducted. The inspections demonstrate that wetland plantings were dormant in the first quarter and flourished once the growing season set in. Previously noted preferential flow channels have filled in with wetland vegetation, but inspection reports continue to monitor for evidence of flow paths. The run-on defense cells demonstrated activity, both anthropogenic and natural. With the first 2016 inspection, the defense cells were functioning as intended. However, in the spring, Los Alamos County began field activities related to a long-term solution to address run-off from the former landfill into this drainage and associated erosion resulting from this runoff. Specifically, Los Alamos County conducted field activities to collect geotechnical data in support of the design. As part of this effort, Los Alamos County removed sediment from behind the upper run-on defense cell to provide additional sediment collection capacity and installed additional best management practices, including straw bales within the drainage, farther upstream. In the latter half of 2016, it was noted that sediments had moved from the County outfall into the upper defense cell. However, additional sediment capture volume remains behind the upstream run-on defense cell because of the sediment removal discussed above. Because the cells continued to function as intended, they did not warrant maintenance. Subsequent inspections will monitor the defense cells for change.

The photographs in the appendix illustrate the health of the wetland in and around the GCS, revegetation of adjacent slopes, and the best management practices in place to help maintain the integrity of the GCS and its associated wetland vegetation.

Additional data on the position of the channel thalweg in the area of the GCS can be found in Appendix B. Quantitative data from vegetation perimeter mapping in and around the GCS can be found in Appendix C.

E-2.0 SANDIA CANYON GCS INSPECTION PHOTOGRAPHS

E-2.1 Vegetation Inspection, 2016

Figure E-2.1-1 March 2016: Vegetation above lower weir, dormant at this time

Figure E-2.1-2 June 2016: Vegetation shows improving density of wetland-type vegetation above and below upper weir

Figure E-2.1-3 November 2016: Vegetation dormant showing good stability and density

Figure E-2.1-4 March 2016: Partial establishment of vegetation on north embankment turf-reinforcement mat

Figure E-2.1-5 June 2016: Closeup of vegetation on north embankment

Figure E-2.1-6 November 2016: Vegetation on north embankment showing improving fill-in from March 2016 inspection

Figure E-2.1-7 March 2016: South bank vegetation

Figure E-2.1-8 June 2016: South bank vegetation

Figure E-2.1-9 November 2016: South bank vegetation

E-2.2 Defense Cells, North Side

Figure E-2.2-1 March 2016: Earthen fill between upper and lower defense cells showing minor knick point (shifting material may lead to rill and erosional features)

Figure E-2.2-2 June 2016: Minor rill showing in earth fill area between defense cells

Figure E-2.2-3 June 2016: Mostly weeds established in area between defense cells

Figure E-2.2-4 June 2016: Newly installed best management practices above upper defense cell. Installation by Los Alamos County landfill operations.

Figure E-2.2-5 June 2016: Upper defense cell, some fine material deposit from Los Alamos County landfill

Figure E-2.2-6 November 2016: Upper defense cell muck intrusion from Los Alamos County landfill slope. Defense cell operating as designed.

Figure E-2.2-7 November 2016: Lower defense cell operating as designed

E-2.3 GCS Inspections

Figure E-2.3-1 March 2016: Middle GCS

Figure E-2.3-2 March 2016: Middle GCS

Figure E-2.3-3 June 2016: Upper GCS

Figure E-2.3-4 June 2016: Middle GCS

Figure E-2.3-5 June 2016: Lower GCS

Figure E-2.3-6 November 2016: Upper GCS

Figure E-2.3-7 November 2016: Lower GCS

E-2.4 Other Inspection Photographs

Figure E-2.4-1 March 2016: Straw wattle damaged by animal or persons walking on wattle. Recommend maintenance action.

Figure E-2.4-2 March 2016: Previous crack repair on middle grade-control structure. No change from past inspections.

Figure E-2.4-3 June 2016: Crack repair on middle GCS. No change from past inspections.

Figure E-2.4-4 November 2016: Crack repair on middle GCS. No change from past inspections.

Figure E-2.4-5 March 2016: Crack monitoring. No change from last inspection.

Figure E-2.4-6 March 2016: Preferential flow path monitoring on north bank between lower and middle GCS

Figure E-2.4-7 June 2016: Preferential flow path not evident from vegetation in-fill. Continued monitoring recommended.

Appendix F

Analytical Data
(on CD included with this document)